MPR ASSOCIATES, INC.

OYSTER CREEK
NUCLEAR GENERATING STATION
MARK I CONTAINMENT LONG-TERM PROGRAM

PLANT-UNIQUE ANALYSIS REPORT
SUPPRESSION CHAMBER AND VENT SYSTEM

MPR-733

Prepared for:

General Public Utilities Nuclear
Parsippany, New Jersey

August 1982

1140 CONNECTICUT AVENUE, N. W. WASHINGTON, D. C. 20036 202 - 659-2320

TABLE OF CONTENTS

List of Tables

List of Figures

List of Acronyms

1.0 INTRODUCTION

- 1.1 Background
- 1.2 Short-Term Program
- 1.3 Long-Term Program
- 1.4 Scope of this Report
- 1.5 Summary of Results

2.0 DESIGN CRITERIA

- 2.1 Design Specifications
  - 2.1.1 Original Design Specification
  - 2.1.2 Specifications for Modifications
- 2.2 Long-Term Program Structural Acceptance Criteria
- 2.3 Material Parameters

3.0 COMPONENT DESCRIPTIONS

- 3.1 Suppression Chamber
- 3.2 Vent System
- 3.3 Internal Structures

4.0 LOAD DEFINITIONS

4.1 Original Design Loads
4.2 LOCA Containment Pressure and Temperature
4.3 LOCA Loads on the Torus Shell
4.3.1 Pool Swell
4.3.2 Condensation Oscillation
4.3.3 Chugging
4.4 LOCA Loads on the Vent System
4.4.1 Pool Swell
4.4.2 Condensation Oscillation
4.4.3 Chugging
4.5 LOCA Loads on Internal Structures
4.5.1 Pool Swell
4.5.2 Condensation Oscillation and Chugging
4.6 Safety Relief Valve Induced Loads
4.6.1 SRV Discharge Loads on the Piping
4.6.2 SRV Discharge Loads on the Torus Shell
4.6.3 SRV Discharge Loads on Internal Structures

5.0 GENERAL ANALYTICAL PROCEDURES

5.1 Coupled Torus-Vent System Computer Model
5.2 Vent System Beam Model
5.3 Generic Mark I Program Computer Programs
5.4 Seismic Analysis

6.0 DESIGN STRESS ANALYSIS

6.1 Torus and Support System

6.1.1 Torus Shell and Hoop Straps

6.1.1.1 Methods of Analysis

6.1.1.2 Loading and Acceptance Criteria

6.1.1.3 Summary of Results

6.1.2 Torus Ring Girder

6.1.2.1 Methods of Analysis

6.1.2.2 Loading and Acceptance Criteria

6.1.2.3 Summary of Results

6.1.3 Torus Mid-Bay Saddle

6.1.3.1 Methods of Analysis

6.1.3.2 Loading and Acceptance Criteria

6.1.3.3 Summary of Results

6.1.4 Torus Support Columns

6.1.4.1 Methods of Analysis

6.1.4.2 Loading and Acceptance Criteria

6.1.4.3 Summary of Results

6.1.5 Torus Sway Braces

6.1.5.1 Methods of Analysis

6.1.5.2 Loading and Acceptance Criteria

6.1.5.3 Summary of Results

6.2 Vent System

6.2.1 Vent Line, Vent Header and Downcomers

6.2.1.1 Methods of Analysis

6.2.1.2 Loading and Acceptance Criteria

6.2.1.3 Summary of Results

6.2.2 Vent Line-Drywell Intersection

6.2.2.1 Methods of Analysis

6.2.2.2 Loading and Acceptance Criteria

6.2.2.3 Summary of Results

6.2.3 Vent Line-Vent Header Intersection
6.2.3.1 Methods of Analysis
6.2.3.2 Loading and Acceptance Criteria
6.2.3.3 Summary of Results
6.2.4 Downcomer-Vent Header Intersection
6.2.4.1 Methods of Analysis
6.2.4.2 Loading and Acceptance Criteria
6.2.4.3 Summary of Results
6.2.5 Vent Line Bellows
6.2.5.1 Methods of Analysis
6.2.5.2 Loading and Acceptance Criteria
6.2.5.3 Summary of Results
6.2.6 Vent System Support Columns
6.2.6.1 Methods of Analysis
6.2.6.2 Loading and Acceptance Criteria
6.2.6.3 Summary of Results
6.2.7 Vent Header Ring Collar
6.2.7.1 Methods of Analysis
6.2.7.2 Loading and Acceptance Criteria
6.2.7.3 Summary of Results
6.2.8 Vent Header Deflector
6.2.8.1 Methods of Analysis
6.2.8.2 Loading and Acceptance Criteria
6.2.8.3 Summary of Results
6.2.9 Downcomer Bracing
6.2.9.1 Methods of Analysis
6.2.9.2 Loading and Acceptance Criteria
6.2.9.3 Summary of Results
6.3 Torus Internal Structures
6.3.1 Methods of Analysis
6.3.2 Loading and Acceptance Criteria
6.3.3 Summary of Results

7.0 FATIGUE EVALUATION

7.1 ASME Code Jurisdiction and Criteria
7.2 Load Sources, Load Cycles, and Sequence of Loads
7.3 Analysis Methods
7.4 Summary of Results

8.0 REFERENCES

9.0 APPENDIX A

Oyster Creek Plant Unique Load Definition Data

LIST OF TABLES

Table Number	Title
4.5.1-1	Summary of Peak Pool Swell Loads on Oyster Creek Torus Internal Structures
4.6.1-1	Peak Steam Thrust Loads on Oyster Creek SRV Discharge Lines
4.6.1-2	Peak Water Thrust on the Oyster Creek Quencher for Worst-Case SRV Discharge
4.6.2-1	Overall Multipliers for SRV Discharge Analysis of Torus Shell and Supports
4.6.3-1	Summary of Peak Applied SRV Drag Loads on Submerged Structures in the Oyster Creek Torus for Worst-Case SRV Actuation
6.0-1	Summary of Limiting Load Combinations for Torus and Vent System Components
6.1-1	List of Loads Considered for Evaluation of Torus and Support System
6.1.1-1	Summary of Limiting Stresses in Torus Shell
6.1.1-2	Summary of Shear Stresses in Hoop Strap Attachment Fillet Welds for Limiting Load Combination (IBA + POCH + EQ)
6.1.2-1	Summary of Limiting Stresses in Torus Ring Girder and Attachment Welds for the 14 Ring Girders not Supporting the Safety Relief Valve Discharge Piping System
6.1.3-1	Summary of Limiting Stresses in Torus Saddle
6.1.3-2	Summary of Limiting Loads in Saddle Anchorage
6.1.4-1	Stresses in Support Column Attachments to Shell
6.1.4-2	Maximum Stress Interaction of Axial and Bending Loads on Outside Support Column
6.1.4-3	Peak Axial Loads on the Support Columns
6.1.5-1	Bounding Loads on Sway Braces

LIST OF TABLES (Continued)

6.2.1-1	Loads Considered in the Evaluation of Vent Lines, Vent Header and Downcomers
6.2.1-2	Summary of Calculated Stresses at Limiting Vent Line, Vent Header and Downcomer Locations
6.2.1-3	Summary of Limiting Calculated Stresses in Vent Lines, Vent Header and Downcomer
6.2.1-4	Summary of Limiting Calculated Stresses at Vent System Miter Locations
6.2.1-5	Summary of Limiting Stresses in Vent Lines and Vent Header at Support Attachment Points
6.2.1-6	Summary of Limiting Stresses in Vent Line and Vent Header Support Attachment Welds
6.2.1-7	Summary of Limiting Stress Results for Local Impact Pressure Loading on Vent Header During Pool Swell
6.2.2-1	Summary of Controlling Stresses in the Vent Line/Drywell Intersection
6.2.3-1	Summary of Limiting Stresses in Vent Line/Vent Header Intersection
6.2.4-1	Loads Considered in the Evaluation of the Downcomer/Vent Header Intersection
6.2.4-2	Summary of Limiting Stresses at Downcomer/Vent Header Intersection
6.2.5-1	Loads Considered in Torus/Main Vent Line Bellows Analysis
6.2.5-2	Summary of Results for Torus/Main Vent Line Bellows Evaluation
6.2.6-1	Loads Considered in Vent Header Support Column Analysis
6.2.6-2	Combined Axial and Bending Stresses in Support Columns and Attachment Brackets
6.2.6-3a	Limiting Stresses at Pinholes
6.2.6-3b	Limiting Stresses at Pins

LIST OF TABLES (Continued)

6.2.6-4	Limiting Weld Stresses
6.2.7-1	Summary of Limiting Ring Collar Stresses
6.2.8-1	Loads Considered in the Evaluation of the Vent Header Deflector
6.2.8-2	Summary of Limiting Stresses Compared to Allowable Values for the Vent Header Deflector
6.2.9-1	Loads Considered in the Evaluation of the Modified Downcomer Bracing
6.2.9-2	Results of Analysis of Downcomer Bracing
6.3-1	Controlling Load Cases for Oyster Creek Internal Structures
6.3-2	Limiting Components and Calculated Stresses for the Oyster Creek Catwalk
7.4-1	Results of the Fatigue Analysis of Torus and Vent System Components

LIST OF FIGURES

Figure Number	Title
3.0-i	Generic Mark I Containment
3.1-1	Oyster Creek Torus Plan View
3.1-2	Oyster Creek Torus Cross-Section at Ring Girder
3.1-3	Oyster Creek Torus Cross-Section at Saddle and Main Vent
3.1-4	Oyster Creek Torus Sway Braces
3.1-5	Oyster Creek Torus View from Below Showing Shell Straps
3.2-1	Oyster Creek Torus Vent System Plan View
3.2.2	Oyster Creek Torus Cross-Section at Saddle and Main Vent
3.2.3	Oyster Creek Torus Cross-Section at Ring Girder
4.6.1-1	Model/Test Data Comparison for Two Valves, Simultaneous, First Actuation, North Header Discharge Line Pressure Near Relief Valves
4.6.1-2	Pipe Segments for SRV Discharge Thrust Load Calculations for the South Header
4.6.1-3	Pipe Segments for SRV Discharge Thrust Load Calculation for the North Header
4.6.1-4	Load Definition for Oyster Creek Sparger Water Clearing Thrust Loads
4.6.2-1	Oyster Creek Torus Plan View Showing Location of SRV Discharge Quenchers
4.6.2-2	Oyster Creek Torus Attenuation Factors for In-Plant SRV Tests
5.1.1-1	Oyster Creek Torus Finite Element Shell Model
5.1.2-1	Oyster Creek Torus Inside Column Connection Region Model
5.1.2-2	Oyster Creek Torus Outside Column Connection Region Model
5.2-1	Oyster Creek Vent System Finite Element Beam Model

LIST OF FIGURES (Continued)

6.1.2-1	Oyster Creek Torus Plan View Systems which Attach to Ring Girders
6.1.2-2	Oyster Creek Torus Systems Attached to Typical Ring Girder
6.1.2-3	Oyster Creek Torus Systems Attached to Ring Girder Numbers 3, 6, 15 and 18
6.1.2-4	Oyster Creek Torus Systems Attached to Ring Girder Number 7
6.1.2-5	Oyster Creek Torus Systems Attached to Ring Girder Numbers 8 and 13
6.1.2-6	Oyster Creek Torus Systems Attached to Ring Girder Numbers 9 and 12
6.1.2-7	Oyster Creek Torus Systems Attached to Ring Girder Number 14
6.1.2-8	Oyster Creek Torus Ring Girder Finite Element Model for Out-of-Plane Loads
6.1.3-1	Torus Mid-bay Saddle Structure
6.1.3-2	Torus Mid-bay Saddle Anchorage
6.1.3-3	Torus Mid-bay Saddle Finite Element Mesh
6.1.4-1	Outside Support Column
6.1.4-2	Inside Support Column
6.1.5-1	Sway Braces
6.2.1-1	Calculation of Stress Intensity in Vent Lines, Vent Header and Downcomers
6.2.2-1	Vent Line/Drywell Intersection
6.2.2-2	Vent Line/Drywell Intersection Finite Element Model
6.2.3-1	Plan View of Oyster Creek Vent Line/Vent Header Intersection
6.2.3-2	Plan View of Mesh for Vent Line/Vent Header Intersection Finite Element Model

LIST OF FIGURES (Continued)

6.2.4-1	Typical Downcomer/Vent Header Intersection and Reinforcement
6.2.4-2	Downcomer/Vent Header Intersection Finite Element Model
6.2.5-1	Torus/Main Vent Line Bellows Expansion Joint
6.2.6-1	Typical Pair of Vent Header Support Columns
6.2.7-1	Finite Element Mesh of Ring Collar Model
6.2.7-2	Ring Collar Sections for Stress Analysis
6.2.8-1	Side View of Vent System Showing Vent Header Deflector
6.2.9-1	Typical Downcomer Brace Configuration
7.2-1	Load Cycles for Evaluation of All Structures Except Downcomer/Vent Header Intersection
7.2-2	Load Cycles for Evaluation of Downcomer/Vent Header Intersection

LIST OF ACRONYMS

ASME	-	American Society of Mechanical Engineers
ASTM	-	American Society for Testing and Materials
BWR	-	boiling water reactor
CMM	-	consistent mass matrix
CO	-	condensation oscillation
CH	-	chugging
DBA	-	design basis accident
DLF	-	dynamic load factor
DW	-	drywell
ECCS	-	emergency core cooling system
EQ(O)	-	operating basis earthquake
EQ(S)	-	safe shutdown earthquake
FDSAR	-	Facility Design and Safety Analysis Report
FSI	-	fluid-structure interaction
FSTF	-	Full-Scale Test Facility
FSRF	-	fatigue strength reduction factor
IBA	-	intermediate break accident
LDR	-	Load Definition Report
LOCA	-	loss-of-coolant accident
LTP	-	Long-Term Program
OBE	-	operating basis earthquake
PRCH	-	pre-chug
PS	-	pool swell
POCH	-	post-chug
PSTF	-	Pressure Suppression Test Facility
PUA	-	plant-unique analysis
PUAAG	-	Plant-Unique Analysis Application Guide
PULD	-	plant-unique load definition
SBA	-	small break accident
SRV	-	safety relief valve
SSE	-	safe shutdown earthquake
STP	-	Short-Term Program

1.0 INTRODUCTION

The Oyster Creek Nuclear Generating Station uses a containment structure for the BWR (Boiling Water Reactor) nuclear steam supply system designated as the Mark I containment system. It is one of 25 power plants in the United States using this early General Electric (GE) containment design.

This report documents the results of a reevaluation of the modified Oyster Creek containment considering the new suppression pool hydrodynamic loads which were defined in the Mark I Containment Long-Term Program. Finite element model analyses of the major torus and vent system structures which were used in this evaluation were performed by Structural Dynamics Technology, Inc., and Nutech. In addition, Structural Dynamics Technology assisted in the preparation of Sections 5.1 and 5.2 of this report. A companion report entitled "Plant Unique Analysis Report - Torus Attached Piping (Reference 8.5.1) covers the evaluation of the Oyster Creek torus attached piping for the same Mark I Containment Long-Term Program loads.

In order to keep this report brief and avoid unnecessary duplication, the contents of the generic Mark I Containment Long-Term Program documents are not repeated. Specifically, it is assumed that the reader has the following documents available and is familiar with their content:

- NUREG-0661. Safety Evaluation Report Mark I Containment Long-Term Program Resolution of Generic Technical Activity A-7. July 1980. (Reference 8.1.2)

- NEDO-21888 (Revision 2). Mark I Containment Program Load Definition Report. November 1981. (Reference 8.2.1)

- NEDO-24583-1. Mark I Containment Program Structural Acceptance Criteria Plant-Unique Analysis Application Guide. October 1979. (Reference 8.2.3)

1.1 BACKGROUND

The original design of the Mark I containment system considered postulated accident loads previously associated with containment design. These included pressure and temperature loads associated with a loss-of-coolant accident (LOCA), seismic loads, dead loads, jet-impingement loads, and hydrostatic loads due to water in the suppression chamber. However, since the establishment of the original design criteria, additional loading conditions which arise in the functioning of the pressure-suppression concept utilized in the Mark I containment system design have been identified. These additional loads result from dynamic effects of drywell air and steam being rapidly forced into the suppression pool (torus) during a postulated LOCA and from suppression pool response to safety relief valve (SRV) operation generally associated with plant transient conditions.

Because these hydrodynamic loads had not been considered in the original design of the Mark I containment, the Nuclear Regulatory Commission (NRC) required that a detailed reevaluation of the Mark I containment system be made. In February and April 1975, the NRC transmitted letters to all utilities owning BWR facilities with the Mark I containment system design, requesting that the owners quantify the hydrodynamic loads and assess the effect of these loads on the containment structure. The February 1975 letters reflected NRC concerns about the dynamic loads from SRV discharges, while the April 1975 letters indicated the need to evaluate the containment response to the newly identified dynamic loads associated with a postulated design basis LOCA.

As a result of these letters from the NRC, and recognizing that the additional evaluation effort would be very similar for all Mark I BWR plants, the affected utilities formed an "ad hoc" Mark I Owners Group, and GE was designated as the Group's lead technical organization. The objectives of the Group were to determine the magnitude and significance

of these dynamic loads as quickly as possible and to identify courses of action needed to resolve any outstanding safety concerns. The Mark I Owners Group divided this task into two programs: a Short-Term Program (STP) and a Long-Term Program (LTP).

1.2 SHORT-TERM PROGRAM

The objectives of the Short-Term Program (STP) were to verify that each Mark I containment system would maintain its integrity and functional capability when subjected to the most probable loads induced by a postulated design basis LOCA, and to verify that the licensed Mark I BWR facilities could continue to operate safely without endangering the health and safety of the public while a methodical, comprehensive Long-Term Program (LTP) was being conducted.

The STP structural acceptance criteria used to evaluate the design of the torus and related structures were based on providing adequate margins of safety; i.e., a safety-to-failure factor of 2, to justify continued operation of the plant before the more detailed results of the LTP were available.

The results of the Short-Term Program evaluation of the Oyster Creek torus were submitted to the NRC by Jersey Central Power and Light letters in 1976 (References 8.3.2 and 8.3.3). As a part of that program, a drywell-to-wetwell differential pressure was imposed to reduce LOCA loads and a quencher was installed on the SRV discharge line to reduce SRV discharge transient induced loads. The conclusion of the Short-Term Program evaluation was that the Oyster Creek torus met the criteria established for the Short-Term Program.

The NRC concluded that a sufficient margin of safety had been demonstrated to assure the functional performance of the containment system and, therefore, any undue risk to the health and safety of the public was precluded. These conclusions were documented in the "Mark I Containment Short-Term Program Safety Evaluation Report," NUREG-0408, dated December 1977 (Reference 8.1.7). The NRC granted the operating Mark I facilities an exemption relating to the structural factor of safety requirements of 10 CFR 50.55(a) for an interim period while the more comprehensive LTP was being conducted.

1.3 LONG-TERM PROGRAM

The objectives of the Long-Term Program (LTP) were to establish conservative design basis loads that are appropriate for the anticipated life of each Mark I BWR facility (40 years), and to restore the originally intended design safety margins for each Mark I containment system. The plans for the LTP and the progress and results of the program were reviewed with the NRC throughout the performance of the program.

The LTP consisted of:

- the definition of loads for suppression pool hydrodynamic events
- the definition of structural assessment techniques
- the performance of a plant-unique analysis (PUA) for each Mark I facility.

The generic aspects of the Mark I Owners Group LTP were completed with the submittal of the "Mark I Containment Program Load Definition Report" (LDR), (Reference 8.2.1) and the "Mark I Containment Program Structural Acceptance Criteria, Plant Unique Analysis Application Guide" (PUAAG), (Reference 8.2.3). The NRC concluded that load definitions and structural acceptance criteria documented in these two reports were acceptable for use in the plant-unique analysis of each plant. The NRC conclusions and comments were presented in the "Mark I Containment Long-Term Program Safety Evaluation Report, NUREG-0661," dated July 1980 (Reference 8.1.2).

1.4 SCOPE OF THIS REPORT

The purpose of this report is to present the Plant-Unique Analysis (PUA) of the Oyster Creek torus and vent system based on the LDR (Reference 8.2.1), PUAAG (Reference 8.2.3), NUREG-0661, and the plant unique load definition report (PULD) provided by General Electric for Oyster Creek (Reference 8.2.2). This PUA covers all the components specified in the PUAAG except for torus attached piping. A separate document (Reference 8.5.1) presents the results of the plant-unique analysis of the piping systems attached to the Oyster Creek torus.

Section 2.0 of this report describes the design criteria used in this evaluation. Section 3.0 describes the structures and their modifications. Section 4.0 defines the loads used in the analyses and Section 5.0 explains the analytical procedures used. The specific stress analyses and results are presented in Sections 6.0 and 7.0. Section 8.0 lists the references. Section 9.0 is an appendix containing plant-unique load definition data for the Oyster Creek plant.

A summary of the results of this report follows.

1.5 SUMMARY OF RESULTS

The analyses of the Oyster Creek torus and vent system has been performed in conformance with the requirements of the Mark I Containment Long-Term Program as prescribed in the LDR (Reference 8.2.1), the PUAAG (Reference 8.2.3), and NUREG-0661 (Reference 8.1.2). The analyses are complete with the exception of the evaluation of the structure for the loads imposed by the safety relief valve discharge piping on the torus ring girders. This evaluation is in progress and will be submitted separately.

A number of structural modifications were designed for installation in the Oyster Creek containment as part of the Long-Term Program; many of these modifications are already installed in the plant. The analyses described in this report are based on the containment with all the modifications installed.

The results of the analyses of the Oyster Creek torus and vent system show that all components of these structures meet the criteria of the Mark I Long-Term Program with the modifications which will be completed as part of this program. Thus, the functional performance of the containment system will be assured for both LOCA and SRV discharge suppression pool hydrodynamic loading conditions. Specific results of the analyses are given in Sections 6.0 and 7.0.

No evaluation of the Oyster Creek drywell was required in the Mark I Containment Long-Term Program, since the maximum drywell pressure specified for Oyster Creek in the Long-Term Program (Reference 8.2.2) is well within the design value specified in the original containment design.

2.0 DESIGN CRITERIA

The criteria for the original design of the torus and vent system and for the design of modifications are contained in this section. In addition, the acceptance criteria and material parameters for the plant-unique analyses are described.

2.1 DESIGN SPECIFICATIONS

2.1.1 Original Design Specification

The specification used for the design of the Oyster Creek torus and vent system was Burns and Roe Specification S-2299-4, "Reactor Drywell and Suppression Chamber Containment Vessels" (Reference 8.6.1). That specification invoked (1) Sections II, VIII and IX of the ASME Boiler and Pressure Vessel Code of 1962 (References 8.4.2, 8.4.3 and 8.4.4) and Nuclear Code Case Interpretations 1270N5, 1271N, and 1272N5 (References 8.4.5, 8.4.6, and 8.4.7) for the vessels, and (2) the Specification for the Design, Fabrication and Erection of Structural Steel of Buildings of the American Institute of Steel Construction (Reference 8.6.2) for the supports and bracing. The original torus structure is an ASME "U" stamped pressure vessel per ASME Section VIII requirements.

The size, arrangement, and geometry of the torus and vent system were specified by the Burns and Roe Specification. In addition, it specified the design conditions and load combinations for the design. These are discussed further in Section 4.1.

2.1.2 Specifications for Modifications to the Torus and Vent System

A GPUN specification was prepared for each modification to the torus and vent system, which specifies functional and design requirements, stress acceptance criteria and quality assurance requirements for the modification. Modification work is performed under the rules of the ASME Boiler and Pressure Vessel Code, Section XI, 1977 Edition (Reference 8.4.8) for the replacement of nuclear components.

The nuclear containment design rules have been used in this report as the basis for the design evaluation of all torus and vent system

components and their modifications as required by the Mark I Long-Term Program in the PUAAG (Reference 8.2.3). Specifically, the ASME B&PV Code requirements of the 1977 Edition with Addenda through Summer 1977 of Section III, Division I, Subsection NE, "Class MC Components for Nuclear Power Plants," and Subsection NF, "Component Supports for Nuclear Power Plants," have been invoked (Reference 8.4.1).

2.2 LONG-TERM PROGRAM STRUCTURAL ACCEPTANCE CRITERIA

The acceptance criteria used for this evaluation are the criteria specified in the PUAAG (Reference 8.2.3) and NUREG-0661 (Reference 8.1.2). The PUAAG specifies allowable stresses to be used in the Mark I Long-Term Program by specifying service limits for each component of the structure for each load combination. The level of stress or strain permitted for each service limit is also specified.

The resulting matrix of components, load combinations, and service limits for the torus and vent system structures are summarized in Table 5-1 of the PUAAG.

2.3 MATERIAL PARAMETERS

The material parameters used in this report in the evaluation of the structures are based on the requirements of the 1977 Edition with Addenda through Summer 1977 of the ASME B&PV Code, Section III, Division I, Subsections NE and NF (Reference 8.4.1). These parameters included Young's modulus, coefficient of thermal expansion, Poisson's ratio, yield strength, and allowable stress. The appropriate values have been used corresponding to the material temperature existing at the time of each loading condition.

The material of the principal structures of the original torus and vent system was steel plate specified as ASME SA-212, Grade B. This material specification has been superseded in the ASME Code applicable for this evaluation (Reference 8.4.1) by ASME SA-516, Grade 70. Therefore, this current specification is used for purposes of defining material parameters.

All modifications use ASME code materials and material properties as specified in Reference 8.4.1. Weld materials comply with ASME Code requirements, thus weld material properties are based on the ASME Code (Reference 8.4.1).

3.0 COMPONENT DESCRIPTIONS

The Mark I containment system is designed to condense the steam released during a postulated LOCA, to limit the release of any fission products associated with the accident, and to serve as a source of water for the emergency core cooling system (ECCS).

The Mark I containment structures consist of: (1) a drywell which encloses the reactor vessel, the reactor coolant recirculation system, and other branch connections of the reactor coolant system; (2) a toroidal-shaped pressure-suppression chamber (torus) approximately half filled with water; and (3) a vent system connecting the drywell to the water space of the torus. Figure 3.0-1 shows a cutaway of the generic Mark I arrangement.

The drywell is a steel pressure vessel, supported in concrete, with a spherical lower section and a cylindrical upper section. The suppression chamber is a steel pressure vessel in the shape of a torus, located below the drywell and encircling it. The Oyster Creek torus is constructed of 20 truncated cylindrical sections welded together at mitered joints. It is mounted on supports which transmit operational, accident, and seismic loads to the concrete foundation of the reactor building.

The drywell and suppression chamber volumes are interconnected by a vent system. Vent lines connect the drywell to a vent header, which is located in the airspace of the suppression chamber. Projecting downward from the vent header are downcomer pipes which terminate below the surface of the pool. There are 10 vent lines and 120 downcomers in the Oyster Creek design.

In the event of a postulated LOCA, reactor water and steam would expand into the drywell atmosphere. As a result of the increasing drywell

pressure, a mixture of drywell atmosphere, steam, and water would be forced through the vent system into the pool of water which is stored in the suppression chamber. The steam vapor would condense in the suppression pool, thereby reducing the drywell pressure. Noncondensible gases and fission products would be collected and contained in the suppression chamber. Initially, the drywell atmosphere is transferred to the suppression chamber and pressurizes the chamber. At the end of the blowdown, when ECCS water spills out of the break and rapidly reduces the drywell pressure, the suppression chamber is vented to the drywell through installed vacuum breakers to equalize the pressure between the two vessels. The ECCS cools the reactor core and transports the heat to the water in the suppression chamber. Cooling systems are provided to remove heat from the water in the suppression chamber, thus providing a continuous path for the removal of decay heat from the primary system.

The scope of this report includes the evaluation of the torus and its supports, the vent system, and structures inside the torus. Each of these structures is described in the sections below.

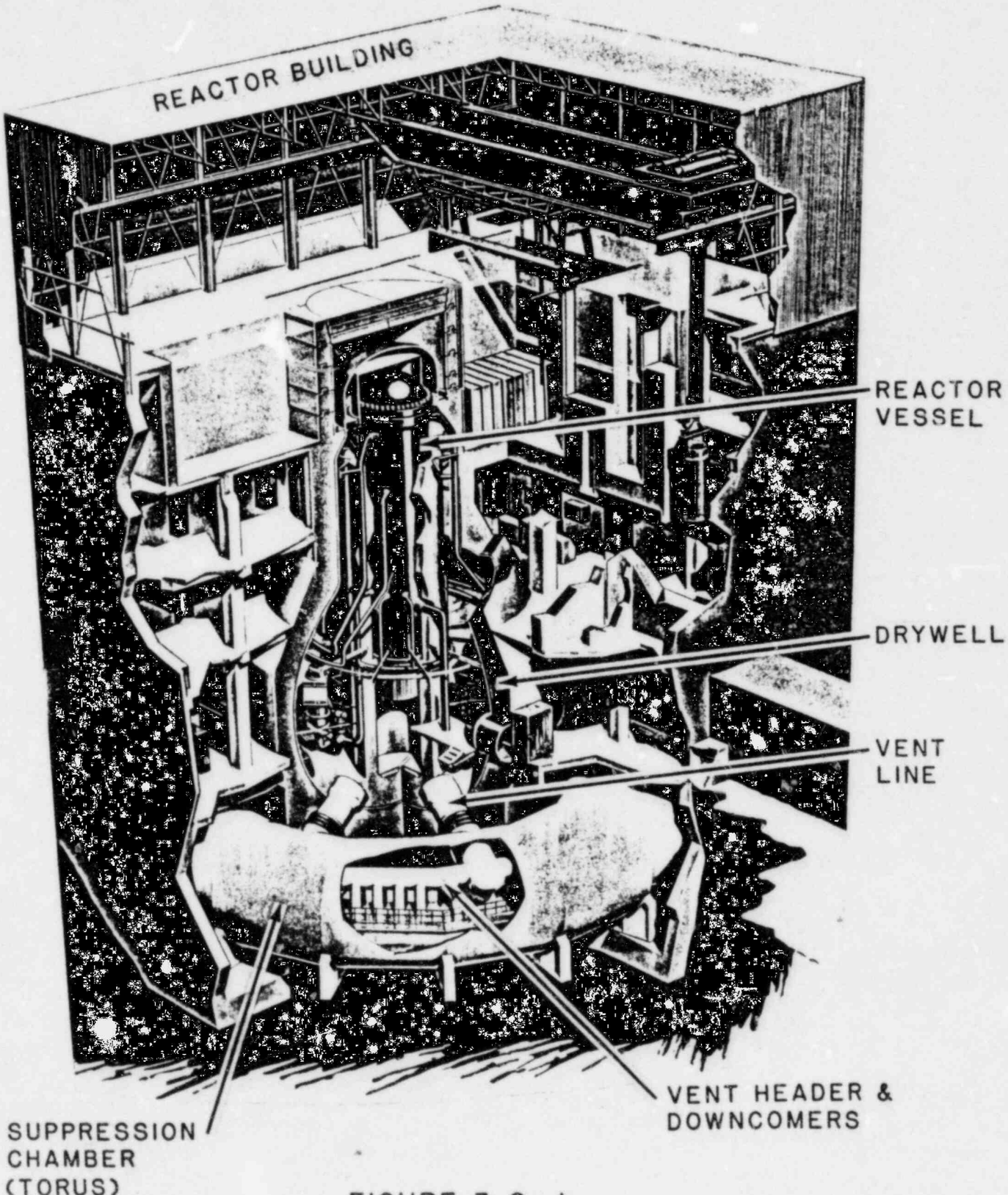

FIGURE 3.0-1

GENERIC
MARK I CONTAINMENT

3.1 SUPPRESSION CHAMBER (TORUS)

General Description

The Oyster Creek torus consists of twenty mitered cylindrical shell segments (bays) as shown in the plan view in Figure 3.1-1. The individual segments are welded together at their intersections. At each of these intersections, the torus is stiffened with an internal "T" shaped ring girder as shown in Figure 3.1-2. Each ring girder is supported by an inner and outer support column resting on the concrete foundation (Figures 3.1-1 and 3.1-2). The torus is also supported by saddles which are located at the middle of each bay of the torus as shown in Figure 3.1-3. These saddle supports were added as part of the Mark I Long-Term Program.

The support columns and saddles are bolted to the concrete foundation to permit them to resist downloads and uploads. Torus lateral displacement radially outward, principally due to thermal growth of the torus, is permitted by pivoting of the columns on pinned joints and sliding of the saddles on Lubrite pads.

Net lateral forces on the torus (such as lateral seismic loads) are resisted by sway braces which are attached to the outer column attachment points on each torus bay as shown in Figure 3.1-4.

Component Descriptions

The torus shell has a major diameter of 101 feet and cross-sectional diameter of 30 feet. The shell thickness is 0.385 inches and is reinforced at penetrations for piping and access hatches. The lower half of the shell is reinforced by eight external straps in each bay as shown in Figures 3.1-4 and 3.1-5. These reinforcing straps have been

added as part of the Mark I Long-Term Program. The straps are 1.25 inches thick and 16 inches wide and are welded continuously to the shell. Four of the straps in each bay extend several feet above the centerline on each side of the torus. As a result of the mitered shape of each bay and the existing reinforcement at the outer support columns, the other four straps in each bay are partial straps extending from the mitered joint to the support column attachment.

The ring girders are constructed of welded plate and the web and flange are one inch thick. The outer support columns are constructed of 10-inch Schedule 120 pipe. They are pinned at the bottom. The inner support columns are constructed of plate material and are pinned top and bottom. They have an "H" cross-section with a 1.25-inch thick flange and 2.75-inch thick web. The support plates for all columns are anchored to the concrete foundation with pre-placed anchors installed at the time of plant construction.

The mid-bay saddle supports, which are being added as part of the Mark I Long-Term Program, are constructed of plate material forming an "H" cross-section; the web and flange are 1.5 inches thick. The saddle is welded continuously to the torus shell. Each saddle rests on, and is bolted to, two base plates which are covered with Lubrite pads. Slotted bolt holes in the saddle permit the saddle to slide for thermal expansion of the torus. The base plates are attached to the concrete foundation with imbedded anchors.

The sway braces are 8-inch, standard schedule pipe and are attached to the upper column attachment plate with bolting and to the lower column base plate with a pinned connection. At the intersection of each pair of sway braces, one brace is slotted and the other brace has the pipe section replaced by a short length of plate which fits through the slot in the first pipe.

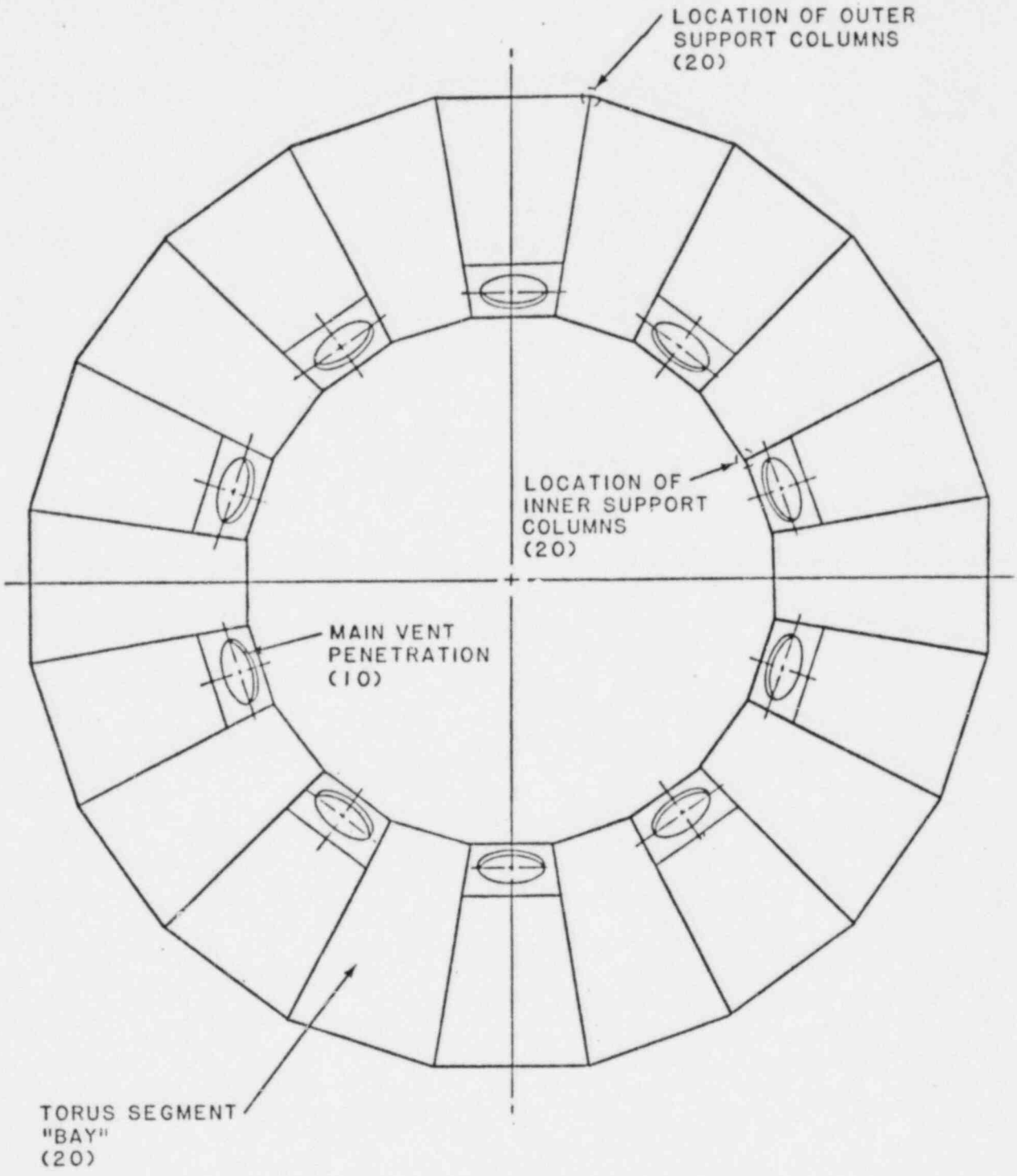

FIGURE 3.1-1

OYSTER CREEK TORUS
PLAN VIEW

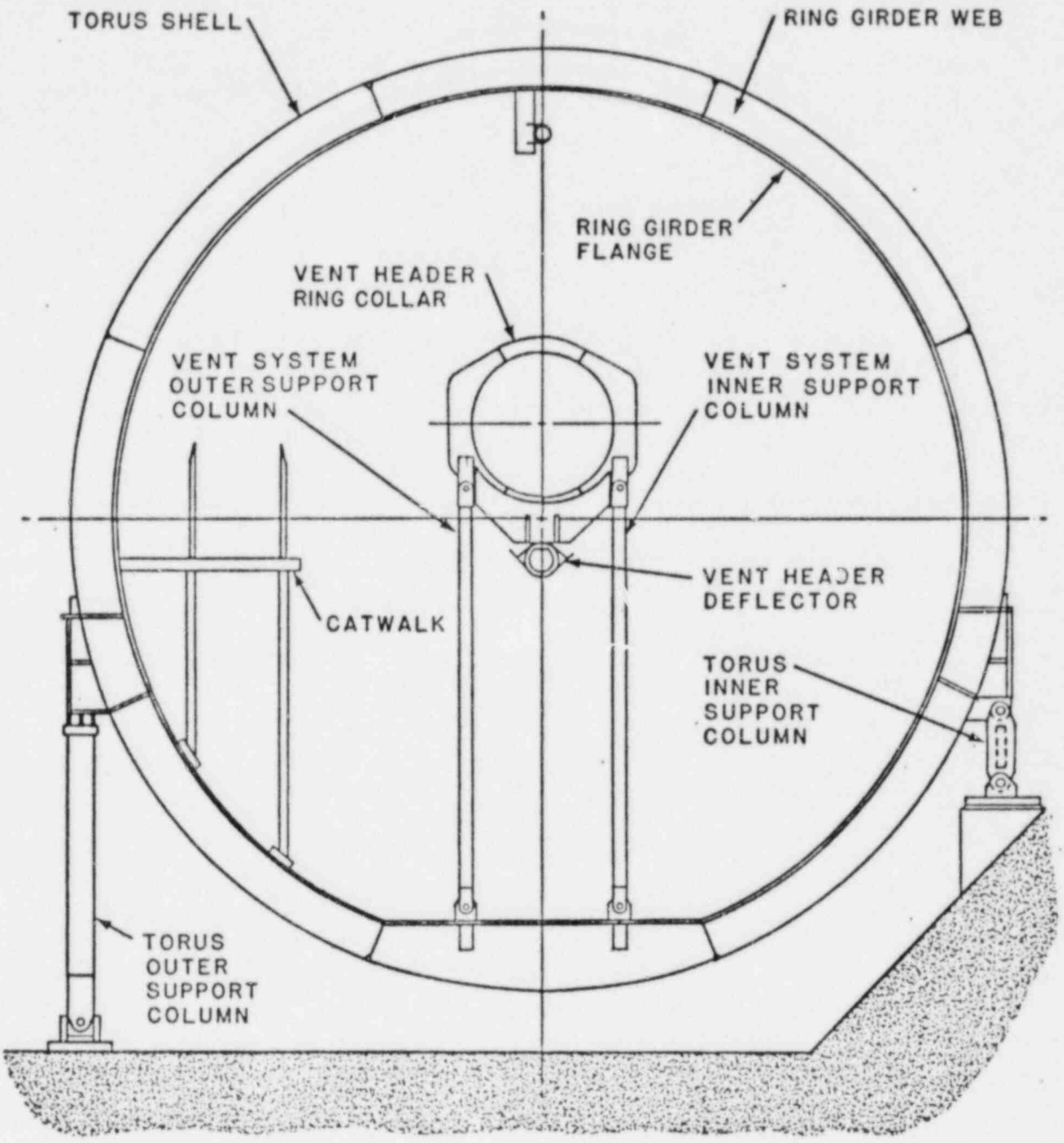

FIGURE 3.1-2

OYSTER CREEK TORUS
CROSS-SECTION AT RING GIRDER

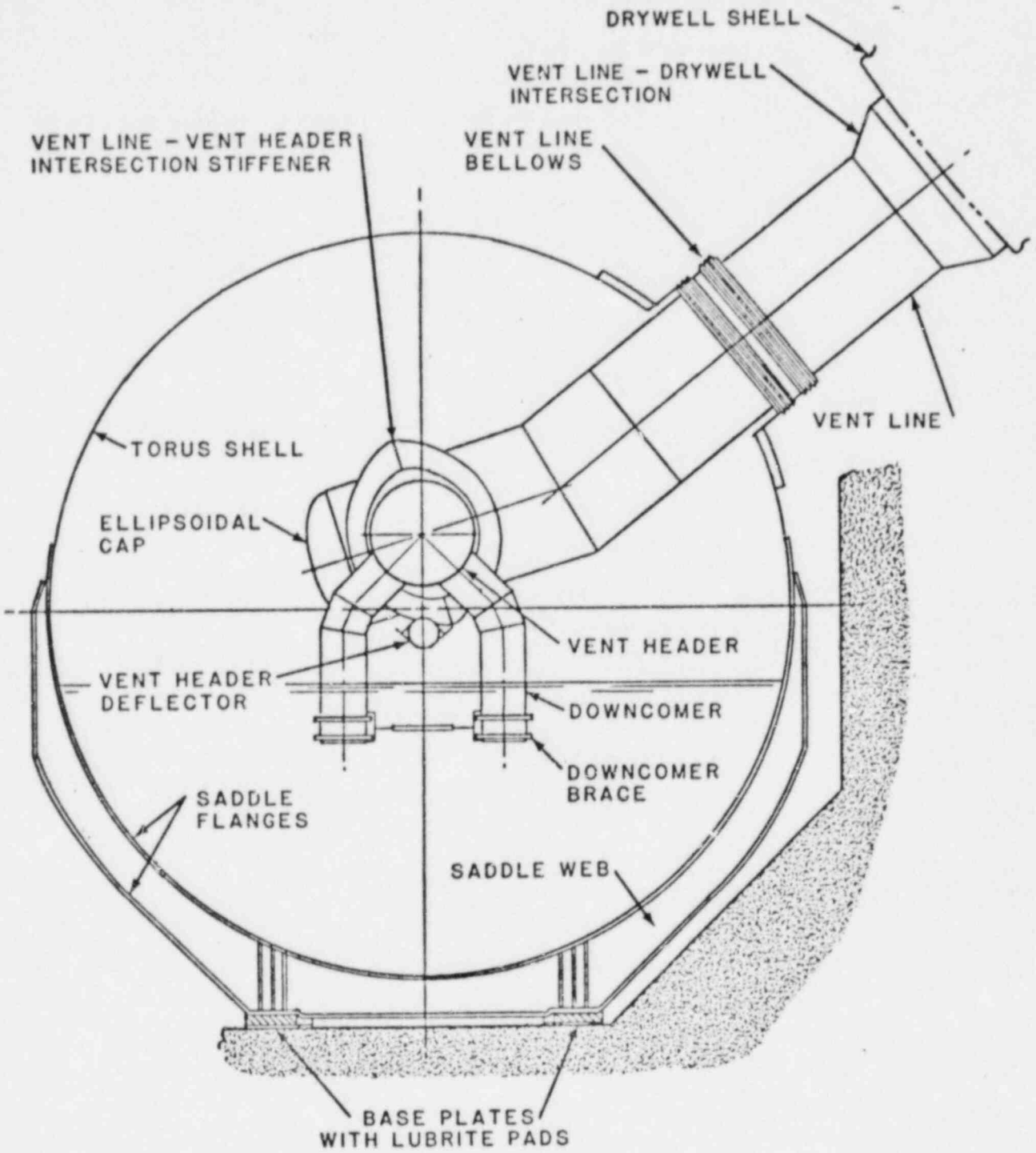

FIGURE 3.1-3

OYSTER CREEK TORUS
CROSS-SECTION AT SADDLE AND MAIN VENT

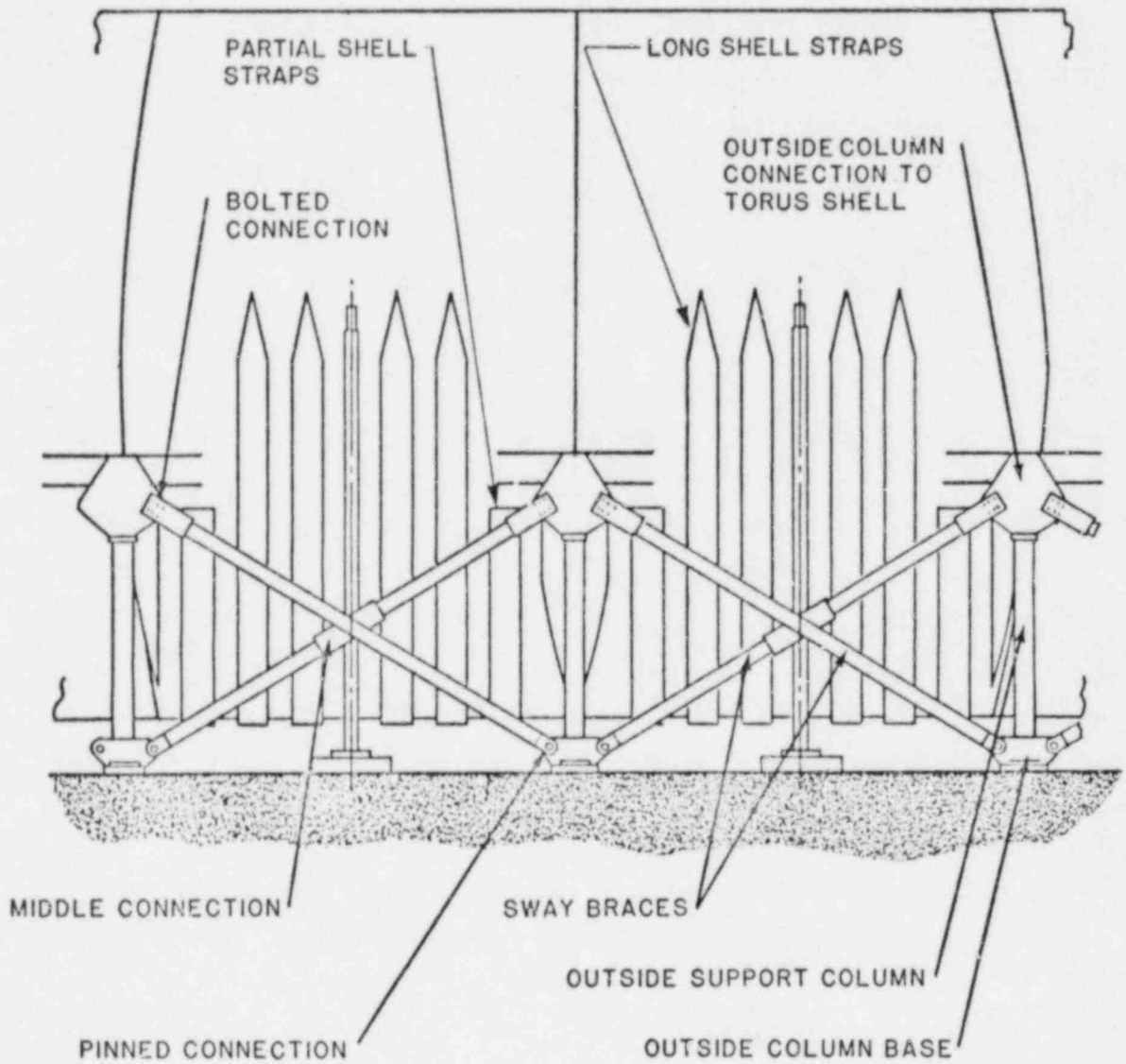

FIGURE 3.1-4
OYSTER CREEK TORUS
SWAY BRACES

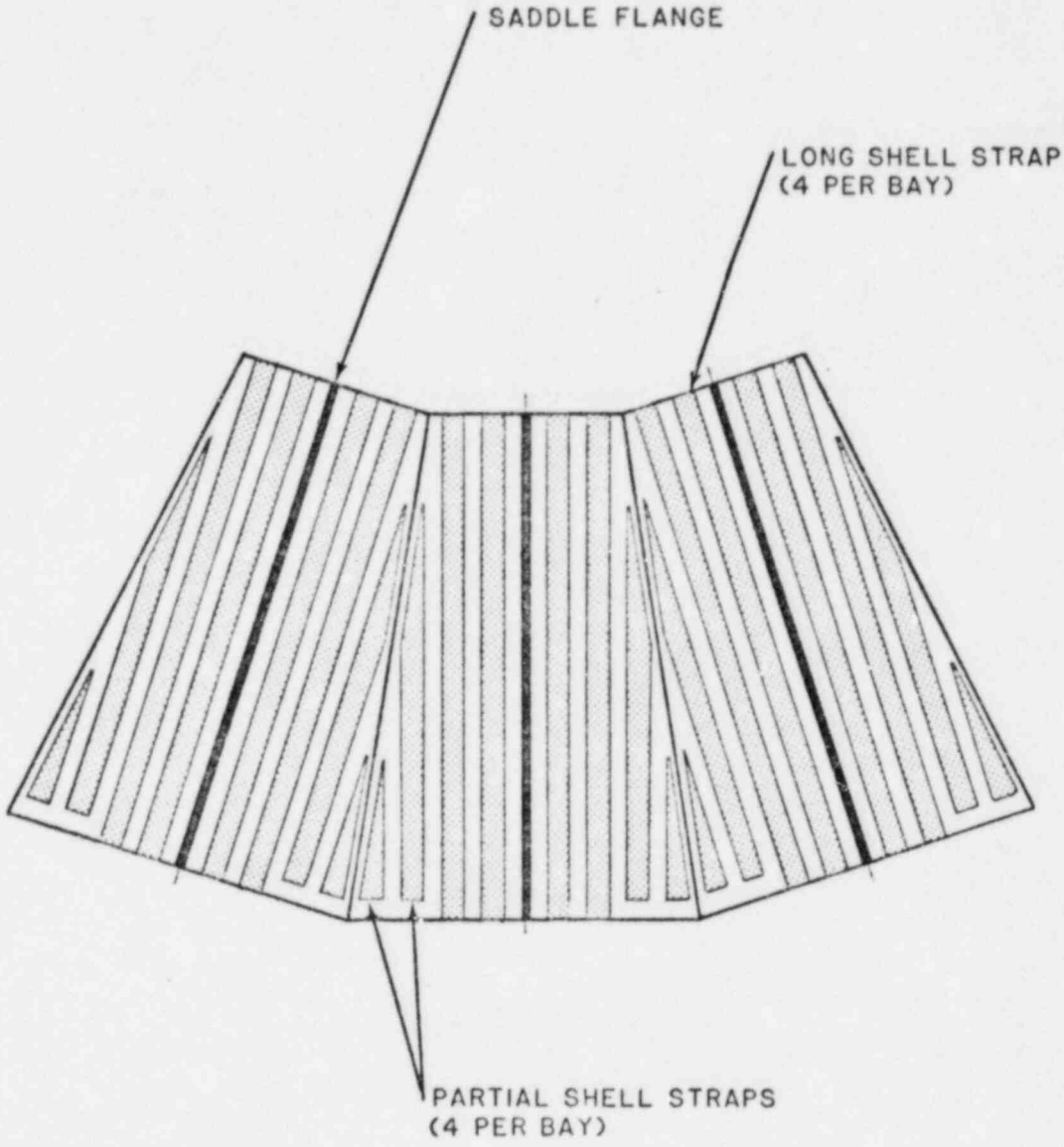

FIGURE 3.1-5

OYSTER CREEK TORUS
VIEW FROM BELOW
SHOWING SHELL STRAPS

3.2 VENT SYSTEM

General Description

The vent system consists of ten vent lines which connect the drywell to the vent header as shown in Figures 3.2-1 and 3.2-2. Figure 3.2-2 also shows the bellows which seal the gap between the vent line and the torus shell while permitting relative motion between the drywell and the torus. One hundred and twenty downcomers (60 pairs) are attached to the vent header and terminate under water. These are also shown on the figures mentioned above. A downcomer brace is located at the lower end of each pair of downcomers (Figure 3.2-2). A strengthened brace has been installed as part of the Mark I Long-Term Program.

At each torus ring girder location, the vent header has a ring collar which is supported by two support columns which in turn are attached to the ring girder (Figure 3.2-3). A vent deflector is installed below the vent header for the entire length of the vent header (i.e., in every torus bay). This deflector was added as part of the Mark I Long-Term Program to shield the vent header from the surge of torus water which could occur as the result of a design basis accident.

Component Description

The vent lines are 78-inch diameter pipes with 0.25-inch thick walls. They are structurally continuous from the drywell to the vent header. Each is connected to the drywell at a reinforced penetration in the drywell shell. The intersections at the vent header are crosses reinforced with stiffener plates and closed with ellipsoidal caps as shown in Figures 3.2-2 and 3.2-1. There is a miter bend in each vent line as shown in Figure 3.2-2. The wall thickness of the vent line is increased to 0.3125 inches at this miter bend.

The vent line is made free to move independently of the torus shell by providing a gap at the snell penetration. The gap is sealed by a universal bellows expansion joint located outside the torus and welded to the torus shell at one end and the vent line at the other (Figure 3.2-2). It consists of two formed, stainless steel bellows (each with five convolutions) connected by a short cylindrical pipe section.

The vent header is a 55-inch diameter pipe with a 0.25-inch thick wall. It is made of straight sections welded together at mitered connections similar to the torus shell geometry (Figures 3.2-1 and 3.2-2).

The sixty pairs of downcomers are distributed on the vent header as shown in Figure 3.2-1. The arrangement of each pair is shown on Figure 3.2-2. Each downcomer is a 24-inch diameter pipe. The downcomer segment nearest the vent header is 0.5 inches thick and the remainder is 0.25 inches thick. The three segments of each downcomer are connected by mitered welded joints. Each of the downcomers was modified to reduce its submergence as part of the Mark I Long-Term Program. This reduced submergence results in lower LOCA loads. The modified downcomer submergence is 4.06 feet at the maximum permissible water level; the minimum submergence is 3.0 feet.

The connection between each downcomer and the vent header is stressed by various loads on the downcomer and vent header and has been reinforced by the addition of a 1.0-inch thick internal reinforcing pad as a part of the Mark I Long-Term Program. A separate pad is placed on the vent header to support each pair of downcomers (i.e., 60 pads total). This reinforcement is described in Subsection 6.2.4 of this report.

The downcomer bracing consists of two heavy clamps attached to each downcomer and a pipe section connecting the clamps on each pair of downcomers (Figure 3.2-2). This stronger bracing system has replaced the original design as part of the Mark I Long-Term Program.

The vent header ring collars are 0.75-inch thick flat plates welded to the vent header. The vent system support columns are pinned to weldments which are attached to the ring collar and are also pinned to attachments on the ring girder (Figure 3.2-3). The original columns have been replaced by 5-inch diameter solid bars and the attachments at each end have been reinforced as part of the Mark I Long-Term Program.

A vent header deflector has been installed in every torus bay at Oyster Creek as part of the Mark I Long-Term Program. It consists of 16-inch diameter, Schedule 120 pipe, with two welded "T" sections as shown in Figure 3.2-3. Each length of deflector spans a bay and is supported at each end by an attachment which is welded to the vent header ring collar.

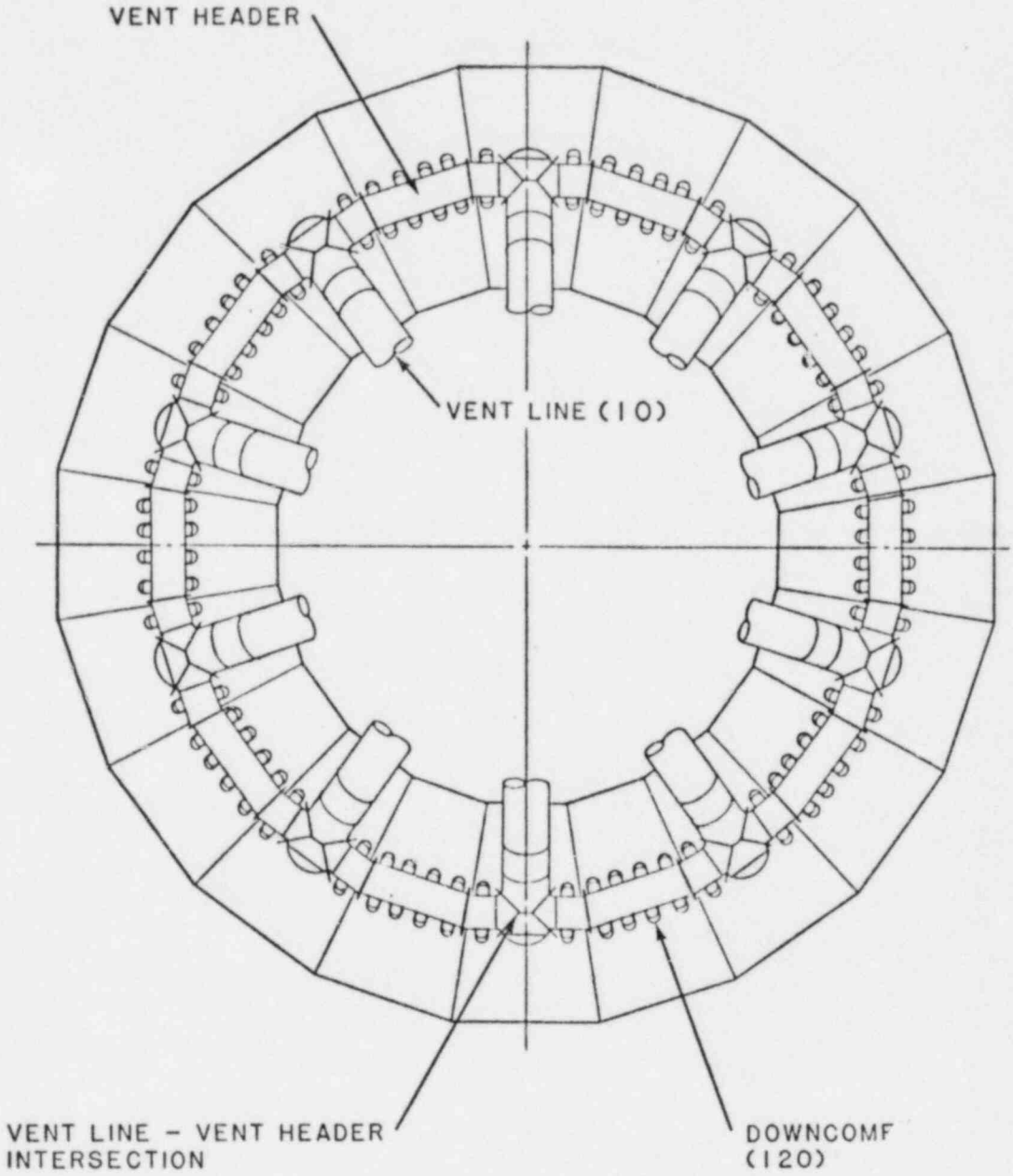

FIGURE 3.2-1

OYSTER CREEK TORUS
VENT SYSTEM
PLAN VIEW

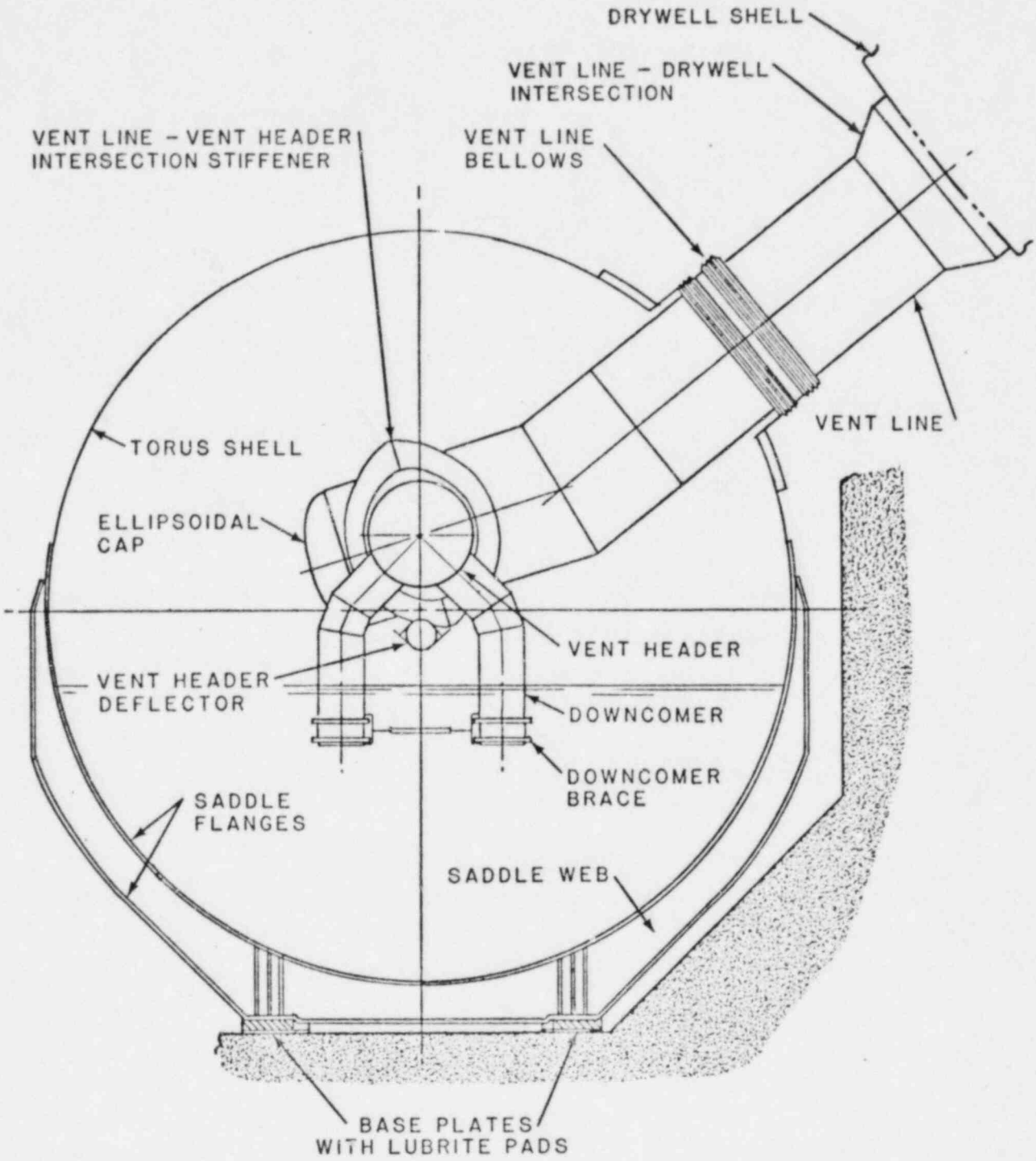

FIGURE 3.2-2

OYSTER CREEK TORUS
CROSS-SECTION AT SADDLE AND MAIN VENT

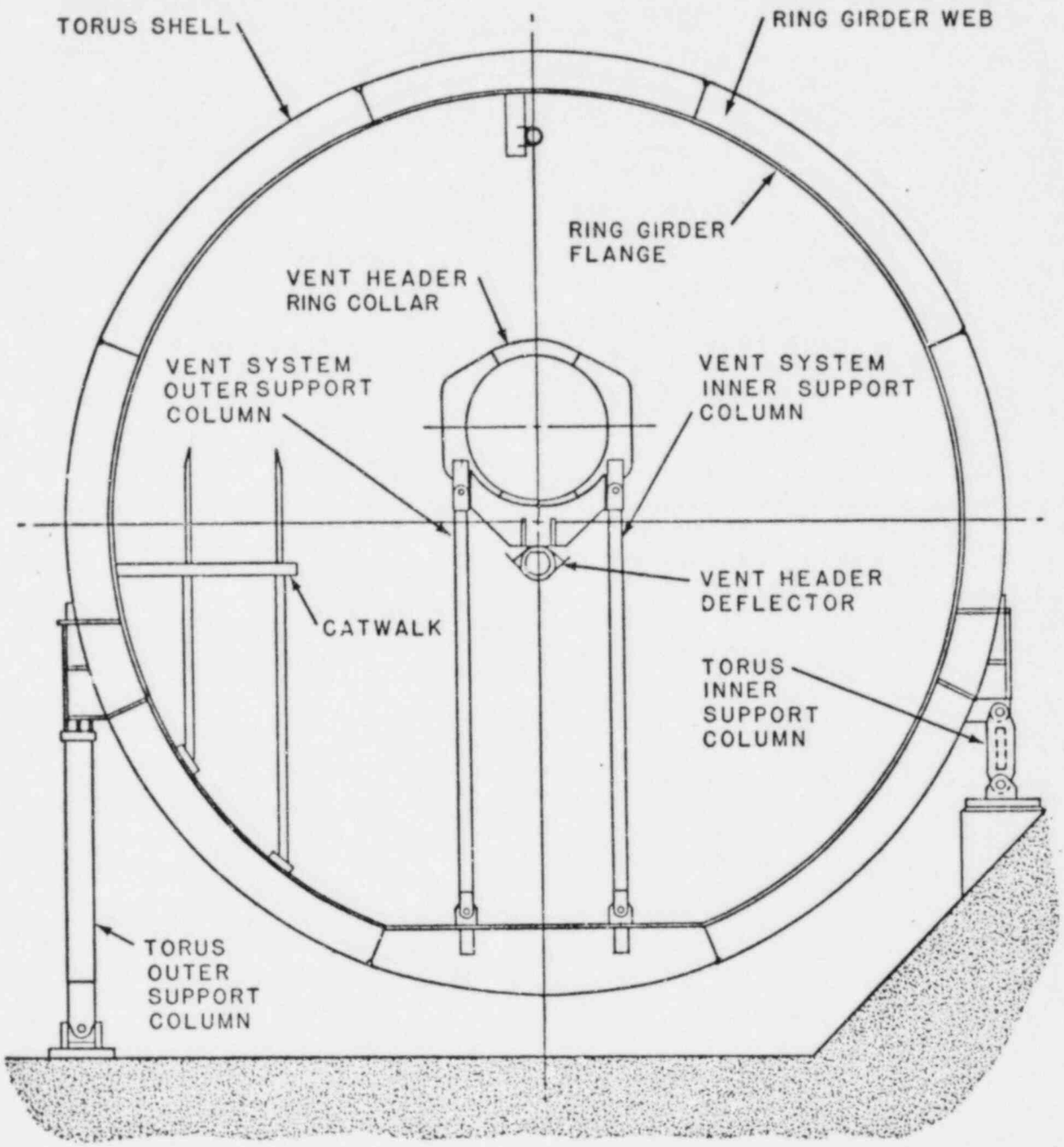

FIGURE 3.2-3

OYSTER CREEK TORUS
CROSS-SECTION AT RING GIRDER

3.3 INTERNAL STRUCTURES

The original Oyster Creek torus design contained several internal structures (other than the torus and vent system components themselves, which are described above) which were subject to hydrodynamic loads. Most of these have been removed. For example, the baffles and catwalk ladders have been removed. The one structure remaining in place is the catwalk.

The catwalk provides a continuous walkway in every bay of the torus. It consists of a walkway grating attached to a framework which is supported at each ring girder (Figure 3.2-3). Additional support columns and reinforcement were added to the catwalk supports and hand rails as part of the Mark I Long-Term Program to strengthen the catwalk.

There are, in addition, several piping systems which have piping runs internal to the torus. These include the containment spray system torus spray line, suction strainers, demineralizer relief valve discharge line, and SRV discharge line. Loads are defined on these piping runs just as on other torus internal structures (Section 4.0). The analyses of these piping systems are described in the Oyster Creek Mark I Containment Long-Term Program Report on piping (Reference 8.5.1).

4.0 LOAD DEFINITIONS

Many diverse loads on the Oyster Creek containment are considered in this Mark I Long-Term Program evaluation. The specific loads used are defined in this section. The response of the structures to each load has been analyzed; the results of these analyses are discussed in Sections 6.0 and 7.0.

The loads used in this evaluation are derived from the requirements of the LDR (Reference 8.2.1), the PULD (Reference 8.2.2), and NUREG-0661 (Reference 8.1.2). Pertinent data from the Oyster Creek PULD are contained in the Appendix in Section 9.0. The sources of the load definitions vary. For example, in some cases, the loads are defined generically by GE in the LDR for all Mark I containments (e.g., chugging loads). Some loads are defined specifically for Oyster Creek in the PULD (e.g., pool swell loads). Some SRV discharge loads are based on data obtained during in-plant tests at Oyster Creek. In each case, the loads used comply with the requirements of NUREG-0661.

For purposes of this discussion, the loads have been divided into several groups. Specifically,

- Original design loads
- LOCA containment pressure and temperature
- LOCA loads on the torus shell
- LOCA loads on the vent system
- LOCA loads on internal structures
- Safety relief valve induced loads on the SRV piping, the torus shell, and internal structures

The source of the load definition and any plant-unique considerations are identified in the following subsections for each load. The requirements for combining these individual loads for purposes of structural assessment are described in Section 2.2.

In the description of the loads, the structures to which they have been directly applied are identified. The structural analyses account for the effects of each load on any additional structures to which the loaded structure is attached.

4.1 ORIGINAL DESIGN LOADS

The original design requirements for the Oyster Creek torus and vent system are contained in Burns and Roe Specification S-2299-4 (Reference 8.8.1) and the Oyster Creek FDSAR (Reference 8.2.4). These documents specified a number of design loads, however they did not address all the hydrodynamic loads which have been developed as part of the Mark I Containment Long-Term Program.

The specific loads specified in the Burns and Roe specification which are applicable to the Mark I Containment Long-Term Program are the following:

- Dead load of structure
- Dead load of water
- Earthquake load

The dead load of the structure and water used in this analysis includes the weight of the modifications which have been made. The high water level limit of 92,000 ft^3 in the torus (12.88 feet) is used.

The earthquake ground spectrum used is the same as that specified in the FDSAR. The calculation of the torus response in this analysis accounts for water sloshing loads. The resulting accelerations on total deadweight loads to account for operating basis earthquake (OBE) seismic loads are:

Structure:	0.22g lateral 0.10g vertical
Water:	0.16g lateral 0.16g vertical

Accelerations for the safe shutdown earthquake (SSE) are twice the values for the OBE.

4.2 LOCA CONTAINMENT PRESSURE AND TEMPERATURE

The containment pressure and temperature response during a LOCA is described in Section 4.1 of the LDR (Reference 8.2.1). The pressures and temperatures used in this analysis for the accident conditions were obtained from the Oyster Creek PULD provided by GE (Reference 8.2.2). Since the Oyster Creek plant will operate with no differential pressure between the drywell and wetwell, the values used are those for the OΔP conditions (0 psi between drywell and wetwell).

The curves of pressure and temperature used were for the plant conditions resulting in the most severe loads. Specifically, for each LOCA break size, the data used were as follows:

- Design Basis Accident (DBA) - PULD Figures O.C.4.1.1-1b and -2b. These figures are for maximum downcomer submergence (4.06 feet) and average pool temperature (77.5^{o}F). The maximum torus pressure and temperature from these figures are 25.4 psig and 115.5^{o}F. In the analysis this pressure is increased by 1 psi up to 30 seconds after the DBA and by 2 psi after that time to adjust for initial pool temperature as required by NUREG-0661 (Reference 8.1.2).

- Intermediate Break Accident (IBA) - PULD Figures O.C. 4.1.2-1a and -2a. These figures are for maximum downcomer submergence (4.06 feet) and maximum pool temperature (95^{o}F). The maximum torus pressure and temperature from these figures are 27.1 psig and 154^{o}F.

- Small Break Accident (SBA) - PULD Figures O.C.4.1.3-1a and -2a. These figures are for maximum downcomer submergence (4.06 feet) and maximum pool temperature (95°F). The maximum torus pressure and temperature from these figures are 25.4 psig and 141°F.

For load combinations, the pressure and temperature from the above figures at the appropriate point in time in each LOCA was used. For example, pressures early in a DBA combine with pool swell loads while pressures late in a DBA combine with chugging loads. The timing of the various loads was based on the requirements in the LDR (Reference 8.2.1). In some cases, for calculational convenience, a bounding value of pressure or temperature was used in the structural analysis to cover the entire transient.

4.3 LOCA LOADS ON THE TORUS SHELL

During the course of a LOCA several types of loads are imposed on the torus shell. These have been defined as pool swell, condensation oscillation, and chugging. Each of these phenomena is described in the LDR (Reference 8.2.1). The load definitions used in this analysis for each of these loads are described in the following subsections.

4.3.1 Pool Swell

The pool swell loads occur as the result of a DBA. As explained in the LDR, the pool swell shell loads are defined for the Oyster Creek plant based on plant-unique tests. The resulting load definitions were provided by GE in the Oyster Creek PULD (Reference 8.2.2).

The specific PULD data used in this analysis were for the following plant conditions:

- Maximum downcomer submergence (4.06 feet), 0ΔP - Table O.C.4.3.1-1
- Minimum downcomer submergence (3.0 feet), 0ΔP - Table O.C.4.3.1-2a

The maximum submergence case results in the highest loads on the shell. The minimum submergence case was also evaluated, since this condition results in the highest total vent system impact loads, and the impact loads and shell loads are coupled through the vent system support columns.

The PULD pool swell shell load definition includes time history data for torus net vertical loads, average submerged pressure, and airspace pressure. To obtain pressure time histories for each point on the shell, longitudinal and azimuthal multipliers were used as described in the LDR (Reference 8.2.1).

The resulting dynamic pressure time histories were increased as required by the NRC in NUREG-0661 (Reference 8.1.2) to account for statistical variance and three dimensional effects. In addition, the 0ΔP loads were further increased to account for the larger statistical variance associated with the smaller number of tests at 0ΔP conditions.

4.3.2 Condensation Oscillation

Condensation oscillation loads on the torus shell occur during a DBA or IBA. The DBA condensation oscillation (CO) loads are discussed in this subsection. The IBA condensation oscillation (CO) loads are defined in the LDR (Reference 8.2.1) to be the same as pre-chug loads, which are discussed in Subsection 4.3.3, below.

The DBA CO shell load definition in the LDR was used in this analysis. Load definition Alternate 2 was found to produce the maximum total response, so it was used. The Oyster Creek plant-unique multiplication factor of 1.0 for pool-to-vent area ratio was used in the analysis.

The DBA CO load definition consists of harmonic loads specified at 1 Hz intervals. The responses to each load were calculated and summed to obtain the total responses. A random phasing methodology which was developed generically for the Mark I owners was used to perform this summation. This methodology was verified by showing that it bounded the test data from the full-scale test facility (FSTF). Specifically, the summation procedure involves adding the individual harmonic responses assuming random phase angles and multiplying the results by 1.3 for shell stress and strain values and by 1.15 for other responses.

4.3.3 Chugging

Chugging loads on the torus shell occur during a DBA, IBA, and SBA when the steam flow rate through the downcomers falls below a certain critical rate. The chugging shell load definition in the LDR (Reference 8.2.1) was used in this analysis.

As described in the LDR, the chugging load definition is divided into a pre-chug load and a post-chug load. The pre-chug load is a single harmonic load which is required to be applied at the frequency in the range of 6.9 to 9.5 Hz which produces the maximum response. For Oyster Creek this frequency is 9.5 Hz.

The post-chug load is defined in the LDR as 50 separate harmonic loads. Analysis showed the contribution of harmonics above 30 Hz was small for the Oyster Creek structure, so the final analysis procedure which was used involved absolute summing of individual harmonic responses up to 30 Hz. Subsequently, a generic Mark I study showed that a random phasing procedure could be used for all these harmonics similar to the CO load procedure discussed in Subsection 4.3.2. This study also showed that absolute summation of harmonics is very conservative compared to the random phasing methodology and compared to the FSTF test data. The chugging load cases were not controlling for the Oyster Creek structures, so there was no incentive to perform a reanalysis using the random phase load definition to reduce the chugging load.

The asymmetric pre-chugging shell load distribution specified in the LDR was used in this analysis to obtain the net lateral load on the torus. For conservatism, this load was assumed to be sinusoidal and coincident with the fundamental structural resonance, therefore a dynamic amplification of 25 was used. This value would be considerably smaller if a realistic time history analysis were performed.

4.4 LOCA LOADS ON THE VENT SYSTEM

During a LOCA, several types of loads are applied to the vent system. These loads can be subdivided into pool swell, condensation oscillation, and chugging. Pool swell loads are applicable only to a DBA, condensation oscillation loads are applicable only to a DBA or an IBA, and chugging loads are applicable to a DBA, an IBA or an SBA. Definitions of the individual loads within each of these categories are described in the following subsections. Loads on the vent system support columns and the downcomer braces, which are fluid drag loads, are covered in Section 4.5.

4.4.1 Pool Swell

During a DBA pool swell, the drywell and vent system are rapidly pressurized and air is discharged into the torus, which results in the pool surface being lifted. The pool swell transient and the resulting loads are described in the LDR. The following loads on the vent system were defined for pool swell:

- Internal pressure in vent system components, and the net thrust loads produced by this internal pressure and momentum changes in the flow through the vent system.
- Impact and drag load on the vent header.
- Impact and drag load on the vent header deflector.
- Impact and drag load on the downcomers.
- Impact and drag load on the main vent line.
- Reaction load at the vent line from impact and drag loads on SRV piping.

A brief discussion of the nature and magnitude of these loads is provided below.

Vent system internal pressure and thrust loads for a DBA were determined as described in Section 4.2 of the LDR. The loads are shown in the Oyster Creek PULD (Reference 8.2.2); Figures OC 4.2-12 through OC 4.2-21 (for 3.53-foot downcomer submergence, OΔP between the drywell and wetwell); and Figures OC 4.2-12a through OC 4.2-21a (for 4.06-foot submergence, OΔP). The submergence has a negligible effect on the loads. The thrust loads are defined as point forces at various vent system locations (intersections, miters, etc.). The internal pressure used in vent system pool swell impact load structural evaluations was 11.2 psi (for OΔP), based on Table 4.3.3-1 of the LDR (Reference 8.2.1).

The impact and drag load on the vent header was determined from Oyster Creek plant-unique quarter-scale test data, as described in Section 4.3 of the LDR. This load is shown in the Oyster Creek PULD, Table OC 4.3.3-2 (4.06-foot submergence, OΔP) and Table OC 4.3.3-1b (3.0-foot submergence, OΔP). The load is of the form of pressure time histories at 12 reference locations on the vent header. Pressures at a total of 59 vent header locations in an 18^{o} symmetrical vent system segment were subsequently determined by applying multipliers and time delays, also given in the PULD, to the reference pressures. The net vertical upload at several points along the vent header (which was used, for example, in the vent system beam model pool swell evaluation) was determined by summing the pressures over the external impacted area of the vent header. Finally, a time delay to account for the delay between time of LOCA break and time of initial vent header impact was determined using the plant-unique pool swell displacement curves in the PULD, and incorporated into the load definition.

The impact and drag load on the vent deflector was determined from Oyster Creek plant-unique quarter-scale test data and analytical methods as described in Section 4.3 of the LDR. The load is presented in the Oyster Creek PULD, Figure OC 4.3.9-1 (4.06-foot submergence, OΔP) and Figure OC 4.3.9-1a (3.0-foot submergence, OΔP). The load is presented as a force-per-unit-length time history at three locations: middle of vent bay, miter joint, and middle of non-vent bay. Linear interpolation was used to determine the load at intermediate points.

The impact and drag load on the downcomers was determined from the Mark I generic downcomer load definition presented in Section 4.3.3.2 of the LDR. An 8-psi load applied over the bottom 50^{o} of the downcomer was used for all DBA initial conditions. An adjustment was made to the load on the lower of the two angled sections of the Oyster Creek downcomer to account for the pool striking this section at a lower angle. The time delay between time of break and time of impact was determined using the

plant-unique pool swell displacement curves in the PULD and incorporated in the load definition. The structural response to this load was analyzed dynamically using a structural model which accounted for added water mass around the downcomers.

The impact and drag load on the main vent line was calculated using the plant-unique pool swell displacement and velocity profiles in the PULD, in accordance with Section 4.3.3.2 of the LDR and NUREG-0661. Time history pressures were determined at several vent line locations. Maximum impact pressure spikes of about 49 psi, and maximum steady velocity plus acceleration drag pressures of about 12 psi were determined. The maximum total upload was found to exist for 4.06-foot submergence and 0ΔP initial conditions.

The impact and drag load on the relief valve piping, which is covered in Section 4.5 below, was applied to a structural model of the relief valve line to determine the maximum reaction where this pipe penetrates the main vent line. The maximum load was then used as a static upload for pool swell analyses. This load was calculated to be 9000 lbs for the 4.06-foot submergence, 0ΔP case, which was the worst case.

By reviewing the various vent system pool swell loads described above, it was found that the loads for 0ΔP initially between drywell and wetwell were more severe than the loads for an initial condition with a ΔP. Also, the Oyster Creek plant intends to operate without ΔP in the future. Accordingly, pool swell analyses were performed using only 0ΔP loads; this explains why only these loads are covered in the discussion above.

It was also determined from a review of the vent system loads that the vent header deflector impact and drag load was most severe at 3.0-foot submergence; the vent header, vent line, and SRV line impact and drag loads were most severe at 4.06-foot submergence; and the thrust and

downcomer impact loads were not sensitive to water level. Structural analyses were performed at each submergence to obtain the limiting load combination for each structure.

4.4.2 Condensation Oscillation

Condensation oscillation (CO) occurs when steam is discharged through the vent system into the suppression pool at some critical flow rate. CO occurs during a DBA or an IBA. The following loads on the vent system occur during condensation oscillation.

- Static internal pressure in vent system components and the net thrust loads produced by internal pressure and momentum changes in the flow through the vent system.
- Constrained thermal expansion of the vent system.
- Dynamic internal pressure loads in vent system components.

Each of these is discussed below.

The vent system internal pressure and thrust loads during DBA CO are given in the Oyster Creek PULD on the same figures as mentioned above for DBA Pool Swell. The time span t=5 to 35 seconds on these figures is applicable to DBA CO. Either actual loads at each point in time or worst-case loads during the whole time period were used in structural evaluations. For IBA, the thrust loads and pressures from the DBA curve at t=30 seconds were used, since explicit IBA results were not calculated and the IBA represents a low steam flow condition like t=30 seconds of a DBA. These loads are relatively minor; for example, the internal pressure is about equal to the downcomer submergence water head, or 1.8 psi maximum.

The constrained thermal expansion loads in the vent system during DBA or IBA CO are caused by heat-up of the drywell, vent system and torus as constrained by the torus and drywell supports. The drywell and torus temperatures are given in the Oyster Creek PULD as described in Section 4.2, above. The vent system temperature was taken to be equal to the drywell temperature.

The dynamic vent system internal pressures for DBA and IBA CO are defined in Sections 4.4.3 and 4.4.4 of the LDR. These loads include vent line and vent header pressures which are analyzed quasi-statically to determine hoop response of these components, and downcomer pressures which are analyzed dynamically to determine net loads and stresses at the downcomer/vent header intersection. The downcomer dynamic pressure load consists of two parts: one part which is uniform in all downcomers and one which exists in only one of each pair of downcomers. Three harmonics are required to be considered: a primary harmonic between 4 and 8 Hz, a secondary harmonic between 8 and 16 Hz, and a tertiary harmonic between 12 and 24 Hz. Since the Oyster Creek downcomer sway natural frequency was calculated to be 12 Hz, the loads were applied at 6, 12 and 18 Hz.

4.4.3 Chugging

Chugging occurs when steam is discharged through the vent system into the suppression pool, below some critical flow rate. Chugging occurs during an SBA, IBA, or DBA. The following loads on the vent system occur during chugging:

- Static internal pressure in vent system components and the net thrust loads produced by internal pressure and momentum changes in the flow through the system.
- Constrained thermal expansion of the vent system.
- Dynamic internal pressure in vent system components.
- Point loads at the downcomer tips.

Each of these is discussed below.

The vent system internal pressure and thrust loads during DBA, IBA and SBA chugging are those defined for a DBA at t=30 seconds in the Oyster Creek PULD. According to Section 4.2 of the LDR, DBA thrust loads are constant after t=30 seconds (i.e., the time when chugging occurs), and DBA loads bound SBA and IBA loads. The appropriate figures in the PULD which show these loads are mentioned in Section 4.4.1, above.

The constrained thermal expansion loads in the vent system during SBA, IBA or DBA chugging are determined from the drywell and torus temperatures during these transients. These temperatures are presented in the PULD as described in Section 4.2, above. The vent system temperature was taken to be equal to the drywell temperature.

The dynamic vent system internal pressures for chugging are defined in Section 4.5.4 of the LDR. These loads include vent line, vent header, and downcomer pressures which are analyzed quasi-statically to determine hoop response of these components. Net load effects are covered by the downcomer tip loads, discussed below.

Chugging point loads at the downcomer tips were determined in accordance with Section 4.5.3 of the LDR. This approach utilizes the static equivalent load from FSTF suitably scaled to account for differences in dynamic amplification at Oyster Creek. A factor of 2.0 was determined to account for differences in dynamic amplification. The maximum plant-unique load was calculated to be 6150 lbs, acting in any direction. It was conservatively assumed that this load could act simultaneously on a pair of tied downcomers, in the same direction. A maximum load range of 7950 lbs was also calculated for use in primary plus secondary stress analyses and fatigue analyses. Once again, it was conservatively assumed that this load range could be applied to both of a pair of tied downcomers, in the same direction. Finally, a tip load to be applied in a uniform direction to a large number of downcomers (synchronous chugging net lateral load) was determined. Two cases were considered: all 120 downcomers chugging together, and 12 adjacent downcomers (in a span between two vent lines) chugging together. A load of 1100 lbs per downcomer bounded the results in both cases.

4.5 LOCA LOADS ON INTERNAL STRUCTURES

During the course of a LOCA, several types of loads are imposed on the torus internal structures. These are separated into pool swell loads and condensation oscillation and chugging loads. All of these loads are described in the LDR (Reference 8.2.1). The load definitions used in the analyses of Oyster Creek torus internal structures comply with the LDR and NUREG-0661 (Reference 8.1.2). They are described in the following sections.

4.5.1 Pool Swell

Pool swell loads occur as the result of a design basis accident (DBA). The LDR (Reference 8.2.1) subdivides pool swell loads on internal structures into pool swell impact and drag, froth impingement (Regions I and II), fallback, LOCA jet and LOCA bubble drag loads. The methodology for defining these pool swell loads is defined generically for the Mark I Containment Long-Term Program in the LDR (Reference 8.2.1). This methodology uses as input plant-unique data from the Oyster Creek PULD (Reference 8.2.2). The PULD data used in this methodology were for the following plant conditions:

- Maximum downcomer submergence (4.06 feet), zero differential pressure.
- Minimum downcomer submergence (3.0 feet), zero differential pressure.

The maximum submergence case results in the highest loads for Region II froth impingement, fallback, LOCA jet and LOCA bubble drag. The minimum submergence case results in maximum pool swell impact and drag and Region I froth impingement loads. Peak pool swell loads on Oyster Creek internal structures are summarized in Table 4.5.1-1.

TABLE 4.5.1-1

SUMMARY OF PEAK POOL SWELL LOADS ON OYSTER CREEK TORUS INTERNAL STRUCTURES

STRUCTURE	PEAK APPLIED LOAD (psi)					
	POOL SWELL IMPACT	POOL SWELL DRAG	FROTH IMPINGEMENT	FALLBACK	LOCA JET	LOCA BUBBLE
1. SRV Line and Quencher	34.2	13.0	N/A	4.9	0.54	1.0
2. Vent Header Support Columns	N/A	N/A	N/A	N/A	1.05	2.3
3. Catwalk	112.2	22.2	N/A	5.7	0.3	2.0
4. Demineralizer Discharge Line	N/A	N/A	6.8	N/A	N/A	2.3
5. ECCS Nozzle and Strainer	N/A	N/A	N/A	N/A	0.56	4.4
6. Ring Girder	N/A	N/A	N/A	N/A	N/A	1.7
7. Downcomer Braces	N/A	N/A	N/A	6.4	N/A	1.3
8. Wetwell Spray Line	N/A	N/A	2.75	N/A	N/A	N/A

NOTE:

Table is for comparison only. Values are based on peak load on worst-case structure and worst-case location on structure. Actual loads are defined as time histories as specified in the LDR and NUREG-0661.

4.5.2 Condensation Oscillation and Chugging

During condensation oscillation and chugging, the oscillation and collapse of steam bubbles at the exits of the downcomers induce velocity and acceleration fields in the torus pool. These result in fluid drag loads on internal structures submerged in the pool. The LDR (Reference 8.2.1) establishes a generic methodology for defining condensation oscillation and chugging drag loads on submerged internal structures. The LDR subdivides this load definition into a condensation oscillation load and two chugging loads based on the two distinct chugging phenomena observed during full-scale testing. The chugging loads are distinguished as the pre-chug and the post-chug loads.

The analytical model which is the basis of all three condensation oscillation/chugging drag loads assumes a series of noninteracting spherical bubbles oscillating in a finite pool. Bubble motions are controlled by the Rayleigh bubble equations using a method of images to account for rigid wall effects. Bubble source strengths for CO, pre-chug, and post-chug are based on full-scale tests. In addition, fluid-structure interaction (FSI) which results from the flexibility of the torus walls is accounted for in the load definitions as required by the LDR and NUREG-0661 (Reference 8.1.2).

Drag loads are defined for the following internal structures in the Oyster Creek torus in accordance with the procedures in the LDR and NUREG-0661:

- SRV line and spargers
- Vent header support columns
- Catwalk supports and braces
- Demineralizer discharge line

- ECCS (Emergency core cooling system) nozzles and strainers
- Ring girders
- Downcomer braces

A separate drag load is defined for each of the following cases:

- Condensation oscillation
- Pre-chug
- Post-chug

For each case, the drag load-time history is expressed as two distinct Fourier series. One Fourier series represents load caused by velocity and acceleration fields resulting directly from steam bubble oscillation. The other Fourier series represents loadings caused by the velocity and acceleration fields resulting from torus fluid-structure interaction (FSI).

Each Fourier series load is defined as a set of vector loads on sections of the submerged internal structures for a unit bubble source strength oscillation independent of frequency and a table of bubble source strengths as a function of frequency. The resulting total load is applied to the structures listed above and their dynamic structural response is calculated.

4.6 SAFETY RELIEF VALVE INDUCED LOADS

Oyster Creek is equipped with five relief valves (SRVs) to provide over pressure protection and automatic depressurization for the primary system. The SRVs are mounted on the main steam lines inside the drywell, with discharge pipes routed into the suppression pool in the torus. Two discharge pipes are installed; three valves discharge into the south discharge pipe, and two discharge into the north discharge pipe. Each discharge pipe terminates in a quencher device under the water in the torus. These quenchers are in a "Y" configuration and were installed and successfully tested in 1977 (Reference 8.3.4).

When an SRV is actuated, steam from the primary system is discharged through the discharge line and quencher into the torus water where it is condensed. The water initially in the quencher is discharged first, followed by the air from the discharge line, and then the steam. This section of the report defines the loads which result from this SRV discharge transient at Oyster Creek. These loads are used in the structural evaluation of the torus, its supports and internal structures, and attached piping systems.

The procedures used for defining the SRV discharge loads for Oyster Creek are in accordance with the LDR (Reference 8.2.1) and NUREG-0661 (Reference 8.1.2). The load definition is based, in part, on in-plant tests which were performed at Oyster Creek as a part of the load definition effort. This approach is in accordance with NUREG-0661 (Reference 8.1.2).

As a result of the excellent performance of the Y-quencher at Oyster Creek, the SRV discharge loads on the torus are relatively small. Consequently, it was possible to use a simple, bounding methodology, based on test data, to define the loads on the torus shell. Analysis

procedures, provided in the LDR (Reference 8.2.1) and approved in NUREG-0661 (Reference 8.1.2), were used to extrapolate shell loads from test conditions to the various design conditions and to define other SRV discharge loads, such as thrust loads on SRV piping and underwater drag loads. These procedures were verified for applicability to the Oyster Creek installation by the successful comparison of calculated predictions with in-plant test data. The definition of the loads caused by the various SRV discharge transients is discussed in the following subsections in three categories, as follows:

- SRV Discharge Loads on the SRV Discharge Piping
- SRV Discharge Loads on the Torus Shell
- SRV Discharge Loads on Torus Internal Structures

4.6.1 SRV Discharge Loads on the SRV Discharge Piping

SRV discharge loads on the SRV discharge piping are caused by transient and steady-state steam and water thrust loads. These loads are calculated for Oyster Creek using the procedures in the LDR (Reference 8.2.1) in accordance with NUREG-0661 (Reference 8.1.2). The methodology used to calculate these loads is discussed below.

4.6.1.1 SRV Discharge Steam Thrust Loads on the SRV Discharge Piping

Actuation of a safety relief valve (SRV) causes the discharge piping to pressurize rapidly. The steam flowing into the discharge line forms a shock wave that travels down the pipe to the water surface and is reflected back. The pressure difference across the shock wave can be large and cause large impulse loadings on straight segments of pipe between elbows and at area changes. The high transient thrust loads exist only as the shock wave travels through the pipe segment with the high pressure behind the wave unbalanced by the lower pressure in front of the wave. As the pressure at the water surface in the piping increases, the water slug in the bottom of the discharge pipe is accelerated until the slug is completely expelled from the pipe. At that time, the pipe depressurizes to a steady-state pressure and steam discharge flow rate. The discharge piping may then experience thrust loads from both the depressurization shock wave moving up the pipe, similar to the initial pressurization wave, and from the steady-state steam flow down the pipe.

This section presents the method used to analyze the thrust loads on the Oyster Creek SRV discharge piping caused by transient and steady-state steam flow during an SRV actuation. The results of these analyses are also presented.

1. Method

The LDR (Reference 8.2.1) procedure for computing transient steam thrust loads on an SRV discharge line was used for Oyster Creek. Adjustments were made to the procedure to account for two variations specific to the Oyster Creek plant. These are:

- Oyster Creek is designed with two or three SRVs discharging to a common header. The LDR procedure assumes one SRV per discharge line.
- Oyster Creek is equipped with Y-quenchers. The LDR procedure assumes a ramshead or GE T-quencher discharge device.

The LDR procedure for defining steam thrust loads on the SRV discharge lines was implemented as follows to define loads on the Oyster Creek SRV discharge piping:

- To Account for Multiple SRVs in a Single Discharge Line

  The Oyster Creek discharge lines have branches running from each SRV to a common header. To calculate thrust loads on each branch line, the LDR analytical model is applied to the branch line and the common header ignoring all other branch lines to the header. To calculate thrust loads on the common header, the branch lines are analytically combined into a single, equivalent line and the calculation repeated. This equivalent line has the correct equivalent volume, flow resistance, and mass flow rate. For conservatism, the line length is set equal to the length of the shortest branch included in the equivalent line. This minimizes sonic transport times and line losses. The adequacy of this approach to model SRV discharge lines was confirmed by comparing results of the analytical model with test data from the in-plant tests as discussed below.

- To Account for Differences Between the GE T-Quencher and the Oyster Creek Y-Quencher

For steam thrust load calculations, the configuration of the discharge fitting has little influence. The large transient steam thrust loads are more a function of the gas space properties and the transmission of sonic shock waves than of the discharge device geometry. Steady-state steam thrust and peak pipe pressures do depend on sparger geometry and properties, specifically flow resistance, but only weakly. Based on the comparisons of the generic analytical model with in-plant test data discussed below, the Oyster Creek SRV discharge piping thrust loads can be calculated using the generic analytical model assuming a T-quencher discharge device.

2. Test Data Comparison

The results of the generic analytical model applied to the Oyster Creek SRV discharge piping were compared to in-plant SRV test data for various SRV actuation conditions. The comparisons show that the analytical model conservatively predicts discharge line pressure for a variety of initial conditions. Figure 4.6.1-1 is an example of the comparisons performed. It shows the comparison of model calculations to test data for the base case SRV test (simultaneous two-valve, first actuation).

3. Results

As discussed in the LDR (Reference 8.2.1), application of the generic analytical model results in a set of load-time histories on each straight line segment of the SRV piping. The piping segments for which steam thrust loads are defined for

Oyster Creek are shown in Figures 4.6.1-2 and 4.6.1-3. Peak transient thrust loads for each segment are tabulated in Table 4.6.1-1.

4.6.1.2 SRV Discharge Water Thrust Loads on the Y-Quencher

Actuation of an SRV causes the discharge piping to pressurize rapidly. As the pressure increases, the water slug in the bottom of the discharge line is accelerated until the slug is completely expelled from the pipe. The acceleration and redirection of the water slug as it clears cause transient thrust loads on the bottom of the discharge line and the discharge device. This section presents the method of analysis used to define the water thrust loads on the Oyster Creek SRV discharge device caused by transient water slug clearing. It also summarizes the results of this analysis.

1. Method

To model the water clearing transient for the Oyster Creek Y-quencher, the two sparger arms are combined analytically and then nodalized. Equations of motion for the water slug are developed for each node. These are solved for water slug acceleration and velocity, pressure along the sparger, and discharge hole velocity. The above analytical model was used in accordance with the procedures, assumptions, and conditions described in the LDR (Reference 8.2.1) to calculate water thrust loads on the Y-quencher.

2. Verification of Oyster Creek Model

To ensure that the model developed to calculate Y-quencher water thrust loads is adequate, the model was used to calculate water thrust loads for the GE T-quencher. These thrust loads were then

compared to those calculated using the generic analytical model from the LDR (Reference 8.2.1). The results of this comparison show that the Oyster Creek model yields more conservative loads than does the LDR model when both are applied to the same quencher geometry. Specifically, loads calculated by the Oyster Creek model are at least 20% greater than those calculated by the LDR model.

3. Results

The water thrust loads calculated for the Oyster Creek Y-quencher are illustrated in Figure 4.6.1-4. Forces F_1, F_3, F_4 result from the redirection of water. Forces F_6, F_7 and F_8 are caused by the acceleration of water in the sparger. Force F_2 and F_5 result from postulating unbalanced water and gas flow into the sparger arms and out of the sparger discharge holes, respectively, as specified in the LDR. For the SRV piping analysis, F_5 is examined both as a net side load (i.e., same directions on both arms) and as a moment (i.e., different directions in each arm). The pressure on the end caps ($P_{end\ cap}$) from internal pressure in the sparger is also calculated. In addition, the analytical model calculates the velocity of water exiting the sparger holes during the transient. This water velocity is required by the LDR as input for calculating SRV water jet loads on torus internal structures (Section 4.6.3.1). Peak water thrust loads, end cap pressures, and hole velocities are tabulated in Table 4.6.1-2 for worst-case SRV actuation.

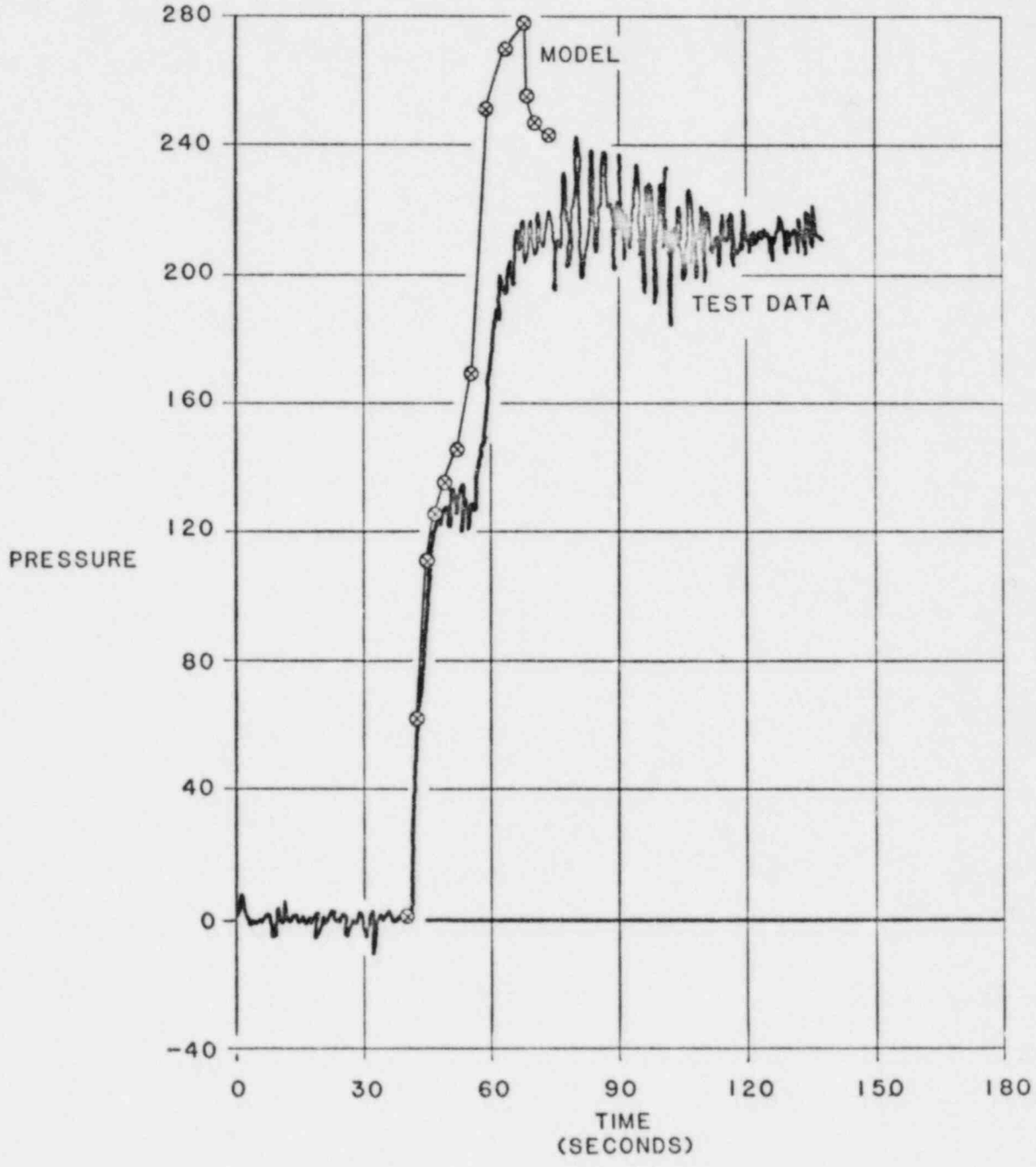

FIGURE 4.6.1-1

MODEL /TEST DATA COMPARISON
FOR TWO VALVES, SIMULTANEOUS, FIRST ACTUATION
NORTH HEADER DISCHARGE LINE PRESSURE NEAR RELIEF VALVES

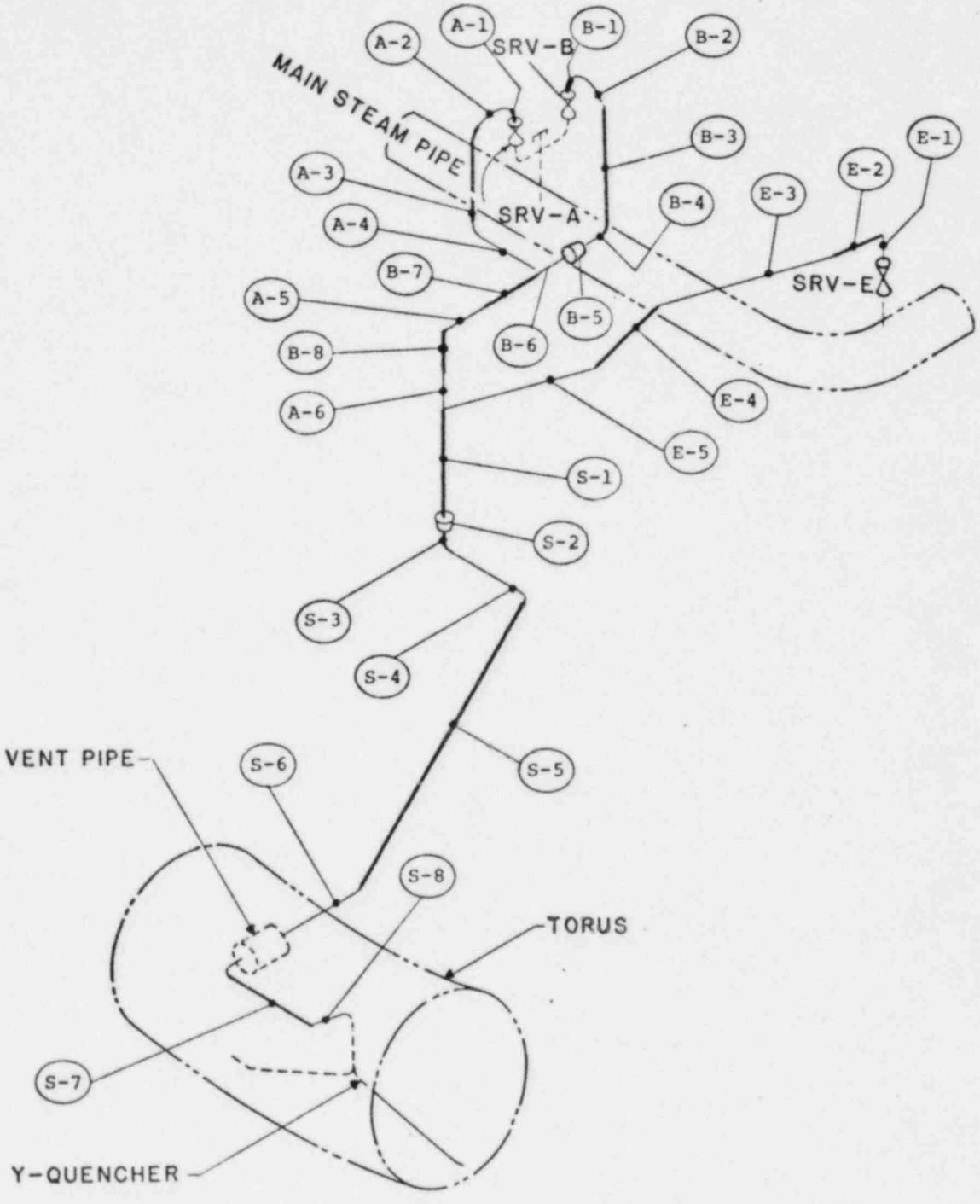

FIGURE 4.6.1 -2
PIPE SEGMENTS FOR
SRV DISCHARGE THRUST LOAD CALCULATIONS
FOR
THE SOUTH HEADER

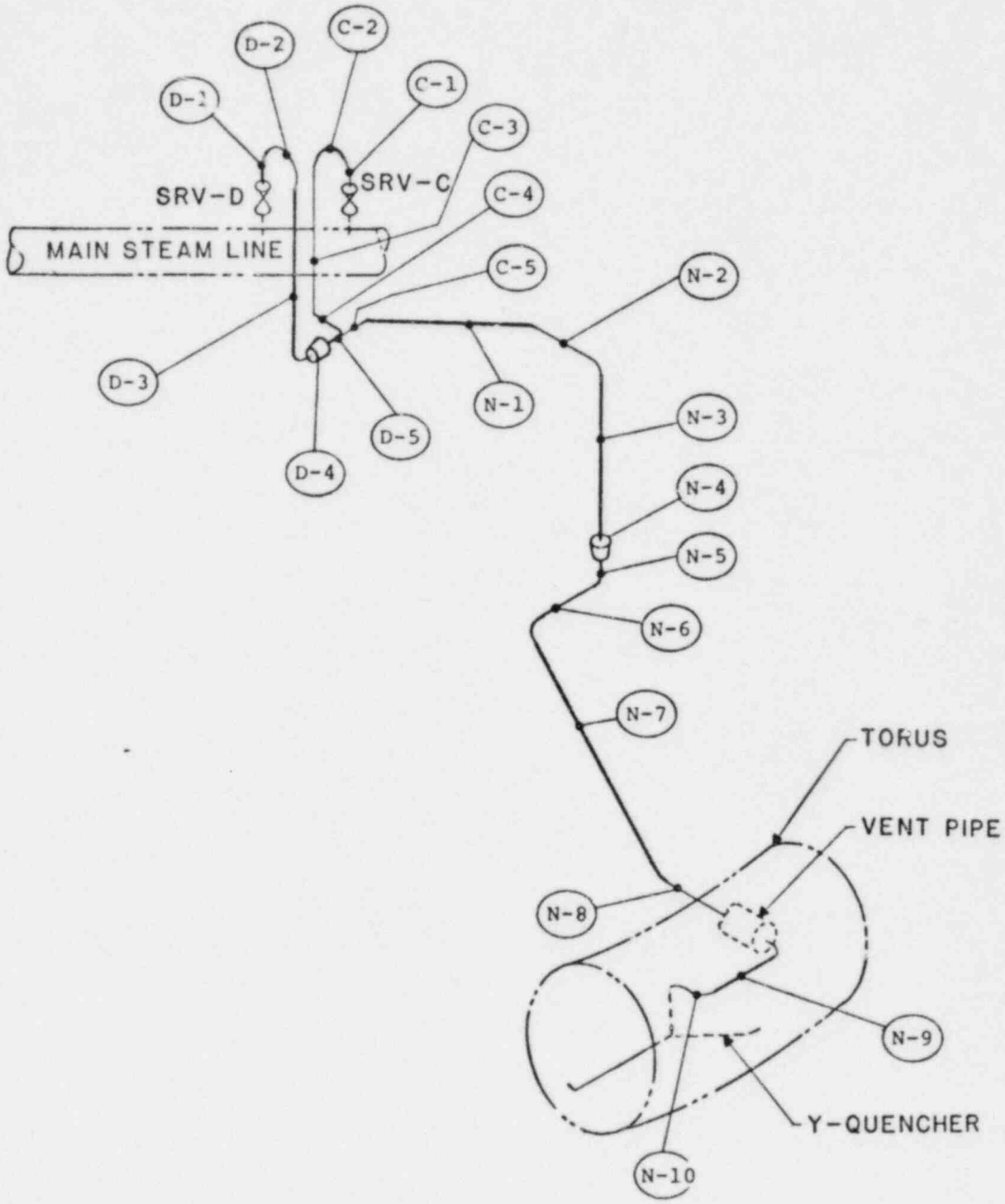

FIGURE 4.6.1-3

PIPE SEGMENTS FOR
SRV DISCHARGE THRUST LOAD CALCULATION
FOR
THE NORTH HEADER

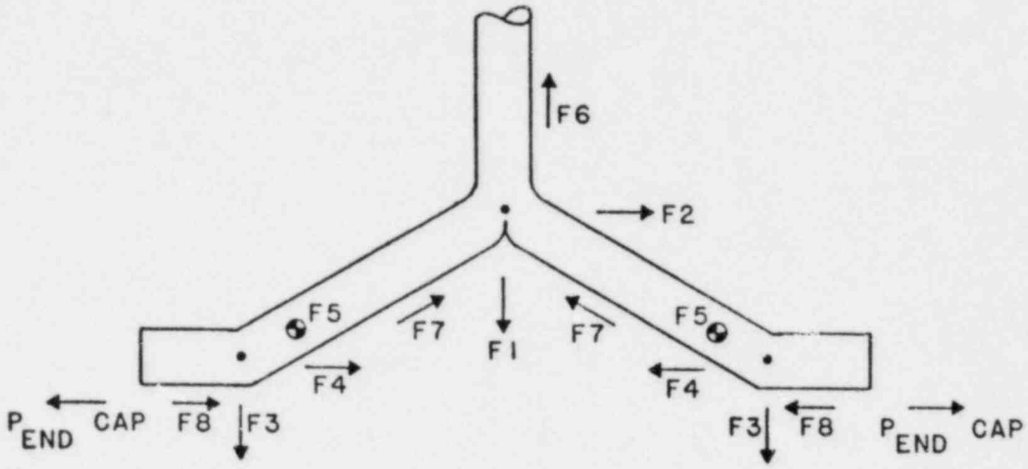

NOTES:

1. ARROWS DENOTE POSITIVE SIGN CONVENTION
2. FORCE F5 IS NORMAL TO THE PLANE OF THE SPARGER AND ASSUMED LOCATED AT WORST-CASE POSITION ALONG SPARGER BUT NO CLOSER THAN 1/2 BAY TO THE CENTER OF THE SPARGER.

4.6.1-4

LOAD DEFINITION
FOR
OYSTER CREEK SPARGER WATER CLEARING THRUST LOADS

TABLE 4.6.1-1

PEAK STEAM THRUST LOADS ON
OYSTER CREEK SRV DISCHARGE LINES

SOUTH HEADER		NORTH HEADER	
Segment	Peak Load (lbf)	Segment	Peak Load (lbf)
A-1	646	C-1	440
A-2	396	C-2	885
A-3	2616	C-3	2550
A-4	1932	C-4	1513
A-5	3121	C-5	2516
B-1	365	D-1	448
B-2	712	D-2	904
B-3	2380	D-3	2317
B-4	1389	D-4	1611
B-5	5254	D-5	4780
B-6/B-7	23389		
E-1	365	N-1	8421
E-2	712	N-2	6990
E-3	3289	N-3	14148
E-4	3094	N-4	6860
E-5	2352	N-5	7090
		N-6	11060
S-1/A-6/B-8	11859	N-7	14382
S-2	2965	N-8	14178
S-3	5057	N-9	13573
S-4	8656	N-10	12875
S-5	13563		
S-6	12513		
S-7	11570		

TABLE 4.6.1-2

PEAK WATER THRUST LOADS ON THE OYSTER CREEK Y-QUENCHER FOR WORST-CASE SRV DISCHARGE

F1	-	14,570 lbf
F2	-	776 lbf
F3	-	3,604 lbf
F4	-	524 lbf
F5	-	7,461 lbf
F6	-	7,422 lbf
F7	-	29,961 lbf
F8	-	3,148 psi
$P_{end\ cap}$	-	383 psi
V_{hole}	-	200 ft/sec

4.6.2 SRV Discharge Loads on the Torus Shell

The definition of shell loads due to SRV discharge was performed in accordance with the LDR (Reference 8.2.1) and NUREG-0661 (Reference 8.1.2). In particular, since Oyster Creek uses a Y-quencher SRV discharge device instead of a standard T-quencher, in-plant tests were used to define shell loads. This is in accordance with the requirements of NUREG-0661 for non-standard quenchers. The Y-quencher design and in-plant test results are described in the report forwarded to the NRC by Reference 8.3.4.

The approach which was used in the analysis of the shell loads and the results of the analysis are described below.

4.6.2.1 Torus Shell and Support Structure

The approach taken to evaluate the Oyster Creek torus for relief valve discharge transients is based on using the data from the tests performed in the plant. The Oyster Creek quencher was tested in the Oyster Creek torus for a number of operating conditions. The pressure on the shell and structural response of the torus were measured, as reported in Reference 8.3.4. Instrumentation used in the tests included:

- strain gages on the shell (inside and outside) and support columns,
- pressure gages on the shell
- displacement transducers on the shell
- accelerometers on the shell and basemat, and
- pressure gages, temperature gages and water level sensors in the discharge piping.

The procedure for evaluating the structure is described in the following paragraphs.

1. Base Case

The first step in the evaluation of the torus structure was to determine the stresses for a base case which was tested. These stresses were based on test results. Stresses for other load cases were then obtained by extrapolation from this base case using the finite element model of the torus.

The base case selected was the event in which two valves simultaneously discharge into one discharge quencher with a cold pipe, normal water slug length in the pipe, and a reactor pressure of 1035 psia. The base case tests were performed using the north discharge quencher because this discharge line was expected to produce higher loads than the south line for the two-valve discharge case. This conclusion was confirmed by the in-plant tests. The results from seven tests for shell stresses and support stresses were statistically evaluated to define 95% confidence values for this base case. These values were used in the definition of SRV loads.

The two-valve test condition was selected as the base case because the stress results are higher than for the one-valve tests. Thus the results require less extrapolation to the design load cases. For this reason, more tests were run at the two-valve condition to obtain better statistical accuracy. The measured stresses (95% confidence values) were used to calibrate the finite element model of the torus in which the SRV load is approximated by a hydrostatic load distribution. The finite element model of the torus was then used to calculate the stresses at locations which were not instrumented.

Calculation of shell stresses for the base case by the method discussed above accounts for the effects of the SRV load

distribution as well as the load magnitude and dynamic effects on the torus shell of the base case. The different magnitudes and dynamic effects of the other SRV discharge conditions which must be evaluated are accounted for separately as discussed below.

Because the loads from the Y-quencher are relatively low, a number of bounding simplifications were made. For example, single bounding scale factors were selected for application to large general areas of the structure, and the peak in the upload transient was smaller than the peak in the download transient, so both peaks were assumed equal to the download value.

2. Design Case Amplitudes

Calculations of stresses and loads for relief valve transient design cases which are different than the tested base case were performed by accounting for the different magnitudes and frequencies of the design cases. The magnitude correction was performed by calculating the peak shell pressure for each design case condition and comparing it to the calculated peak shell pressure for the tested base case. The calculation of these pressures was performed using the procedure required in the LDR (Reference 8.2.1). The shell pressures and frequencies calculated for a number of test conditions were compared to test results from Oyster Creek to confirm that the model correctly predicts the effect of different operating conditions. The comparison showed the predictions bound the test data.

A special design case for Oyster Creek is the opening of an SRV into a discharge quencher into which another SRV is already discharging. This was shown by tests at Oyster Creek to result in lower shell pressures than for the first valve opening. It is therefore treated the same as an initial valve opening transient.

3. Design Case Frequencies

The change in the dynamic response of the structure in the design cases compared to the tested base case was accounted for by performing a dynamic analysis of the torus for each condition. The dynamic load factor (the ratio of the peak dynamic response amplitude to the static response amplitude) was calculated for each case using the coupled load-structure analytical model of the Oyster Creek torus and the bubble time history measured in the Oyster Creek in-plant test as required by NUREG-0661. The bubble time history was shifted in frequency as required for each design case. The frequency used for the analysis of each design load case was selected to coincide with the upper limit of the dominant frequency range predicted for each design load case. The range of frequencies considered were in accordance with the requirements of NUREG-0661. The upper limit of the frequency range was used for the analysis because this results in the highest torus response, since the torus fundamental natural frequency (19 Hz) is above the highest SRV bubble frequency (11.4 Hz). In addition, to reduce the extent of analysis, the frequencies for subsequent actuations were used for the frequencies applicable to first actuations under normal and SBA/IBA (small and intermediate break accidents) conditions. This approach introduces further conservatism, since the SRV bubble frequencies are higher (and thus closer to the torus fundamental natural frequency) for subsequent actuations than for first actuations.

The dynamic load factor for each design case was compared to the dynamic load factor for the tested base case for various parts of the torus and its supports and bounding values of this ratio were selected for use in the structural analyses. This bounding method of adjusting for frequency effects was possible because dynamic amplifications are not large, since the torus structural resonant

frequencies at Oyster Creek are well above SRV discharge bubble frequencies.

4. Simultaneous Discharge from More Than One Quencher

The procedures described above define the loads resulting from the discharge transient from one SRV quencher. At Oyster Creek this transient could be for one, two, or three valves discharging simultaneously through one quencher.

There are two such quenchers installed at Oyster Creek, located as shown in Figure 4.6.2-1; two SRVs discharge into one quencher and three SRVs discharge into the other. Although the two quenchers are widely separated (5 bays apart), some structural loading occurs in the vicinity of one quencher when the other quencher discharges. Consequently, in the event all five SRVs discharge simultaneously, the loads from the two quenchers will superimpose.

The loads on the torus in each bay as a function of the distance from the quencher centerline were obtained, based on test data from the in-plant Oyster Creek test as required by NUREG-0661. The attenuation of load with distance is shown in Figure 4.6.2-2. The load for the five-SRV discharge was then obtained by taking the absolute sum of the loads from each quencher for each bay (as required by NUREG-0661). The most highly loaded bay is the south quencher bay located between 135^{o} and 153^{o}.

5. Overall Multipliers for Analysis of Torus Shell and Supports

For convenience, all the above effects have been combined into one multiplier for evaluation of the torus shell and supports for the SRV discharge transients. The stresses and loads for each SRV discharge case are obtained by using this multiplier to factor the

results of the analysis of the hydrostatic load case. The values of this multiplier for the cases of interest are listed in Table 4.6.2-1.

The vertical reaction due to the net lateral SRV load on the torus is discussed in the following section. The magnitude of this vertical load in the most highly affected bay is equivalent to 0.01 times the hydrostatic load. Although this is a small effect, it has been added to the other SRV loads in Table 4.6.2-1 for the evaluation of the torus shell and its supports.

6. The Effect of the Net Lateral SRV Load

When a discharge transient occurs in one or both discharge quenchers, a net lateral load is imposed on the torus. This occurs because the discharge air bubble pressure acts mainly on the shell surface area in the bays of the torus nearest the quencher. The shell area on the side away from the reactor is greater than the area on the side toward the reactor. Thus a net unbalanced lateral force acts on the torus structure.

The magnitude of this force was calculated by integrating the pressure on the shell over the submerged torus shell surface for each SRV discharge design case. In addition, a dynamic load factor was applied to this static force value. Considering the wide range of bubble frequencies required to be considered by the LDR (Reference 8.2.1), the calculation of the dynamic load factor for each load case assumed the dominant bubble frequency coincides with the major torus structural lateral resonance frequency. The dynamic load factor calculation used the measured bubble pressure time history and 2% structural damping. The results are conservative, since a forced vibration model was used instead of a free vibration interaction model, and coincident frequencies were assumed for the bubble load and structural resonance.

The resulting dynamic forces are listed below:

SRV Design Case	Total Lateral Load (kips)
1 valve, initial actuation, design basis accident	82
5 valves, subsequent actuation, normal operating conditions	264
5 valves, subsequent actuation, IBA/SBA conditions	355

These values are used in the analysis of the structure to calculate stresses and deflections. The deflections are included in the evaluation of attached piping and other structures.

The net lateral force on the torus shell is located at some elevation above the support points for the torus support columns. Consequently, an overturning moment is created. This moment is resisted by a couple formed by an upload on the bays on one side of the torus and a download on the bays 180^{0} opposite. These loads have been included in the SRV shell load definitions described in the preceding section.

4.6.2.2 Response Spectra and Deflections

The response spectra and deflections resulting from the SRV design case transients were obtained by dynamic analyses using the finite element model of the torus. Test data from the in-plant SRV test at Oyster Creek were also used. A standard bubble pressure time history was defined based on data from the tested base case and the response of the torus was calculated by applying this time history to the analytical model of the torus. To scale this analytical response to the actual test response, the analytical response was empirically corrected by comparing the response calculated for the tested base case conditions to the actual response measured during the tests (95% confidence value).

The torus response (response spectrum and deflection) was calculated for each attachment point on the torus using the analytical model of the torus and the standard bubble pressure time history. The bubble pressure time history was first shifted in frequency to correspond to the frequency of the desired design load case. The calculated response was then multiplied by a factor which accounted for the calculated amplitude of the bubble for each design load case compared to the tested base case.

The response (response spectra or deflection) of the torus in each bay depends on the longitudinal distance of the bay from the quencher. The attenuation results discussed in Subsection 4.6.2.1, above, were used to calculate response at each attachment point location. The responses for the two-quencher (five SRVs) discharge were obtained by taking the absolute sum of the responses from each quencher's discharge transient (as required in NUREG-0661).

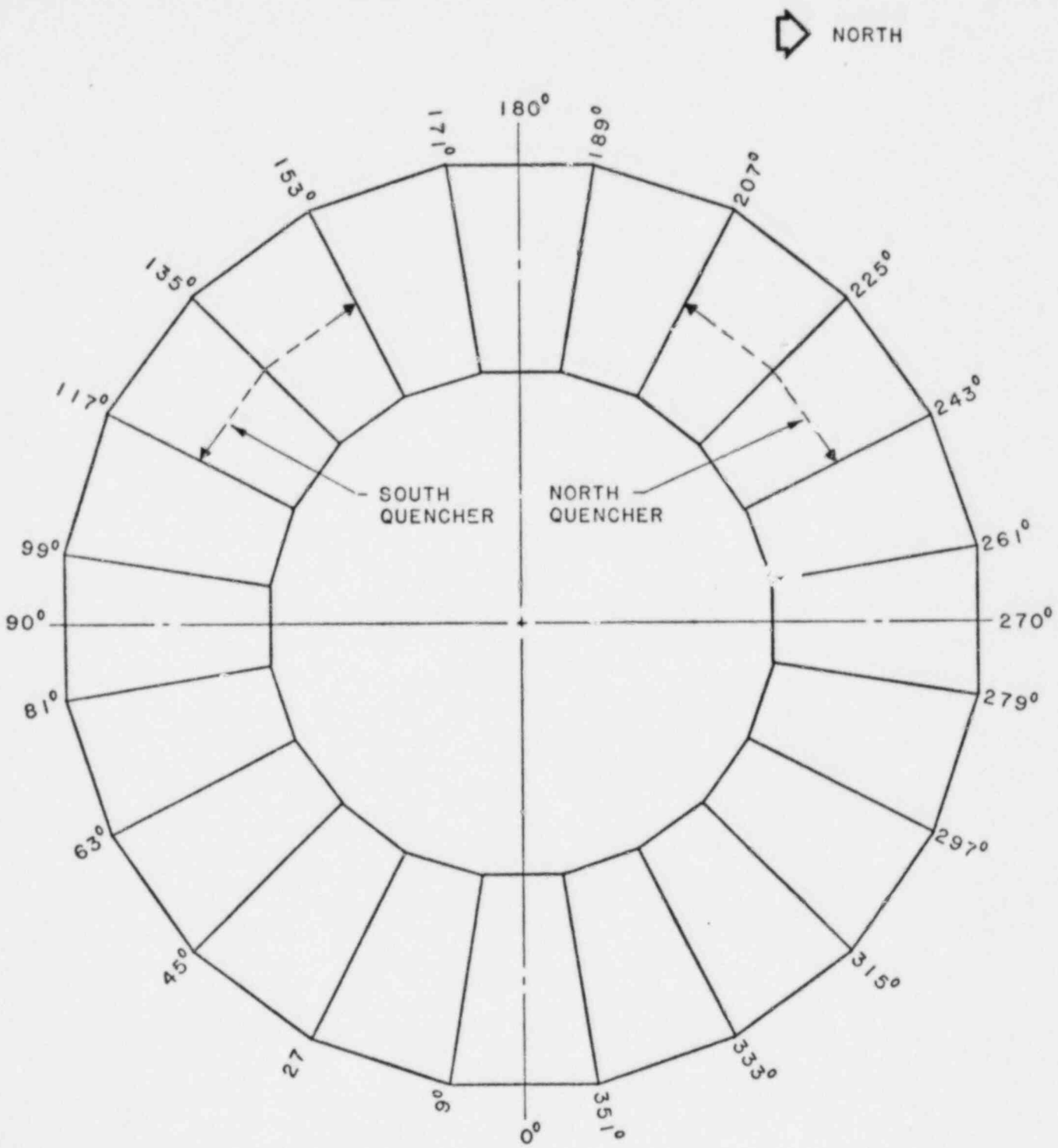

FIGURE 4.6.2-1

OYSTER CREEK TORUS
PLAN VIEW
SHOWING LOCATION OF SRV DISCHARGE QUENCHERS

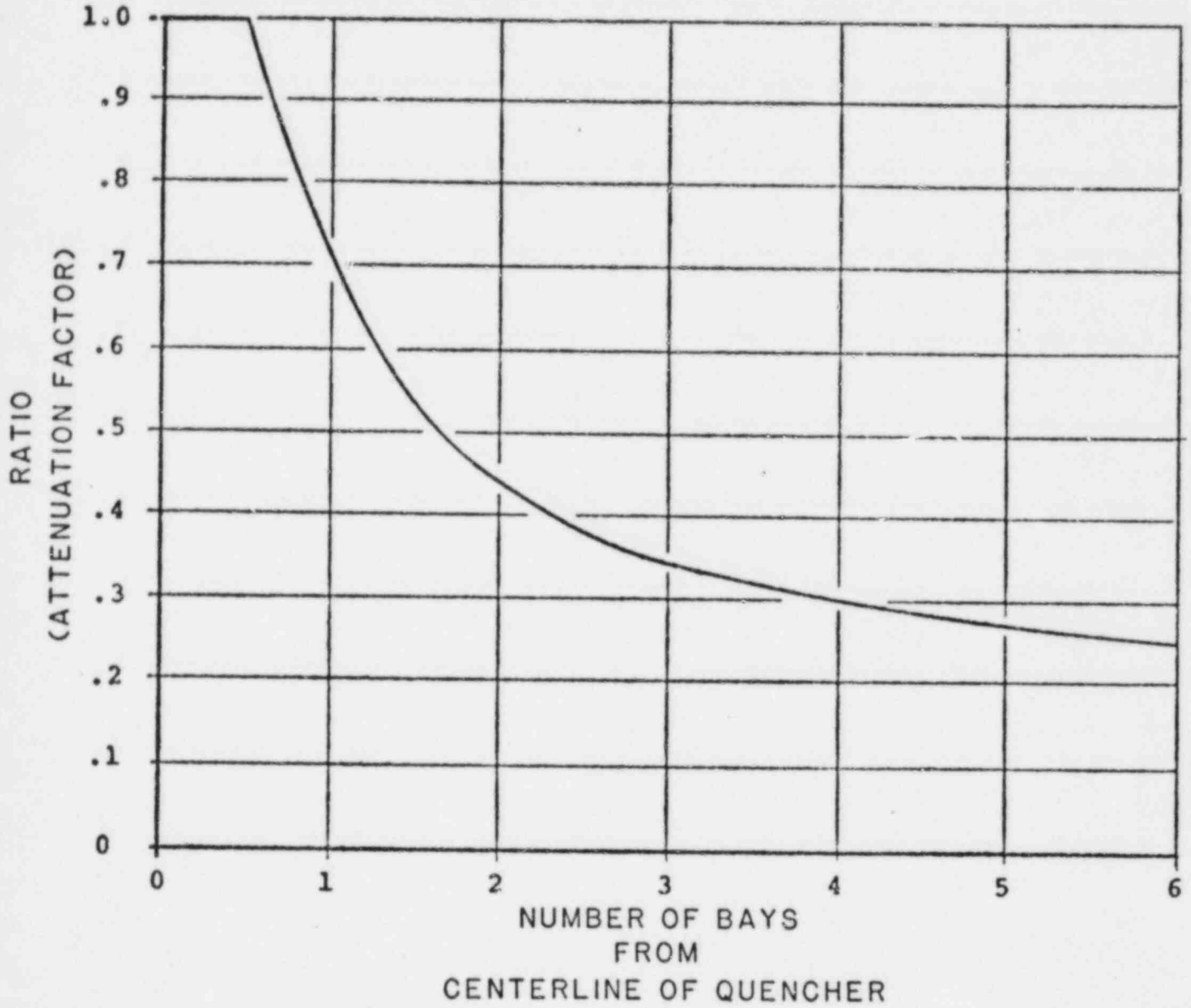

FIGURE 4.6.2-2

OYSTER CREEK TORUS
ATTENUATION FACTORS
IN- PLANT SRV TESTS

TABLE 4.6.2-1

OVERALL MULTIPLIERS FOR SRV DISCHARGE ANALYSIS OF TORUS SHELL AND SUPPORTS

Design Case	OVERALL MULTIPLIER ON HYDROSTATIC LOAD RESULTS		
	Shell Extreme Fiber Stress		
	a. Shell Near Columns	b. Remainder of Shell	c. Column, Column Attachments, Ring Girder, Saddle
1. DBA conditions, One Valve Actuation	0.36	0.42	0.18
2. Normal Operating Conditions, 5 Valves, First Actuation	1.11	1.16	0.56
3. Normal Operating Conditions, 5 Valves, Subsequent Actuation	1.24	1.30	0.63
4. SBA/IBA Conditions, 5 Valves, First Actuation	2.08	2.38	0.93
5. SBA/IBA Conditions, 5 Valves, Subsequent Actuation	2.16	2.48	0.97

Notes:

1. To obtain overall multipliers for shell membrane stress, multiply the values in this table by 0.8.
2. Values in this table apply to both positive and negative peaks.
3. SRV load case results are obtained by multiplying the multipliers in this table times the results of the maximum water level (12.88-foot) hydrostatic load case.

4.6.3 SRV Discharge Loads on Torus Internal Structures

Loads on torus internal structures resulting from SRV discharge are caused by water jet impingement and SRV bubble drag. Plant-unique loads for Oyster Creek internal structures were calculated in accordance with the procedures, assumptions, and conditions specified in the LDR (Reference 8.2.1) and NUREG-0661 (Reference 8.1.2). The detailed methodology that is used is described below.

4.6.3.1 SRV Discharge Jet Impingement Loads on Torus Internal Structures

Following the actuation of an SRV, water initially contained in the submerged portion of the discharge line is expelled into the suppression pool through the discharge device. This can result in water jet impingement loads on structures submerged in the suppression pool. This section presents the method of analysis used to define SRV water jet impingement loads on all Oyster Creek submerged structures and the results of this analysis.

1. Method

   The LDR (Reference 8.2.1) presents a method for determining jet impingement loads on submerged structures caused by an SRV discharge through a GE T-quencher. To determine jet impingement loads on submerged structures in the Oyster Creek torus, the analytical method presented in the LDR is used with the specific Oyster Creek Y-quencher geometry.

2. Results

Only the vent header support columns are subject to SRV jet impingement loads. Other submerged structures are either not in the path of the jets or are beyond the point of maximum jet penetration. Total load on the vent header support columns from SRV jet impingement is conservatively calculated as 700 lbf distributed over the bottom approximately 2.0 feet of the support column.

4.6.3.2 SRV Discharge Bubble Drag Loads on Torus Internal Structures

As a result of an SRV actuation, air initially in the SRV discharge line is forced through the SRV sparger device beneath the torus pool. The air forms oscillating bubbles which rise to the pool surface. As the bubbles oscillate, they induce velocity and acceleration fields in the pool which cause drag loads on torus internal submerged structures.

This section discusses the method of analysis used to define SRV air bubble drag loads on torus submerged structures at Oyster Creek and the results of that analysis.

1. Method

The LDR (Reference 8.2.1) discusses an analytical model developed to predict SRV air bubble drag loads on submerged structures for a GE T-quencher. SRV air bubble drag loads on submerged structures for Oyster Creek were calculated using the LDR model adapted as follows:

a. The LDR analytical model uses an empirical factor to ensure loads calculated by the model conservatively bound the test data for the GE T-quencher. A similar factor is developed for the Oyster Creek Y-quencher. This factor was developed using the in-plant test data for the Oyster Creek Y-quenchers, following the same method as that used to develop the empirical factor for the GE T-quencher.

b. The frequency of bubble oscillation, and hence the forcing frequency for the drag load, is that calculated for the SRV loads on the torus shell. Frequency is taken from the SRV shell load analysis since it has been verified to calculate correct SRV bubble frequencies within the limits specified by the LDR and NUREG-0661 (Section 4.6.2.1).

2. Verification of Model

Following the same method used to compare the LDR analytical model to in-plant test data for the GE T-quencher, the LDR analytical model was compared to the Oyster Creek Y-quencher. The results of this comparison based on measured and calculated pressures indicate that the LDR analytical model is about 20 percent more conservative for the Oyster Creek Y-quencher than it is for the GE T-quencher.

3. Results

The peak applied SRV drag loads for the worst-case SRV actuation are summarized in Table 4.6.3-1.

TABLE 4.6.3-1

SUMMARY OF PEAK APPLIED SRV DRAG LOADS
ON SUBMERGED STRUCTURES IN THE
OYSTER CREEK TORUS FOR WORST-CASE SRV ACTUATION

SUBMERGED STRUCTURE	PEAK APPLIED DRAG LOAD (lbf/ft)
Vent Header Support Columns	22
Catwalk Support Column and Braces	33
Demineralizer Relief Valve Discharge Line	No Load
ECC Nozzle and Strainer	No Load
SRV Line Y-Quencher and Supports	710
Downcomers and Downcomer Braces	1650
Ring Girder	446

NOTE:

Table is for comparison only. Values are based on worst-case structure at worst-case location.

5.0 GENERAL ANALYTICAL PROCEDURES

This section describes the general procedures followed in evaluating the response of the Oyster Creek torus and vent system to the Mark I Long-Term Program loads. The section is divided into four parts.

Section 5.1 discusses the coupled torus/vent system finite element model and associated substructure models used to predict the overall static and dynamic behavior of the suppression chamber. Section 5.2 describes the vent system finite element beam model used to analyze structural components of the vent system. Several generic computer programs provided by General Electric to define special load effects are described in Section 5.3. Finally, the seismic analysis methods followed in the Oyster Creek Mark I Long-Term Program are presented in Section 5.4.

5.1 COUPLED TORUS - VENT SYSTEM COMPUTER MODEL

The primary analysis tool for the structural evaluation of the Oyster Creek pressure-suppression containment is the finite element model of the coupled torus/vent system. The term "coupled" is used to indicate that this model includes the interaction effects between the torus structure and the vent system. Specifically, it combines the mass and stiffness characteristics of the vent system beam model (Section 5.2) and the torus shell model described below.

These finite element analyses were performed using the STARDYNE finite element code (Reference 8.6.6), which is a verified industry-proven computer program for static and dynamic structural analysis.

5.1.1 1/40 Sector Torus Shell Model

The 1/40 sector torus shell model was developed to analyze overall shell and support response for static and hydrodynamic Mark I symmetric loads. Because of the symmetry of these loads and the Oyster Creek torus structure (the Oyster Creek suppression chamber is composed of 20 identical symmetrical linear cylindrical segments), it was possible to accurately capture such responses for the Oyster Creek torus geometry with a representative 1/40 sector model of the torus.

5.1.1.1 Model Description

The torus shell model is a state-of-the-art finite element representation of a typical 1/40 sector of the Oyster Creek torus suppression chamber. A view of the model is shown in Figure 5.1.1-1. It is comprised of over 7000 degrees of freedom and approximately 2000 discrete elements. The structure was modeled using a carefully refined mesh to correctly identify stress distribution and, since the model is dynamically analyzed using modal superposition methods, the modeling detail was rigorously verified to ensure that the significant modes of this structure are captured.

The model includes the support columns at the miter and the saddle at mid-bay. Symmetry boundary conditions were imposed on the mid-bay and mitered joint planes. The stiffness of the ring girder was modeled with beam elements that are tied to the shell nodes on the miter. The mid-bay saddle was modeled with both plate and beam elements to accurately represent the stiffness of the saddle and its gussets and flanges. The gussets and flanges in the support column connection regions were also explicitly modeled with plate elements. Thus the interaction of the supports and the torus shell is properly modeled.

The model shown in Figure 5.1.1-1 includes an explicit representation of the shell straps which are being added as a part of the Mark I Long-Term Program. Some analyses were performed on an earlier model which did not include the straps. The results of these analyses have been used in the final evaluation in some cases, where the particular component or load is not affected by the presence of the straps.

Another significant modeling characteristic of the torus model is the suppression pool water mass representation. This mass representation was derived from an explicit model of the fluid and then distributed in matrix form to the wetted surface nodes on the torus shell with the cross-coupling of the pool mass accounted for at all appropriate shell nodes. Specifically, this distribution was accomplished by adding a consistent mass matrix (CMM) formulation of the three-dimensional pool to the explicit torus shell model.

The Oyster Creek vent system is supported by columns attached to the torus ring girder. The effect of the vent system was modeled by synthesizing the vent system modal mass and stiffness terms (determined from the vent system beam model, Section 5.2) into the explicit torus shell model. Convergence studies demonstrated that this coupling adequately represents the participation of the vent system in the torus response for Mark I static and dynamic loads.

The coupled torus/vent system model was used to determine dynamic characteristics of the torus, general shell stresses, support reactions, attachment point motions for piping and internal structures, and input for substructure models. Since local discontinuities such as attachment penetrations do not significantly influence any of these overall torus responses, a clean shell model was used. Piping systems attached to the shell can be omitted from the model because they are small compared to

the torus structure and the vent line from the drywell can be neglected since it is decoupled from the torus by a bellows.

Since torus response can be accurately captured with a clean shell model, the only asymmetry of the torus structure that could necessitate a more complex general torus model than the 1/40 sector is the offset of the ring girder from the mitered joint. Therefore, in order to quantify the significance of this offset, a 1/20 sector model comprised of shell elements extending from mid-bay to mid-bay on either side of a mitered joint was developed. The correlation of response data from this 1/20 model with 1/40 model data indicated, however, that this offset has a negligible effect on overall torus behavior. It was thereby established that the more practical 1/40 shell model shown in Figure 5.1.1-1 is adequate to calculate torus response for the Oyster Creek Mark I plant unique analysis.

5.1.1.2 Loading Analyses

The 1/40 sector coupled torus/vent system model was used to evaluate torus response for the applicable Mark I loads specified in the Load Definition Report (LDR), (Reference 8.2.1). To facilitate the discussion of these Mark I loading analyses, each static and dynamic load case is discussed individually herein.

The analysis of the coupled torus/vent system model included several static load cases for normal operating and loss-of-coolant accident conditions. These load cases included torus self-loads, such as dead-weight, hydrostatic and internal pressure, and reaction loads imposed on the torus from the vent system and other structures that the torus supports.

When appropriate for these loadings, unit loads were applied instead of loads with unique magnitudes. For example, for the internal pressure

load case, nodal forces equivalent to a one psi uniformly-distributed internal torus pressure were used instead of forces corresponding to specific accident condition pressure amplitudes. Similarly, 1000-lb concentrated loads and 1000-lb-in applied moments were used to represent various reaction loads. Results for actual loadings were obtained by factoring the appropriate unit load cases during the post-processing of the loads and during the formation of final load combinations for comparison to stress allowables.

Lateral and vertical ground acceleration load cases were also analyzed using one "g" as the acceleration amplitude. These cases permitted the evaluation of various seismic conditions by factoring, as well as the evaluation of torus dead weight. The results of this model were used to obtain local shell stresses and strains due to lateral seismic forces; the overall response of the torus due to lateral seismic accelerations was evaluated separately as described in Section 5.4.

Specific loading conditions were imposed for some load cases when it was not useful to employ a unit load representation. In particular, the hydrostatic loading was defined for maximum suppression pool water depth; i.e., 4.06-foot downcomer submergence. Also, the thermal load on the torus was specified as a 100^{o} Fahrenheit heat-up from a 70^{o} initial temperature.

Following verification of the static torus responses, the modal (i.e., frequency-dependent) characteristics of the coupled torus/vent system were extracted prior to performing the dynamic load analyses. These modal characteristics were used together with static response data to select critical monitor locations on the torus for the dynamic analyses.

Two types of dynamic analyses were performed: time history and harmonic analysis. Both used two percent of critical damping for the viscous damping of the coupled torus/vent system structure. The dynamic

analyses of the design basis accident (DBA) pool swell submerged pressure transient was performed using the time history method. This load was applied in accordance with LDR specifications using the most severe pool swell load definition for the Oyster Creek torus shell; i.e., the 4.06-foot downcomer submergence, zero drywell to wetwell differential pressure load. The internal pressurization component of the pool swell load, which is a static pressure ramp, was subsequently included in the solution by applying appropriate time-varying factors to the unit internal pressure static load case. Also, there are significant dynamic loads on the vent system during pool swell, and it was necessary to evaluate the torus for these loads. It was possible, based on the frequency content of the loads relative to the torus structural frequencies, to calculate the effects of these reaction loads using time-varying, statically applied factors.

The other type of dynamic analysis, a harmonic analysis, was performed for the various DBA, IBA and SBA condensation oscillation and chugging loads that are defined in the LDR as steady-state, frequency dependent pressures. The technique used for these analyses is analogous to the unit static load method described earlier in that a unit harmonic load profile was used; i.e., the hydrostatic torus load distribution was normalized to a one psi pressure at bottom dead center. This normalized harmonic load profile was applied to the torus model at all torus natural frequencies and at additional intermediate frequencies. This provided at least one harmonic response case in each one-Hertz band. Response to the specific LDR condensation oscillation and chugging loads was then obtained by applying the appropriate LDR load amplitude factors to respective individual unit harmonic responses. These factored responses were then summed using accepted phasing conventions (Section 4.3) to obtain total responses for each load case.

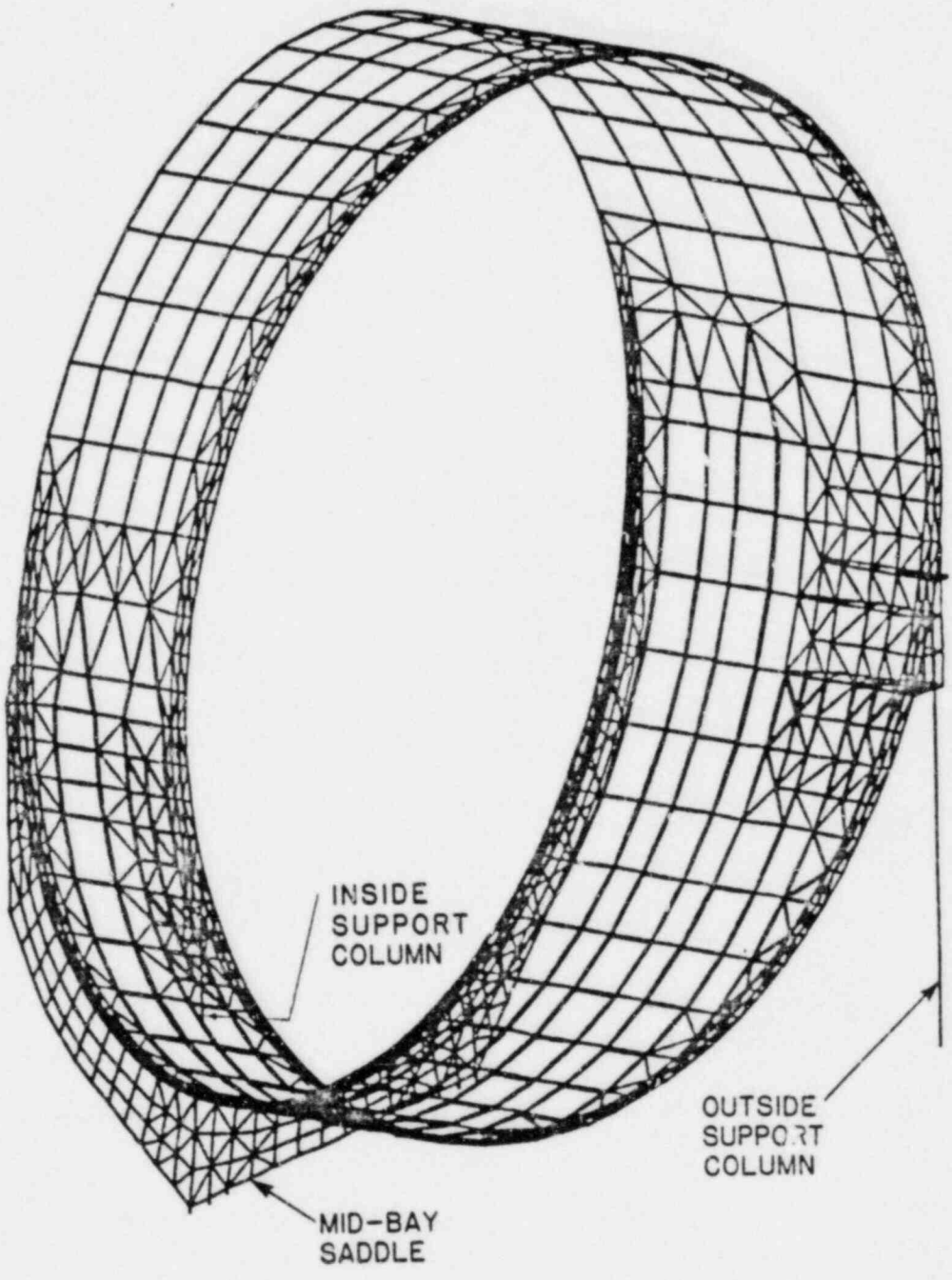

FIGURE 5.1.1-1

OYSTER CREEK TORUS
FINITE ELEMENT SHELL MODEL

5.1.2 Substructuring Models

While the 1/40 sector torus model was used to evaluate general torus response, three additional models, described below, were developed to investigate local torus and column attachment stresses. These models were used to rigorously represent components of the overall torus.

5.1.2.1 Detailed Connection Region Models

As discussed earlier, the reaction loads from the torus support columns are transferred to the torus shell and ring girder through vertical and horizontal gussets. Although the 1/40 model captures the general stress distribution in these connection regions, it is not refined enough to identify the specific stress intensifications at the various discontinuities in these areas. Therefore, more refined finite element shell models of the inner and outer torus support column to torus shell connection regions were developed to obtain the local stress intensification due to geometric discontinuities at the miter near the connection gussets and flanges. These models are shown in Figures 5.1.2-1 and 5.1.2-2. They were defined using the same state-of-the-art modeling techniques and finite elements used in the 1/40 torus model.

In both of these models, the torus shell is extended to both sides of the miter and above and below the gussets far enough that at the boundaries of these models general shell response is obtained. In addition to providing a refined mesh of the shell and column connections, these models also permit a detailed evaluation of the effects of the ring girder offset from the miter.

Validation of these models was performed using boundary displacements from both the 1/20 and 1/40 torus models, together with local loads to insure that connection region stresses could be calculated using these models with boundary data from the 1/40 model. After demonstrating the

compatibility of using 1/40 model displacement data with the connection region models, boundary displacements from the 1/40 model static analysis were imposed. The resulting stress states in the respective regions were then examined to identify connection region stress extrapolation factors. These factors were then subsequently used to adjust 1/40 model shell stresses from both static and dynamic analyses to obtain local connection stress intensities.

5.1.2.2 Ring Girder Shell Model

The third detailed three-dimensional substructure model was developed to examine local ring girder response. This model represents the ring girder web and flange with plate elements to analyze local stresses due to loads on the ring girder normal to the plane of the ring girder. These loads come from structures and piping supported by the ring girder and from hydrodynamic loads on the ring girder. As with the connection models, enough torus shell is included in this model to facilitate the application of realistic boundary conditions. This model is described in more detail in Section 6.1.2.

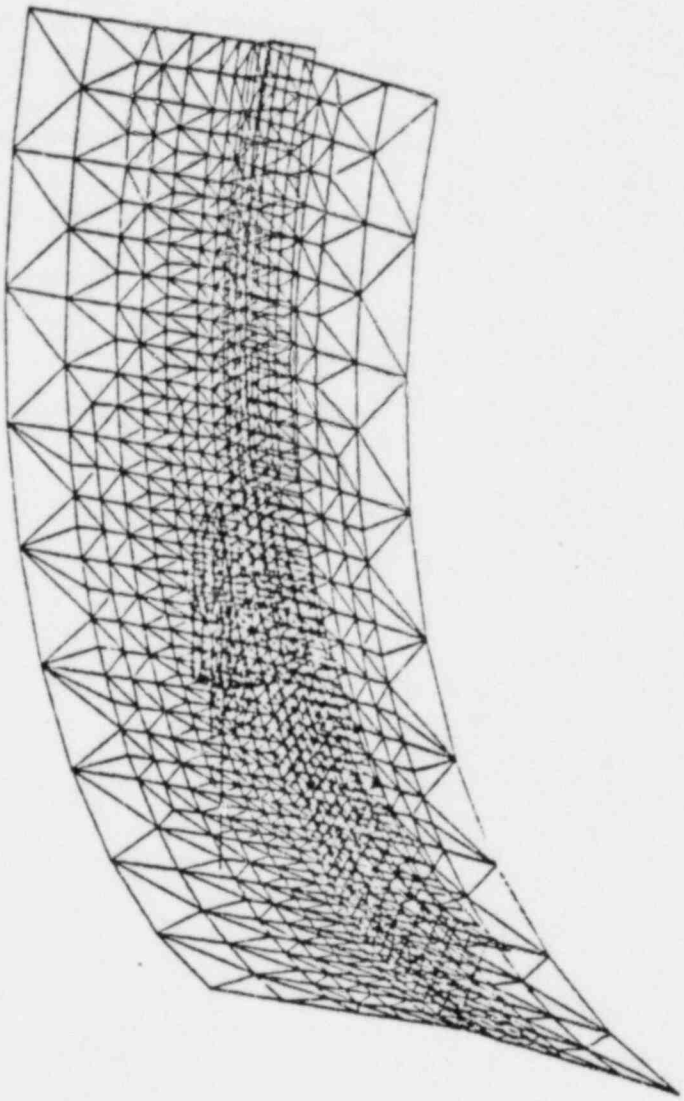

FIGURE 5.1.2-1

OYSTER CREEK TORUS
INSIDE COLUMN CONNECTION REGION MODEL

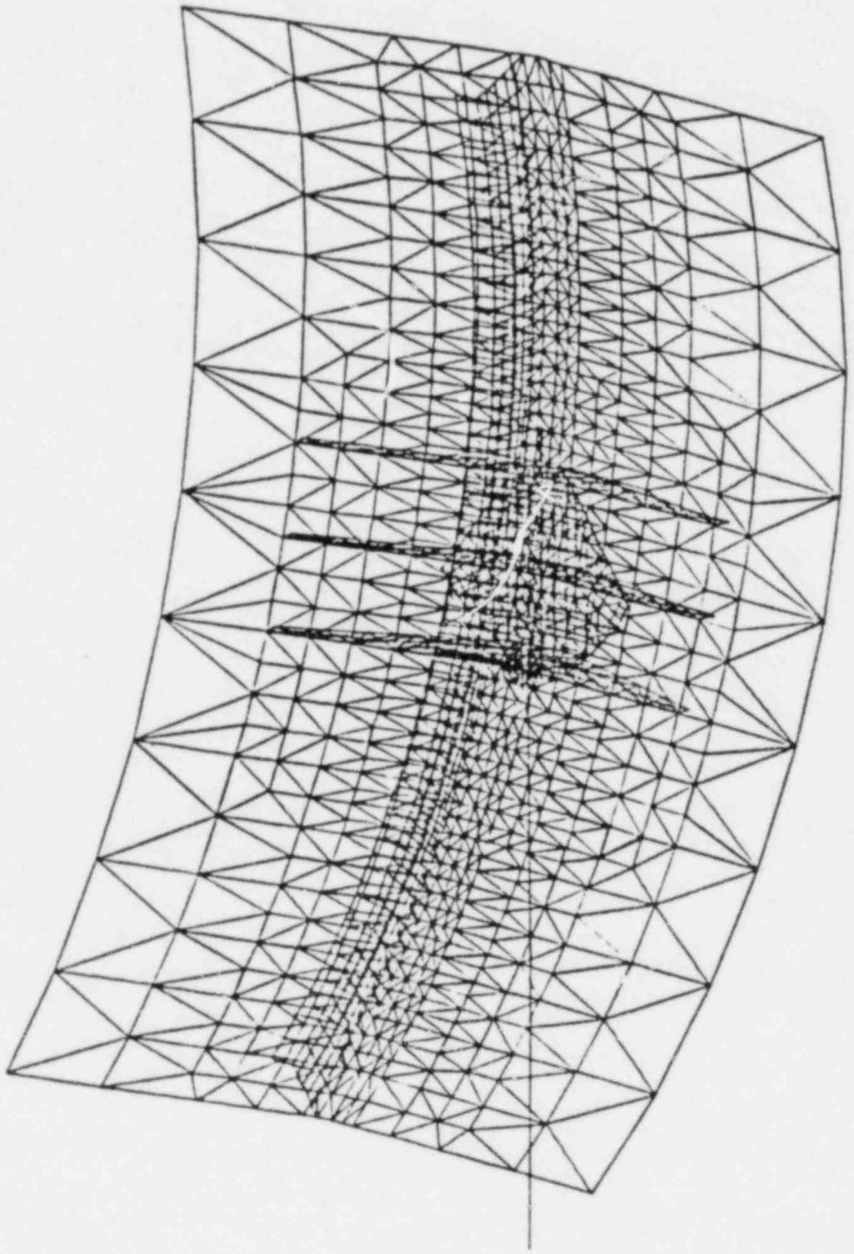

FIGURE 5.1.2-2

OYSTER CREEK TORUS
OUTSIDE COLUMN CONNECTION REGION MODEL

5.1.3 Post-Processing

Following the individual analyses of the torus and its various components, the resulting data base of digitized response was used in several post-processing efforts. The extensive digitized data base, containing the results of the detailed torus analyses, permitted the rigorous automated evaluation of the many load cases and load combinations required by the PUAAG (Reference 8.2.3).

The post-processing provided stress components, stress intensities and weld forces in a form which permitted evaluation of each to the applicable ASME Code criteria. In addition, the final post-processing of torus data involved the determination of differential displacements and acceleration response spectra at locations where piping and internal structures are attached to the torus. This was accomplished using techniques appropriate for all dynamic torus loads. Specifically, two techniques were used to generate acceleration response spectra for torus attached systems due to torus motion at attachment locations. A state-of-the-art numerical integration solution was used for the transient loads (i.e., SRV discharge and pool swell), while a closed form method was used to calculate response spectra for the steady-state condensation oscillation and chugging loads. All response spectra were peak-broadened in accordance with NRC Regulatory Guidelines prior to being used as input for subsequent analyses.

The use of the analysis results in the evaluation of the torus is discussed in Section 6.1.

5.2 VENT SYSTEM BEAM MODEL

The 1/20 sector vent system beam model shown in Figure 5.2-1 was used to determine vent system response, including the displacements and accelerations at points where piping or other internal structures are attached. This model included the modifications to the system which are being made as part of the Mark I Long-Term Program (the vent header deflector, downcomer penetration reinforcement and vent system support columns). Local structural effects were evaluated using a number of detailed vent system component models and the structural characteristics from these models were included in the beam model. This modeling is described below.

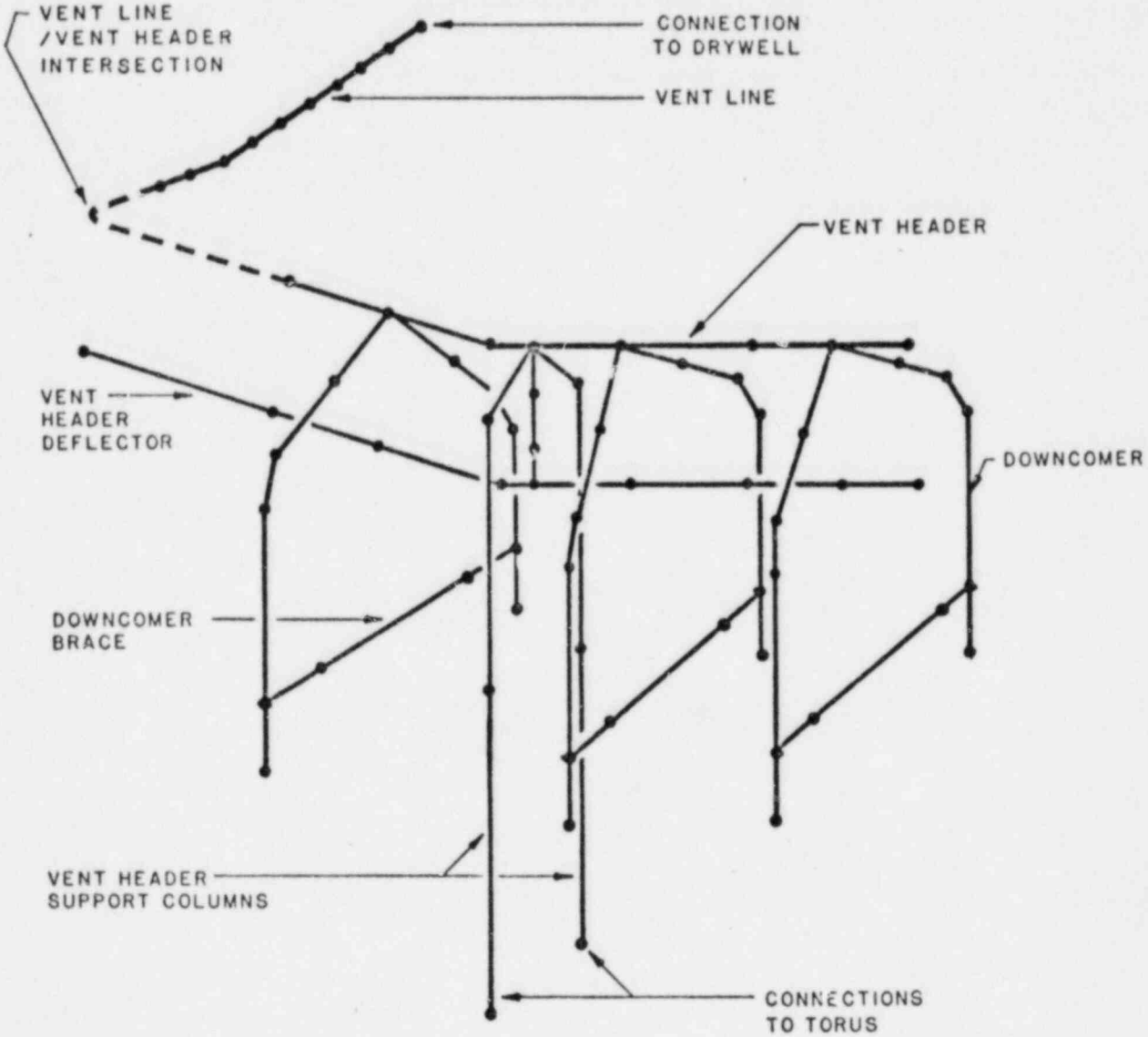

FIGURE 5.2-1

OYSTER CREEK VENT SYSTEM
FINITE ELEMENT BEAM MODEL

5.2.1 1/20 Sector Vent System Beam Model

Vent system symmetry extends from mid-bay of a vent bay to mid-bay of a non-vent bay. Therefore, the 1/20 sector model is defined between two adjacent mid-bay symmetry planes as shown in Figure 5.2-1. The model includes representations of the vent line, vent header, vent deflector, downcomers, vent header support columns, downcomer braces, vent deflector supports and the intersections between these components. The water mass associated with the submerged portion of the downcomers was included appropriately in the model. Although the overall behavior of the vent system can be modeled with typical beam elements, the three types of cylindrical intersections in the vent system required special consideration as described below.

5.2.1.1 Vent Line/Drywell Intersection

In order to approximate the boundary condition imposed on the vent line at its penetration through the drywell containment, a separate detailed finite element model of this intersection was used to calculate the stiffness of this penetration. The resulting stiffness matrix was used to define the boundary in the 1/20 beam model. The analysis of this intersection is described in Section 6.2.2.1.

5.2.1.2 Vent Line/Vent Header Intersection

The second cylindrical intersection, the vent line/vent header tee, was also modeled with a stiffness matrix representation of the actual intersection geometry. This matrix was determined analytically in a generic Mark I analysis program. The analysis of this intersection is described in Section 6.2.3.1.

5.2.1.3 Downcomer/Vent Header Intersection

An explicit finite element model was developed for the downcomer/vent header intersection. The stiffness matrix obtained from this model was used at the appropriate locations in the 1/20 beam model. The analysis of this intersection is described in Section 6.2.4.1.

5.2.2 Vent System Loadings

Two types of vent system loads were considered: vent system self-loads, and loads imposed on the vent system by the displacement of the torus at the base of the vent header support columns.

5.2.2.1 Vent System Self-Loads

As with the torus, both static and dynamic loads for the vent system are defined in the Mark I LDR (Reference 8.2.1). Explicit dynamic analysis was performed for the DBA pool swell impact and thrust loads, and for the downcomer CO loads. Other loads were evaluated using statically applied forces including dynamic load factors where appropriate.

In order to evaluate both static and static equivalent dynamic loads, unit loads similar to those used with the torus model were employed. Overall vent system loadings such as deadweight, distributed pressure loads, and unit displacements and reactions were applied to the 1/20 beam model. Actual results for design loads were obtained by factoring these unit cases.

The dynamic analysis of vent system self-loads due to DBA pool swell impact and drag involved explicit transient analyses of the vent system. In order to ensure a conservative evaluation for this loading, the limiting loads for each component were applied (Section 4.4).

The downcomer CO loads were analyzed using a harmonic analysis technique, where the loads were applied at the natural frequency associated with the downcomers swaying. A unit harmonic load was utilized and actual results were obtained by factoring this unit harmonic response.

5.2.2.2 Torus Imposed Loads

In addition to vent system self-loads, the deformation of the torus ring girder due to static and dynamic loads on the torus imposes forces on the vent system through the vent header support columns. These loads were analyzed using the results of the coupled torus/vent system model analyses. Specifically, for static loads, the calculated displacements at the bases of the vent header support columns were applied to the vent system by factoring imposed unit displacement results. For dynamic loads, the calculated response of the vent system modal representation was used to determine the overall vent system response.

5.2.3 Vent System Post-Processing

Vent system analysis results were post-processed similar to the torus shell results to permit evaluation of the system for the applicable ASME Code criteria and to provide input for the attached piping analyses. The use of the analysis results in the evaluation of the vent system is discussed in Section 6.2.

5.3 GENERAL ELECTRIC COMPANY MARK I LONG-TERM PROGRAM COMPUTER CODES

Many of the calculational methods described in the LDR (Reference 8.2.1) for defining LOCA and SRV loads are generally applicable to all Mark I plants but require plant-specific information; e.g., on structure or component geometry, initial conditions, etc. In order to ensure plant-unique application of these calculational methods is uniformly carried out in accordance with the LDR and NUREG-0661 (Reference 8.1.2), General Electric Company (GE) has automated several of the more complex LDR analytical models using computer programs. Each GE computer program implements a single LDR calculational method in accordance with the LDR and NUREG-0661. The programs are maintained and controlled by GE and are accessible for execution only. The programs are designed to accept plant-unique input data for structure and component geometry, initial conditions, etc. as part of the execution of the program. GE computer programs used in the Oyster Creek Mark I Containment Long-Term Program analyses are as follows:

LOCAFOR This code calculates LOCA bubble-induced drag loads on submerged structures as described in Section 4.3.8 of the LDR. The code was used to calculate Oyster Creek LOCA bubble drag loads discussed in Section 4.5.1 of this report.

LOCAFOR was developed based on analytical models formulated by GE (F. J. Moody, et.al.), (Reference 8.2.7). LOCAFOR has been proven to calculate conservative LOCA bubble-induced drag loads based on direct comparison to quarter-scale test data (Reference 8.2.8). The analytical model, and the comparison to test data were reviewed by the NRC (NUREG-0661). The analytical model, including resolution of NRC comments, has been included in the LOCAFOR code used to define LOCA drag loads for Oyster Creek. The LOCAFOR code performs two distinct operations. First, the code calculates the flow

field local to the structure under consideration. Second, the drag load on the structure caused by the calculated flow is determined.

CONDFOR This code calculates loads on submerged structures due to main vent steam condensation oscillation and chugging as described in Sections 4.4.2 and 4.5.2 of the LDR. The code was used to calculate Oyster Creek condensation oscillation and chugging drag loads discussed in Section 4.5.2 of this report.

CONDFOR uses the same basic analytical models as does LOCAFOR for bubble dynamics, flow field evaluation, and drag load calculations. The analytical models and methods (Reference 8.2.10) on which CONDFOR is based, have been reviewed by the NRC (NUREG-0661). Resulting NRC comments were incorporated into the CONDFOR program used to define condensation oscillation and chugging drag loads for Oyster Creek.

Note, because of the manner of establishing condensation oscillation and chugging source strength, the effects of fluid-structure interaction (FSI) on drag loads must be computed separately from CONDFOR. The FSI drag loads are added to the drag loads calculated by CONDFOR.

TEEQFOR This code calculates SRV bubble-induced drag loads on submerged structures for discharge lines with quenchers. This code was used to calculate Oyster Creek SRV bubble drag loads discussed in Section 4.6.3.2 of this report.

The analytical models used in TEEQFOR are described in Reference 8.2.12. Comparisons of calculated results with test data (Reference 8.2.12) have shown that the models in TEEQFOR conservatively predict the effects of SRV discharge on the

torus pool. The NRC has reviewed the models and data comparisons (NUREG-0661). The resulting NRC comments have been incorporated into the TEEQFOR code used to calculate SRV-induced drag loads at Oyster Creek. As previously discussed, TEEQFOR has also been assessed for its applicability to the Oyster Creek Y-quencher. The results of this assessment indicate that TEEQFOR is applicable to Oyster Creek (Section 4.6.3.2). The TEEQFOR code used for the Oyster Creek load definition used no empirical damping of bubble oscillation; i.e., it was based on an analytically derived waveform for the SRV bubble.

QBUBS — This code calculates torus shell pressures caused by SRV discharge through a GE T-quencher. The analytical method is described in Section 5.2.2 of the LDR. This code was used to extrapolate SRV test data to design SRV actuation conditions as discussed in Section 4.6.2.1 of this report.

The analytical models used in QBUBS and their ability to predict conservatively torus shell pressures caused by SRV actuation are discussed in Reference 8.2.11. The NRC has reviewed these models and comparisons of their results to test data (NUREG-0661). Resulting NRC comments have been incorporated into the QBUBS code used for Oyster Creek. In addition, QBUBS has been shown to be applicable to the Oyster Creek Y-quencher by comparison of its results to Oyster Creek in-plant test data (Section 4.6.2.1 herein).

RVFOR — This code calculates SRV discharge line clearing transient loads as described in Section 5.2.1 of the LDR. It was used to calculate steam thrust loads on the Oyster Creek SRV discharge lines as discussed in Section 4.6.1.1 of this report. Reference 8.2.12 describes the analytical models and

their ability to predict conservatively the results of SRV discharge line clearing. The NRC has reviewed these and found them acceptable (NUREG-0661).

RVRIZ — This code calculates the SRV discharge line reflood transient as described in Section 5.2.3 of the LDR. It was used to calculate initial conditions in the Oyster Creek SRV discharge line for the SRV clearing transient analyses discussed in Section 4.6.1.1 of this report.

Reference 8.2.13 describes the analytical models and compares model results to test data for an SRV discharge line reflood. The NRC has reviewed these and found them acceptable (NUREG-0661).

5.4 SEISMIC ANALYSIS

Seismic analyses for the torus were performed using the methods employed in the original plant design. This approach is in conformance with the analysis guidelines in the Plant Unique Analysis Application Guide (PUAAG), (Reference 8.2.3), and NUREG-0661 (Reference 8.1.2).

The seismic analysis procedures which were used are those reported in the Oyster Creek primary containment design report (Reference 8.2.4). The method is an equivalent static stress analysis in which the seismic load is a static acceleration force. The peak acceleration is calculated by applying the seismic ground motion specified for Oyster Creek in the containment design report (Reference 8.2.4) to a single degree of freedom oscillator with the same natural frequency as the lateral mode of the torus.

The results of this analysis showed a maximum lateral acceleration of 0.44g and a maximum vertical acceleration of 0.2g for the safe shutdown earthquake. These results are conservative in that they are based on a torus natural frequency which is calculated assuming all the torus water moves with the structure. Actually, only a fraction of the water moves laterally with the structure. As a result, the natural frequency is really higher than the calculated value. Consequently, the dynamic response is actually lower than the value used in the calculation.

The forces on the torus shell and its supports due to the seismic acceleration were calculated accounting for the masses of the structure and the water and the sloshing behavior of the water. The water sloshing analysis was performed using the procedures in TID-7024, Nuclear Reactors and Earthquakes (Reference 8.1.4). Methods for applying these procedures to the torus geometry were verified by analyzing the seismic slosh tests performed by Lawrence Berkeley Laboratory for the USNRC (References 8.1.5 for annular geometry and

8.1.6 for torus geometry) and the seismic slosh tests performed as part of the Mark I Containment Long-Term Program (Reference 8.2.5 for torus geometry).

The net lateral load on the torus causes an overturning moment which is resisted by an upload on one end of the torus and a download on the opposite end. The magnitude of this vertical load was calculated and added absolutely to the vertical load due to the vertical seismic acceleration.

6.0 DESIGN STRESS ANALYSIS

This section presents the structural analyses of the torus, torus support system, vent system and torus internal structures. The analyses are based on the Mark I Long-Term Program criteria in Section 2.2 of this report, using the loads defined in Section 4.0. The geometries of the structural components are described in Section 3.0.

Initially, all the loads described in Section 4.0 were considered in the analysis of each component. Engineering judgment and scoping calculations were then used to determine which of the loads were significant and which had only a negligible effect on a particular component. For example, underwater drag loads on the torus attached piping systems and the catwalk were neglected in the analysis of the vent system. In general it was found that most of the loads on the vent system components, the torus shell, and the relief valve piping (which is attached to the vent system and torus ring girder) were required to be considered in the structural analyses covered by this report. Local reaction loads on the torus shell, hoop straps and vent lines due to motions of torus-attached piping at shell penetrations are evaluated separately in the Mark I Long-Term Program report for the piping (Reference 8.5.1).

Large finite element analytical models were developed to determine the general structural responses to the major loads. For most static and dynamic loads on the vent system, including the reaction loads from the relief valve piping attachment, the vent system model described in Section 5.2 was used. For most static and dynamic loads on the torus shell, the coupled torus/vent system model described in Section 5.1 was used. In addition, supplemental computer and hand analyses were performed for many of the structural components to evaluate local effects.

Based on the acceptance criteria described in Section 2.2, it was possible to identify a set of six event combinations which were potentially limiting for most components. These load combinations are shown in Table 6.0-1. These six cases correspond to six of the columns in Table 5-1 of the PUAAG (Reference 8.2.3).

Conservative techniques have been used to combine responses due to the several individual loads within a given load combination. In some cases, the maximum individual responses have been combined at the stress intensity level, or on an absolute sum basis at the reaction component level. For combinations of loads such as pool swell where mechanistic timing is known, algebraic summation of responses with proper timing was employed.

Specific information about the loads, load combinations, methods of analysis, and evaluation results for each structural component are given in the following sections. Section 6.1 covers the torus and support system, Section 6.2 covers the vent system, and Section 6.3 covers torus internal structures.

TABLE 6.0-1

SUMMARY OF LIMITING LOAD COMBINATIONS
FOR TORUS AND VENT SYSTEM COMPONENTS

PUAAG[3] LOAD CASE	DESCRIPTION	ASME SERVICE LEVEL
14	Intermediate or Small Break Accident occurring simultaneously with normal loads, an operating basis earthquake and a relief valve discharge event (IBA/SBA + EQ(O) + SRV)	A/B[1]
15	Same as 14, except the earthquake is a safe shutdown earthquake (IBA/SBA + EQ(S) + SRV)	C
18	Design Basis Accident (Pool Swell Phase), occurring simultaneously with normal loads, and an operating basis earthquake (DBA(PS) + EQ(O))	A/B[1]
20	Design Basis Accident (CO or Chugging phase), occurring simultaneously with normal loads, and an operating basis earthquake (DBA(CO/CH) + EQ(O))	A/B[1]
25	Same as 18, except the earthquake is a safe shutdown earthquake and an SRV discharge event is included (DBA(PS) + EQ(S) + SRV)	C
27	Same as 20, except the earthquake is a safe shutdown earthquake and an SRV discharge event is included (DBA(CO/CH) + EQ(S) + SRV)[2]	C

(1) ASME Code Criteria for these structures are identical for Service Levels A and B.

(2) It was determined on a mechanistic basis that SRV discharge loads could not occur simultaneously with DBA(CO/CH); however, many of the structural components were conservatively analyzed including SRV discharge stresses in this combination.

(3) Mark I Containment Program Plant-Unique Analysis Application Guide (Reference 8.2.3).

6.1 TORUS AND SUPPORT SYSTEM

Mark I Long-Term Program analyses of the torus and support system components are summarized in this section. For convenience in evaluation and presentation of results, these components have been divided into several categories, as follows:

- Torus Shell and Hoop Straps
- Torus Ring Girder
- Torus Mid-Bay Saddle
- Torus Support Columns
- Torus Sway Braces

Each of these categories is covered in the sections below. A list of the individual loads considered in the evaluation of all of these components is shown on Table 6.1-1. Other loads judged important for specific components were also evaluated. These are discussed in the pertinent sections that follow. As mentioned previously, all loads defined in Section 4.0 were initially screened using engineering judgment and scoping calculations to establish the significant loads on each component.

TABLE 6.1-1

LIST OF LOADS CONSIDERED FOR
EVALUATION OF TORUS AND SUPPORT SYSTEM

GENERAL CATEGORY	INDIVIDUAL LOADS CONSIDERED
Deadweight	Deadweight of torus steel Deadweight of vent system steel Deadweight of torus water
Earthquake (Operating Basis or Safe Shutdown)	Vertical acceleration of vent system Horizontal acceleration of vent system Vertical acceleration of torus and water Horizontal acceleration of torus and water
SRV Discharge	Bubble pressure on torus shell Discharge sparger flow reaction loads on ring girder attachment Relief valve pipe reaction load on main vent line
Intermediate or Small Break Accident	Pre-chug and post-chug harmonic pressures on torus shell Static internal pressure on torus shell Constrained thermal expansion of vent system and torus Vent system thrust load Chugging synchronous downcomer tip load
Design Basis Accident (Pool Swell Phase)	Transient pressure load on torus shell Static internal pressure on torus shell Vent system thrust load Impact and drag on vent header deflector Impact and drag on vent header Impact and drag on vent line Impact and drag on downcomers Impact and drag on SRV piping
Design Basis Accident (CO/CH Phase)	Condensation oscillation harmonic pressures on torus shell Pre-chug and post-chug harmonic pressures on torus shell Static internal pressure on torus shell Constrained thermal expansion of vent system and torus Vent system thrust load Chugging synchronous downcomer tip load

6.1.1 Torus Shell and Hoop Straps

A description of the torus shell and hoop straps is given in Section 3.1. As mentioned in that section, the hoop straps were installed on the shell as part of the Mark I Long-Term Program. In continuous welded contact with the shell, the straps help reduce radial displacements and resulting membrane stresses due to pressure loads on the shell.

6.1.1.1 Methods of Analysis

The torus shell and hoop straps were analyzed as a Class MC component and integral attachments, respectively, to the ASME Boiler and Pressure Vessel Code, Section III, Subsection NE (Reference 8.4.1) in accordance with the criteria of Section 2.2 of this report. The shell was built of full penetration welded ASME SA-212, Grade B plate, and was evaluated to the ASME Code allowable stresses of the equivalent ASME SA-516, Grade 70 material, as discussed in Section 2.3. The straps were built of full penetration welded ASME SA-516, Grade 70 plate, and are attached to the shell with continuous fillet welds.

The primary analytical model used to evaluate the torus shell was the coupled torus/vent system finite element model discussed in Section 5.1. The shell is composed of more than 1000 plate elements representing one-half of a torus bay in the model. Stresses from all shell elements were screened for several important load cases to select a set of 41 limiting element locations for complete stress evaluation. Combined element centroidal stresses and stress intensities at these locations were then computed for the six potentially limiting PUAAG (Reference 8.2.3) cases described in Table 6.0-1.

To investigate local stress gradients at structural discontinuities including the three-inch ring girder offset at the miter joint, several

detailed finite element substructure models were built and analyzed. Results from these models were used to develop extrapolation factors to predict maximum local stresses based on nearby element centroid stresses. In addition, local stresses in the shell near the ring girder due to concentrated loads on the girder were calculated using a detailed model of the ring girder. Also, local shell stresses caused by vent bellows reactions at the vent line penetration were calculated by conventional nozzle analysis methods. The limiting general and local stress intensity results were then compared to the applicable ASME Code criteria.

Results from the detailed substructure models were used to show that the stress intensities in the hoop straps were less limiting than the stress intensities in the torus shell when compared to ASME Code criteria. As a consequence, the hoop straps meet the stress criteria of the ASME Code whenever the torus shell does and an explicit evaluation of the straps for each load combination was not required.

The fillet welds attaching the hoop straps to the torus shell were evaluated for forces in the welds which occur as a result of the constraint of the torus shell by the hoop straps. The resulting shear stresses were compared to the applicable ASME Code criteria.

Separate evaluations of the finite element model stress results were made to satisfy ASME Code limits on buckling and fatigue. Compressive circumferential and longitudinal membrane stresses were tabulated for the buckling analysis. Combined primary-plus-secondary-plus-peak alternating stress intensity ranges were tabulated for fatigue.

6.1.1.2 Loading and Acceptance Criteria

Loads considered in the analysis of the torus shell and hoop straps are those defined in Table 6.1-1. These loads were grouped into the six potentially limiting PUAAG load combinations listed in Table 6.0-1. For shell pressure load definitions, such as pool swell, whose magnitudes are not identical in every torus bay, the worst-loaded bay was analyzed. (Note: This evaluation does not include the loads on the ring girders from the safety relief valve (SRV) discharge piping. The evaluation of the shell for these loads is not complete.) As mentioned in Section 6.0, local piping nozzle reaction loads on the torus shell are evaluated separately in Reference 8.5.1.

Acceptance criteria for the torus shell were developed based on Section 2.2 and the PUAAG (Reference 8.2.3) using the ASME service levels specified for the six limiting load combinations. Stress allowables were determined from the ASME Code Section III (Reference 8.4.1). Stress intensities were classified as follows: In regions of the shell adjacent to or between straps, membrane stress intensities are general primary membrane (P_m) and bending stress intensities are secondary bending (Q). At all other structural discontinuities (the ring girder, support column attachment gussets, and saddle top flange), membrane stress intensities are local primary membrane (P_L) and bending stress intensities are secondary bending (Q). All stresses due to thermal effects were considered secondary (Q). Material allowable stresses for the shell and hoop straps are evaluated at the maximum accident wetwell temperature of approximately 170^{o}F from the PULD (Reference 8.2.2).

6.1.1.3 Summary of Results

Table 6.1.1-1 shows a summary of the limiting calculated stresses in the torus shell except for the effect of the SRV discharge piping loads on

the ring girder. All the calculated stresses meet the applicable ASME Code limits. The results of the torus shell fatigue evaluation are presented in Section 7.0. The results of the buckling analysis showed that the shell meets the ASME Code limits.

Table 6.1.1-2 shows a summary of the limiting calculated shear stresses in the hoop strap attachment welds. All these stresses are below allowables. As discussed in Section 6.1.1.1, the stresses in the straps are less limiting than those in the shell and the acceptability of the hoop straps is indicated by the torus shell results.

TABLE 6.1.1-1

SUMMARY OF LIMITING STRESSES IN TORUS SHELL

LOCATION	TYPE OF STRESS	ASME SERVICE LEVEL	CALCULATED STRESS (ksi)	ALLOWABLE STRESS (ksi)	LOAD COMBINATION
Clean Shell	General Primary Membrane Stress Intensity (P_m)	A/B	14.3	19.3	DBA(CO) + EQ(O)
		C	14.4	35.6	DBA(CO) + EQ(S)
Shell Between Straps	General Primary Membrane Stress Intensity (P_m)	A/B	19.1	19.3	IBA(CO) + SRV + EQ(O)
		C	19.1	35.6	IBA(CO) + SRV + EQ(S)
Shell at Edge of Straps	Primary + Secondary Stress Intensity (P_m + Q)	A/B	50.3	69.5	IBA(POCH) + SRV + EQ(O)
Shell at Tip of Straps	Local Primary Membrane Stress Intensity (P_L)	A/B	22.2	29.0	DBA(POCH) + EQ(O)
		C	22.2	53.4	DBA(POCH) + EQ(S)
Shell at Saddle Flange Edge	Local Primary Membrane Stress Intensity (P_L)	A/B	17.6	29.0	IBA(POCH) + SRV + EQ(O)
		C	30.9	53.4	DBA(PS) + SRV + EQ(S)
	Primary + Secondary Stress Intensity (P_L + Q)	A/B	57.4	69.5	IBA(POCH) + SRV + EQ(O)
Shell at Saddle Flange Tips	Local Primary Membrane Stress Intensity (P_L)	A/B	15.0	29.0	DBA(CO) + EQ(O)
		C	15.1	53.4	DBA(CO) + EQ(S)
	Primary + Secondary Stress Intensity (P_L + Q)	A/B	24.2	69.5	DBA(CO) + EQ(O)
Shell at Ring Girder	Local Primary Membrane Stress Intensity (P_L)	A/B	24.2	29.0	IBA(POCH) + SRV + EQ(O)
		C	31.7	53.4	DBA(PS) + SRV + EQ(S)
	Primary + Secondary Stress Intensity (P_L + Q)	A/B	67.7	69.5	DBA(POCH) + EQ(O)
Shell at Column Connection	Local Primary Membrane Stress Intensity (P_L)	A/B	15.5	29.0	DBA(POCH) + EQ(O)
		C	23.1	53.4	DBA(PS) + SRV + EQ(S)
	Primary + Secondary Stress Intensity (P_L + Q)	A/B	21.4	69.5	IBA(POCH) + SRV + EQ(O)
Shell at Vent Penetration	Local Primary Membrane Stress Intensity (P_L)	A/B	8.4	29.0	IBA(CO) + SRV + EQ(O)
		C	8.4	53.4	IBA(CO) + SRV + EQ(S)
	Primary + Secondary Stress Intensity (P_L + Q)	A/B	10.7	69.5	SBA(PRCH) + SRV + EQ(O)

TABLE 6.1.1-2

SUMMARY OF SHEAR STRESSES IN
HOOP STRAP ATTACHMENT FILLET WELDS FOR
LIMITING LOAD COMBINATION (IBA + POCH + EQ)

LOCATION	CALCULATED STRESS (ksi)	ALLOWABLE STRESS (ksi)
Fillet Welds not at Hoop Strap Ends	11.9	15.0
Fillet Welds at Full Strap Ends	10.8	15.0
Fillet Welds on Tapered Strap Ends	12.0	15.0
Fillet Welds on Squared Strap Ends	12.2	15.0

6.1.2 Torus Ring Girder

A description of the torus ring girder is given in Section 3.1. The ring girder is an integral part of the torus and its support structure and is stressed as a result of loads on the torus shell. In addition, there are six systems attached to the ring girder which also cause stresses in the ring girder. These are the following:

- Vent Header Support Columns
- Catwalk
- Torus Spray Header Piping System
- Core Spray Suction Header Horizontal Restraint Snubber
- Demineralizer Relief Valve Discharge Piping System
- Safety Relief Valve Discharge Piping System

Figures 6.1.2-1 through 6.1.2-7 show which of the 20 ring girders are used to support these systems and the cross-sectional view of the ring girders with the systems attached.

6.1.2.1 Methods of Analysis

The torus ring girder was analyzed as a Class MC integral attachment to the ASME Boiler and Pressure Vessel Code, Section III, Subsection NE (Reference 8.4.1) in accordance with the criteria of Section 2.2, herein. The flange and web were each built of full penetration welded ASME SA 212, Grade B plate, and were evaluated to the ASME Code allowable stresses of the equivalent ASME SA 516, Grade 70 material, as discussed in Section 2.3 of this report. The flange was attached to the web with continuous 5/16-inch leg fillet welds. The web was attached to the torus shell with continuous 5/16-inch leg fillet welds.

Two primary analytical models were used to evaluate the torus ring girder and its attachment welds. The first model was the coupled torus/vent system finite element model discussed in Section 5.1. This model was used to evaluate the stresses caused by in-plane loads applied to the shell and ring girder. (In-plane loads are defined as pressures, forces, and moments whose effects are primarily to cause the ring girder to move in the plane of the ring girder; e.g., internal pressure, deadweight of water and steel, vertical forces from the vent header support columns, etc.).

The second analytical model used to evaluate the ring girder was a finite element model of a ring girder attached to some of the torus shell on either side of the ring girder. This model was used to evaluate the stresses caused by out-of-plane loads applied to the ring girder; e.g., drag loads from water going from one bay to another. This model, shown in Figure 6.1.2-8, contains about 2000 elements. The model includes the plates and gussets for the two torus support columns; these are modeled in a manner very similar to the analytical model used for in-plane loads (discussed in Section 5.1). The ring girder is modeled with plate elements and is offset 3 inches from the miter joint consistent with the design of the torus.

6.1.2.2 Loading and Acceptance Criteria

The loads defined in Table 6.1-1 were considered in the analysis of the ring girder. In addition, the reaction loads imposed on the ring girder by the six systems attached to it were also considered. The effect of each of these individual load cases was evaluated in a scoping analysis and it was found that the stresses in the ring girder were significantly higher at the outside vent header support column during design basis accident (DBA) pool swell (PS) than for any other location or load combination. (Note: This evaluation was limited to the 14 ring girders not supporting the safety relief valve (SRV) discharge piping. The

evaluation of the ring girders for the SRV discharge piping system loads is not complete.) Based on this result, stress analyses were performed for Plant Unique Analysis Application Guide (PUAAG), (Reference 8.2.3), load combination No. 25 (DBA(PS) + EQ(S) + SRV) for a typical ring girder at a cross section where the outside vent header support column is attached. These analyses also included the effects of the core spray suction header horizontal restraint snubbers so that this analysis was bounding for all of the ring girders except the six which support the SRV discharge piping system.

Acceptance criteria for the torus ring girder were based on Section 2.2 and the PUAAG for the ASME Service Level A/B. This is a more restrictive service level than required for PUAAG load combination No. 25; however, this was done to make the one stress analysis applicable to all the other load combinations. All the stress intensities, including any secondary effects in the ring girder and welds, were considered general primary membrane (P_m) or primary membrane plus bending ($P_m + P_b$). Material allowable stresses for the ring girder were evaluated at the maximum accident wetwell temperature of about 170°F as specified in the PULD (Reference 8.2.2).

6.1.2.3 Summary of Results

Table 6.1.2-1 shows a summary of the calculated stresses in the torus ring girders except those supporting the SRV discharge piping system. The stresses in the table are for the most highly stressed location (near the outside vent header support column) due to the most severe load combination (PUAAG load combination No. 25: DBA (PS) + EQ(S) + SRV). All the calculated stresses meet the applicable ASME Code limits. The results of the torus ring girder fatigue evaluation are presented in Section 7.0.

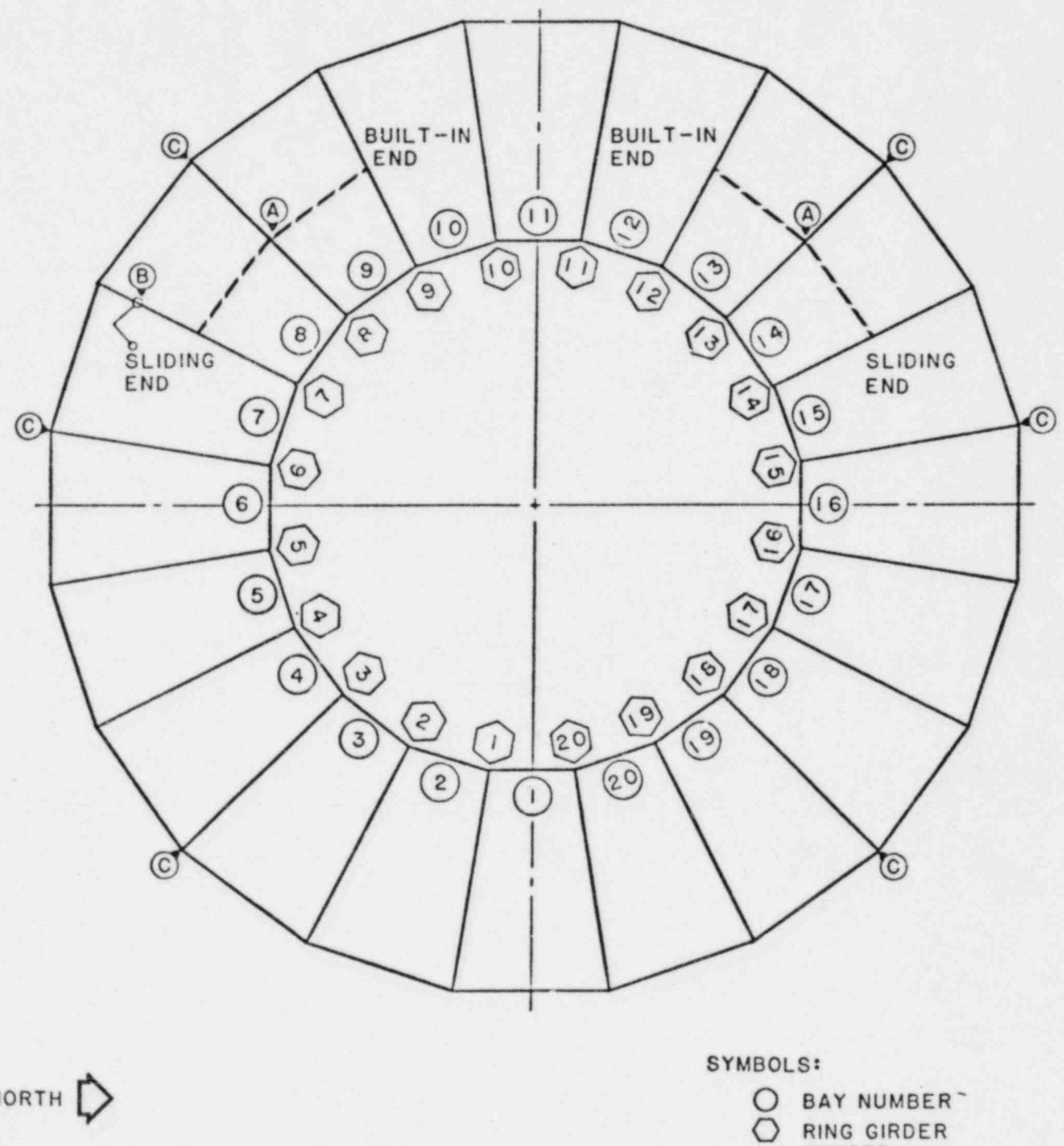

FIGURE 6.1.2-1

OYSTER CREEK TORUS
PLAN VIEW
SYSTEMS WHICH ATTACH TO RING GIRDERS

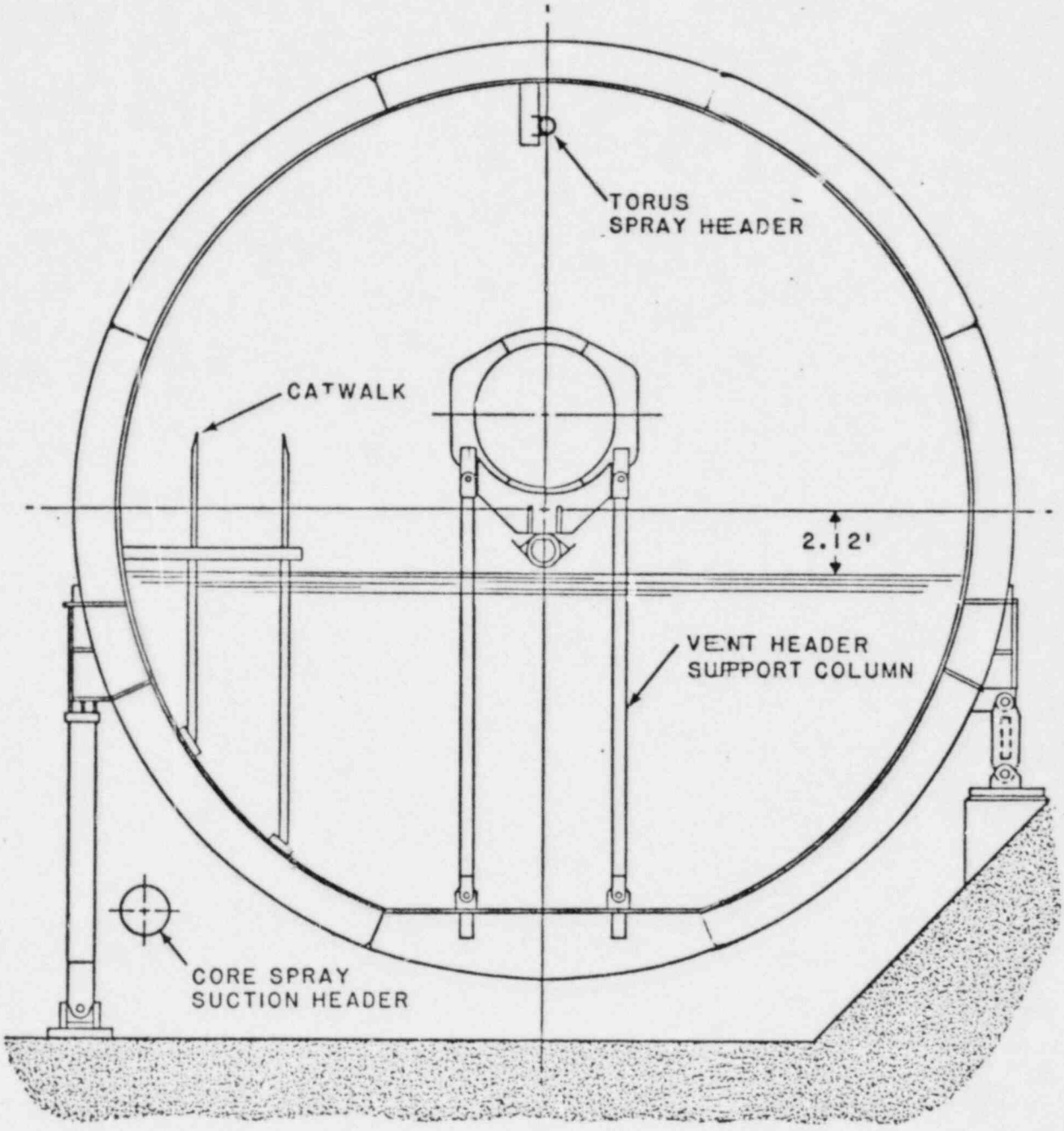

FIGURE 6.1.2-2

OYSTER CREEK TORUS
SYSTEMS ATTACHED TO TYPICAL RING GIRDER

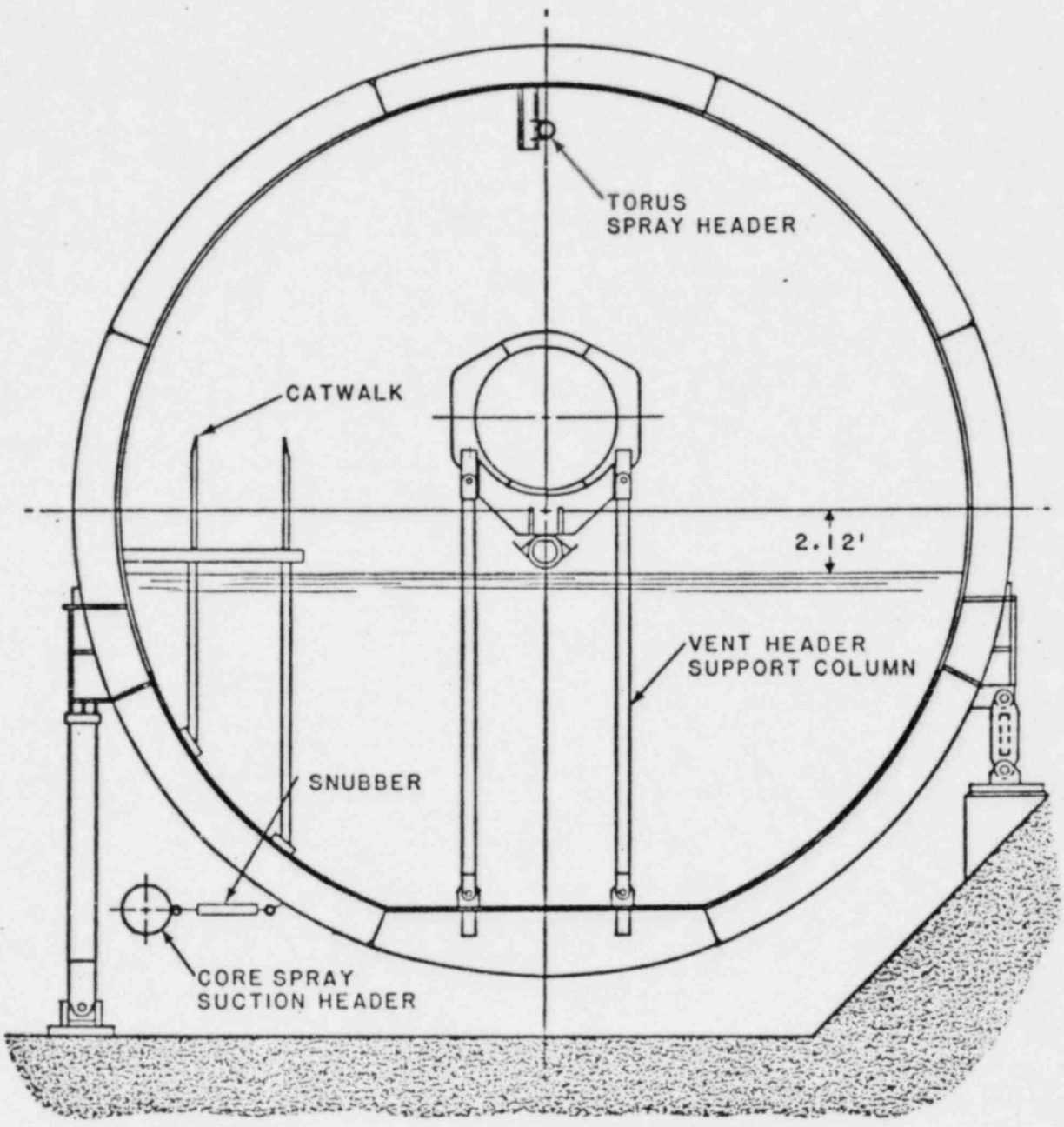

FIGURE 6.1.2-3

OYSTER CREEK TORUS
SYSTEMS ATTACHED TO RING GIRDER
NUMBERS 3,6,15 AND 18

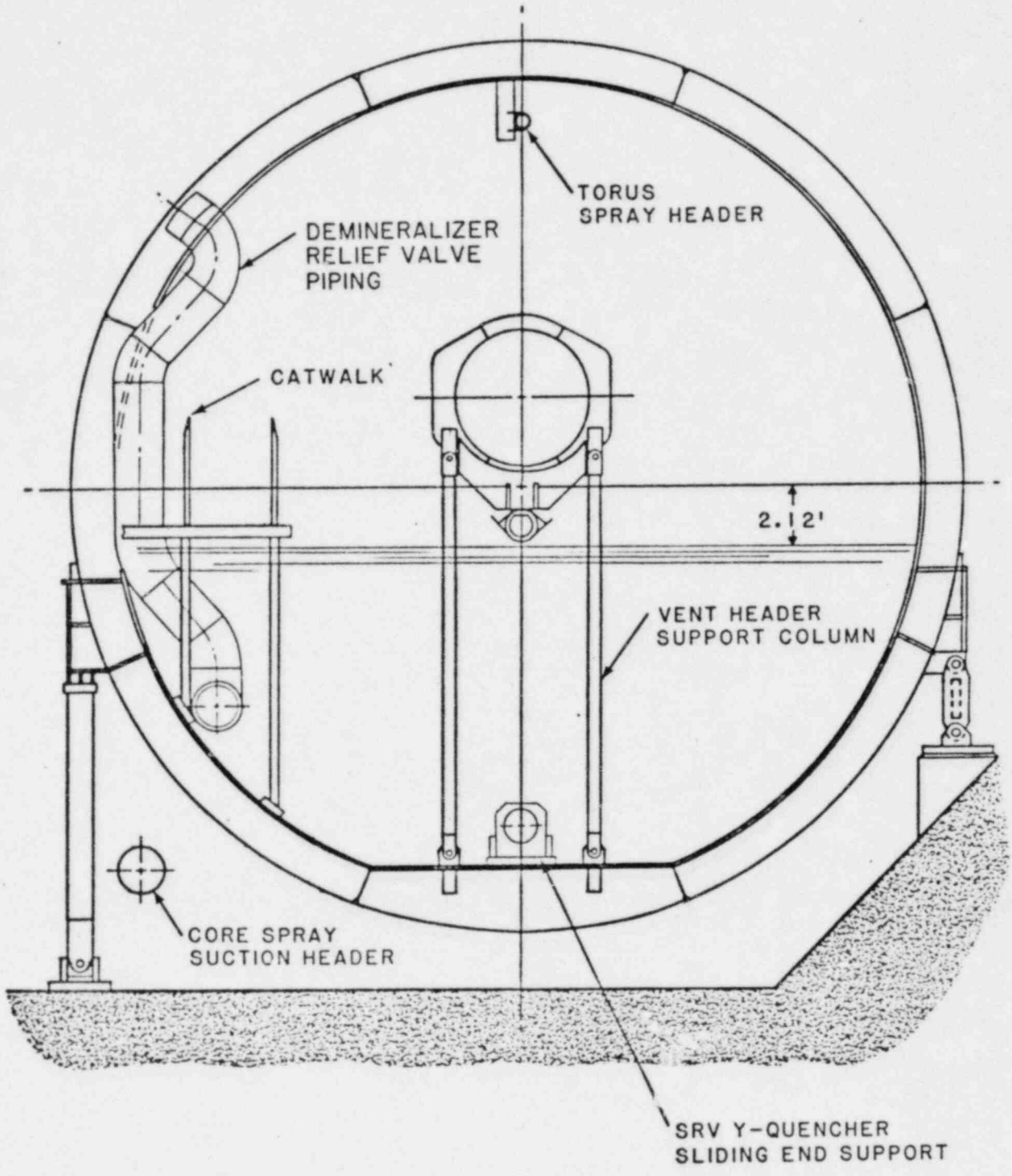

FIGURE 6.1.2-4

OYSTER CREEK TORUS
SYSTEMS ATTACHED TO RING GIRDER
NUMBER 7

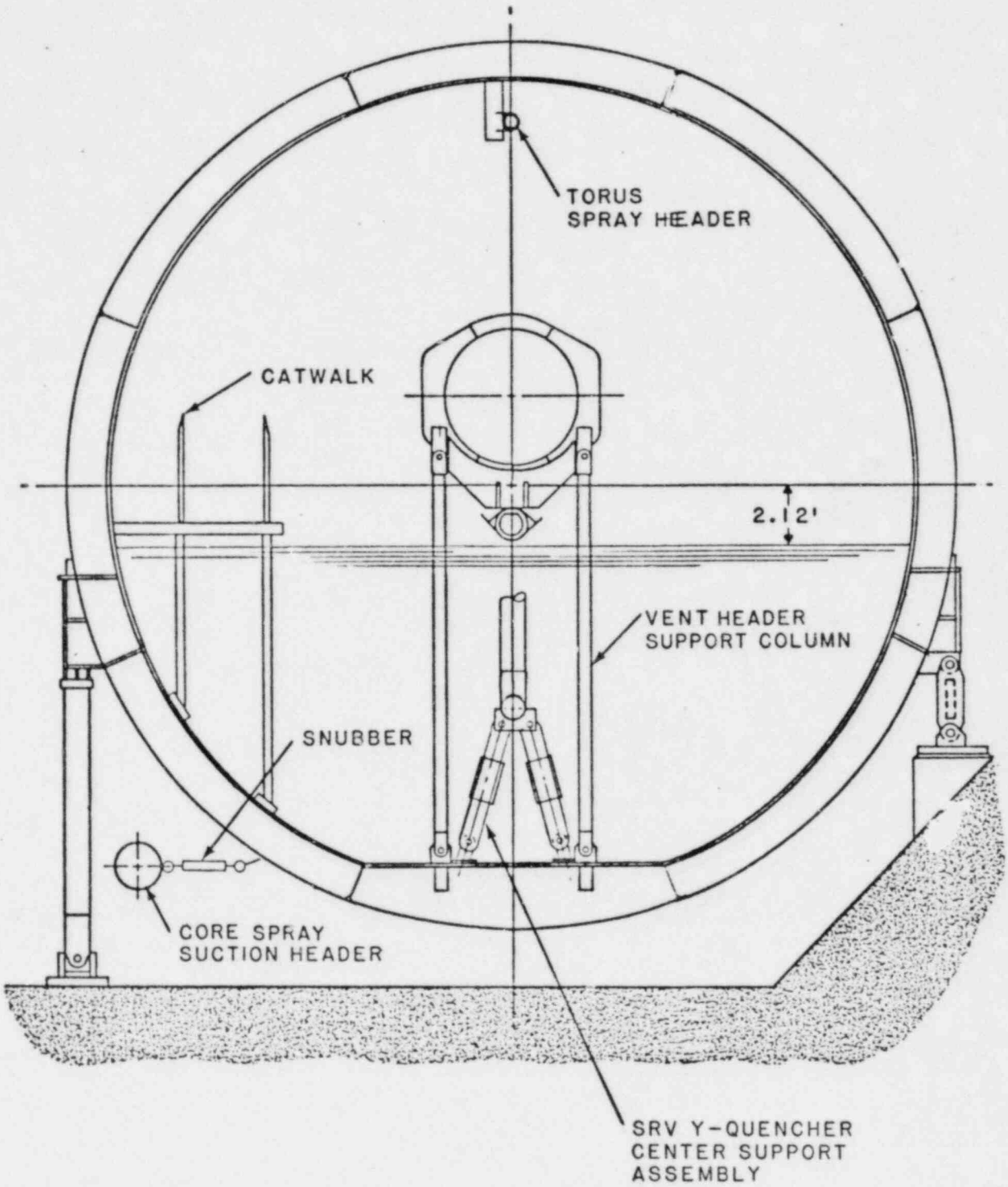

FIGURE 6.1.2-5

OYSTER CREEK TORUS
SYSTEMS ATTACHED TO RING GIRDER
NUMBERS 8 AND 13

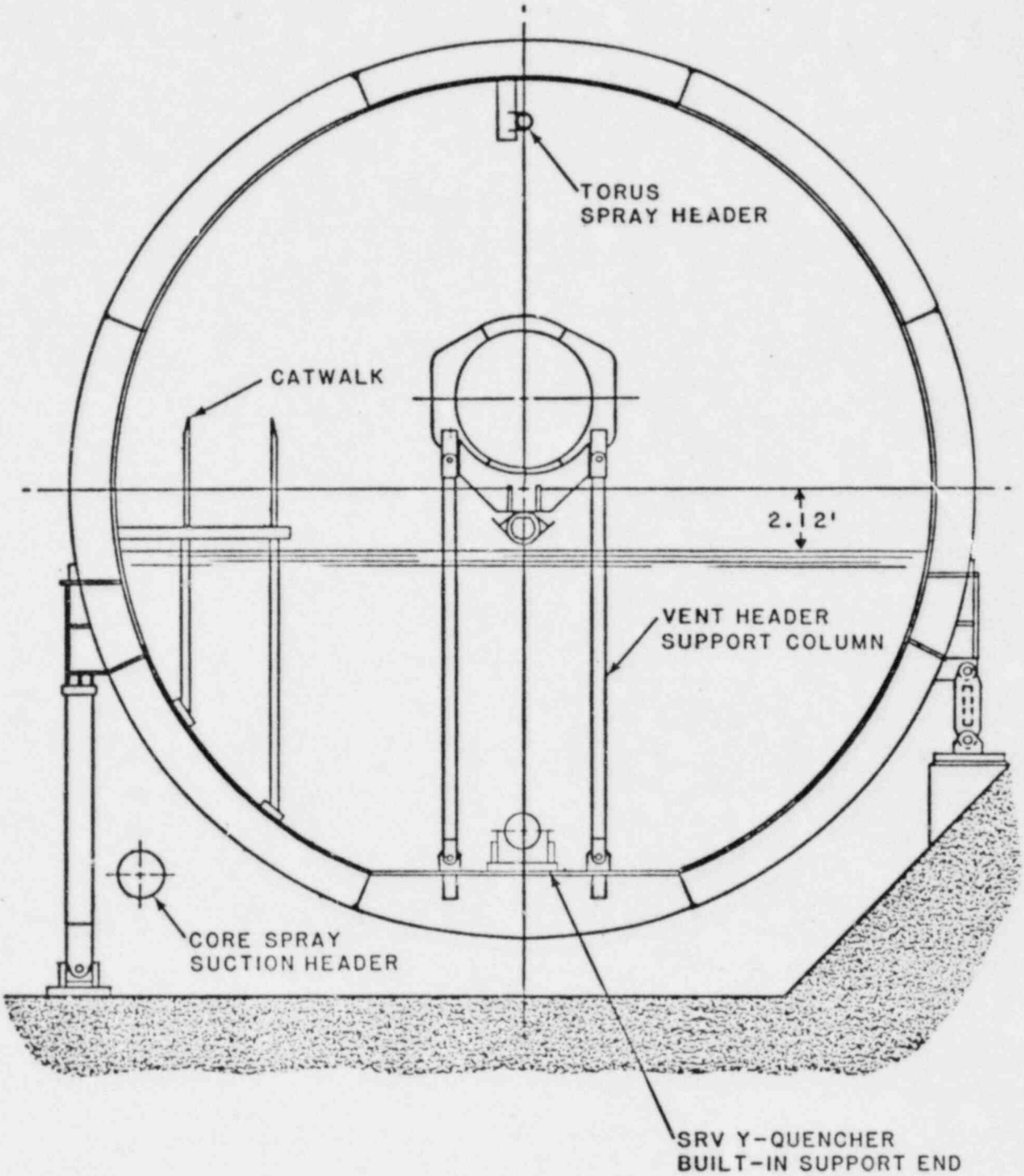

FIGURE 6.1.2-6

OYSTER CREEK TORUS
SYSTEMS ATTACHED TO RING GIRDER
NUMBERS 9 AND 12

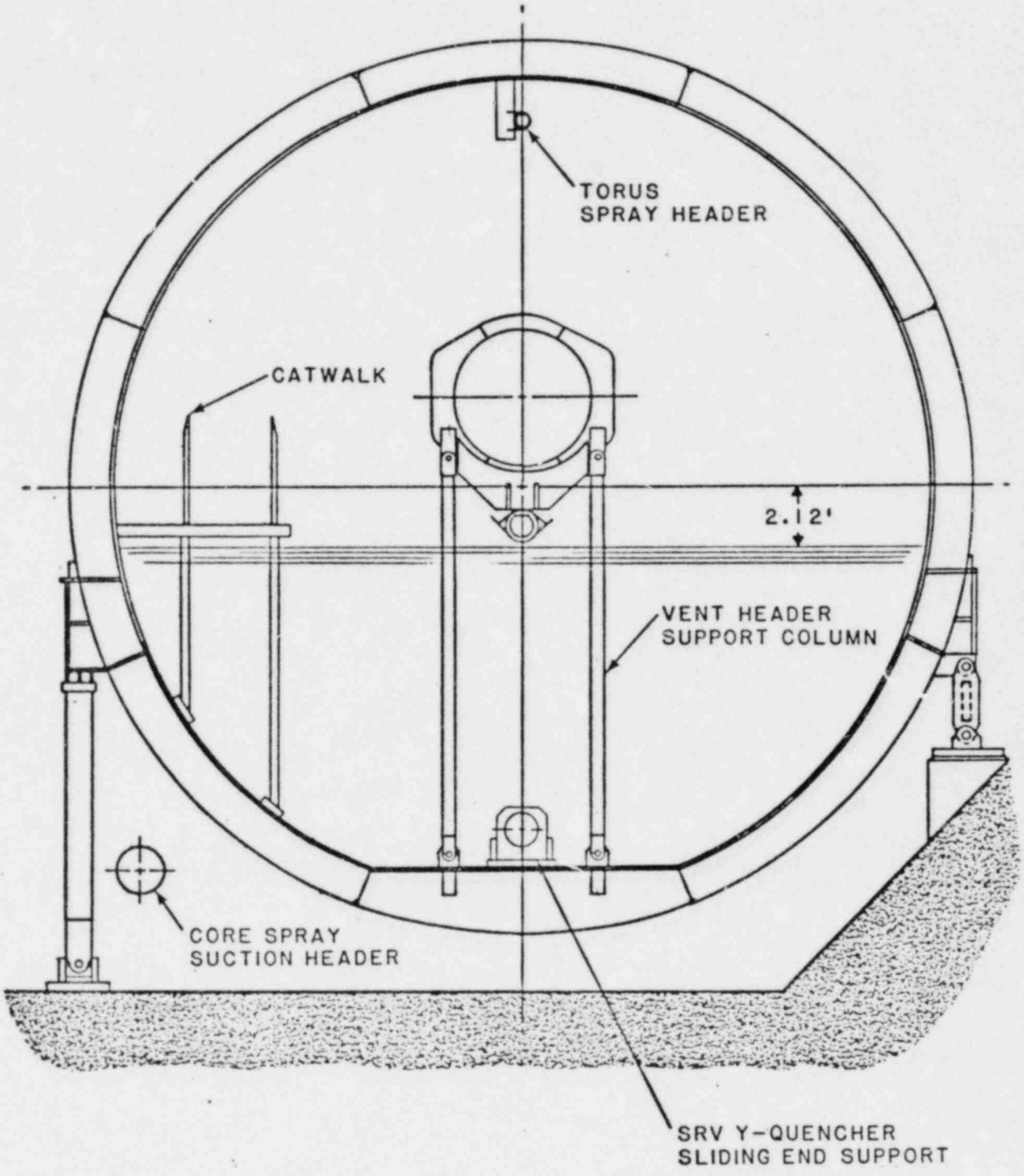

FIGURE 6.1.2-7

OYSTER CREEK TORUS
SYSTEMS ATTACHED TO RING GIRDER
NUMBER 14

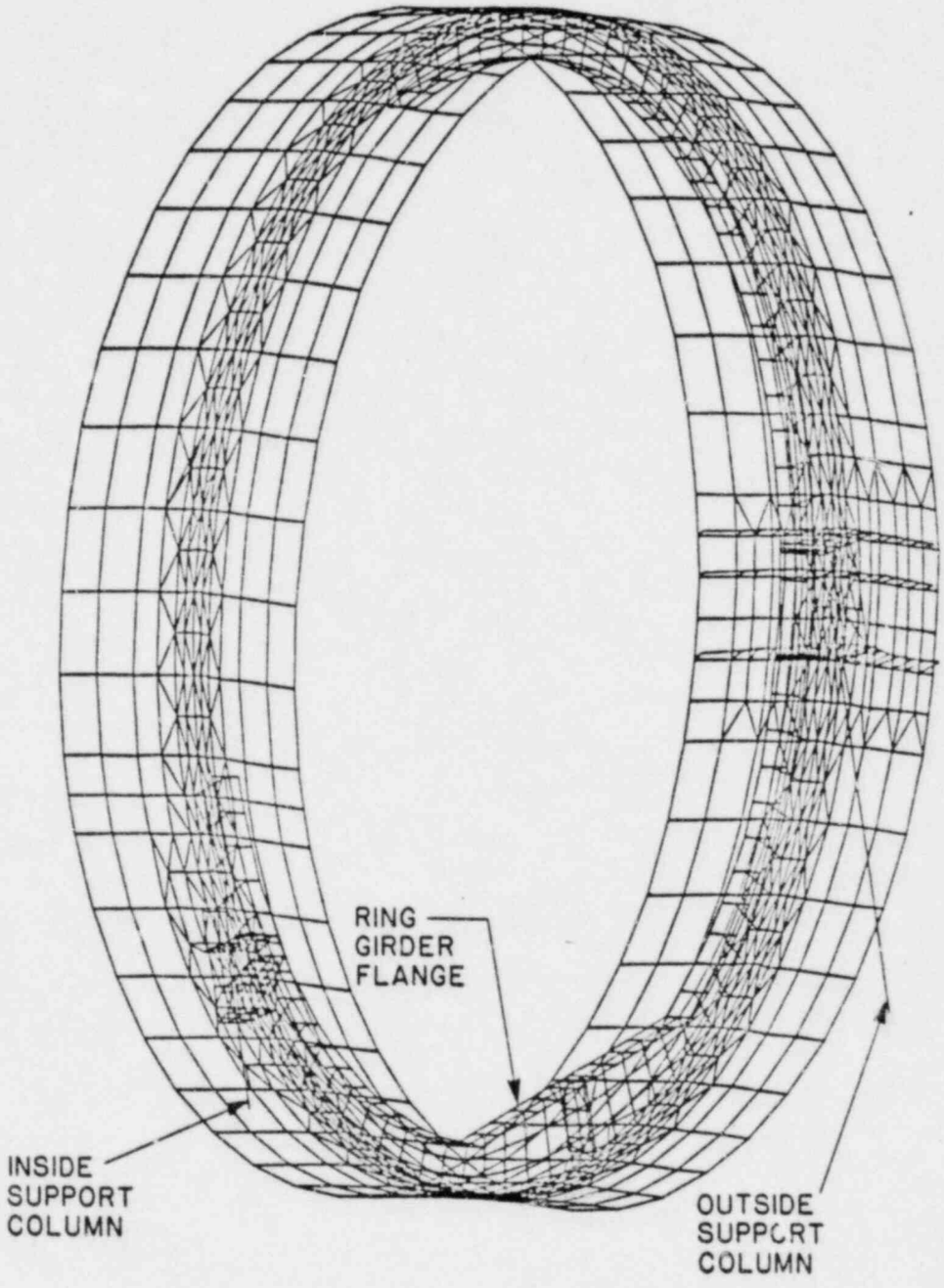

FIGURE 6.1.2-8

OYSTER CREEK TORUS
RING GIRDER FINITE ELEMENT MODEL
FOR OUT-OF-PLANE LOADS

TABLE 6.1.2-1

SUMMARY OF LIMITING STRESSES IN TORUS RING GIRDER AND ATTACHMENT WELDS
FOR THE 14 RING GIRDERS NOT SUPPORTING THE SAFETY RELIEF VALVE DISCHARGE PIPING SYSTEM

LOCATION	TYPE OF STRESS	ASME SERVICE LEVEL	CALCULATED STRESS (ksi)	ALLOWABLE STRESS (ksi)
Web-at-the-Shell	General Primary Membrane Stress Intensity (P_m)	A/B	5.4	19.3
	Primary Membrane Plus Bending Stress Intensity ($P_m + P_b$)	A/B	26.8	29.0
Web-at-the-Flange	General Primary Membrane Stress Intensity (P_m)	A/B	9.0	19.3
	Primary Membrane Plus Bending Stress Intensity ($P_m + P_b$)	A/B	24.3	29.0
Flange at its Edge	General Primary Membrane Stress Intensity (P_m)	A/B	12.8	19.3
	Primary Membrane Plus Bending Stress Intensity ($P_m + P_b$)	A/B	23.7	29.0
Web-to-Shell Weld	Primary Shear Stress	A/B	14.1	15.0
Web-to-Flange Weld	Primary Shear Stress	A/B	8.7	15.0

6.1.3 Torus Mid-Bay Saddle

The torus mid-bay saddle is composed of two subassemblies: the saddle structure and the saddle anchorage. The saddle structure geometry is shown in Figure 6.1.3-1. The saddle anchorage geometry is shown in Figure 6.1.3-2. As described in Section 3.1, the saddle is free to slide radially on Lubrite pads to permit unrestrained thermal expansion. Net vertical loads on the torus are shared among the saddle and the support columns. The saddle was added as part of the Mark I Long-Term Program.

6.1.3.1 Methods of Analysis

The criteria of Section 2.2 require analysis of saddle components to several classifications of the ASME Boiler and Pressure Vessel Code Section III (Reference 8.4.1). The saddle top flange and attachment fillet weld to the torus shell are classified as Class MC component integral attachments to Subsection NE of Reference 8.4.1. The saddle web, bottom flange, gussets, bearing plates and associated welds and bolts are classified as a Class MC Plate and Shell Type Support to Subsection NF of Reference 8.4.1. The base plates are classified as Linear Type Supports to Subsection NF of Reference 8.4.1. The anchor bolts are Drillco Maxi-bolts classified as Component Standard Supports to Subsection NF of Reference 8.4.1. Finally, the local reaction load effects on the reactor building basemat are analyzed as a ductile anchorage to the American Concrete Institute Standard 349, Appendix B (Reference 8.8.4).

A plate element representation of the saddle is included in the coupled torus/vent system finite element model described in Section 5.1. In the model, three beam elements which are free to slide horizontally

represent the saddle support connections to the anchorage at the inner and outer supports. An illustration of the saddle mesh is given in Figure 6.1.3-3.

This model was used to obtain reactions in the saddle supports for the static and dynamic load cases described in Table 6.1-1. For dynamic cases, the maximum and minimum saddle reaction forces and moments were selected to represent the entire load time history. These bounding values were combined algebraically with static load reactions to form the load combinations specified in Table 6.0-1.

These bounding combined reactions were used with hand models to evaluate the stresses in the local saddle support area, including the anchor bolts, base plate, Lubrite, bearing plates and bolts, gussets, local web, and associated welds.

The top flange, web, bottom flange and connecting welds were evaluated as a composite beam structure by considering 13 radial cross sections. Detailed element stresses were obtained from the finite element results for the hydrostatic and unit uniform internal pressure static cases. The stresses at the 13 sections were processed to determine total section shear force, axial force, and in-plane bending moments for the two cases. The saddle reactions and internal pressure conditions for the limiting load combinations in Table 6.0-1 were compared to the two static cases to develop factors on the unit section resultants. These factored resultants were then used along with the section properties to calculate section stresses.

A similar approach was followed to evaluate the top flange-to-torus shell weld. This weld is represented as a series of beam element connectors between the shell and saddle nodes in the finite element model. Complete beam reactions were obtained for the hydrostatic and unit uniform internal pressure static cases. These unit reactions were

factored to obtain limiting load combination results and processed with the weld geometry properties to determine combined stresses.

6.1.3.2 Loading and Acceptance Criteria

Loads considered in the analysis of the saddle are those defined in Table 6.1-1. These loads were grouped into the six potentially limiting PUAAG (Reference 8.2.3) load combinations listed in Table 6.0-1. For shell pressure load definitions, such as pool swell, whose magnitudes are not equal in each torus bay, the worst-loaded bay was analyzed.

Acceptance criteria for the saddle are derived based on Section 2.2 and the Code classifications for each component mentioned in Section 6.1.3.1. Material allowable stresses are evaluated at the maximum accident wetwell temperature of about 170^{o}F from the PULD (Reference 8.2.2). All plate material is ASME SA-516, Grade 70. The bolts are ASME SA-193, Grade B7 material.

6.1.3.3 Summary of Results

Tables 6.1.3-1 and 6.1.3-2 show a summary of the limiting calculated stresses in the saddle and its anchorage. All the calculated stresses meet the applicable Code limits. The results of a fatigue evaluation of the saddle top flange are presented in Section 7.0. Also, the anchor bolt anchorage design meets the requirements of ACI-349-76 (Reference 8.6.4) for a ductile anchorage.

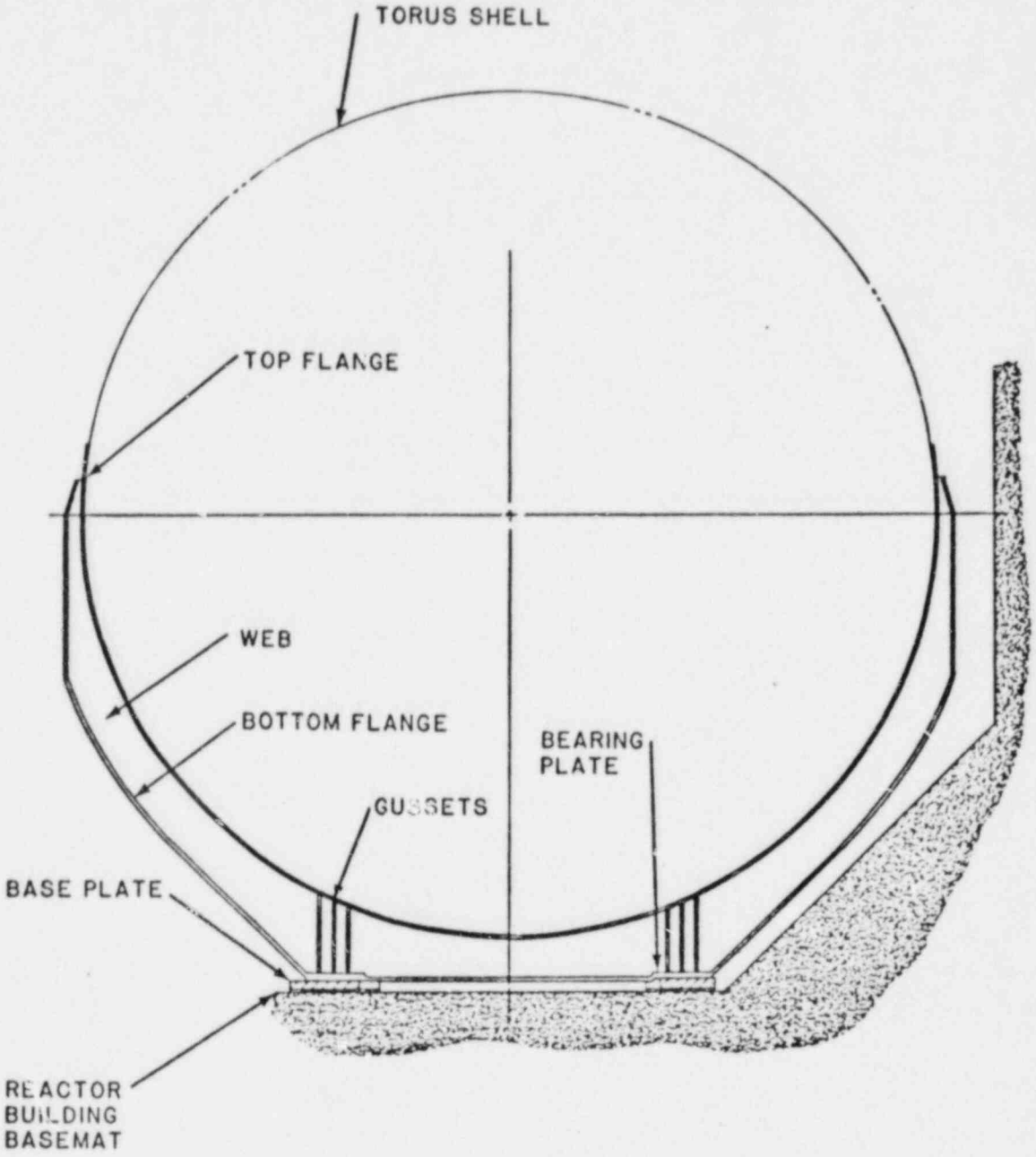

FIGURE 6.1.3-1

TORUS MID-BAY SADDLE STRUCTURE

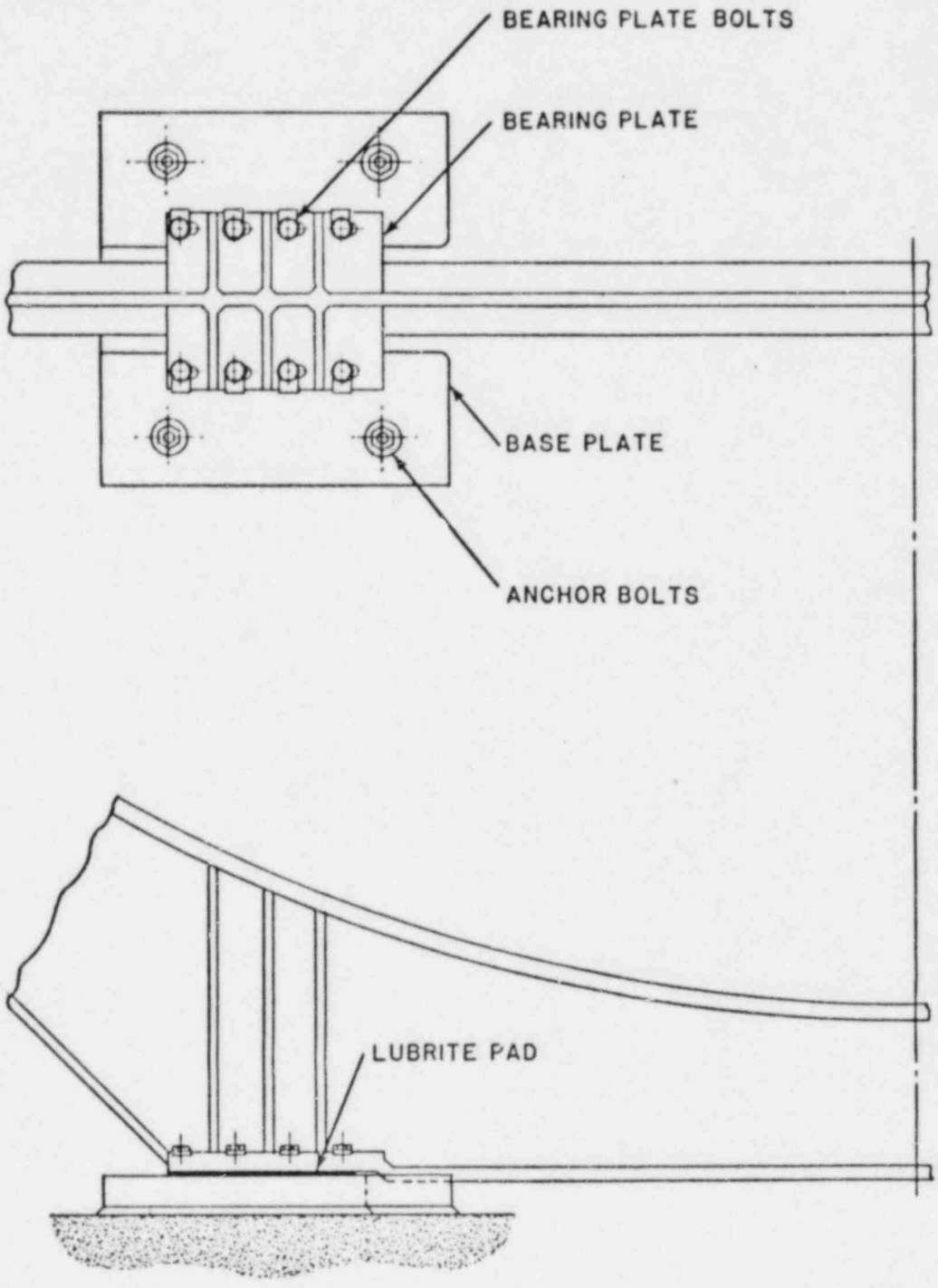

FIGURE 6.1.3-2

TORUS MID BAY SADDLE ANCHORAGE

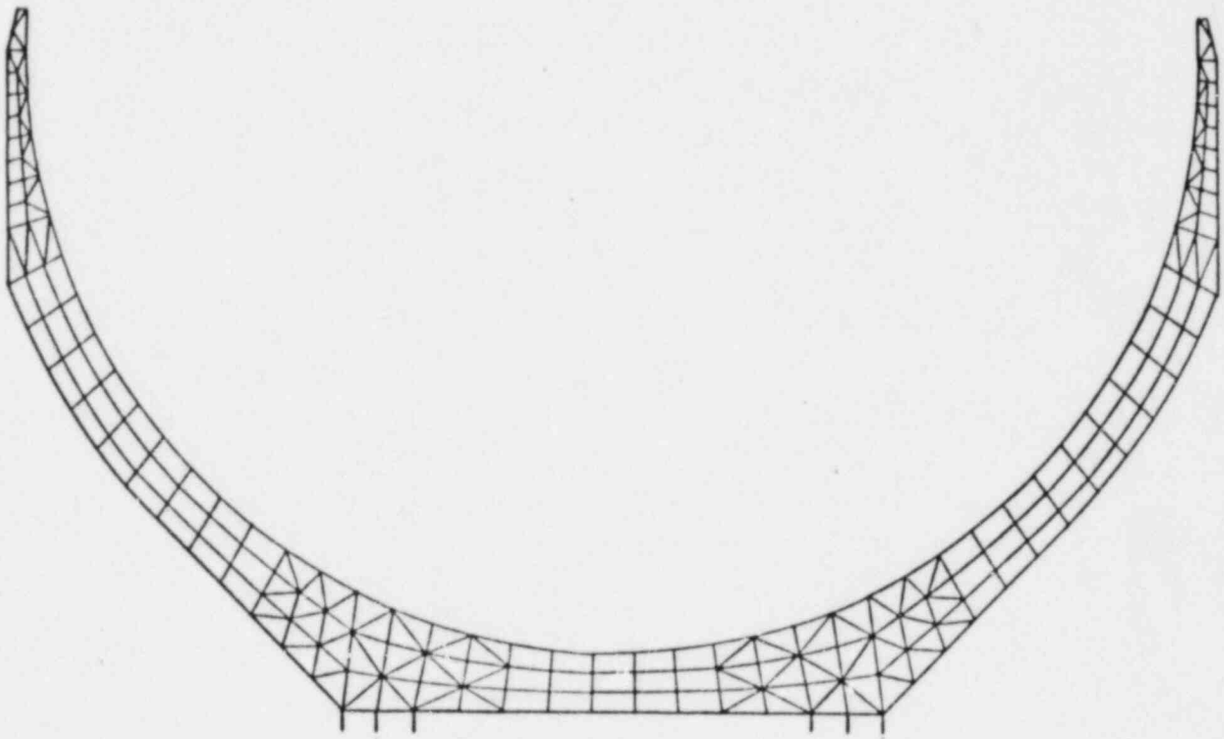

FIGURE 6.1.3-3

TORUS MID-BAY SADDLE
FINITE ELEMENT MESH

TABLE 6.1.3-1

SUMMARY OF LIMITING STRESSES IN TORUS SADDLE

LOCATION	TYPE OF STRESS	ASME SERVICE LEVEL	CALCULATED STRESS (ksi)	ALLOWABLE STRESS (ksi)	LOAD COMBINATION
Top Flange-to-Torus Shell Weld	Shear Stress on Weld Throat	A/B	11.6	15.0	DBA(CO) + EQ(O) + DW
		C	11.9	15.0	DBA(CO) + EQ(S) + DW
Top Flange	General Primary Membrane Stress Intensity (P_m)	A/B	10.4	19.3	DBA(PS) + EQ(O) + DW
		C	11.0	38.0	DBA(PS) + SRV + EQ(S) + DW
	Primary Membrane + Bending Stress Intensity ($P_m + P_b$)	A/B	10.7	29.0	DBA(PS) + EQ(O) + DW
		C	11.3	57.0	DBA(PS) + SRV + EQ(S) + DW
Radial Beam Section	Membrane Stress (40^o Toward Outside)	A/B	11.3	19.3	DBA(PS) + EQ(O) + DW
		C	12.0	23.2	DBA(PS) + SRV + EQ(S) + DW
	Membrane + Bending Stress (26^o Toward Outside)	A/B	16.0	29.0	DBA(PS) + EQ(O) + DW
		C	16.9	34.7	DBA(PS) + SRV + EQ(S) + DW
Top Flange-to-Web Weld	Primary Shear Stress	A/B/C	3.5	21.0	DBA(PS) + SRV + EQ(S) + DW
Web-to-Bottom Flange Weld	Primary Shear Stress	A/B/C	6.0	21.0	DBA(PS) + SRV + EQ(S) + DW
Bearing Plate	Membrane + Bending Stress	A/B	12.5	29.0	DBA(PS) + EQ(O) + DW
		C	17.2	34.7	DBA(PS) + SRV + EQ(S) + DW
Gussets	Membrane + Bending Stress	A/B	0.5	29.0	DBA(PS) + EQ(O) + SRV
		C	0.7	34.7	DBA(PS) + SRV + EQ(S) + DW
Support Attachment Weld	Primary Shear Stress	A/B/C	5.1	21.0	DBA(PS) + SRV + EQ(S) + DW
Bearing Plate Bolts	Tensile Stress	A/B/C	21.1	45.2	DBA(PS) + SRV + EQ(S) + DW

TABLE 6.1.3-2

SUMMARY OF LIMITING LOADS IN SADDLE ANCHORAGE

LOCATION	TYPE OF LOAD	LIMITING COMPONENT	ASME SERVICE LEVEL	CALCULATED LOAD (KIPS)	ALLOWABLE LOAD (KIPS)
Outer Baseplate	Upload	Baseplate	A/B	150.2	193.5
		Baseplate	C	207.4	257.4
	Download	Lubrite Pad	A/B	-589.0	-2112.
		Lubrite Pad	C	-627.1	-2112.
Inner Baseplate	Upload	Anchor Bolt	A/B	110.0	160.3
		Anchor Bolt	C	152.6	213.2
	Download	Lubrite Pad	A/B	-408.8	-2112.
		Lubrite Pad	C	-432.1	-2112.

Limiting Load Combinations:

Service Level A/B - DBA(PS) + EQ(O) + DW
Service Level C - DBA(PS) + SRV + EQ(S) + DW

6.1.4 Torus Support Columns

In addition to the 20 mid-bay saddles, the torus is supported by 20 outside support columns and 20 inside support columns located as shown on Figure 3.1-1. Each column is connected to the torus shell by a welded attachment which is offset three inches from the miter joint to coincide with the position of the ring girder. The outside support column, which is shown in Figure 6.1.4-1, is welded to the torus attachment at top and pinned at the base, and is supported laterally by sway bracing. The inside support column, which is shown in Figure 6.1.4-2, is pinned to the torus attachment at top and pinned at its base.

The outside support column is made of ASME SA-53, Grade B material. The components of the column attachment to the shell are made of ASME SA-212, Grade B, which is equivalent to ASME SA-516, Grade 70. The pin connecting the outside support column to the base is made of C1018 material; the anchor bolts are ASME A-36, and the anchor bolt nuts are ASTM A-307, Grade B. All other components of the outside support column analyzed in this report are made of ASTM A-201, Grade B material, which is equivalent to ASTM SA-516, Grade 60. The inside support column is made of ASTM A-201, Grade B; all other components for the inside support column are made of the same material as the corresponding components for the outside support column.

6.1.4.1 Methods of Analysis

Except for the attachments to the torus shell, the inside and outside support column assemblies were classified as linear supports and were analyzed to the requirements of Subsection NF of the ASME B&PV Code, Section III (Reference 8.4.1). Subsection NE of Reference 8.4.1 was used to analyze the attachments welded to the torus shell, since these are classified as integral attachments to the pressure boundary.

The approach used was to: (1) calculate the column reaction forces and moments for each load case, (2) calculate stresses in the columns and their attachments for unit load cases, and (3) calculate the stresses for combined load cases by appropriately scaling up the stresses for the unit load cases.

The inside and outside torus support columns were modeled as beam elements in the coupled torus/vent system computer model described in Section 5.1. This finite element model was used to obtain reactions in the support columns for the static and dynamic load cases described in Section 6.1. Other support column reactions, such as those caused by the lateral torus motion resulting from SRV discharge, pre-chug, and seismic loads, were calculated using a dynamic model consisting of the torus, the support columns, and the sway braces.

For dynamic load cases, the maximum and minimum column axial loads and bending moments (where applicable) were determined from computer data, and these bounding values were used to represent the column reactions for the entire dynamic load time history. These bounding values were combined algebraically with static and dynamic loads as required in Table 6.0-1. Loads caused by lateral torus motion were added to the column reactions.

The portion of each support column which was not welded to the torus shell was analyzed to linear support rules. Components and welds of these portions were analyzed by hand to determine the allowable tensile and compressive loads on the columns. For the outside support column, interaction formulas for bending and axial load were calculated to determine the magnitude of stress interaction.

Since the inside and outside support column attachments to the torus shell were analyzed as integral attachments to the torus shell, a finite element substructure model of these attachments was used to determine

stresses in the welds and components of each attachment for two unit load cases (torus uniform internal pressure and torus water deadweight). To determine the stress in each component or weld for each PUAAG (Reference 8.2.3) load combination, these unit load case results were multiplied by the appropriate load factors for column reactions and torus uniform internal pressure for that PUAAG combination.

6.1.4.2 Loading and Acceptance Criteria

The loads on the support columns were calculated for the static and dynamic loads listed in Table 6.1-1. In addition to these loads, reactions in the support columns were calculated for torus lateral displacements caused by earthquake, SRV, and pre-chug loads, and for the reaction in the support columns caused by the initial displacement of the base of the outside support columns which was made at the time of construction. The loads were then summed in the load combinations described in Table 6.0-1.

Acceptance criteria for the support column components which are welded directly to the torus shell are described in Subsection NE of Reference 8.4.1. For the anchor bolts and concrete bases of the support columns, applicable acceptance criteria are described in ACI-349-76 (Reference 8.6.4). Acceptance criteria for all other components and welds are obtained from Subsection NF of Reference 8.4.1

6.1.4.3 Summary of Results

Bounding combinations of stresses due to column axial load and torus internal pressure were determined for each service level. In Table 6.1.4-1, the stresses in the support column connection components resulting from these bounding combinations are presented and compared to allowables.

Stress interactions on the outside support column due to combined bending and axial loads are presented in Table 6.1.4-2 for the bounding PUAAG load combinations. The stress interactions are compared to an allowable of unity.

Peak tensile and compressive axial loads on the inside and outside support columns for each service level are listed in Table 6.1.4-3. Also listed in the table are the magnitude and description of the limiting allowable loads for tension and compression in the columns.

In summary, all components and welds of the outside and inside support columns are stressed below the allowable stress limits. Fatigue evaluation of the support columns is presented in Section 7.0 of this report.

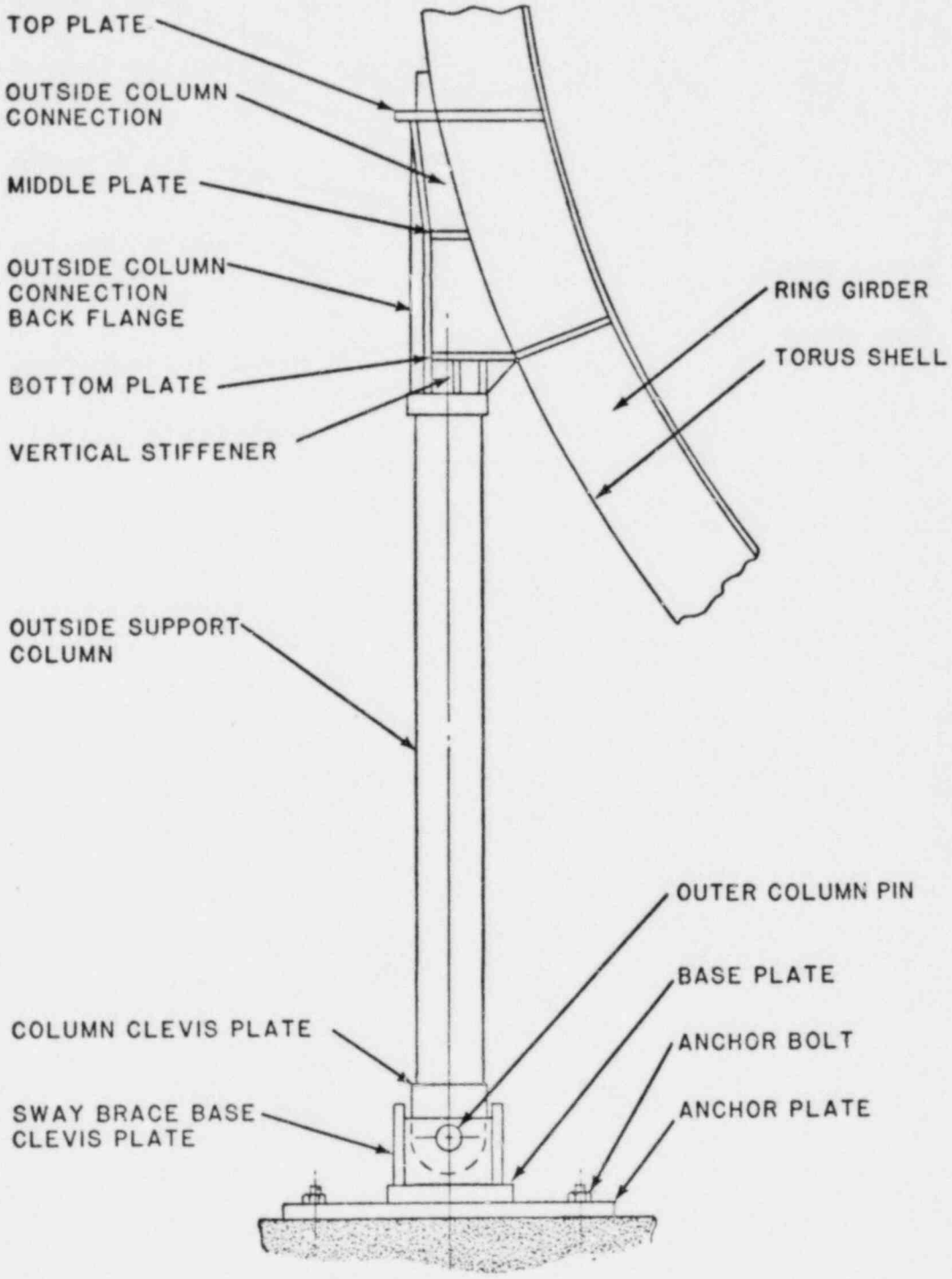

FIGURE 6.1.4-1

OUTSIDE SUPPORT COLUMN

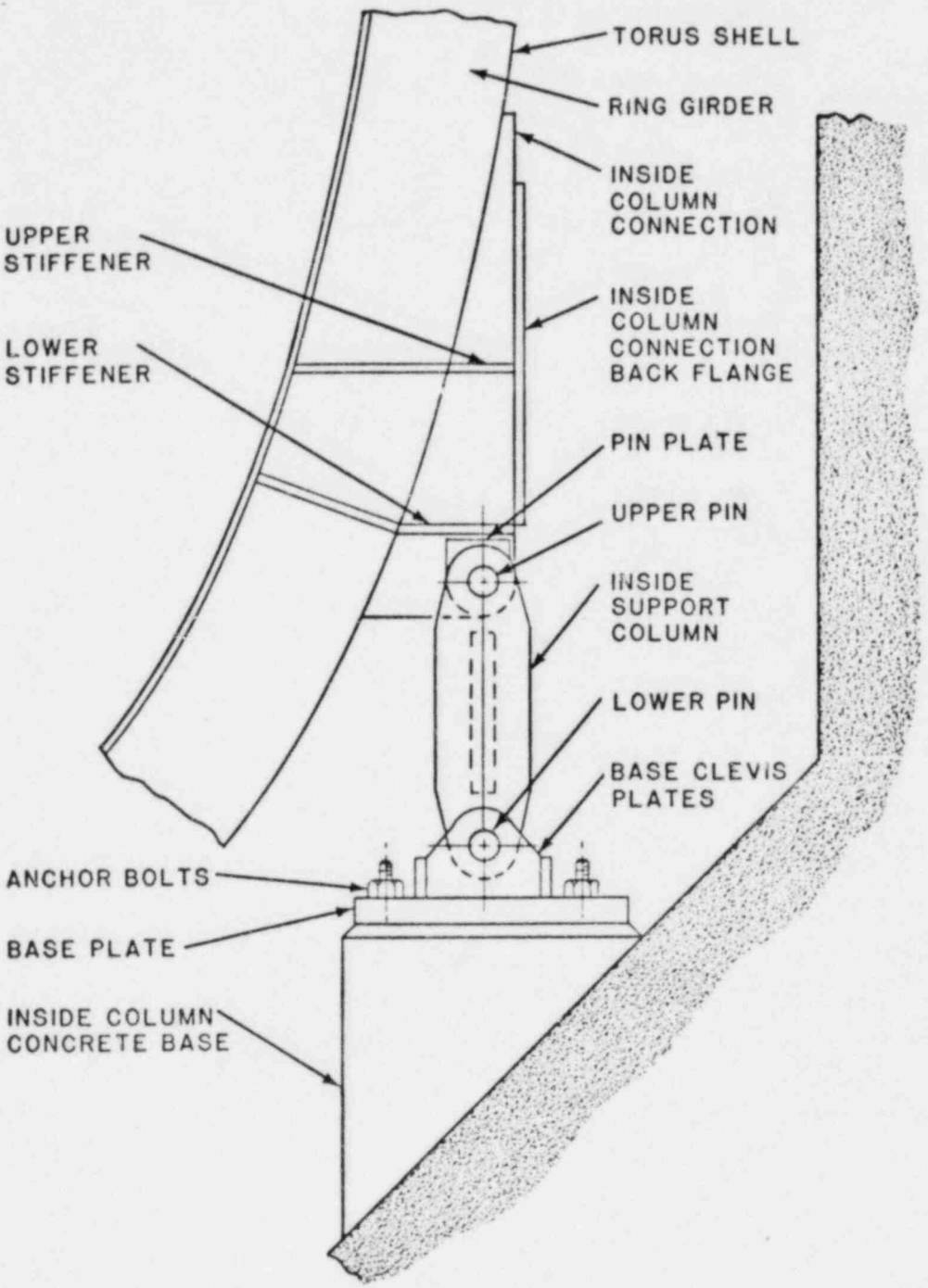

FIGURE 6.1.4-2

INSIDE SUPPORT COLUMN

TABLE 6.1.4-1

LIMITING STRESSES IN SUPPORT COLUMN ATTACHMENTS TO SHELL

	TYPE OF STRESS	ASME SERVICE LEVEL	LIMITING LOAD COMBINATION	STRESS IN HIGHEST STRESS AREA (ksi)	ALLOWABLE STRESS (ksi)
OUTSIDE SUPPORT COLUMN	Membrane Stress in Integral Attachment	A/B	DBA (CO) + OBE	15.1	19.3
		C	DBA (CO) + SSE	15.4	28.95
	Membrane + Bending Stress in Integral Attachment	A/B	DBA (Pool Swell) + OBE	18.3	28.95
		C	DBA (Pool Swell) + SRV + SSE	24.0	28.95
	Membrane Stress in Weld	A/B	DBA (Pool Swell) + OBE	12.2	15.0
		C	DBA (Pool Swell) + SRV + SSE	12.8	15.0
	Membrane + Bending Stress in Weld	A/B	DBA (Pool Swell) + OBE	19.8	22.5
		C	DBA (Pool Swell) + SRV + SSE	20.8	22.5
INSIDE SUPPORT COLUMN	Membrane Stress in Integral Attachment	A/B	DBA (CO) + OBE	17.6	19.3
		C	DBA (CO) + SSE	18.1	28.95
	Membrane + Bending Stress in Integral Attachment	A/B	DBA (Pool Swell) + OBE	25.3	28.95
		C	DBA (Pool Swell) + SRV + SSE	26.7	28.95
	Membrane Stress in Weld	A/B	DBA (Pool Swell) + OBE	13.4	15.0
		C	DBA (Pool Swell) + SRV + SSE	14.1	15.0
	Membrane + Bending Stress in Weld	A/B	DBA (CO) + OBE	17.1	22.5
		C	DBA (CO) + SSE	17.6	22.5

TABLE 6.1.4-2

MAXIMUM STRESS INTERACTION OF AXIAL
AND BENDING LOADS ON OUTSIDE SUPPORT COLUMN

BOUNDING LOAD CASE	ASME SERVICE LEVEL	MAGNITUDE OF INTERACTION	ALLOWED INTERACTION
DBA (Pool Swell) + OBE	A/B	0.89	1.00
DBA (Pool Swell) + SRV + SSE	C	0.74	1.00

TABLE 6.1.4-3

PEAK AXIAL LOADS ON THE SUPPORT COLUMNS

	TYPE OF LOAD	ASME SERVICE LEVEL	LIMITNG LOAD COMBINATION	CORRESPONDING AXIAL LOAD (kips)	ALLOWED AXIAL LOAD (kips)
OUTSIDE SUPPORT COLUMN	Tension	A/B	DBA (Pool Swell) + OBE	88	91
	Tension	C	DBA (Pool Swell) + SRV + SSE	107	112
	Compression	A/B	DBA (Pool Swell) + OBE	391	605
	Compression	C	DBA (Pool Swell) + SRV + SSE	410	807
INSIDE SUPPORT COLUMN	Tension	A/B	DBA (Pool Swell) + OBE	57	85
	Tension	C	DBA (Pool Swell) + SRV + SSE	71	93
	Compression	A/B	DBA (Pool Swell) + OBE	310	360
	Compression	C	DBA (Pool Swell) + SRV + SSE	326	480

6.1.5 Torus Sway Braces

The outside support columns are braced against lateral loads by a network of sway braces, which are shown in Figure 6.1.5-1. The sway braces experience tensile and compressive forces as a result of vertical and horizontal forces exerted on the torus outside support columns by the torus.

The sway braces and components are constructed of the following metals: sway brace body, ASME A-53, Grade B; bolts to top flange, ASME A-325; pins at base, C1018; all other components, ASME A-201, Grade B (equivalent to ASME SA-516, Grade 60).

6.1.5.1 Methods of Analysis

The sway braces were classified as linear supports and analyzed according to Subsection NF of the ASME B&PV Code, Section III (Reference 8.4.1). Reactions in the sway braces due to symmetrical loads were calculated in the coupled torus/vent system computer model discussed in Section 5.1 of this report. A separate dynamic model of the torus, support column and braces was used to determine the reactions in the sway braces due to asymmetric loads which result in a net lateral load on the torus.

As shown in Figure 6.1.5-1, the sway braces are pinned to the outside support column base at the bottom, and bolted to the outside support column attachment at the top. Allowable compressive axial loads on the sway braces were determined for the longest section of the sway brace assembly, which was assumed to be pinned at both ends. Allowable loads for other types of stresses (such as shear pullout, net section tension, bearing, etc.) were calculated for each component of the sway brace assembly. These load allowables were then compared to the applied loads in the sway brace.

6.1.5.2 Loading and Acceptance Criteria

Loads on the sway bracing are caused by a combination of vertical and horizontal loads applied to the top of the outside support column; the loads considered are described in Table 6.1-1. In addition, the sway braces are loaded by torus lateral displacements caused by earthquake, SRV and pre-chug loads, and by the reaction in the outside support column caused by the initial outside support column base displacement.

The sway brace loads due to the various static and dynamic loads were combined in the bounding load combinations described in Table 6.0-1. Since the sway braces are considered linear supports, the combined loads were compared to allowable loads for Service Levels A, B and C which were based on Subsection NF of Reference 8.4.1.

6.1.5.3 Summary of Results

For Service Level B, the bounding vertical support column load occurred during pool swell. The worst-case lateral loads, caused by SRV discharge, operating basis earthquake and pre-chug were combined with this pool swell load to give an overall sway brace load which conservatively bounded all other load combinations, since pre-chug and pool swell cannot actually occur simultaneously.

Three bounding combinations were analyzed for Service Level C loads. The first load case combined the outside column vertical load occurring during pool swell, which bounds all other vertical column loads for Level C, with the lateral torus loads caused by SRV discharge and SSE; the pre-chug lateral load was not considered since pre-chug does not occur during pool swell. The second load case analyzed combined the vertical column load caused by condensation oscillation during a DBA, which is the second highest column load for any case, with the lateral load caused by a safe shutdown earthquake. This is the only lateral

load which can mechanistically occur during DBA(CO). The third case considered was an envelope of the third highest vertical column load for any Level C combination, and the worst-case lateral load caused by pre-chug, SRV, and a safe shutdown earthquake.

Table 6.1.5-1 lists the load combinations considered and the resulting sway brace axial column loads. The sway brace allowable axial load is also listed. As seen in the table, the sway braces are loaded below the allowable loads. Fatigue evaluation of the sway braces is considered in Section 7.0 of this report.

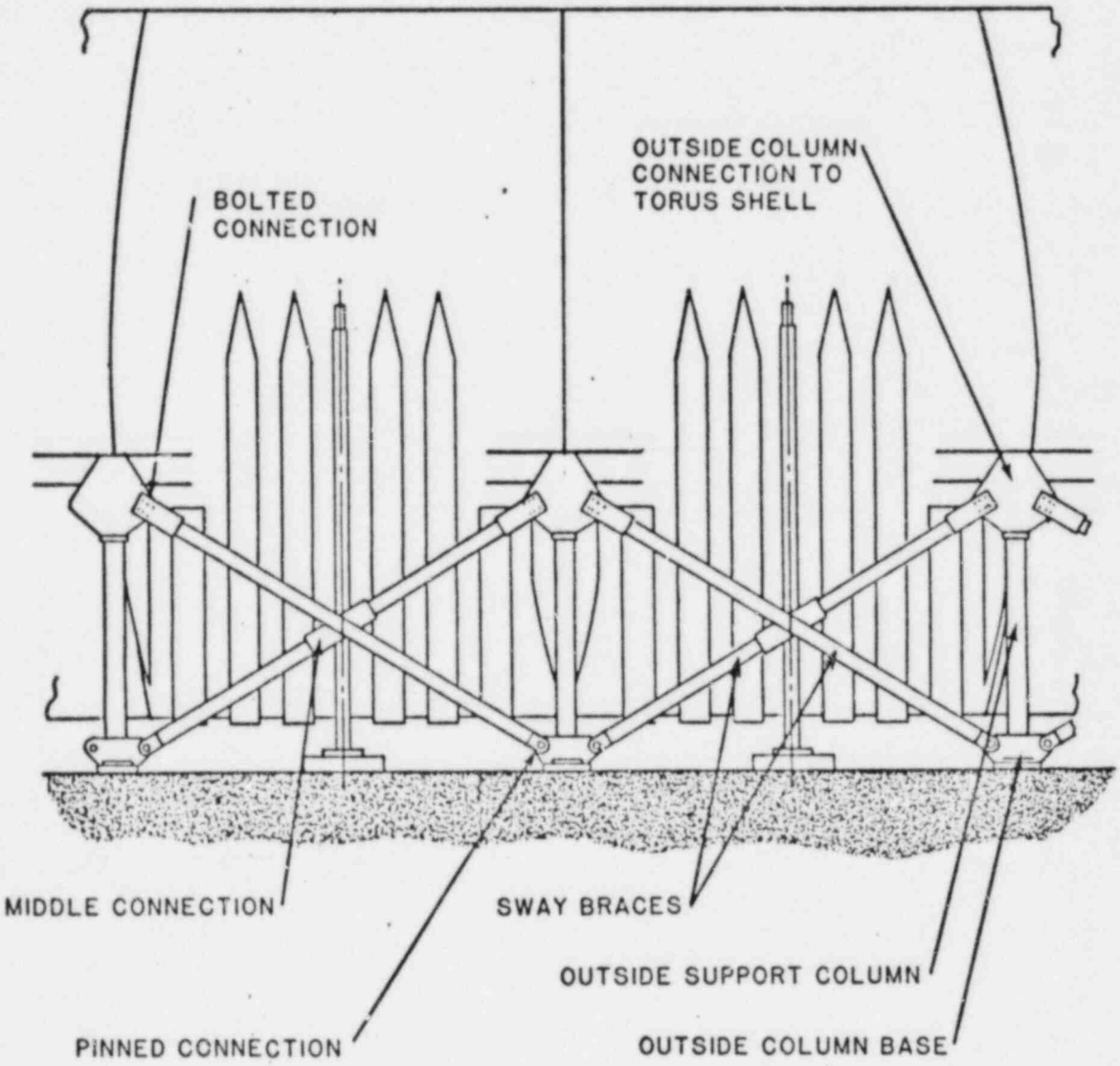

FIGURE 6.1.5-1
SWAY BRACES

TABLE 6.1.5-1

BOUNDING LOADS ON SWAY BRACES

LOAD COMBINATION	ASME SERVICE LEVEL	CALCULATED SWAY BRACE AXIAL LOAD (kips)	ALLOWABLE SWAY BRACE AXIAL LOAD (kips)
DBA (Pool Swell) + OBE + SRV + Static loads + Lateral Loads due to OBE, SRV and Pre-chug	A/B(1)	140	155(2)
DBA (Pool Swell) + SSE + SRV + Static Loads + Lateral Loads due to SSE and SRV	C	127	184.8(2)
DBA (CO) + SSE + Static Loads + Lateral Loads due to SSE	C	106	184.8(2)
Bounding Case of Third Highest Axial Load + Lateral Loads Caused by SSE, SRV, and Pre-chug	C	169	184.8(2)

(1) Service Levels A and B are identical for linear supports.

(2) The limiting allowable loads on the sway brace assembly listed are for sway brace column buckling.

6.2 VENT SYSTEM

A description of the Oyster Creek Vent System is provided in Section 3.2 of this report. The vent system was analyzed in accordance with the criteria defined in Section 2.2, using the loads defined in Section 4.0 of this report. For convenience in evaluation and presentation of results, the vent system has been divided into several categories, by components, as follows:

-- Vent Lines, Vent Header and Downcomers, including local features such as welds, miters and support attachments, but not including intersections
-- Vent Line/Drywell Intersection
-- Vent Line/Vent Header Intersection
-- Downcomer/Vent Header Intersection
-- Vent Line/Torus Bellows
-- Vent System Support Columns
-- Vent Header Ring Collar
-- Vent Header Deflector
-- Downcomer Braces

Each of these categories is covered individually in the sections below. Each section contains a description of the methods of analysis, the individual loads and load combinations which were considered, the structural acceptance criteria, and the results of the evaluations.

6.2.1 Vent Lines, Vent Header and Downcomers

6.2.1.1 Methods of Analysis

The geometry of the vent lines, vent header, and downcomers is covered in Section 3.2. These components were analyzed and evaluated as Class MC vessels in accordance with Subsection NE of the ASME Boiler and Pressure Vessel Code (Reference 8.4.1).

The vent lines, vent header and downcomers were evaluated as beams with cylindrical shell cross sections. Stresses in the shell were calculated based on beam theory along with a hoop stress (due to pressure) calculated by hand. Final stress intensities were determined considering both the pressure and beam stresses. The ratio of radius to thickness (r/t) for the vent system components was sufficiently high that all the stresses described above could be treated as constant across the thickness of the shell; hence, the calculated stresses are membrane stresses and were compared with general primary membrane allowable stress values from the ASME Boiler and Pressure Vessel Code. Figure 6.2.1-1 shows how the stresses were calculated, including the equations which were used.

At discontinuities such as intersections, miter joints and support attachments, local shell bending effects were considered and appropriate stresses for comparison with both membrane and membrane plus bending allowables were determined. For the intersections (vent line/drywell, vent line/vent header, and downcomer/vent header) separate sections are contained below describing these results. For the miters and support attachments, separate structural models were formulated, and the results of the analyses are described in this section.

One loading effect which could produce local shell bending effects in the "clean" parts of the vent system is the pool swell local external pressure impact load. In accordance with the acceptance criteria

described in Section 2.2 of this report and documented in the PUAAG (Reference 8.2.3), a separate special analysis was performed to evaluate these effects, and the results of this special analysis are included in this section of the report.

The primary analytical tools which were used to calculate responses in the vent lines, vent header, and downcomers were the coupled torus/vent system model (Section 5.1) and the vent system beam model (Section 5.2). For net lateral loads such as horizontal earthquake and synchronous chugging, hand calculations were used. Analysis was performed for each individual load, and then the extreme reaction forces and moments were summed in a worst-case manner to obtain final load combinations. The exception to this general rule was the pool swell analysis, where the mechanistic time/history relationship of the loads was used in combining responses to obtain more realistic results.

6.2.1.2 Loading and Acceptance Criteria

A list of the individual loads considered in the evaluation of the vent lines, vent header and downcomers is shown in Table 6.2.1-1. As mentioned previously, this list was selected from all of the loads defined in Section 4.0 using engineering judgment and scoping calculations to determine which loads had a significant effect on the vent system.

Acceptance criteria for the vent system were developed based on Section 2.2 of this report and the PUAAG (Reference 8.2.3). Specifically, as described previously, it was found that six limiting load combinations could be identified for analysis purposes (Table 6.0-1). The ASME service level for each of these six cases is shown on Table 6.0-1. Stress allowables for different stress classifications were determined directly from Section III of the ASME Boiler and Pressure Vessel Code (Reference 8.4.1) for each service level. In

the clean sections of the vent line, vent header and downcomers, calculated stresses were compared to a general primary membrane stress allowable of 19.3 ksi (Service Level A/B) or 33.3 ksi (Service Level C). Near miter joints and support attachments, calculated membrane stresses were compared with a primary local membrane stress allowable of 29.0 ksi (Service Level A/B) and 50.0 ksi (Service Level C); membrane plus bending stresses were compared with a primary plus secondary stress range allowable of 66.6 ksi (Service Level A/B). Primary plus secondary stresses are not considered for Service Level C in accordance with the ASME Code. The allowable values of stress are based on the maximum drywell temperature which occurs during all Mark I loading conditions ($340^{o}F$).

6.2.1.3 Summary of Results

Limiting values of calculated general primary membrane stress in the vent lines, vent header and downcomers are shown in Table 6.2.1-2. Also shown on this table is the allowable value for general primary membrane stress for these load combinations. As can be seen in Table 6.2.1-2, the limiting stresses are within the allowable values. It was determined that no primary bending stresses exist at these portions of the vent lines, vent header and downcomers; hence, the membrane plus bending allowable stress values are implicitly satisfied by the general primary membrane stress comparison.

Table 6.2.1-3 contains a summary of the maximum compressive hoop and longitudinal stresses in the vent lines, vent header and downcomers. Allowable values for these stresses, which were determined from stability (buckling) considerations, are also shown on this table. The maximum stresses are less than the allowable values.

A summary of limiting calculated stresses at the vent line miter joint, the vent header miter joint, and the downcomer miter joints is shown in

Table 6.2.1-4. In this table both primary local membrane stress and primary plus secondary stress range are shown. Allowable stress values are also shown on the table. As can be seen, the limiting calculated miter joint stresses are within the allowable values.

A summary of limiting calculated stresses in the vent system in local regions adjacent to support attachments is shown on Table 6.2.1-5. Three locations were considered: one in the vent header near the vent support column ring collar attachment, one in the vent header near the attachment point for a brace which helps support the vent header deflector, and one in the vent line near the attachment collar for the torus/vent line bellows. The stresses in Table 6.2.1-5 include the effects of amplification, if any, of those stresses existing in the vent header or vent line at the particular location, as well as those local stresses directly caused by loads transmitted through the support. Table 6.2.1-5 also shows the allowable stress values to be compared with the calculated local membrane and membrane plus bending stresses. As can be seen in Table 6.2.1-5 the limiting calculated stresses are less than the allowable values.

Table 6.2.1-6 shows a summary of limiting calculated stresses and allowable stresses in the support welds for the three locations discussed above. As can be seen on this table, the weld stresses for the limiting load combinations are less than the allowable values.

Finally, the results of the special evaluation of the vent header for pool swell local impact pressure loading are summarized in Table 6.2.1-7. In accordance with the acceptance criteria described in Section 2.2, ASME Service Level C allowables were considered in this evaluation.

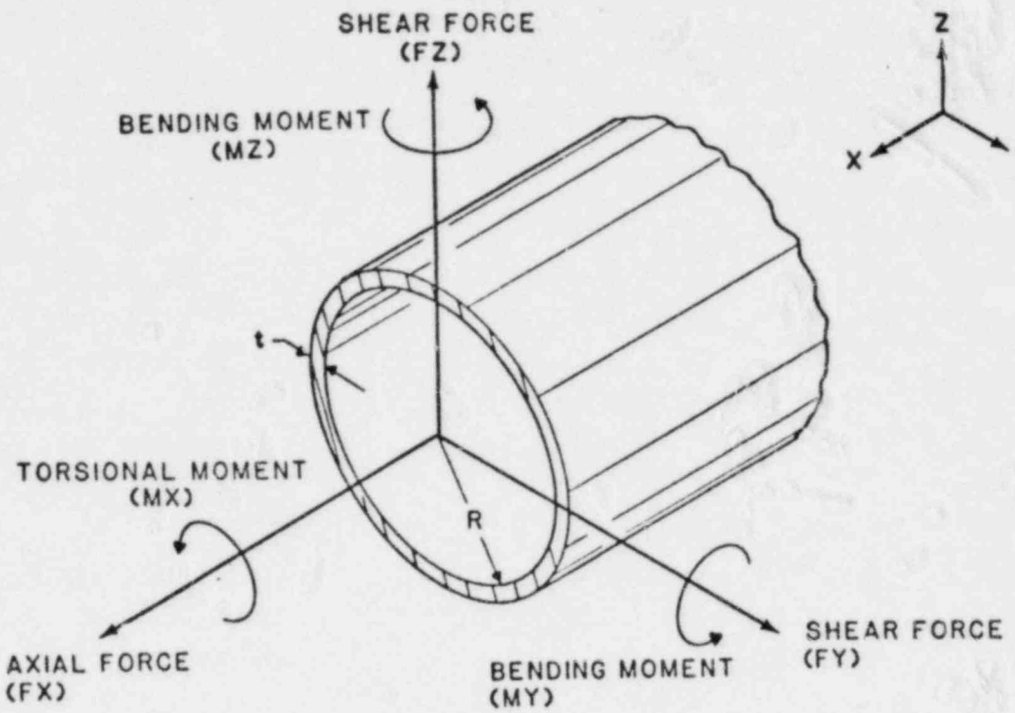

P = INTERNAL PRESSURE

σ_H = HOOP STRESS = $\frac{PR}{t}$

σ_L = LONGITUDINAL STRESS = $\frac{FX}{A} \pm \frac{\sqrt{MY^2 + MZ^2}}{Z}$

τ_{LH} = SHEAR STRESS = $\frac{MX}{2Z} \pm \frac{2\sqrt{FY^2 + FZ^2}}{A}$

A = AREA = $2\pi Rt$

Z = SECTION MODULUS = $\pi R^2 t$

STRESS INTENSITY CALCULATED ASSUMING σ_H, σ_L AND τ_{LH} EXIST AT A SINGLE POINT

FIGURE 6.2.1-1

CALCULATION OF STRESS INTENSITY IN VENT LINES, VENT HEADER AND DOWNCOMERS

TABLE 6.2.1-1

LOADS CONSIDERED IN THE EVALUATION OF
VENT LINES, VENT HEADER AND DOWNCOMERS

General Category	Individual Loads Considered
Deadweight	Deadweight of vent system steel
	Deadweight of torus steel
	Deadweight of torus water
Earthquake (Operating Basis or Safe Shutdown)	Vertical acceleration of vent system
	Horizontal acceleration of vent system
	Vertical acceleration of torus and water
SRV Discharge	Relief valve piping reaction load on the main vent line
	Bubble drag load on downcomers
	Bubble pressure on torus shell
Intermediate or Small Break Accident	Pre- and post-chugging harmonic pressures on torus shell
	Static pressure on torus shell
	Constrained thermal expansion of vent system and torus
	Vent system thrust load
	Vent system static internal pressure load
	Vent system harmonic internal pressure load
	Chugging synchronous downcomer tip load

TABLE 6.2.1-1 (Cont'd)

LOADS CONSIDERED IN THE EVALUATION OF
VENT LINES, VENT HEADER AND DOWNCOMERS

General Category	Individual Loads Considered
Design Basis Accident (Pool Swell Phase)	Impact and drag on vent header
	Impact and drag on vent line
	Impact and drag on downcomers
	Impact and drag on vent header deflector
	Impact and drag on relief valve piping
	Vent system thrust load
	Vent system internal pressure
	Transient down/up load on torus shell
	Static internal pressure in torus
Design Basis Accident (CO/CH Phase)	Condensation oscillation harmonic pressure on torus shell
	Pre- and post-chugging harmonic pressures on torus shell
	Static pressure on torus shell
	Constrained thermal expansion of vent system and torus
	Vent system thrust load
	Vent system static internal pressure load
	Vent system harmonic internal pressure load

TABLE 6.2.1-2

SUMMARY OF CALCULATED STRESSES AT LIMITING
VENT LINE, VENT HEADER AND DOWNCOMER LOCATIONS

COMPONENT	LOCATION	LOAD	ASME SERVICE LEVEL	TYPE OF STRESS	VALUE OF STRESS (ksi)	ALLOWABLE STRESS VALUE (ksi)
Vent Line	Adjacent to drywell	DBA(Pool Swell) + Seismic	A/B	General Primary Membrane (P_m)	13.2	19.3
Vent Line	Adjacent to drywell	DBA(Pool Swell) + SRV + Seismic	C	General Primary Membrane (P_m)	16.1	33.3
Vent Header	Near miter joint between bays	DBA(CO) + Seismic	A/B	General Primary Membrane (P_m)	11.5	19.3
Vent Header	Near miter joint between bays	DBA(CO) + SRV + Seismic	C	General Primary Membrane (P_m)	15.3	33.3
Downcomer	Adjacent to vent header	IBA/SBA(Chugging) + SRV + Seismic	A/B	General Primary Membrane (P_m)	4.9	19.3
Downcomer	Adjacent to vent header	DBA(Chugging) + SRV + Seismic	C	General Primary Membrane (P_m)	4.9	33.3

TABLE 6.2.1-3

SUMMARY OF LIMITING CALCULATED COMPRESSIVE STRESSES IN VENT LINES, VENT HEADER AND DOWNCOMERS

COMPONENT	LOCATION	LOAD	TYPE OF STPESS	VALUE OF STRESS (ksi)	ALLOWABLE STRESS VALUE (ksi)
Vent Line	Adjacent to drywell	DBA (Pool Swell) + SRV + Seismic	Longitudinal	9.5	11.4
Vent Line	Internal to torus	IBA/SBA/DBA (Chugging) + SRV + Seismic	Hoop	0.09	1.3
Vent Header	Near middle of nonvent bay	DBA(Pool Swell) + SRV + Seismic	Longitudinal	10.4	12.5
Vent Header	Any	SBA/IBA/DBA(Chugging) + SRV + Seismic	Hoop	0.13	1.1
Downcomer	Adjacent to vent header	SBA/IBA/DBA(Chugging) + SRV + Seismic	Longitudinal	4.0	17.0
Downcomer	Adjacent to vent header	SBA/IBA/DBA(Chugging) + SRV + Seismic	Hoop	0.26	10.0

TABLE 6.2.1-4

SUMMARY OF LIMITING CALCULATED STRESSES AT VENT SYSTEM MITER LOCATIONS

STRUCTURE	LOAD CASE	ASME SERVICE LEVEL	TYPE OF STRESS	VALUE OF STRESS (ksi)	ALLOWABLE STRESS VALUE (ksi)
Vent Line Miter	DBA(CO) + Seismic	A/B	Local Membrane (P_L)	21.0	29.0
	DBA(CO) + Seismic	A/B	Primary + Secondary ($P_L + P_b + Q$)	42.0(range)	66.6(range)
Vent Header Miter	DBA(Pool Swell) + Seismic	A/B	Local Membrane (P_L)	25.2	29.0
	DBA(CO) + Seismic	A/B	Primary + Secondary ($P_L + P_b + Q$)	45.4(range)	66.6(range)
Downcomer Miter (Bounding Case to Cover Both Upper and Lower Miter)	IBA/SBA(Chugging) + SRV + Seismic	A/B	Local Membrane (P_L)	23.0	29.0
	IBA/SBA(Chugging) + SRV + Seismic	A/B	Primary + Secondary ($P_L + P_b + Q$)	46.0(range)	66.6(range)

TABLE 6.2.1-5

SUMMARY OF LIMITING STRESSES IN VENT LINES AND VENT HEADER AT SUPPORT ATTACHMENT POINTS

LOCATION	LOAD CASE	ASME SERVICE LEVEL	TYPE OF STRESS	VALUE OF STRESS (ksi)	ALLOWABLE STRESS (ksi)
Vent Header Shell Adjacent to Ring Collar Attachment	IBA(Chugging) + SRV + Seismic	A/B	Local Membrane (P_L)	11.5	29.0
	DBA(CO) + Seismic	A/B	Primary + Secondary ($P_L + P_b + Q$)	17.9(range)	66.6(range)
Vent Header Adjacent to Deflector Diagonal Brace Attachment	DBA(Pool Swell) + Seismic	A/B	Local Membrane (P_L)	20.3	29.0
	DBA(CO) + Seismic	A/B	Primary + Secondary ($P_L + P_b + Q$)	39.6(range)	66.6(range)
Vent Line Adjacent to Bellows Collar Attachment	IBA(Chugging) + SRV + Seismic	A/B	Local Membrane (P_L)	14.0	29.0
	IBA(Chugging) + SRV + Seismic	A/B	Primary + Secondary ($P_L + P_b + Q$)	26.7(range)	66.6(range)

TABLE 6.2.1-6

SUMMARY OF LIMITING STRESSES IN VENT LINE AND VENT HEADER SUPPORT ATTACHMENT WELDS

LOCATION	LOAD CASE	ASME SERVICE LEVEL	TYPE OF STRESS	VALUE OF STRESS(ksi)	ALLOWABLE STRESS VALUE (ksi)
Fillet Weld Between Ring Collar and Vent Header	DBA(Pool Swell) + SRV + Seismic	C	Shear Stress Across Weld Throat	7.5	10.6
Fillet Weld Between Deflector Diagonal Brace Base Pad and Vent Header	DBA(Pool Swell) + SRV + Seismic	C	Shear Stress Across Weld Throat	3.0	10.6
Weld Between Bellows Collar and Vent Line	DBA(CO) + Seismic	C	Shear Stress Across Weld Throat	0.5	10.6

TABLE 6.2.1-7

SUMMARY OF LIMITING STRESS RESULTS FOR LOCAL IMPACT PRESSURE LOADING ON VENT HEADER DURING POOL SWELL

STRUCTURE	TYPE OF STRESS	VALUE OF STRESS(ksi)	ALLOWABLE STRESS VALUE (ksi)
Vent Header	Membrane Hoop Stress (Compressive)	0.9	1.1
Vent Header	Primary Local Membrane Plus Bending ($P_L + P_b$)	54.4	57.0

6.2.2 Vent Line/Drywell Intersection

A description of the Oyster Creek vent system is provided in Section 3.2 of this report. The vent line/drywell intersection connects the vent line with the drywell. Figure 6.2.2-1 illustrates the Oyster Creek vent line/drywell intersection. The vent line/drywell intersection was analyzed as a Class MC vessel in accordance with the requirements of the ASME Boiler and Pressure Vessel Code, Section III, Subsection NE, 1977 Edition with Addenda through Summer 1977 (Reference 8.4.1). The results of fatigue analysis are included in Section 7.0.

6.2.2.1 Method of Analysis

Stresses in the vent line/drywell intersection were calculated with an axisymmetric finite element model, using the ANSYS computer program (Reference 8.6.7). The finite element mesh used in the model is shown in Figure 6.2.2-2. This model was analyzed for unit applied loads, including: internal pressure, shear force, axial force and moment. These cases reflect the type of loadings actually calculated to occur at this intersection.

The results of the unit loading of the model were used to determine membrane and bending stress influence coefficient matrices at three controlling locations. These locations, which represent the major structural discontinuities in the intersection, are shown in Figure 6.2.2-1. The stress influence coefficient matrices were incorporated into a computer program which was used to complete the final stress analyses presented in this report. This program calculates the stress state for a given combination of pressure, shear force, axial force, and moment as follows:

- For each load, the influence coefficient matrices are used to calculate resultant shear and normal stress components at three

circumferential locations (0^{o}, 90^{o} and 180^{o}) at each of the three controlling discontinuities.

- The resultant shear and normal stresses from the simultaneous loads are added algebraically to determine the final shear and normal stresses.

- The final stress state is evaluated for maximum stress intensity using the classical methods of mechanics of materials.

The reaction forces and internal pressure at the vent line/drywell intersection (which are the inputs to the stress analysis methodology described above) were determined as described in the analysis of the vent lines, vent headers and downcomers, in Section 6.2.1, above.

6.2.2.2 Loading and Acceptance Criteria

The loading and acceptance criteria considered for the vent line/drywell intersection is identical to that considered for the vent line, vent header and downcomers as described in Section 6.2.1.2. Calculated membrane stress intensities at the intersection discontinuity locations were compared to primary local membrane stress allowables. Calculated extreme fiber stress intensities were compared to primary plus secondary stress allowables.

6.2.2.3 Summary of Results

Limiting values of calculated general primary membrane, local primary membrane and primary plus secondary stress intensities for the locations of interest in the vent line/drywell intersection are shown in Table 6.2.2-1. Also shown on this table are the allowable values for each type of stress and ASME Code service level. As can be seen in Table 6.2.2-1, all of the stresses are within the allowable values.

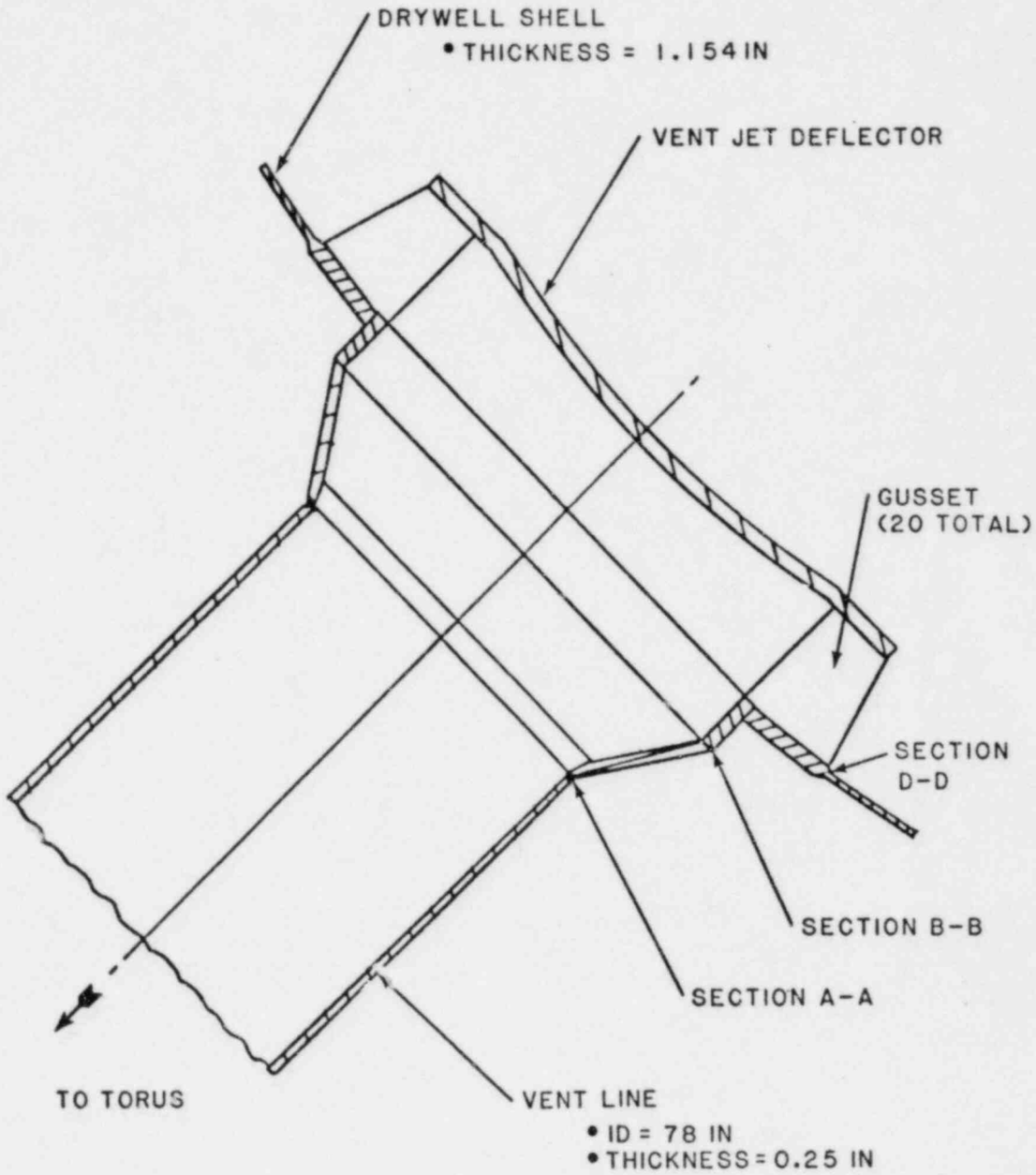

FIGURE 6.2.2-1

VENT LINE / DRYWELL INTERSECTION

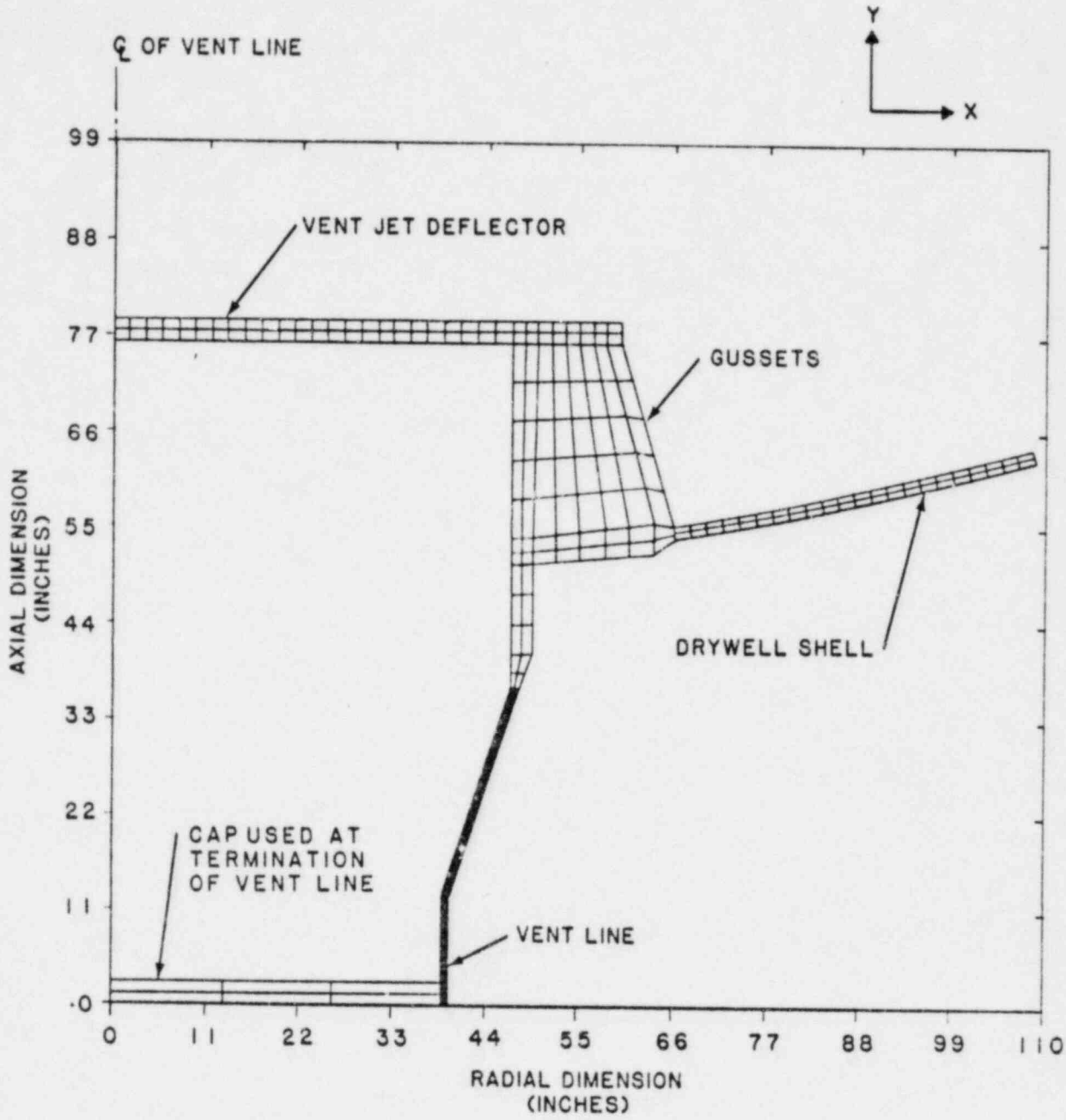

FIGURE 6.2.2-2

VENT LINE / DRYWELL INTERSECTION
FINITE ELEMENT MODEL

TABLE 6.2.2-1

SUMMARY OF CONTROLLING STRESSES IN THE VENT LINE/DRYWELL INTERSECTION

LOCATION	TYPE OF STRESS	ASME CODE LEVEL	CALCULATED STRESS INTENSITY (ksi)	ALLOWABLE STRESS INTENSITY (ksi)	CONTROLLING LOADING CONDITION
Vent Line	General Primary Membrane Stress (P_m)	A/B	13.2	19.3	DW + EQ(S) + DBA (POOL SWELL)
		C	16.1	33.3	DW + EQ(S) + SRV + DBA (POOL SWELL)
Section A-A	Local Primary Membrane Stress (P_L)	A/B	26.8	29.0	DW + EQ(S) + DBA (POOL SWELL)
		C	34.8	50.0	DW + EQ(S) + SRV + DBA (POOL SWELL)
	Primary + Secondary Stress ($P_L + P_b + Q$)	A/B	52.7	66.6	DW + EQ(S) + SRV + SBA/DBA (CHUG)
Section B-B	Local Primary Membrane Stress (P_L)	A/B	6.0	29.0	DW + EQ(S) + DBA (POOL SWELL)
		C	7.6	50.0	DW + EQ(S) + SRV + DBA (POOL SWELL)
	Primary + Secondary Stress ($P_L + P_b + Q$)	A/B	11.6	66.6	DW + EQ(S) + SRV + SBA/DBA (CHUG)
Section D-D	Local Primary Membrane Stress (P_L)	A/B	9.0	29.0	DW + EQ(S) + DBA (CO)
		C	10.0	50.0	DW + EQ(S) + SRV + DBA (CO)
	Primary + Secondary Stress ($P_L + P_b + Q$)	A/B	18.5	66.6	DW + EQ(S) + DBA (CO/CHUG)

6.2.3 Vent Line/Vent Header Intersection

6.2.3.1 Methods of Analysis

There are ten nominally identical vent line/vent header intersections in the Oyster Creek vent system. Two of the intersections are slightly different in that relief valve piping penetrates through the elliptical closure head. The reaction loads transmitted into the intersection by this relief valve piping were considered in the structural analysis described below. However, local stresses at the nozzle penetration are not covered here; they are covered in a separate report which describes the piping analyses (Reference 8.5.1).

Figure 6.2.3-1 shows the Oyster Creek vent line/vent header intersection. A finite element model of this intersection type was formulated and analyzed as part of the Mark I Program. The finite element mesh for this model is shown in Figure 6.2.3-2.

The model shown in Figure 6.2.3-2 was analyzed for six unit loads applied to one of the locations where the vent header connects to the intersection. The loads were reacted at the opposing vent header connection and the vent line connection in a manner consistent with symmetry. The model was also analyzed for a unit internal pressure. Maximum local membrane and membrane plus bending stress intensities were calculated as factors of the nominal stresses produced by these loads in the vent header. Also, maximum stress intensities for a selected combined beam load case were calculated as factors of the nominal combined beam stress in the vent header.

The final analysis of the Oyster Creek vent line/vent header intersection was performed by determining the net loads in the vent header where it connects to the vent line/vent header intersection and the internal pressure in the intersection for each load combination. Then, nominal stresses in the vent header for the combined beam reaction loads and for the internal pressure were determined. Next, maximum stress intensities in the vent line/vent header intersection for combined beam loads and for internal pressure were separately calculated using the factors developed from the finite element stress analysis. Finally, maximum stress intensities for beam loads and internal pressure were added absolutely to obtain final results. This last step entails considerable conservatism in that it assumes the maximum stresses due to beam loads and pressure occur in the same location, and that the principal stresses are similarly oriented such that a direct addition is appropriate.

The analytical tools and methodology used in determining the reaction loads in the vent header where it connects to the vent line/vent header intersection are the same as those described for the vent lines, vent header, and downcomers (Section 6.2.1.1). Specifically, responses to individual loads within a given combination were added in a worst-case manner. This approach is conservative because the limiting load combinations include dynamic loads from independent sources (e.g., earthquake, LOCA, SRV).

6.2.3.2 Loading and Acceptance Criteria

The loads considered in the evaluation of the vent line/vent header intersection are the same as those considered in the evaluation of the vent lines, vent header and downcomers, as discussed in Section 6.2.1.2.

Acceptance criteria for the vent line/vent header intersection were developed based on Section 2.2 and the PUAAG (Reference 8.2.3), and are identical to those developed for the evaluation of the vent lines, vent

header and downcomers, as discussed in Section 5.2.1.2. Specifically, six limiting load combinations were considered (Table 6.0-1). Allowable stresses were determined from the ASME Boiler and Pressure Vessel Code (Reference 8.4.1). Calculated membrane stress intensities were compared to primary local membrane stress allowable values of 29.0 ksi (Service Level A/B) and 50.0 ksi (Service Level C). Calculated membrane plus bending stress intensities were compared to a primary plus secondary allowable stress range value of 66.6 ksi for an SBA or IBA, or 67.5 ksi for a DBA (Service Level A/B). This latter stress is not applicable for Service Level C evaluations. The allowable stresses are based on the maximum drywell temperatures which occur during the accidents.

6.2.3.3 Summary of Results

Table 6.2.3-1 shows a summary of limiting calculated stresses in the Oyster Creek vent line/vent header intersection. As can be seen in this table, limiting calculated stresses slightly exceed the allowable values (by a maximum of 7%). The vent line/vent header intersection is considered to be acceptable on the basis that the methods of analysis are conservative, and the conservatisms more than offset the small amount by which the calculated stresses exceed the allowable values. The primary conservative features of the analysis are the worst-case summation of vent system responses due to dynamic loads from diverse sources, and the absolute addition of beam reaction stress intensity and pressure stress intensity in the vent line/vent header intersection. These conservatisms were discussed above in Subsection 6.2.3.1.

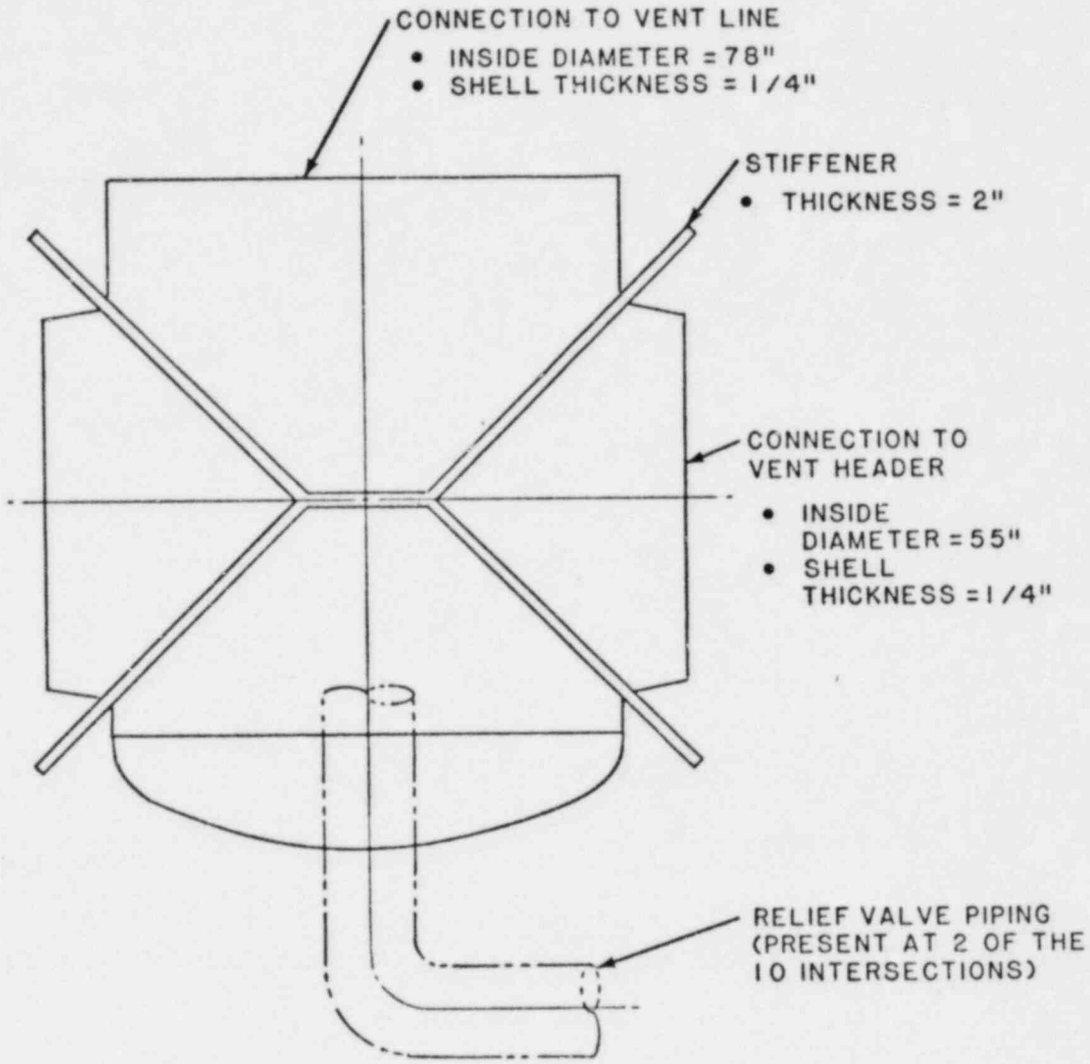

FIGURE 6.2.3-1

PLAN VIEW
OF OYSTER CREEK
VENT LINE / VENT HEADER INTERSECTION

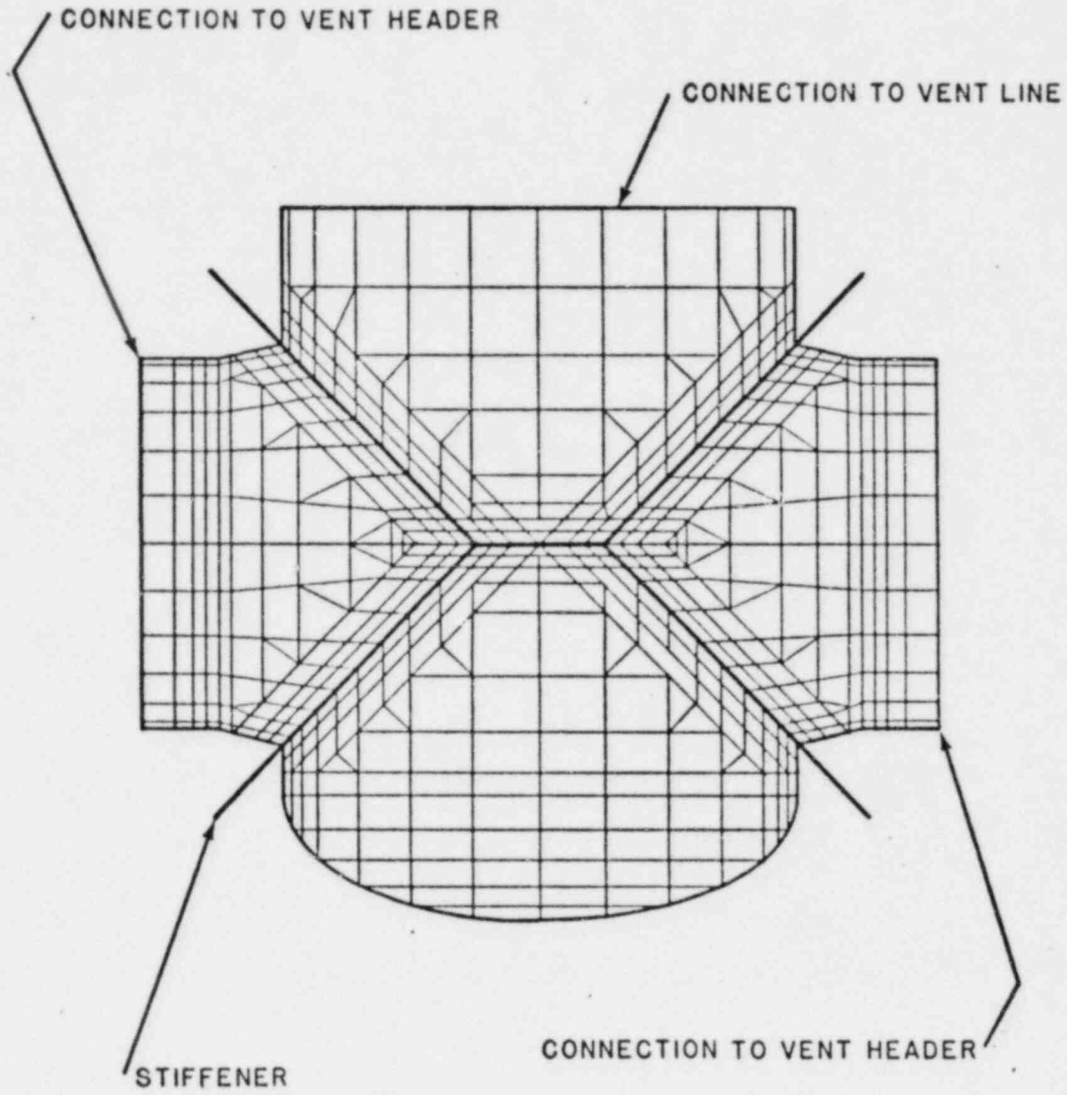

FIGURE 6.2.3-2

PLAN VIEW OF MESH
FOR VENT LINE / VENT HEADER INTERSECTION
FINITE ELEMENT MODEL

TABLE 6.2.3-1

SUMMARY OF LIMITING STRESSES IN VENT LINE/VENT HEADER INTERSECTION

LOAD COMBINATION	ASME SERVICE LEVEL	TYPE OF STRESS	VALUE OF STRESS (ksi)	ALLOWABLE VALUE (ksi)
SBA/IBA (Chugging) + SRV + Seismic	A/B	Primary Local Membrane (P_L)	29.4	29.0
		Primary Plus Secondary ($P_L + P_b + Q$)	71.5 (range)	66.6 (range)
DBA (Pool Swell) + Seismic	A/B	Primary Local Membrane (P_L)	29.3	29.0
DBA(CO) + Seismic	A/B	Primary Local Membrane (P_L)	30.9	29.0
		Primary Plus Secondary ($P_L + P_b + Q$)	69.4 (range)	67.5 (range)
DBA (Pool Swell) + SRV + Seismic	C	Primary Local Membrane (P_L)	49.4	50.0

6.2.4 Downcomer/Vent Header Intersection

6.2.4.1 Methods of Analysis

As mentioned in Section 3.2, the downcomer/vent header intersection was modified as a part of the Mark I Containment Long-Term Program by adding a 1.0-inch thick reinforcement pad to the vent header in the region around each pair of downcomers. Figure 6.2.4-1 shows the physical configuration of this added reinforcement.

A finite element shell model of a typical downcomer/vent header intersection was formulated. The model included a four-foot length of vent header, the penetrations for a pair of downcomers, and the upper region (including the two upper mitered sections and a short portion of the vertical section) of each of the two downcomers. The reinforcement plate which was added to the vent header at each pair of downcomers as a part of the Mark I Program was included in the model as a separate shell. Also, a beam element representation of the lower portion of each downcomer and the brace between the two downcomers was included. Figure 6.2.4-2 shows the mesh of the finite element model of the intersection region.

The model described above was subjected to several unit static loads, including internal pressure, and in-plane and out-of-plane loads at the downcomer tips. The results from these unit load analyses were used in determining the final stresses in the intersection for the CO and chugging load combinations. The actual loads at the intersection, or the factors used to scale the unit load cases, were determined directly from the load definitions (e.g., downcomer chugging load) or from hand calculations (e.g., lateral seismic) or from the results of dynamic analyses of the vent system using the vent system beam model (e.g., downcomer CO load).

In addition to the analyses described above, pool swell external pressure loads on the vent header and downcomer and pool swell beam loads in the vent header were analyzed. This evaluation was performed with a version of the finite element model which did not include the reinforcement plate, and hence represented a conservative approach.

Finally, the model shown in Figure 6.2 4-2 was used to determine appropriate stiffness coefficients for the intersection region for incorporation into the vent system beam model, as described in Section 5.2 of this report. These analyses were performed using a version of the model which included only the vent header and a short section of each downcomer (out to the first miter joint), to isolate the stiffness of the intersection region.

6.2.4.2 Loading and Acceptance Criteria

Loads considered in the analysis of the downcomer/vent header intersection are those defined in Section 4.0 of this report. It was identified in preliminary analyses that the stresses in the intersection were most strongly influenced by the local loads applied to the downcomers and by loads applied elsewhere which could cause the downcomers to sway. Table 6.2.4-1 shows the loads which were considered in the analysis of the downcomer/vent header intersection.

Acceptance criteria for the downcomer/vent header intersection were developed based on Section 2.2 and the PUAAG (Reference 8.2.3). As described previously, it was found that six limiting load combinations could be identified for analysis purposes (Table 6.0-1). The ASME service level for each of these six cases is shown in Table 6.0-1. Stress allowables were determined from the ASME Boiler and Pressure Vessel Code (Reference 8.4.1) for each service level. In the region around the intersection, calculated membrane stresses were compared to primary local membrane stress allowable values of 37.6 ksi (Service

Level A/B) and 50.0 ksi (Service Level C). The primary local membrane stress allowable for Level A/B was increased by the factor 1.3 from the normal allowable of 29.0 ksi based on the PUAAG (Reference 8.2.3) requirements for this intersection. Membrane plus bending stresses were compared to a primary plus secondary stress range allowable value of 66.6 ksi for an SBA or an IBA, or 67.5 ksi for a DBA (Service Level A/B). Primary plus secondary stresses are not considered for Service Level C in accordance with the ASME Code. The allowable stresses are based on the maximum drywell temperature which occurs during the accidents.

6.2.4.3 Summary of Results

The limiting load combinations were found to be DBA CO and SBA/IBA chugging, depending on which stress quantity was being evaluated. Table 6.2.4-2 summarizes the stresses for limiting load combinations. For primary local membrane stress, the limiting condition was SBA/IBA chugging, and for primary plus secondary stress, the limiting condition was DBA CO. As can be seen in Table 6.2.4-2, the stresses in the intersection region are less than their allowable values.

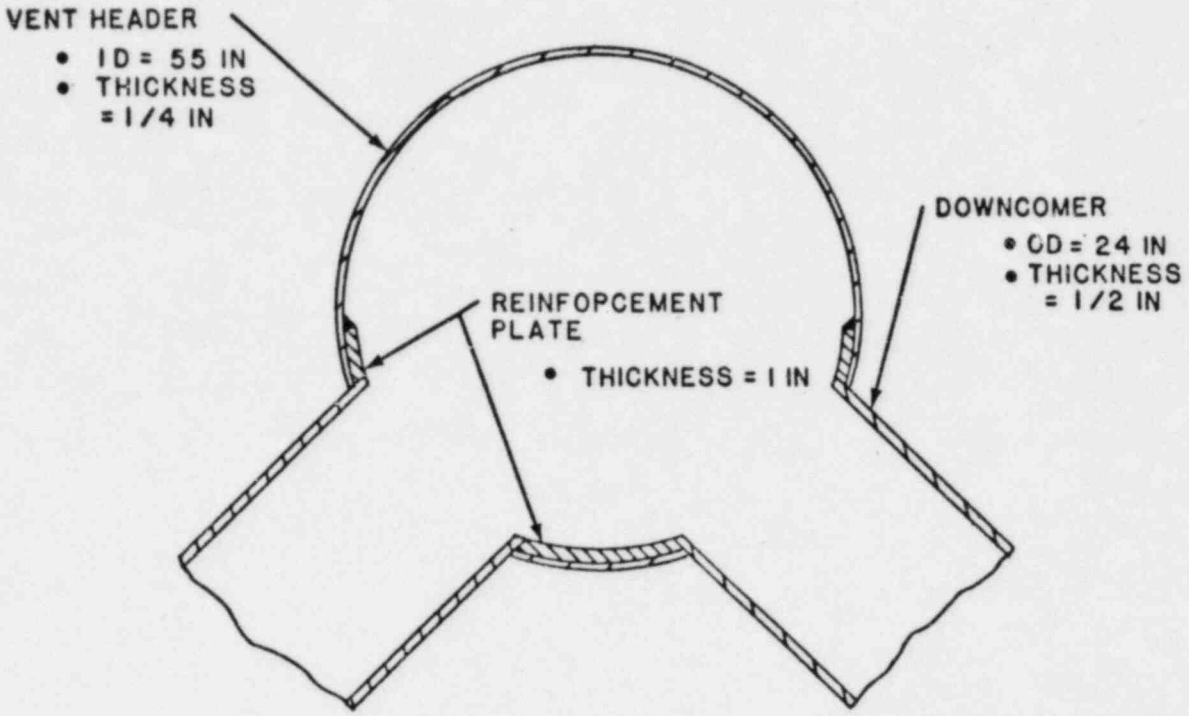

SECTIONAL VIEW AT TYPICAL DOWNCOMER PAIR

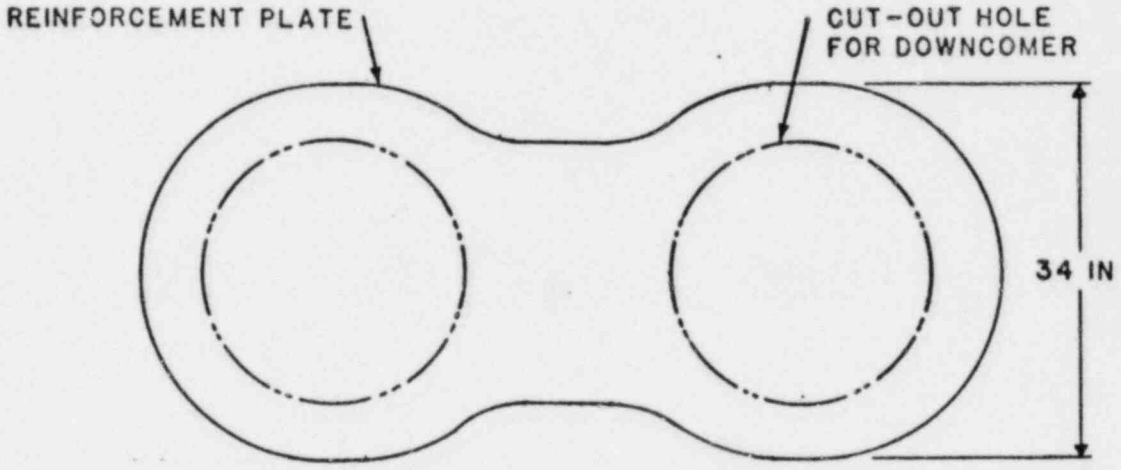

UNWRAPPED VIEW OF REINFORCEMENT PLATE

FIGURE 6.2.4-1

TYPICAL DOWNCOMER/VENT HEADER INTERSECTION AND REINFORCEMENT

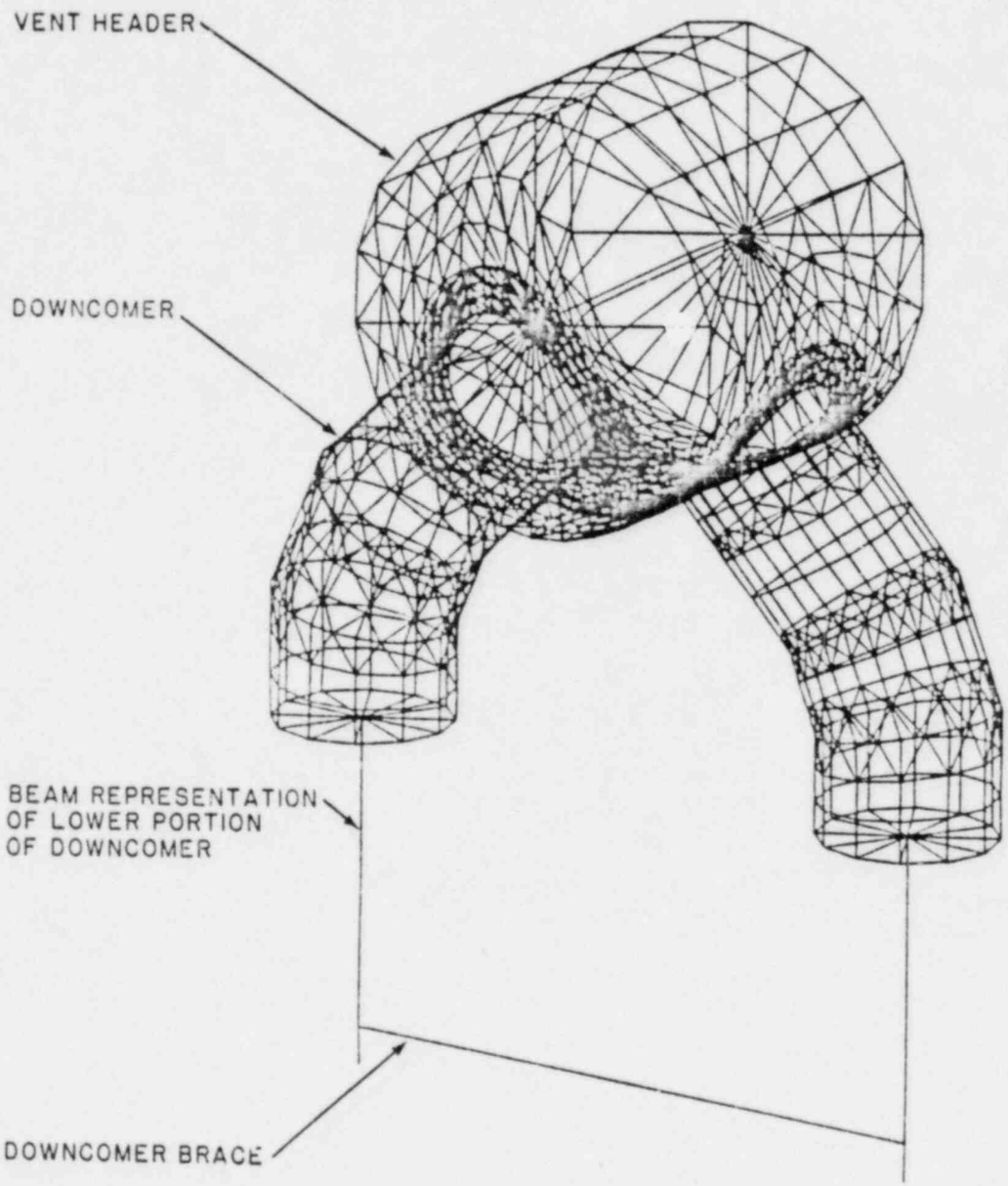

FIGURE 6.2.4-2

DOWNCOMER/VENT HEADER INTERSECTION
FINITE ELEMENT MODEL

TABLE 6.2.4-1

LOADS CONSIDERED IN THE EVALUATION OF THE DOWNCOMER/VENT HEADER INTERSECTION

General Category	Individual Loads Considered
Earthquake	Vertical Acceleration of Vent System.
	Horizontal Acceleration of Downcomers.
SRV Discharge	Bubble Drag Load on Downcomers.
Intermediate or Small Break Accident	Chugging Downcomer Tip Load.
	IBA CO Harmonic Internal Pressure Load in Downcomers.
Design Basis Accident (Pool Swell Phase)	Impact and Drag on Vent Header.
	Impact and Drag on Downcomers.
	Impact and Drag on Vent Header Deflector.
	Impact and Drag on Vent Line.
	Impact and Drag on Relief Valve Piping.
	Vent System Thrust Load.
Design Basis Accident Pressure (CO or Chugging Phase)	DBA CO Harmonic Internal
	Load in Downcomer.
	Chugging Downcomer Tip Load.

TABLE 6.2.4-2

SUMMARY OF LIMITING STRESSES AT DOWNCOMER/VENT HEADER INTERSECTION

LOAD COMBINATION	SERVICE LEVEL	LOCATION OF STRESS	TYPE OF STRESS	VALUE OF STRESS (ksi)	ALLOWABLE STRESS VALUE (ksi)
DBA(CO) + EQ	A/B	Vent Header	Local membrane (P_L)	19.3	37.6
	A/B	Downcomer	Primary + Secondary $P_L + P_b + Q$	64.0 (Range)	67.5 (Range)
SBA/IBA (Chugging) + SRV + EQ	A/B	Vent Header	Local membrane (P_L)	26.8	37.6
	A/B	Downcomer	Primary + Secondary ($P_L + P_b + Q$)	58.3 (Range)	66.6 (Range)
SBA/IBA (Chugging) + SRV + EQ	A/B	Fillet Weld (Pad-to-Header)	Shear Stress	5.4	10.6

6.2.5 Torus/Main Vent Line Bellows

The analyses of the torus/main vent line bellows expansion joint are described in this section. The torus/main vent line bellows provide a flexible seal between the torus shell and the main vent line at the points where the main vent lines penetrate the torus shell (Figure 3.1-3). Figure 6.2.5-1 illustrates the bellows in detail.

6.2.5.1 Methods of Analysis

The torus/main vent line bellows were analyzed using analysis techniques described in the Expansion Joint Manufacturers Association (EJMA) standards (Reference 8.6.5). The following effects were considered:

- Maximum bellows deflections
- Cyclic fatigue of the bellows
- Pressure-induced stress
- Pressure-induced instability

The bellows were assumed to completely absorb relative deflections between the torus and vent line. The expansion joint deflections due to loads applied to the torus shell were calculated from coupled torus/vent system finite element model results. Expansion joint deflections due to loads applied to the vent system were calculated using a combination of vent system beam model results and hand calculations. Dynamic effects were considered for dynamically applied loads. Maximum and minimum values of deflections for each applied load were combined in a worst-case manner when analyzing load combinations.

The torus/main vent line bellows form part of the torus pressure boundary and experience an internal pressure equal to the torus internal pressure. For analysis purposes, the torus design pressure of 35 psig was used. The torus design pressure exceeds the torus internal

pressures for all of the load combinations defined in the Mark I Containment Long-Term Program and therefore provides a conservative upper bound on the torus internal pressure.

6.2.5.2 Loading and Acceptance Criteria

Section 4.0 of this report covers all of the loads for the Mark I Containment Long-Term Program. For the torus/main vent line bellows, loads applied to the torus shell and to the vent system were considered since the bellows are connected to both. Table 6.2.5-1 summarizes the loads which were considered in the analysis.

Acceptance criteria for the bellows were developed based on Section 2.2 and the PUAAG (Reference 8.2.3). The allowable stresses were determined from Subsection NE of the ASME Boiler and Pressure Vessel Code (Reference 8.4.1). The allowable stress in the bellows is 18.3 ksi (Material Specification ASME SA-240-T304). The allowable stress in the attachment collars is 15.1 ksi. (The collar material specified was ASTM A-2018 which has been superseded by ASTM A-516 Grade 60.) The allowable axial and lateral deflections of the bellows were those specified by the bellows manufacturer. The stability and fatigue allowables were calculated using formulas from the EJMA standard (Reference 8.6.5). The material properties specified in Subsection NE of the ASME Boiler Pressure Vessel Code (Reference 8.4.1) were used for the bellows material (ASME SA-240-T304).

6.2.5.3 Summary of Results

The results of the evaluation of the torus/main vent line bellows are shown in Table 6.2.5-2. The results for the most limiting load cases are shown. As can be seen on Table 6.2.5-2, all of the calculated values are within their allowable values.

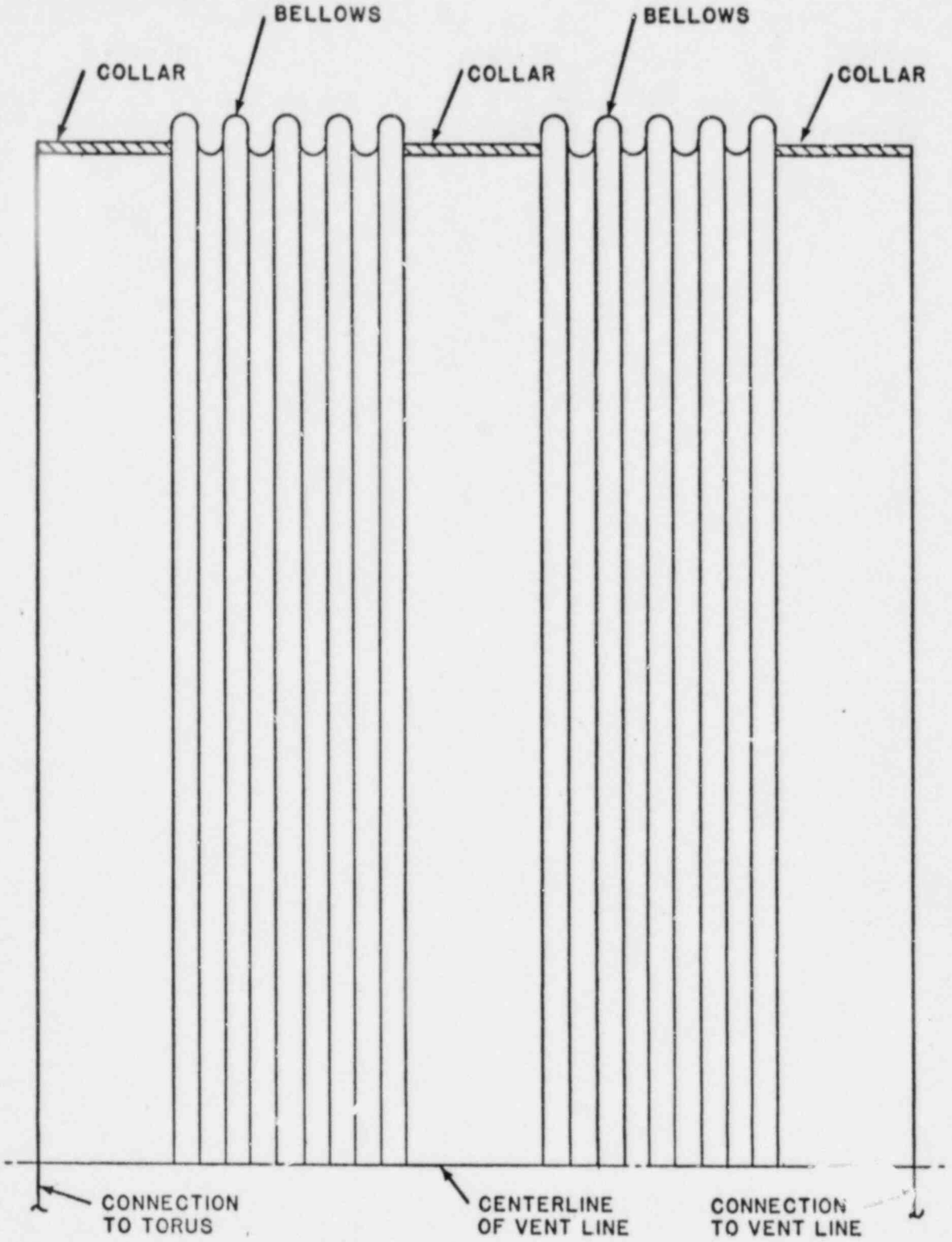

FIGURE 6.2.5-1

TORUS/MAIN VENT LINE
BELLOWS EXPANSION JOINT

TABLE 6.2.5-1

LOADS CONSIDERED IN TORUS/MAIN VENT LINE BELLOWS ANALYSIS

General Category	Individual Loads Considered
Deadweight	Deadweight of torus and vent system steel
	Deadweight of torus water
Earthquake	Vertical acceleration of vent system
	Vertical acceleration of torus and water
	Horizontal acceleration of vent system
	Horizontal acceleration of torus and water
SRV Discharge	Relief valve pipe reaction on main vent line
	Air bubble load on torus shell
	Air bubble drag load on vent system
Intermediate or Small Break Accident	Pre- and post-chugging harmonic pressure on torus shell
	Static torus internal pressure
	Thermal expansion of torus, vent system, and expansion joint
	Vent system thrust load
	Synchronous chugging load on downcomers

TABLE 6.2.5-1 (Continued)

General Category	Individual Loads Considered
Design Basis Accident (Pool Swell Phase)	Impact and drag loads on vent line, vent header, downcomers, vent header deflector, and relief valve piping
	Vent system thrust load
	Transient pressure on torus shell
	Static torus internal pressure
	Thermal expansion of torus, vent system, and expansion joint
Design Basis Accident (CO and Chugging Phase)	CO, pre- and post-chugguing harmonic pressure on torus shell.
	Static torus internal pressure.
	Vent system thrust loads
	Thermal exansion of torus, vent system, and expansion joint
	Synchronous chugging load on downcomers

TABLE 6.2.5-2

SUMMARY OF RESULTS FOR TORUS/MAIN VENT LINE BELLOWS EVALUATION

ITEM	CALCULATED VALUE	ALLOWABLE VALUE	NOTES
Maximum Axial Deflection (extension)	.168 in	.275 in	(1)
Maximum Axial Deflection (compression)	-.340 in	-.800 in	(2)
Maximum Lateral Deflection	.430 in	.500 in	(3)
Maximum Pressure Stress in Bellows	10.9 ksi	18.3 ski	(4)
Maximum Pressure Stress in Collar	2.8 ksi	15.1 ksi	(4)
Stability Against Pressure			
- In-plane	35 psig	320 psig	(5)
- Column	35 psig	499 psig	(5)
Fatigue Usage	.0238	1.0	(6)

Notes

1. Limiting load combination was IBA (Pre-chugging) + SRV + EQ
2. Limiting load combination was SBA (Pre-chugging) + SRV + EQ
3. Limiting load combination was SBA (Pre-chugging) + SRV + EQ
4. The calculated stresses are those due to 35 psig of internal pressure. This pressure is the torus design pressure which bounds all values for Mark I load combinations.
5. The calculated pressure is the torus design pressure which bounds the values for Mark I load combinations. The allowable value is that pressure required to stress the bellows to the stability limits.
6. Fatigue usage was calculated for the most limiting plant cycle history identified in Section 7.0 of this report.

6.2.6 Vent Header Support Columns

The analyses of the vent header support columns and the hardware required to attach them to the vent header and the ring girder are described in this section. Modifications to these structures have been designed and installed as a part of the Mark I Containment Long-Term Program. The major structural components are (see Figure 6.2.6-1):

- The attachment plate at the vent header ring collar
- The clevises on the support column
- The support column
- The attachment bracket at the torus ring girder
- The support column connecting pins

6.2.6.1 Methods of Analysis

The vent header support columns and attachment hardware were analyzed as Class MC component linear supports in accordance with Subsection NF of the ASME Boiler and Pressure Vessel Code (Reference 8.4.1). The vent header support columns were modeled as beam-columns. The end conditions were pinned-pinned. Both axial and lateral loads were considered. The attachment brackets at the ring collar and ring girder and the clevis plates on the vent header support columns were modeled as beam-columns. The end conditions were fixed-free. Appropriate interaction formulas for combination of axial and bending loads were used for all structures modeled as beam-columns, based on Appendix XVII of the ASME Boiler and Pressure Vessel Code (Reference 8.4.1). The attachment brackets were also analyzed for shear pullout, net-section tension, and bearing at the pin holes.

The pins connecting the support columns to the attachment brackets were analyzed for bearing stress and shear stress. The welds in the support columns, the attachment hardware and the welds between the attachment

brackets and the ring collar and ring girder were analyzed for shear stress at the weld throat. The ring girder top flange was analyzed for through-thickness tensile stress at the welds between the ring girder attachment bracket and the top flange.

Reaction forces and moments in the vent header support columns due to loads applied directly to the support columns were determined by hand calculations. Reactions for loads applied to the vent system and torus shell were determined using the coupled torus/vent system model described in Section 5.0. Dynamic effects were considered for dynamically applied loads. Maximum and minimum values of reactions for each applied load were combined in a worst-case manner in analyzing load combinations.

6.2.6.2 Loading and Acceptance Criteria

Section 4.0 of this report covers all of the loads for the Mark I Containment Long-Term Program. For the vent header support columns, loads applied directly to the torus shell and the vent system, (including the support columns) were considered, since the vent header support columns tie the torus and vent system together. Table 6.2.6-1 summarizes the loads which were considered in the analysis.

Acceptance criteria for the support columns were developed based on Section 2.2 and the PUAAG (Reference 8.2.3). The load combinations defined in Reference 8.2.3 were considered and a set of potentially limiting load combinations were identified for analysis. These limiting load combinations and the ASME service levels for each case are summarized in Table 6.0-1.

The allowable stresses were determined from the Class MC component linear support rules of the ASME Boiler and Pressure Vessel Code (Reference 8.4.1). The allowable stresses are a function of the

material yield strength, which was 36 ksi for the columns and pin (material specification ASME SA-36) and 38 ksi for the attachment brackets (material specification ASME SA-516, Grade 70).

6.2.6.3 Summary of Results

The results of the evaluation of the vent header support columns and the attachment brackets are shown in Table 6.2.6-2. The most limiting load combinations for Service Levels A/B and C and the combined stress as a fraction of allowable are shown. The results for the pins and pinholes for the most limiting load combinations for ASME Service Levels A/B and C are summarized in Tables 6.2.6-3a and 6.2.6-3b. The welds were evaluated for two bounding load cases. The first case considered the maximum axial force and maximum lateral forces encountered in all the ASME Service Level A/B load combinations. The second case considered the analogous quantities for the ASME Service Level C load combinations. The limiting weld stresses calculated for these bounding loads are summarized in Table 6.2.6-4. As can be seen on Tables 6.2.6-2 through 6.2.6-4, all of the calculated stresses in the vent header support columns and attachment components are less than the allowable values.

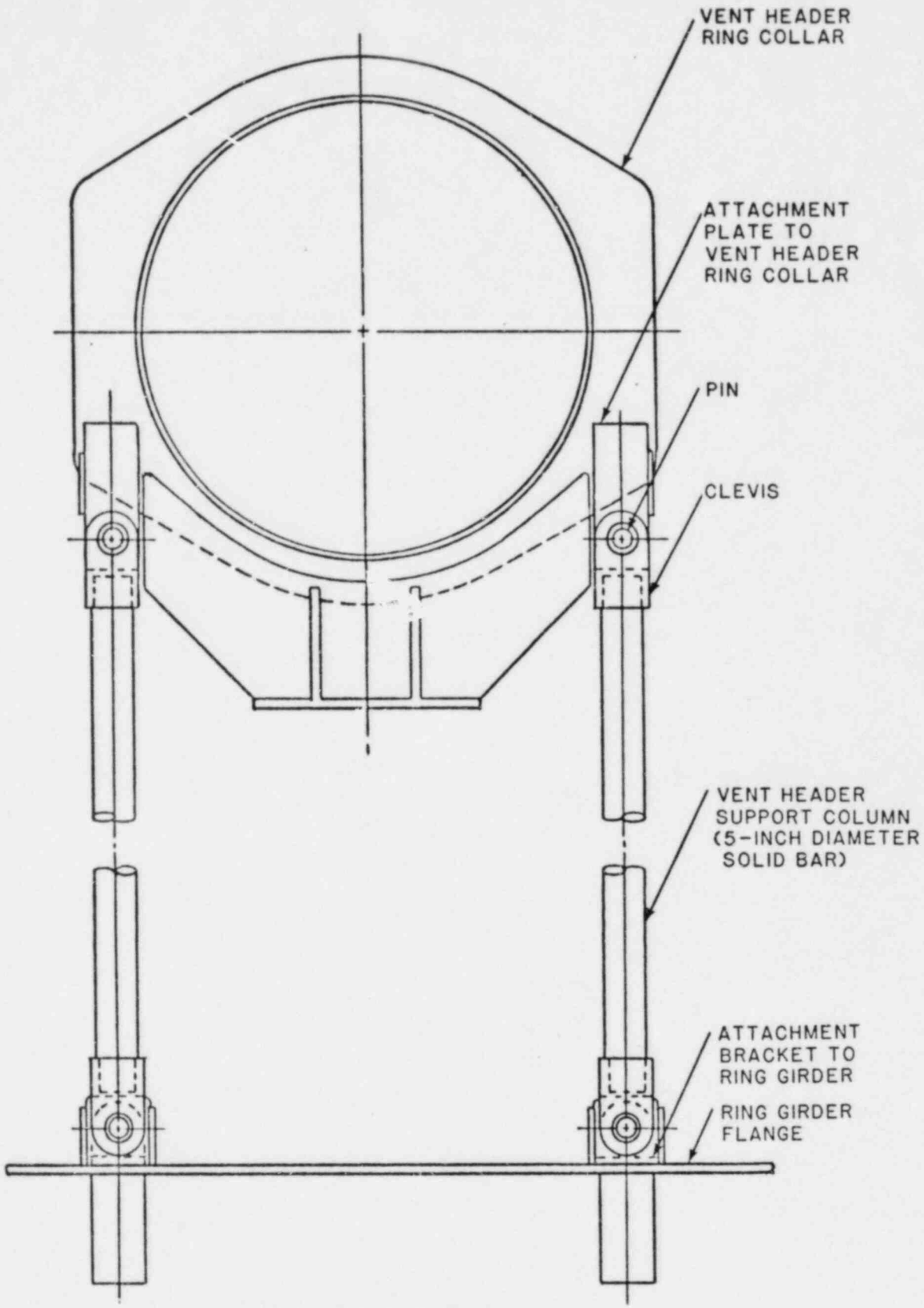

FIGURE 6.2.6-1

TYPICAL PAIR OF VENT HEADER SUPPORT COLUMNS

TABLE 6.2.6-1 (Continued)

General Category	Individual Loads Considered
Intermediate or Small Break Accident (continued)	Chugging synchronous downcomer tip load
	Pre- and post chugging fluid drag loads on columns
Design Basis Accident (Pool Swell Phase)	Impact and drag load on vent line, vent header, downcomers, vent header deflector, and relief valve piping
	Vent system thrust load
	Transient pressure on torus shell (up/down load)
	Static torus internal pressure
	Drag loads on columns due to water-clearing from downcomers
	Drag loads on columns due to LOCA air bubble expansion
Design Basis Accident (CO/Chugging Phase)	CO, pre- and post-chugging harmonic pressure on torus shell
	Static torus internal pressure
	Constrained thermal expansion of vent system and torus
	Vent system thrust load
	Chugging synchronous downcomer tip load
	CO, pre-, and post-chugging fluid drag loads on columns

TABLE 6.2.6-2

COMBINED AXIAL AND BENDING STRESSES
IN SUPPORT COLUMNS AND ATTACHMENT BRACKETS

Component	ASME Service Level	Load Combination(1)	Maximum Stress / Allowable Stress
Support Column Body	A/B C	IBA(POCH)+SRV+EQ+DW DBA(PS)+SRV+EQ+DW	0.94 0.27
Support Column Clevis	A/B C	IBA(POCH)+SRV+EQ+DW DBA(PS)+SRV+EQ+DW	0.68 0.36
Ring Collar Attachment Bracket	A/B C	IBA(POCH)+SRV+EQ+DW DBA(PS)+SRV+EQ+DW	0.63 0.55
Ring Girder Attachment Bracket	A/B C	DBA(PS)+EQ+DW DBA(PS)+SRV+EQ+DW	0.36 0.33

(1) The expression POCH refers to the post-chugging load. The expression PS refers to the pool swell load.

TABLE 6.2.6-3a

LIMITING STRESSES AT PINHOLES

Pinhold Location	ASME Service Level	Load Combination	Maximum Stress/ Allowable Stress		
			Shear Pullout	Net-Section Tension	Bearing
Ring Collar Attachment Bracket	A/B	DBA(PS)+EQ+DW	.53	.93	.67
	C	DBA(PS)+SRV+EQ+DW	.46	.81	.59
Support Column Clevis	A/B	DBA(PS)+EQ+DW	.63	.85	.67
	C	DBA(PS)+SRV+EQ+DW	.55	.74	.59
Ring Girder Attachment Bracket	A/B	DBA(PS)+EQ+DW	.56	.75	.67
	C	DBA(PS)+SRV+EQ+DW	.49	.65	.59

TABLE 6.2.6-3b

LIMITING STRESSES IN PINS

ASME Service Level	Load Combination	Maximum Stress/Allowable Stress	
		Shear	Bearing
A/B	DBA(PS)+EQ+DW	.81	.71
C	DBA(PS)+SRV+EQ+DW	.71	.62

TABLE 6.2.6-4

LIMITING WELD STRESSES

Weld Location	ASME Service Level	Maximum Weld Stress / Allowable Weld Stress
Ring Collar-to Attachment Bracket Weld	A/B C	.63 .69
Weld Within Ring Collar Attachment Bracket	A/B C	.79 .92
Support Column-to-Clevis Weld	A/B C	.78 .81
Weld Within Ring Girder Attachment Bracket	A/B C	.57 .65
Attachment Bracket-to-Ring Girder Weld	A/B C	.74 .75

6.2.7 Vent Header Ring Collar

6.2.7.1 Methods of Analysis

Ring collar stress analysis was performed using both a finite element computer model and hand calculations. The computer model represented one-half of the ring collar and attached vent header deflector support. Figure 6.2.7-1 shows the finite element mesh used for the model. The computer model was used to calculate stresses due to vertical loads on the ring collar applied by the vent header deflector and by the vent header, and torsional loads applied by the vent header. The loads were considered to be reacted by the vent header support columns. Hand calculation methods were used to calculate ring collar stresses due to horizontal deflector loads in the plane of the ring collar, and due to in-plane and out-of-plane horizontal loads on the ring collar applied by the support columns. All hand calculations were based on ring theory.

Stress intensities were calculated at six ring collar sections (Figure 6.2.7-2). Four of the sections (top, bottom, and each side at horizontal centerline) were chosen for analysis because they are the sections with the smallest cross-sectional areas. The other two sections (inside and outside support column connection locations) were chosen for analysis because of the concentrated loading at these locations. At each of the six analyzed sections, the membrane stress intensity, membrane plus bending stress intensity at the inside fiber (adjacent to vent header), and membrane plus bending stress intensity at the outside fiber were calculated.

Loads and load combinations used for ring collar analysis are described below in Subsection 6.2.7.2, Loading and Acceptance Criteria. The actual reactions in the ring collar for most of the loads were determined using the vent system beam model and the coupled torus/vent system model

(Sections 5.1 and 5.2). Reactions for other loads were calculated by hand (e.g., reactions due to drag loads on the vent header support columns). For each load, maximum and minimum reactions were determined at each loading point (i.e., at each attachment to another component). To calculate stresses for combinations of loads, the reactions for individual loads were summed in a worst-case manner.

6.2.7.2 Loading and Acceptance Criteria

All loads described in Section 4.0 of this report were initially considered for ring collar analysis. A reduced set of loads which produce significant reactions in the ring collar was selected on the basis of engineering judgment and scoping calculations. These loads are the same as shown for the vent header support columns in Table 6.2.6-1. Load combinations considered were those in Table 6.0-1, with the exception that the two IBA/SBA events in Table 6.0-1 were conservatively combined (i.e., a safe shutdown earthquake was assumed, but stresses were compared to ASME Service Level A/B allowables).

Ring collar acceptance criteria were developed based on Section 2.2 and the PUAAG (Reference 8.2.3). The ring collar is classified as a Class MC component for ASME Code analysis. Stress allowables are a function of the stress type (membrane or membrane plus bending) and the ASME service level for the load combination under consideration (as defined in Table 6.0-1).

Specifically, allowable stresses are as follows:

ASME Service Level	ASME Stress Type	Allowable Stress Intensity (ksi)
A/B	General Primary Membrane(P_m)	19.3
A/B	General Primary Membrane Plus Primary Bending (P_m+P_b)	29.0
A/B	Primary Plus Secondary (P_m+P_b+Q) (Range)	69.3
C	General Primary Membrane (P_m)	38.0
C	General Primary Membrane Plus Primary Bending (P_m+P_b)	57.0

Ring collar membrane stress intensities were compared with the general primary membrane allowable stress intensity. Stress intensities at the inside and outside fibers were compared with the general primary membrane plus primary bending allowable stress intensity, and with primary plus secondary allowable stress intensity range (Service Level A/B only).

6.2.7.3 Summary of Results

Results of ring collar analysis are summarized in Table 6.2.7-1. Limiting membrane and membrane plus bending stress intensity values for each load combination are shown. Corresponding allowable stress intensities are also shown for comparison. For all load combinations, maximum ring collar stress intensities are less than allowable values.

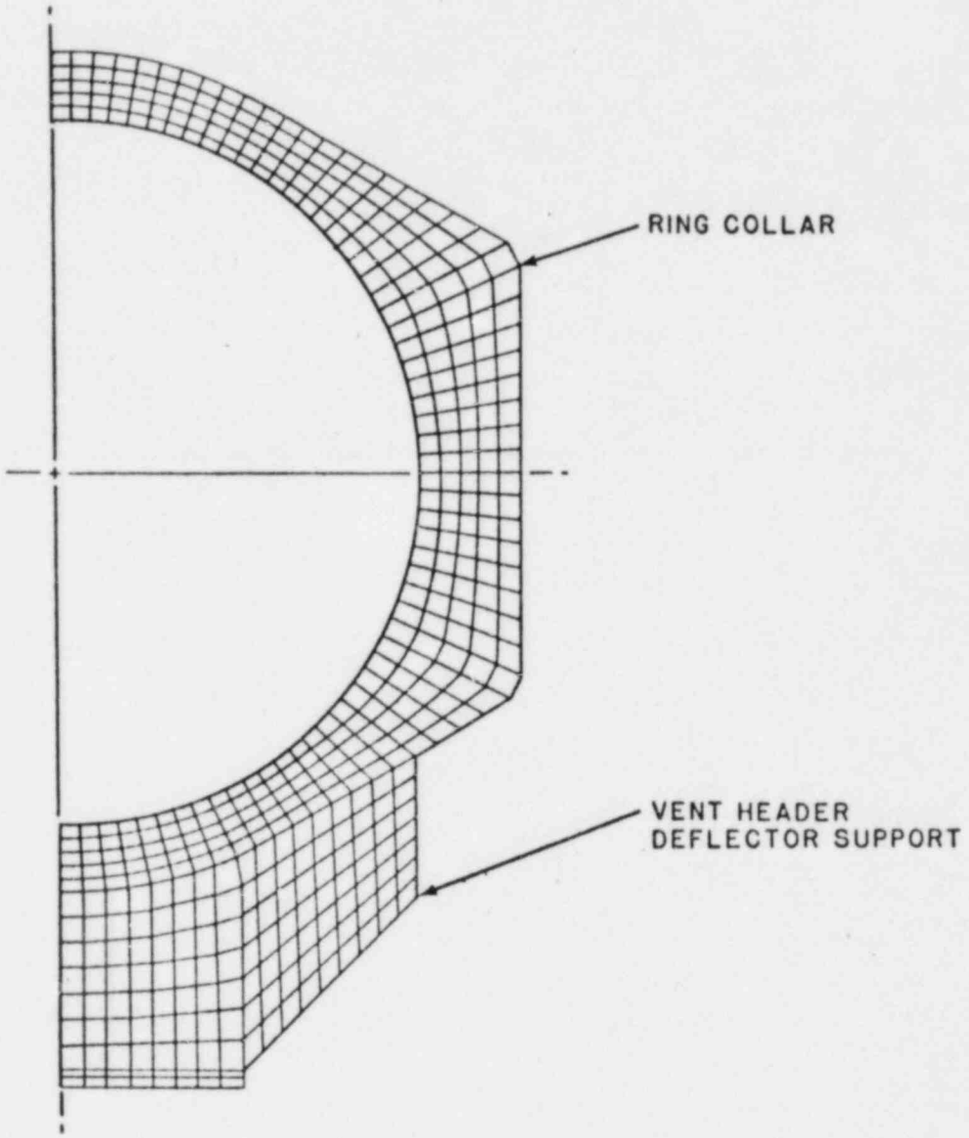

FIGURE 6.2.7-1

FINITE ELEMENT MESH
OF
RING COLLAR MODEL

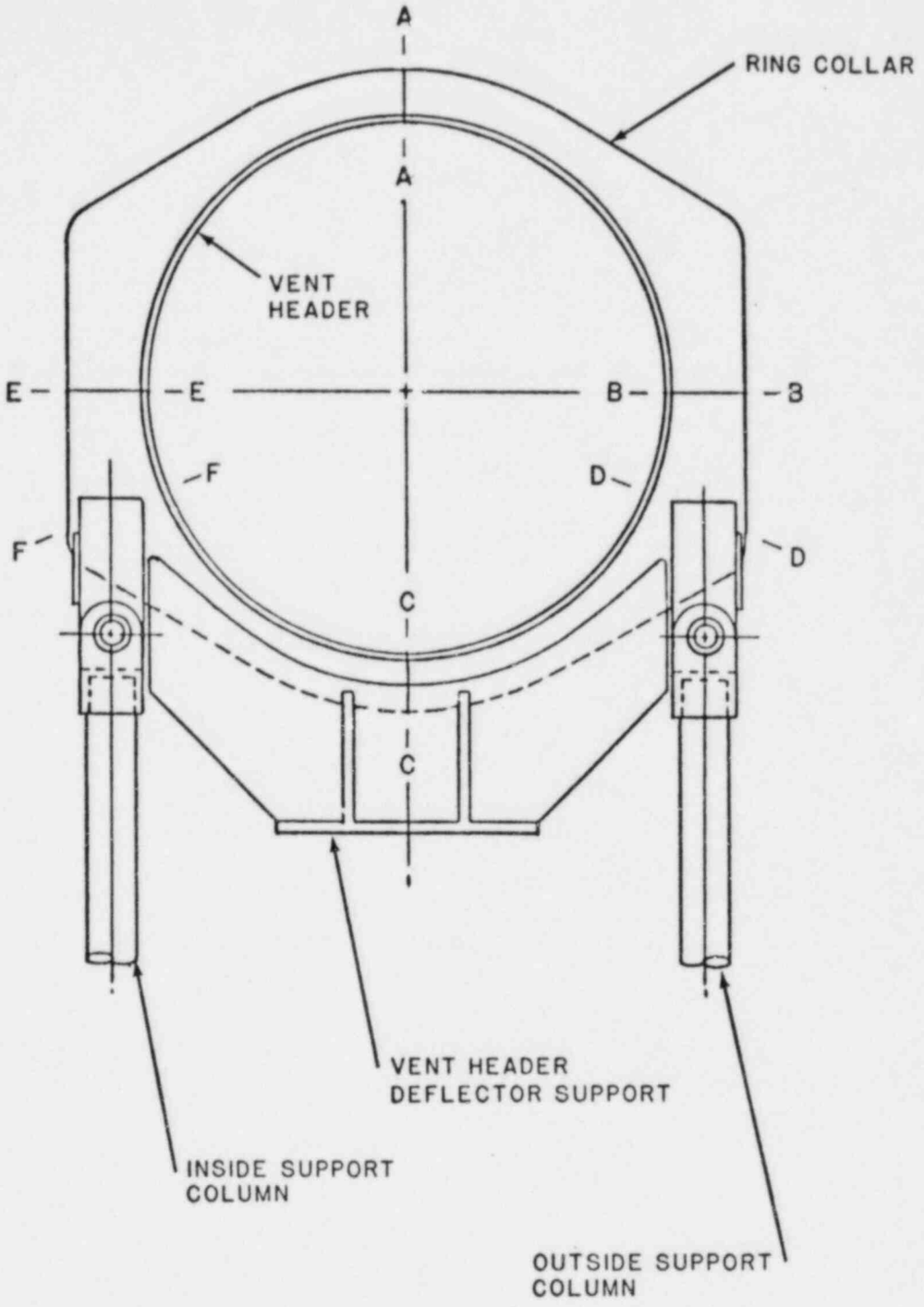

FIGURE 6.2.7-2

RING COLLAR SECTIONS
FOR
STRESS ANALYSIS

TABLE 6.2.7-1

SUMMARY OF LIMITING RING COLLAR STRESSES

Load Combination	ASME Service Level	Type of Stress	Limiting Stress Location(1,2)	Stress Intensity Value (ksi)	Allowable Stress Value (ksi)
IBA/SBA +EQ+SRV	A/B	P_m	E-E	6.3	19.3
		P_m+P_b	F-F (Inside Fiber)	25.4	29.0
		P_m+P_b+Q	F-F (Inside Fiber)	59.2 (Range)	69.3 (Range)
DBA(PS)+EQ +EQ(3)	A/B	P_m	D-D	13.1	19.3
		P_m+P_b	D-D (Inside Fiber)	27.8	29.0
DBA(CO/CH) +EQ	A/B	P_m	B-B	6.5	19.3
		P_m+P_b	F-F (Inside Fiber)	27.8	29.0
		P_m+P_b+Q	F-F (Inside Fiber)	61.6 (Range)	69.3 (Range)
DBA(PS)+EQ +SRV	C	P_m	D-D	15.1	38.0
		P_m+P_b	D-D (Inside Fiber)	37.3	57.0
DBA(CO/CH) +EQ+SRV	C	P_m	E-E	10.2	38.0
		P_m+P_b	F-F (Inside Fiber)	38.6	57.0

(1) See Figure 6.2.7-2 for identification of locations.

(2) Inside fiber is adjacent to vent header.

(3) Primary plus secondary stress not considered for this load combination, per Reference 8.2.3.

6.2.8 Vent Header Deflector

The vent header deflector was installed in the Oyster Creek torus as a part of the Mark I Containment Long-Term Program. A brief description of the geometry of the vent header deflector is given in Section 3.2. The vent header deflector is composed of 20 sections, each spanning the length of a bay between miter joints. Figure 6.2.8-1 shows a typical vent header deflector span. The deflector is attached at each end of its span to a vent header deflector support plate, which is in turn attached to the vent header ring collar.

6.2.8.1 Methods of Analysis

The vent header deflector was modeled as a beam. Beam elements were included in the vent system beam model (Section 5.2) to represent the vent header deflector. This model was used to determine the reactions in the deflector for all the loads which were considered, except for the deadweight and seismic loads, and the horizontal component of the pool swell impact load. Hand calculations were used for these other loads. Dynamic analyses were performed for dynamically applied loads.

Stresses in the vent header deflector were determined based on beam theory, using the calculated reactions. Stresses in the vent header deflector support plate were determined using beam and plate models. The extreme calculated reaction loads at the ends of the deflector spans were used as the applied loads on the support plate.

6.2.8.2 Loading and Acceptance Criteria

Section 4.0 describes the loads on the Oyster Creek Mark I containment system. The loads which produced significant structural response in the vent header deflector were considered in the analysis. These loads include loads applied directly to the deflector (deadweight, seismic,

and pool swell impact) and several dynamic loads applied to the vent system and torus shell, which result in excitation of the deflector as a suspended mass. The loads which were considered are presented in Table 6.2.8-1.

Acceptance criteria for the vent header deflector were developed based on Section 2.2 and the PUAAG (Reference 8.2.3). The load combinations defined in the PUAAG were considered in the structural evaluation. Two limiting load combinations conservatively bounded all of the required combinations. One of these two was a limiting pool swell combination, and the other was a limiting non-pool swell combination. Based on the PUAAG, ASME Service Level D was used in determining allowable stresses for the first case, and ASME Service Level A was used for the second case.

Stress allowable values were determined from the ASME Boiler and Pressure Vessel Code, Section III, (Reference 8.4.1), Subsection NF. Allowable stresses were a function of material minimum yield strength, which ranged from 35.0 to 38.0 ksi for the materials used to construct the vent header deflector and its supports. Allowable stresses were also developed for the welds and bolts used in the vent header deflector.

6.2.8.3 Summary of Results

The limiting load combination for the vent header deflector is the pool swell load combination. A dominant portion of the structural response in the vent header deflector for this load combination is due to the pool swell impact and drag load on the vent header deflector. Table 6.2.8-2 summarizes limiting calculated stresses in the vent header deflector and supports for this load combination and compares them to allowable values. As can be seen in this table, the limiting stresses are less than the allowable values.

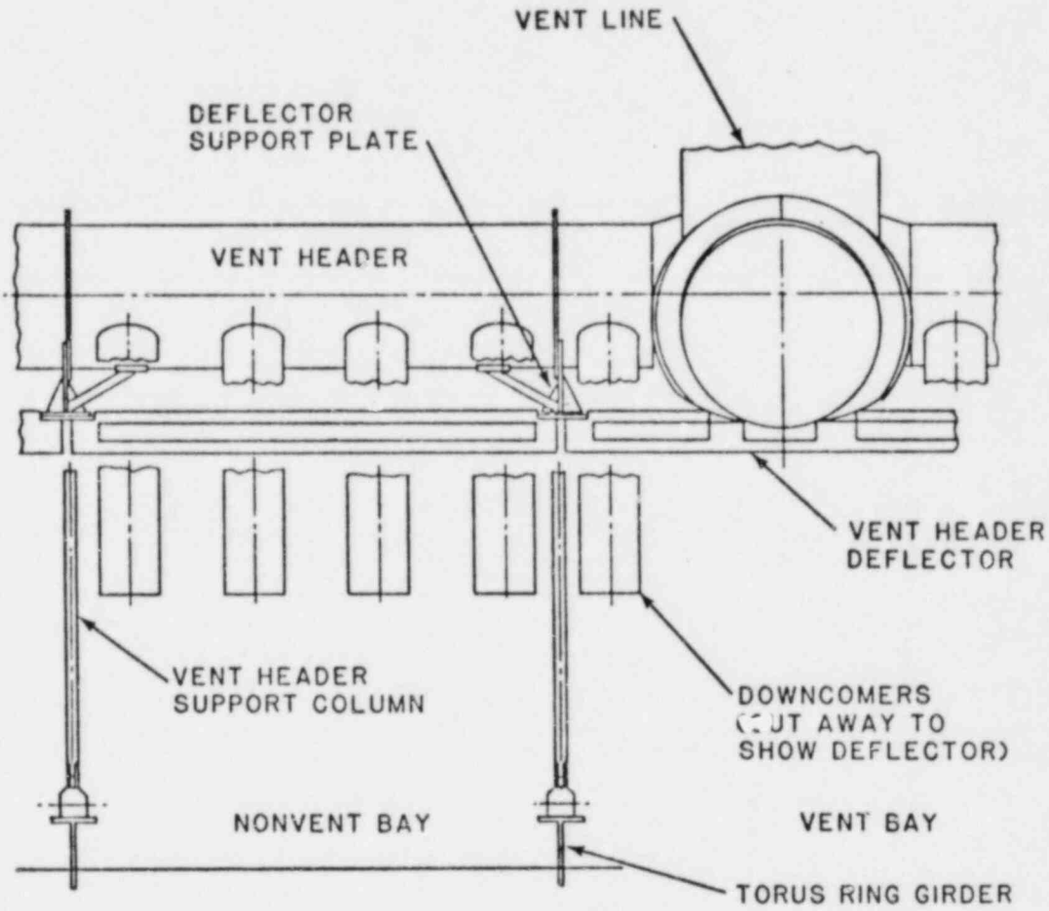

FIGURE 6.2.8-1

SIDE VIEW OF VENT SYSTEM
SHOWING VENT HEADER DEFLECTOR

TABLE 6.2.8-1

LOADS CONSIDERED IN THE EVALUATION OF THE VENT HEADER DEFLECTOR

General Category	Individual Loads Considered
Deadweight	Deadweight of deflector and supports
Earthquake (Operating Basis or Safe Shutdown)	Vertical acceleration of deflector
	Horizontal acceleration of deflector
SRV Discharge	Dynamic pressure load on torus shell
Intermediate or Small Break Accident	Pre- and post-chugging harmonic pressure on torus shell
Design Basis Accident (Pool Swell Phase)	Impact and drag on deflector
	Impact and drag on vent header, vent line, downcomers, and relief valve piping
	Vent system thrust loads
	Transient pressure load on torus shell
Design Basis Accident (Condensation Oscillation and Chugging Phase)	Condensation oscillation harmonic pressure on torus shell
	Pre- and post-chugging harmonic pressure on torus shell

TABLE 6.2.8-2

SUMMARY OF LIMITING STRESSES COMPARED TO ALLOWABLE VALUES FOR THE VENT HEADER DEFLECTOR

Component	Type of Stress	Ratio of Stress to Allowable Value
Deflector Span	Bending	0.60
Support Plate	Bending	0.96
Weld Between Support Plate and Ring Collar	Shear	0.88
Weld Between Support Plate and Diagonal Brace	Shear	0.90
Bolts Which Attach Deflector to Special I-Beam Member*	Tension	0.94
Weld Which Attaches Bolt Seating Block to Special I-Beam Member*	Shear	0.96

* The special I-beam member is utilized as a short portion of the deflector span in 2 of the 20 torus bays, for the purpose of avoiding a physical interference with the relief valve piping inside the torus.

6.2.9 Downcomer Bracing

As mentioned in Section 3.2, a modified downcomer brace was installed at each pair of downcomers as a part of the Mark I Long-Term Program. Figure 6.2.9-1 shows the primary features of the downcomer brace and its attachment to the downcomer.

The material of the downcomer brace body is steel pipe specified as ASME SA-53, Grade B. The downcomer clamps, attachment plates and eyebolts are ASME SA-36 steel, and the downcomer clamp bolts are ASME SA-307 steel.

6.2.9.1 Methods of Analysis

The downcomer braces were analyzed as pin connected beams, subject to axial loads as well as horizontal and vertical bending loads. The clamp assemblies used to attach the braces to the downcomers were analyzed by comparing the axial load in the braces to the manufacturer's specified capacity for the clamps. Finally, the local details of the connection between the brace and the clamp (attachment plates, eyebolts, and bolts) were analyzed using beam and plate models.

Reaction forces and moments in the downcomer braces for loads applied to the downcomers and braces were determined by hand calculations. Reactions for loads applied to other parts of the vent system and the torus shell were determined using the coupled torus/vent system model described in Section 5.1. Dynamic effects were considered for dynamically applied loads. Absolute values of reaction loads were summed in performing load combinations.

6.2.9.2 Loading and Acceptance Criteria

Loads considered in the analyses of the downcomer bracing are those defined in Section 4.4. Scoping calculations and engineering judgment were used to determine which of the loads had a significant effect on the downcomer braces. The loads used in the analyses are shown in Table 6.2.9-1.

Acceptance criteria for the braces were developed based on Section 2.2 of this report and the PUAAG (Reference 8.2.3). The downcomer braces were considered to be Class MC linear supports, in accordance with the PUAAG. The six limiting load cases identified in Table 6.0-1 were analyzed and compared to the most stringent allowables, i.e., ASME Service Level A/B allowables. Since the braces are subjected to axial loads as well as vertical and horizontal bending loads, appropriate interaction allowables for combinations of axial and bending loads were determined in accordance with Appendix XVII of the ASME Boiler and Pressure Vessel Code (Reference 8.4.1).

6.2.9.3 Summary of Results

A summary of the calculated loads on the downcomer braces is listed in Table 6.2.9-2. In the table, the maximum value of each of the types of loads applied to the braces in any of the six limiting load cases is listed, along with the Service Level A/B allowable load. As seen in Table 6.2.9-2, all loads on the braces are lower than Service Level A/B allowable loads.

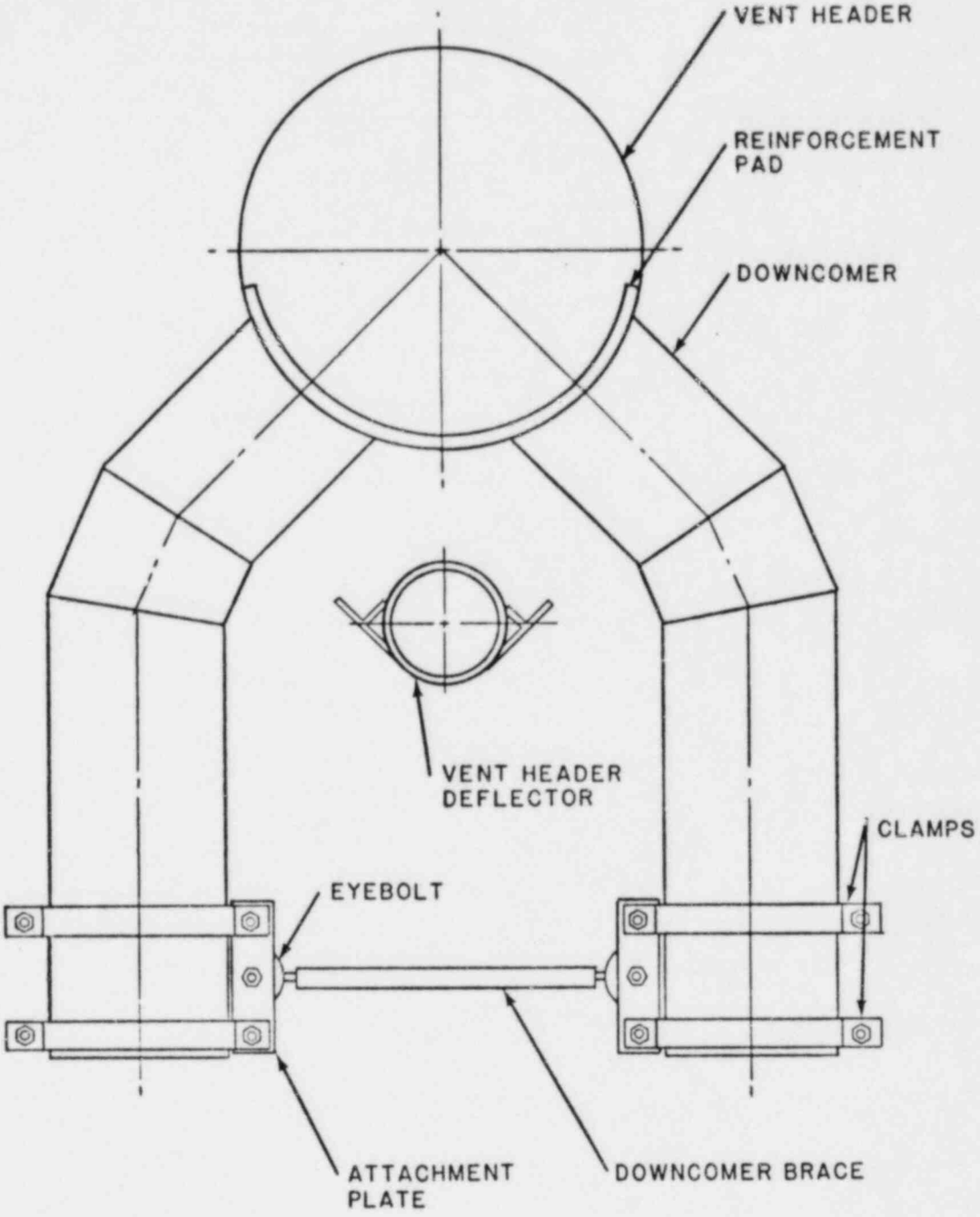

FIGURE 6.2.9-1

TYPICAL DOWNCOMER BRACE CONFIGURATION

TABLE 6.2.9-1

LOADS CONSIDERED IN THE EVALUATION
OF THE MODIFIED DOWNCOMER BRACING

General Category	Individual Load Considered
Deadweight	Deadweight of downcomer braces
	Deadweight of torus steel
	Deadweight of vent system steel
	Deadweight of torus water
Earthquake (Operating Basis or Safe Shutdown)	Vertical acceleration of vent system and torus
	Horizontal and vertical acceleration of downcomer braces
SRV Discharge	Relief valve piping reaction load on the main vent line
	Bubble drag on downcomers
	Bubble drag on downcomer bracing
	Discharge pressure on torus shell
Intermediate or Small Break Accident	Pre- and post-chugging harmonic pressure on torus shell
	Static pressure on torus shell
	Constrained thermal expansion of vent system and torus
	Constrained thermal expansion of downcomers and downcomer braces
	Pre- and post-chugging drag loads on braces
	Vent system thrust load
	Vent system static and harmonic internal pressure load
	Chugging downcomer tip load
Design Basis Accident (Pool Swell Phase)	Impact and drag on vent line
	Impact and drag on vent header
	Impact and drag on downcomer
	Impact and drag on vent deflector
	Impact and drag on relief valve piping
	Transient down/upload on torus shell
	Static internal pressure in torus
	Bubble drag load on braces
	Fallback drag loads on bracing
Design Basis Accident (CO/Chugging Phase)	Condensation oscillation harmonic pressure on torus shell
	Pre-and post-chugging harmonic pressure on torus shell
	Static pressure on torus shell
	Constrained thermal expansion of vent system and torus
	Constrained thermal expansion of downcomers and downcomer bracing
	CO, pre- and post-chugging drag loads on braces
	Vent system thrust load
	Vent system static and harmonic internal pressure loads
	Chugging downcomer tip load

TABLE 6.2.9-2

RESULTS OF ANALYSIS OF DOWNCOMER BRACING

TYPE OF LOAD	LIMITING LOAD COMBINATION	VALUE OF LOAD	SERVICE LEVEL A/B ALLOWABLE
Axial Force in Brace	IBA/SBA (CO/Chug) + SRV + EQ(S) + DW	10.4 kip	13.6 kip
Bending Moment in Brace	DBA (PS) + SRV + EQ(S) + DW	9.2 kip-in (1)	22.8 kip-in
Vertical Shear Force at End of Brace	IBA (CO/Chug) + SRV + EQ(S) + DW	0.6 kip	2.7 kip
Horizontal Shear Force at End of Brace	IBA (CO/Chug) + SRV + EQ(S) + DW	0.1 kip	2.0 kip
Combined Bending Moment and Axial Force in Brace	DBA(PS) + SRV + EQ(S) + DW	0.64	1.0
Interaction of Axial Force and Shear Force in Attachment Components	(Envelope)	0.85	1.0

NOTES:

(1) The bending moment listed is the resultant of horizontal and vertical bending moments.

6.3 INTERNAL STRUCTURES

As noted in Section 3.3, the only internal structure remaining in the Oyster Creek torus is the catwalk. The catwalk has been analyzed for the following loads:

- LOCA Loads on Internal Structures (Section 4.5)
- SRV Induced Loads on Internal Structures (Section 4.6.3)
- Base excitation resulting from LOCA and SRV loads on the torus and vent header. (Sections 4.3, 4.4, and 4.6.2)

Combinations of the loads were considered in accordance with the Plant Unique Analysis Application Guide (PUAAG), (Reference 8.2.3). The controlling load combinations for the catwalk are listed in Table 6.3-1.

The catwalk structural analysis was performed in accordance with the requirements of the PUAAG (Reference 8.2.3) and NUREG-0661 (Reference 8.1.2). Specifically, catwalk analyses were based on a computer code beam model of the catwalk. This model was used to determine distribution of forces and stresses in the catwalk structural elements for unit static loads and to determine the frequencies of vibration and the shape of the natural modes of the structure. The results of the computer code model were then used in conservative hand calculations of the stresses in the various catwalk components for the load combinations specified in the PUAAG (Reference 8.2.3). These hand calculations used equivalent static loads based on the response of single degree of freedom, linear systems. Calculated stresses were compared to allowables in the ASME Boiler and Pressure Vessel Code, Section III, Appendix XVII (Reference 8.4.1) as permitted for linear component supports by subsection NF of Section III of the ASME Code. For Service Level D, the allowables of Appendix XVII were increased in accordance with Appendix F of Section III of the ASME Code. Also for Service Level D, the analyses used the provisions of Appendix XVII, Paragraph 4000, for limit analyses design of continuous beams.

Preliminary analyses had indicated that the catwalk, as-built, would be incapable of withstanding DBA pool swell impact and drag loads. Hence, the catwalk was modified to withstand pool swell loads as follows:

- Diagonal braces were added to the walkway span. These were attached at the one-third points of the walkway span and were anchored to the ring girders. There are two pairs of braces in each torus bay. Braces are approximately 9-feet long and are fabricated of 3-inch Schedule 80 pipe. The braces reduce the unsupported span of the catwalk to one-third the original span; thus they reduce the beam bending stresses. Also they reduce the loads on the original support brackets.

- The original catwalk handrails were replaced with 1-1/4-inch, double extra-strong (XXS) pipe. The new handrails are much stronger then the originals. They are also more streamlined and hence reduce applied pool swell drag loads. The original handrails were 2 x 1-1/2 x 1/4 angles.

- The catwalk ladder was removed. A temporary ladder is now installed for torus access only during plant outages when internal torus work or inspections must be performed.

The final analyses of the Oyster Creek catwalk for the Mark I Containment Long-Term Program included the above-mentioned modifications to the original catwalk. The analyses demonstrated that the catwalk meets allowables for all load combinations of the PUAAG (Reference 8.2.3). For the worst-case load combination (Case 25 - LOCA pool swell), the catwalk is within the Service Level D allowables of the ASME Code; the more liberal limits of the special non-code Service Level E established by the PUAAG have not been used for Oyster Creek internal structures. The limiting components of the catwalk and their calculated stresses are listed and compared to appropriate allowables in Table 6.3-2.

TABLE 6.3-1

CONTROLLING LOAD CASES FOR OYSTER CREEK INTERNAL STRUCTURES

PUAAG LOAD CASE	SERVICE LEVEL	DESCRIPTION OF LIMITING CASE
5	A/B	SBA/IBA CO/Chugging
15	C	SBA/IBA CO/Chugging plus SRV and Safe Shutdown Earthquake
25(1)	D/E(2)	DBA Pool Swell plus SRV and Safe Shutdown Earthquake

NOTES

(1) PUAAG Load Case 27 was also analyzed and found not to control stresses for Service Levels D/E.

(2) The PUAAG non-Code Service Level E was not invoked for Oyster Creek internal structures. Rather PUAAG Load Cases with Service Level E Limits were analyzed to the more restrictive requirements of Service Level D.

TABLE 6.3-2

LIMITING COMPONENTS AND
CALCULATED STRESSES FOR THE OYSTER CREEK CATWALK

LOAD CASE	LIMITING COMPONENTS	CALCULATED STRESS		ALLOWABLE (ksi)	PERCENT OF ALLOWABLE (%)
		TYPE	VALUE (ksi)		
5	Midrail	Bending	13.5	21.6	63
15	Midrail	Bending	17.3	28.7	60
25	Vertical Support Column Bolt	Shear	25.4	27.0	94

7.0 FATIGUE EVALUATION

This section describes the methodology used to determine the lifetime fatigue usage of torus and vent system components and the results of the analysis. The fatigue evaluation of piping and torus shell regions adjacent to piping penetrations (nozzles) is covered separately in the plant-unique analysis of the torus attached piping (Reference 8.5.1). The fatigue analysis methodology is based on the Mark I Long-Term Program criteria discussed in Section 2.2, using the loads described in Section 4.0.

7.1 ASME CODE JURISDICTION AND CRITERIA

The ASME Boiler and Pressure Vessel Code (ASME Code), Reference 8.4.1, criteria for the acceptability of a component under cyclic loading conditions are established based on component classification. Relevant classifications for the Oyster Creek Mark I Long-Term Program components are:

- Class MC Components - Torus Shell and Vent System Pressure Boundary Parts

- Class MC Integral Attachments - Shell Hoop Straps, Support Column Attachments to the Shell, Mid-Bay Saddle Upper Flange, Ring Girder, Vent System Support Collar and Vent Deflector Brace Pad

- Class MC Linear Supports - Torus Support Columns, Vent System Support Columns, Vent System Downcomer Bracing and Vent Deflector and Supports

Descriptions of these component locations are given in Section 3.0 of this report.

For those components classified as MC components or MC integral attachments, methods of fatigue analysis are given in the ASME Code, Paragraph NE 3221.5. This paragraph requires that the range of the peak stress intensity be limited to certain values, based on the number of cycles anticipated.

Paragraph NF 3132.3 of the ASME Code covers the methods for high cycle fatigue analysis of MC Linear Supports. Those supports with less than 20,000 fatigue cycles do not require an analysis. For the Oyster Creek torus and v[illegible] system, no support equaled or exceeded this value, and, therefore [illegible]atigue analysis was required.

7.2 LOAD SOURCES, LOAD CYCLES AND SEQUENCE OF LOADS

The following load sources were considered in the fatigue analysis of the torus and vent system:

- Normal Operating Loads
- SRV Discharge
- Small Break Accident (SBA)
- Intermediate Break Accident (IBA)
- Design Basis Accident (DBA)
- Operating Basis Earthquake (OBE)

Figure 7.2-1 displays the number of load cycles and sequence considered in the evaluation of all structures except the downcomer/vent header intersection. Figure 7.2-2 gives this information for the downcomer/vent header intersection. A more detailed description of the loads is given in the notes following these figures.

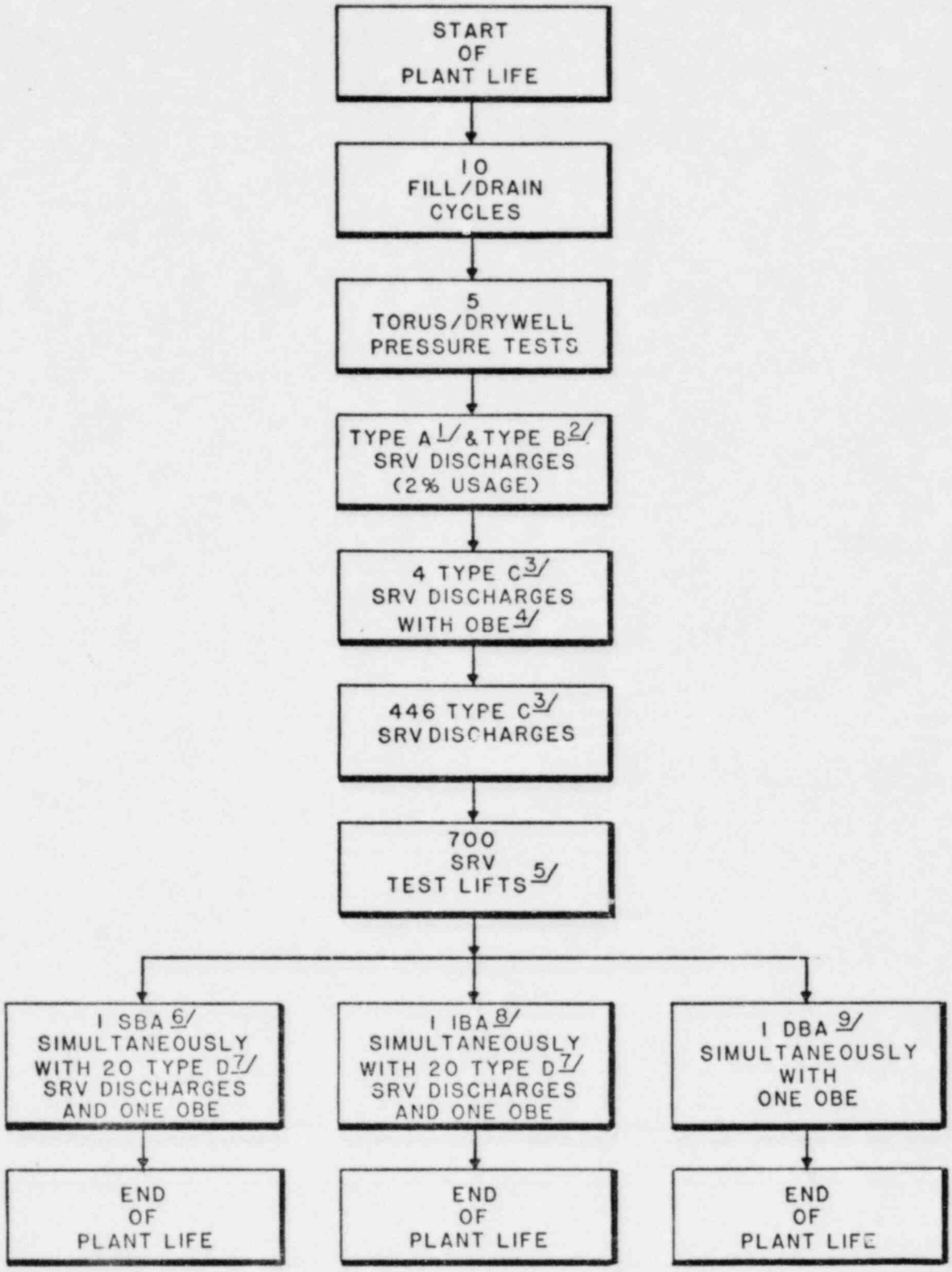

FIGURE 7.2-1

LOAD CYCLES FOR EVALUATION OF ALL STRUCTURES EXCEPT DOWNCOMER/VENT HEADER INTERSECTION

NOTES FOR FIGURE 7.2-1

1. Type A SRV discharges are those with the original design relief valve discharge fitting (i.e., no quencher) and the original design torus structure (i.e., no saddle). Usage for these and the TYPE B[2/] discharges was estimated to be 2% everywhere.

2. A Type B SRV discharge is a one-valve, normal operating condition initial actuation with the modified relief valve discharge fitting (quencher), and the original design torus structure (i.e., no saddle).

3. A Type C SRV discharge is a five-valve, normal operating condition discharge, subsequent actuation, with the modified relief valve discharge fitting (quencher) and the modified torus structure (saddle).

4. The OBE transient involves ten cycles of maximum amplitude.

5. An SRV Test Lift is a one-valve cold discharge at normal operating pressure.

6. The SBA includes 900 seconds of chugging. For all analyses, the chugging load was modeled with 900 seconds of continuous post-chug load; this bounds the combined pre-chug and post-chug load.

7. A Type D SRV discharge is a five-valve, accident (SBA or IBA) condition discharge, with subsequent actuation, and with the modified relief valve discharge fitting (quencher) and the modified torus structure (saddle).

8. The IBA includes a total of 900 seconds of chugging. (IBA CO loads are bounded by chugging loads.) For all analyses, IBA (CO) and chugging were modeled with the post-chug load running continuously for 900 seconds.

9. The DBA includes 30 seconds of DBA condensation oscillation concurrent with the OBE and 30 seconds of chugging. For all analyses, pre-chugging and post-chugging loads were enveloped with 30 seconds of continuous post-chug load.

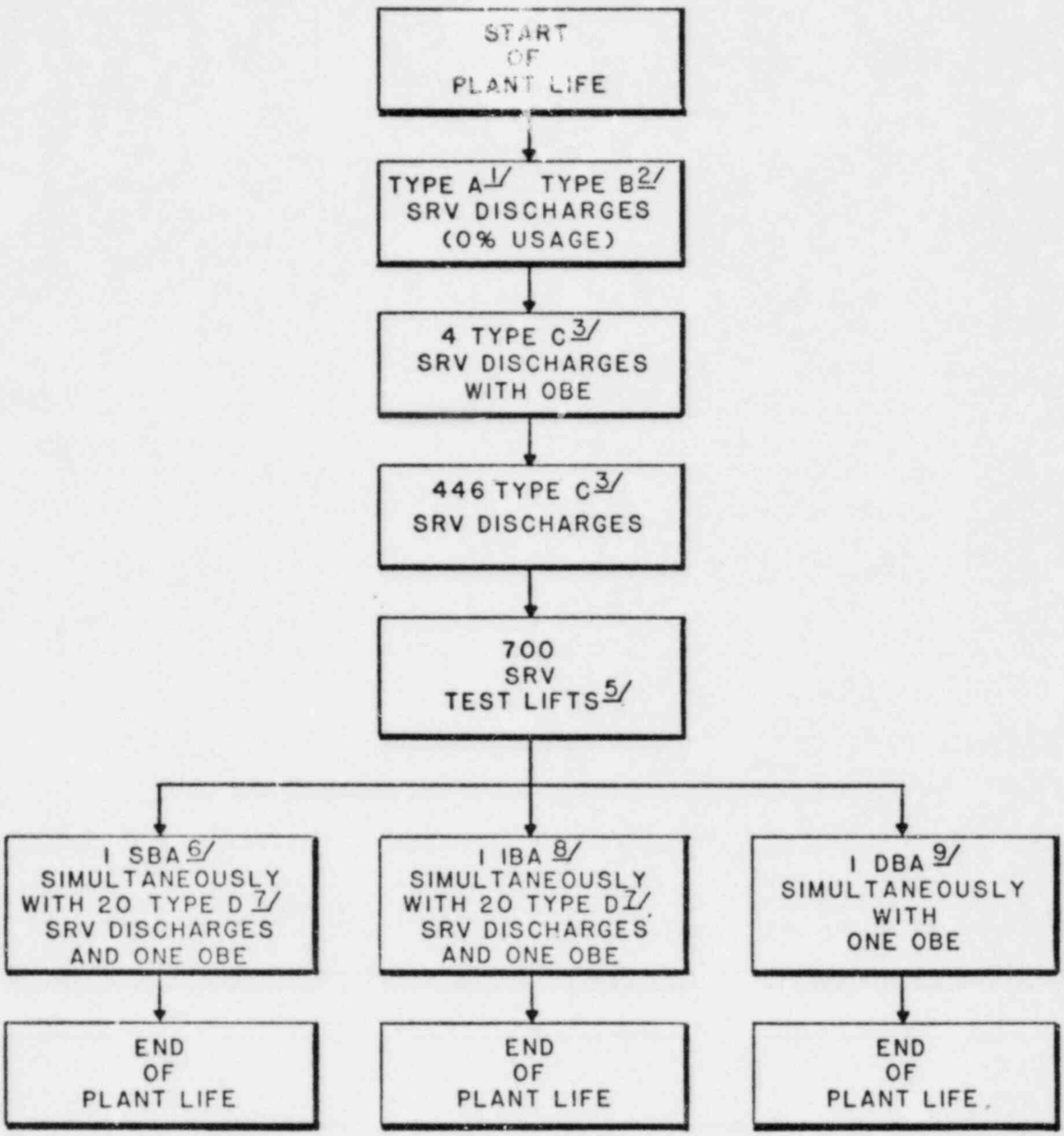

FIGURE 7.2-2

LOAD CYCLES FOR EVALUATION OF
DOWNCOMER/VENT HEADER INTERSECTION

NOTES FOR FIGURE 7.2-2

1. Type A SRV discharges are those with the original design relief valve discharge fitting (i.e., no quencher) and the original design torus structure (i.e., no saddle). Usage for these and the Type B[2/] discharges was assumed to be 0% at the limiting DC/VH locations, based on the fact that new limiting locations are created by the DC/VH reinforcement modification.

2. A Type B SRV discharge is a one-valve, normal operating condition initial actuation with the modified relief valve discharge fitting (quencher) and the original design torus structure (i.e., no saddle).

3. A Type C SRV discharge is a five-valve, normal operating condition discharge, subsequent actuation, with the modified relief valve discharge fitting (quencher) and the modified torus structure (saddle).

4. The OBE transient involves ten cycles of maximum amplitude.

5. An SRV Test Lift is a one-valve cold discharge at normal operating pressure.

6. The SBA includes 900 seconds of chugging. Chugging loads on downcomers in accordance with Section 4.5.3 of Reference 8.2.1 were used.

7. A Type D SRV discharge is a five-valve, accident (SBA or IBA) condition discharge, with subsequent actuation, and with the modified relief valve discharge fitting (quencher) and the modified torus structure (saddle).

8. The IBA includes a total of 900 seconds of IBA CO and 200 seconds of chugging. The IBA chugging load was considered for 900 seconds for evaluation purposes, since this bounds the combined IBA CO and chugging event.

9. The DBA includes 30 seconds of DBA condensation oscillation concurrent with the OBE and 30 seconds of chugging.

7.3 ANALYSIS METHODS

7.3.1 Torus

Stress intensity ranges for the life scenarios depicted in Figure 7.2-1 were determined using the finite element computer model of the coupled torus/vent system described in Section 5.1 and the analysis procedures described in Section 6.1. Appropriate stress extrapolation factors were applied to computer monitor element results in order to estimate local primary plus secondary stresses at the location of the structural discontinuity of interest. A fatigue strength reduction factor (FSRF) was applied to this result in order to account for the small scale (on the order .1 mm) effects of weld toe geometry. That is, the peak stress was determined as follows:

$$FSRF \times (P_L + P_B + Q) = P_L + P_B + Q + F$$

in the terminology of Section III of the ASME Code (Reference 8.4.1). When two or more cycle types occur simultaneously, stress intensity ranges for each were separately determined and added in order to conservatively estimate total range for the combined event.

Cycle counting for the events was accomplished as torus follows:

a. For DBA(CO) and post-chug loads, time histories of torus support column reactions generated by the computer model were used to determine the number of cycles and their relative magnitudes.

b. For SRV loads, SRV bubble time histories were used to estimate number of cycles per event.

c. Each earthquake event was assumed to have ten cycles duration, as specified in NUREG-0800 (Reference 8.1.8).

Fatigue usage factors, as defined in Section III of the ASME Code (Reference 8.4.1), Paragraph NE 3221.5, were determined for each load cycle type and for combined load cycle types. Limiting locations in the torus were determined and results are reported in Section 7.4, below.

7.3.2 Vent System

Vent system stress intensity ranges were calculated from beam reactions and equivalent stress ranges determined using the vent system beam model described in Section 5.2 and the analysis procedures described in Section 6.2. Local primary plus secondary stresses at the location of the structural discontinuities were calculated and FSRF's were used to determine peak stress intensity ranges for each location of interest.

For regions other than the vent header/downcomer intersection, cycle counting was performed on the basis of vent system column reaction time histories for CO, chugging and SRV loads. For the intersection, actual time histories of local stresses were used to count cycles. For all locations, the earthquake was counted as a ten-cycle load acting on the vent system.

Fatigue usage factors were determined as for the torus, described above. Limiting locations and results are given in Section 7.4, below.

7.4 SUMMARY OF RESULTS

Fatigue usage factors for the limiting locations in the torus and vent system are listed in Table 7.4-1. The results show all locations meet the acceptance criteria for the Mark I Containment Long-Term Program.

TABLE 7.4-1

RESULTS OF THE FATIGUE ANALYSIS OF
TORUS AND VENT SYSTEM COMPONENTS

Component	Location	Usage	Scenario[1/]
Torus Shell	Near Hoop Strap Fillet Weld	< .62[2/]	IBA
Torus Shell	Near Ring Girder Fillet Weld	< .62[2/]	IBA
Torus Shell	Near Saddle Flange Fillet Weld	.62	IBA
Torus Shell	Near Support Column Connections	< .62[2/]	IBA
Support Column Attachments	Integral Attachments	.37	IBA
Vent Header	Vent Line Intersection	.82	IBA
Downcomer	Vent Header Intersection	.88	DBA
Vent Header	Ring Collar	.51	IBA
Vent Line	At Drywell Intersection	.46	DBA

1/ The term "scenario" indicates which of the three accident conditions described in Figures 7.2-1 and 7.2-2 lead to the usage reported.

2/ Fatigue was calculated for the areas of highest stress. The shell area near the saddle flange bounds all other areas.

8.0 REFERENCES

The following documents are referenced in this report. The documents are grouped by issuing organization.

8.1 U.S. NUCLEAR REGULATORY COMMISSION

8.1.1 NUREG-0484 (Revision 1). Mattu, R. K. Methodology for Combining Dynamic Responses. May 1980.

8.1.2 NUREG-0661. Safety Evaluation Report, Mark I Containment Long-Term Program Resolution of Generic Technical Activity A-7. July 1980.

8.1.3 Crutchfield, D.M. Letter to I.R. Finfrock, Jr. (JCP&L) . Transmitting the "Order of Modification of License and Grant of Extension of Exemption." January 19, 1980.

8.1.4 TID-7024. Nuclear Reactors and Earthquakes, Appendix F. Lockheed Aircraft Corporation and Holmes and Narver, Inc. for the Division of Reactor Development, U.S.A.E.C. August 1963.

8.1.5 NUREG/CR-1083, LBL-6754. Aslam, M; Godden, W.G.; and Scalise, T. Sloshing of Water i Annular Pressure-Suppression Pool of Boiling Water Reactors Under Earthquake Ground Motions. Lawrence Berkeley Laboratory for U.S.N.R.C. October 1979.

8.1.6 NUREG/CR-1082, LBL-7984. Aslam, M; Godden, W.G.; and Scalise,T. Sloshing of Water in Torus Pressure-Suppression Pool of Boiling Water Reactors Under Earthquake Ground Motions. Lawrence Berkeley Laboratory for U.S.N.R.C. October 1979.

8.1.7 NUREG-0408. Mark I Containment Short-Term Program Safety Evaluation Report. December 1977.

8.1.8 NUREG-0800. Standard Review Plan for the Review of Safety Analysis Reports for Nuclear Power Plants: Section 3.7.3, Revision 1, "Seismic Subsystem Analysis". July 1981.

8.2 GENERAL ELECTRIC COMPANY

8.2.1 NEDO-21888 (Revision 2). Mark I Containment Program Load Definition Report. November 1981.

8.2.2 NEDO-24572 (Revision 2). Mark I Containment Program Plant Unique Load Definition Oyster Creek Nuclear Generating Station. July 1982. (Pertinent data from this document are contained in the Appendix in Section 9.0, herein.)

8.2.3 NEDO-24583-1. Mark I Containment Program Structural Acceptance Criteria Plant-Unique Analysis Application Guide. October 1979.

8.2.4 Amendment 15 to Oyster Creek FDSAR. Oyster Creek Nuclear Power Plant, Primary Containment Design Report. The Ralph M. Parsons Company. October 1967.

8.2.5 NEDC-23702-P. Arain, S. M. Mark I Containment Program, Seismic Slosh Evaluation. March 1978.

8.2.6 (Deleted)

8.2.7 NEDC-21471-2. Analytical Model for Estimating Drag Forces on Rigid Submerged Structures Caused by LOCA and Safety Relief Valve Ramshead Air Discharges. April 1979.

8.2.8 NEDE-21983-P. Mark I Containment Program Submerged Structures Model Main Vent Air Discharges Evaluation Report. March 1979.

8.2.9 NEDE-24539-P. Full-Scale Test Program Final Report. April 1979.

8.2.10 NEDO-25070. Analytical Model for Estimating Drag Forces on Rigid Submerged Structures Caused by Condensation Oscillation and Chugging. April 1979.

8.2.11 NEDE-21878-P. Mark I Containment Program Analytical Model for Computing Air Bubble and Boundary Pressures Resulting from an SRV Discharge Through a T-Quencher Device. January 1979.

8.2.12 NEDE-23749-P. Mark I Containment Program Analytical Model for Computing Transient Pressures and Forces in the Safety/Relief Valve Discharge Line. February 1978.

8.2.13 NEDE-23898-P. Mark I Containment Program Analytical Model for Computing Water Rise in a Safety/Relief Valve Discharge Line Following Valve Closure. October 1978.

8.3 JERSEY CENTRAL POWER AND LIGHT COMPANY

8.3.1 Finfrock, I. R., Jr. Letter to G. Lear (USNRC) . Oyster Creek Nuclear Generating Station Docket No. 50-219, Relief Valve Line Restraints. October 31, 1975.

8.3.2 _____. Letter EA-76-737 to G. Lear (USNRC) . Transmitting the "Oyster Creek Nuclear Generating Station Short-Term Program Plant-Unique Torus Support Systems Analysis." August 2, 1976.

8.3.3 _____. Letter EATE-4 to G. Lear (USNRC) Transmitting the "Oyster Creek Nuclear Generating Station Short-Term Program Plant Unique Torus Attached Piping Analysis." September 1, 1976.

8.3.4 _____. Letter to the Director of Nuclear Reactor Regulation . Transmitting the "Oyster Creek Nuclear Generating Station Test Report on the Modified Electromatic Relief Valve Discharge Device." May 11, 1978.

8.4 AMERICAN SOCIETY OF MECHANICAL ENGINEERS

8.4.1 Boiler and Pressure Vessel Code, Section III. "Rules for Construction of Nuclear Power Plant Components; Division 1." 1977 Edition with Addenda through Summer 1977.

8.4.2 Boiler and Pressure Vessel Code, Section II. "Material Specifications." 1962.

8.4.3 Boiler and Pressure Vessel Code, Section VIII. "Rules for Construction of Pressure Vessels." 1962.

8.4.4 Boiler and Pressure Vessel Code, Section IX. "Welding and Brazing Qualifications." 1962.

8.4.5 Boiler and Pressure Vessel Code Interpretations (Case 1270N-5). "General Requirements for Nuclear Vessels." September 15, 1961.

8.4.6 Boiler and Pressure Vessel Code Interpretations (Case 1271N). "Safety Devices." April 17, 1959.

8.4.7 Boiler and Pressure Vessel Code Interpretations (Case 1272N-5). "Containment and Intermediate Containment Vessels." September 15, 1961.

8.4.8 Boiler and Pressure Vessel Code, Section XI. "Inservice Inspection." 1977.

8.5 MPR ASSOCIATES, INC.

8.5.1 MPR-734. Oyster Creek Nuclear Generating Station, Mark I Containment Long-Term Program -- Plant-Unique Analysis Report: Torus Attached Piping. August 1982.

8.6 OTHER

8.6.1 Burns and Roe, Inc. Reactor Drywell and Suppression Chamber Containment Vessels; Jersey Central Power and Light Company, Oyster Creek, New Jersey. Specification S-2299-4.

8.6.2 American Institute of Steel Construction. Specification for the Design Fabrication and Erection of Structural Steel for Buildings. April 17, 1963.

8.6.3 Chicago Bridge and Iron Company. Drawings of Oyster Creek Pressure Suppression Containment Vessels. Contract No. 9-0971.

8.6.4 American Concrete Institute. Code Requirements for Nuclear Safety Related Concrete Structures and Commentary. ACI 349-76 with 1979 Supplement.

8.6.5 Expansion Joint Manufacturers Association, Inc. Standards of the Expansion Joint Manufacturers Association, Inc. Fifth Edition. 1980.

8.6.6 Control Data Corporation. STARDYNE User Information Manual, Revision C. April 1, 1980; Publication No. 76079900C.

8.6.7 _____. ANSYS User Information Manual, Revision B. September 17, 1979; Publication No. 84000660B.

9.0 APPENDIX A, OYSTER CREEK PLANT UNIQUE LOAD DEFINITION DATA

Pertinent data from the Mark 1 Containment Program Plant Unique Load Definition Report (PULD) for the Oyster Creek Nuclear Generating Station (Reference 8.2.2) which was used in the Oyster Creek plant-unique analysis are presented in this appendix.

TABLE OF CONTENTS FOR APPENDIX A

Figure/Table Number	Title
Figure OC 4.1.1-1b	DBA Containment Pressure Response, Zero Δ P, 4.06ft Submergence
Figure OC 4.1.1-2b	DBA Containment Temperature Response Zero Δ P, 4.06ft Submergence
Figure OC 4.1.2-1a	IBA Containment Pressure Response Zero Δ P, 4.06ft Submergence
Figure OC 4.1.2-2a	IBA Containment Temperature Response Zero Δ P, 4.06ft Submergence
Figure OC 4.1.3-1a	SBA Containment Pressure Response, Zero Δ P, 4.06ft Submergence
Figure OC 4.1.3-2a	SBA Containment Temperature Response, Zero Δ P, 4.06ft Submergence
Table OC 4.2-1	Nomenclature for DBA Vent System Thrust Load Section
Figure OC 4.2-1	Definition of Positive Thrust Loads
Figure OC 4.2-12 through 4.2-21	Vent System Internal Pressure and Thrust Loads, Zero Δ P, 3.53ft Submergence
Figure OC 4.2 - 12a through 4.2 - 21a	Vent System Internal Pressure and Thrust Loads, Zero Δ P, 4.06ft Submergence
Table OC 4.3.1-1	Net Torus Vertical Loads, Average Submerged Pressure and Torus Air Pressure (Filtered), Zero Δ P, 4.06ft Submergence

Table OC 4.3.1-2a	Net Torus Vertical Load, Average Submerged Pressure and Torus Air Pressure (Filtered), Zero Δ P, 3.0ft Submergence
Table OC 4.3.3-2	Vent Header Local Impact/Drag Pressure Transients, Zero Δ P, 4.06ft Submergence
Table OC 4.3.3-1b	Vent Header Local Impact/Drag Pressure Transients, Zero Δ P, 3.0ft Submergence
Figure OC 4.3.3-1	Location of Impact/Drag Pressure Transducers on Header
Figure OC 4.3.3-2	Longitudinal Vent Header Impact Velocity Distribution Based on EPRI Main Vent Orifice Tests, Operating and Zero Δ P, 4.06ft Submergence
Figure OC 4.3.3-3	Longitudinal Time Delay Distribution Based on EPRI Main Vent Orifice Tests, Operating and Zero ΔP, 4.06ft Submergence
Figure OC 4.3.3-5	Circumferential Time Delay Distribution, Zero Δ P, 4.06ft Submergence
Figure OC 4.3.3-1a	Longitudinal Vent Header Impact Velocity Distribution Based on EPRI Main Vent Orifice Tests, Operating and Zero Δ P, 3.0ft Submergence
Figure OC 4.3.3-2a	Longitudinal Time Delay Distribution Based on EPRI Main Vent Orifice Tests, Operating and Zero Δ P, 3.0ft Submergence
Figure OC 4.3.3-1b	Circumferential Time Delay Distribution, Zero ΔP, 3.0ft Submergence
Figure OC 4.3.4-1a	Pool Swell Displacement Distribution, Zero Δ P, 4.06ft Submergence
Figure OC 4.3.4-2a	Pool Swell Velocity Distribution, Zero Δ P, 4.06ft Submergence
Figure OC 4.3.4-1c	Pool Swell Displacement Distribution, Zero Δ P, 3.0ft Submergence

Figure OC 4.3.4-2c	Pool Swell Velocity Distribution, Zero ΔP, 3.0ft Submergence
Figure OC 4.3.9-1	Vent Header Deflector Loads, Zero ΔP, 4.06ft Submergence
Figure OC 4.3.9-1a	Vent Header Deflector Loads, Zero ΔP, 3.0ft Submergence

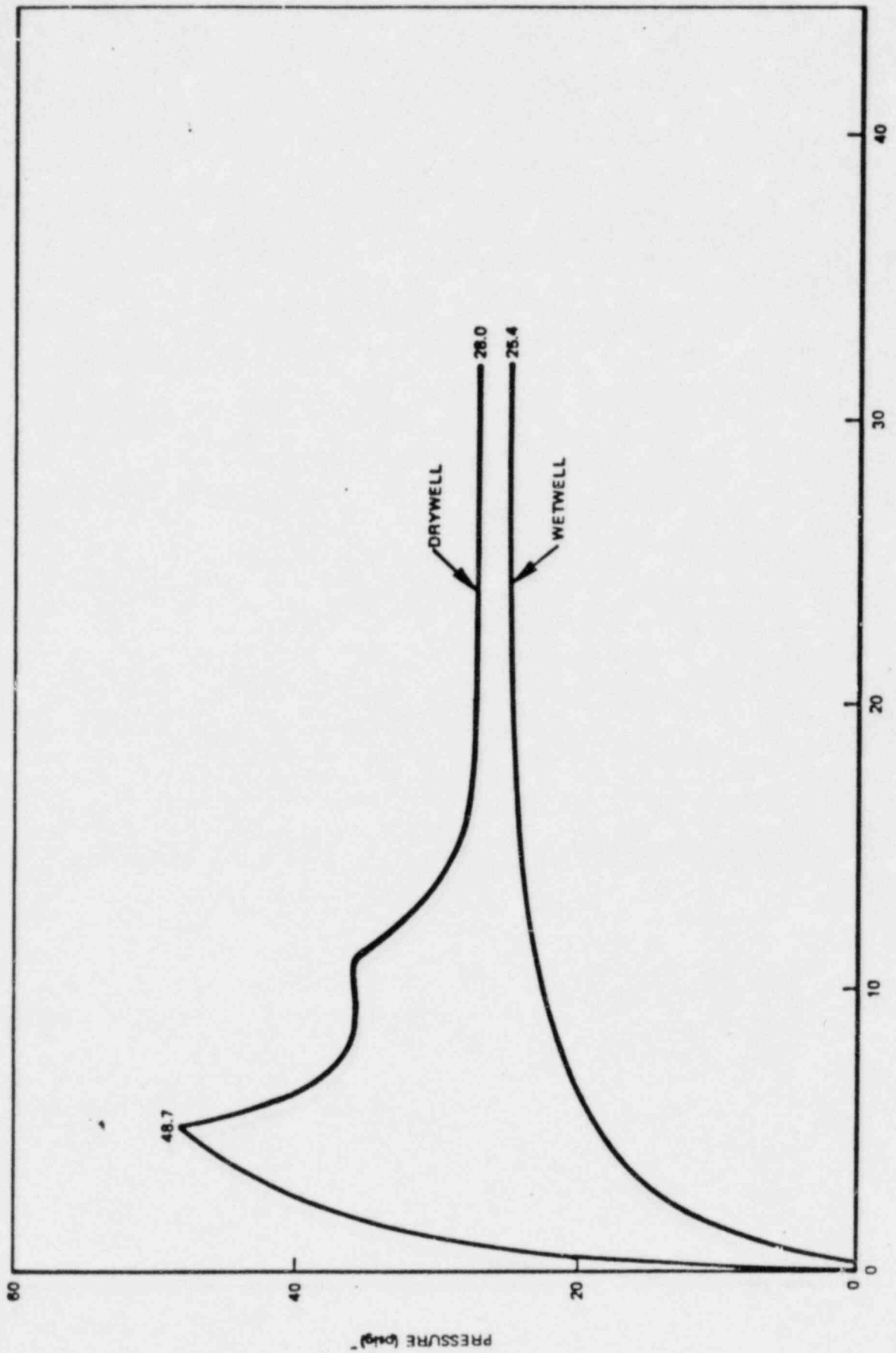

Figure OC 4.1.1-1b. DBA Containment Pressure Response (Zero ΔP), 4.06 ft Submergence

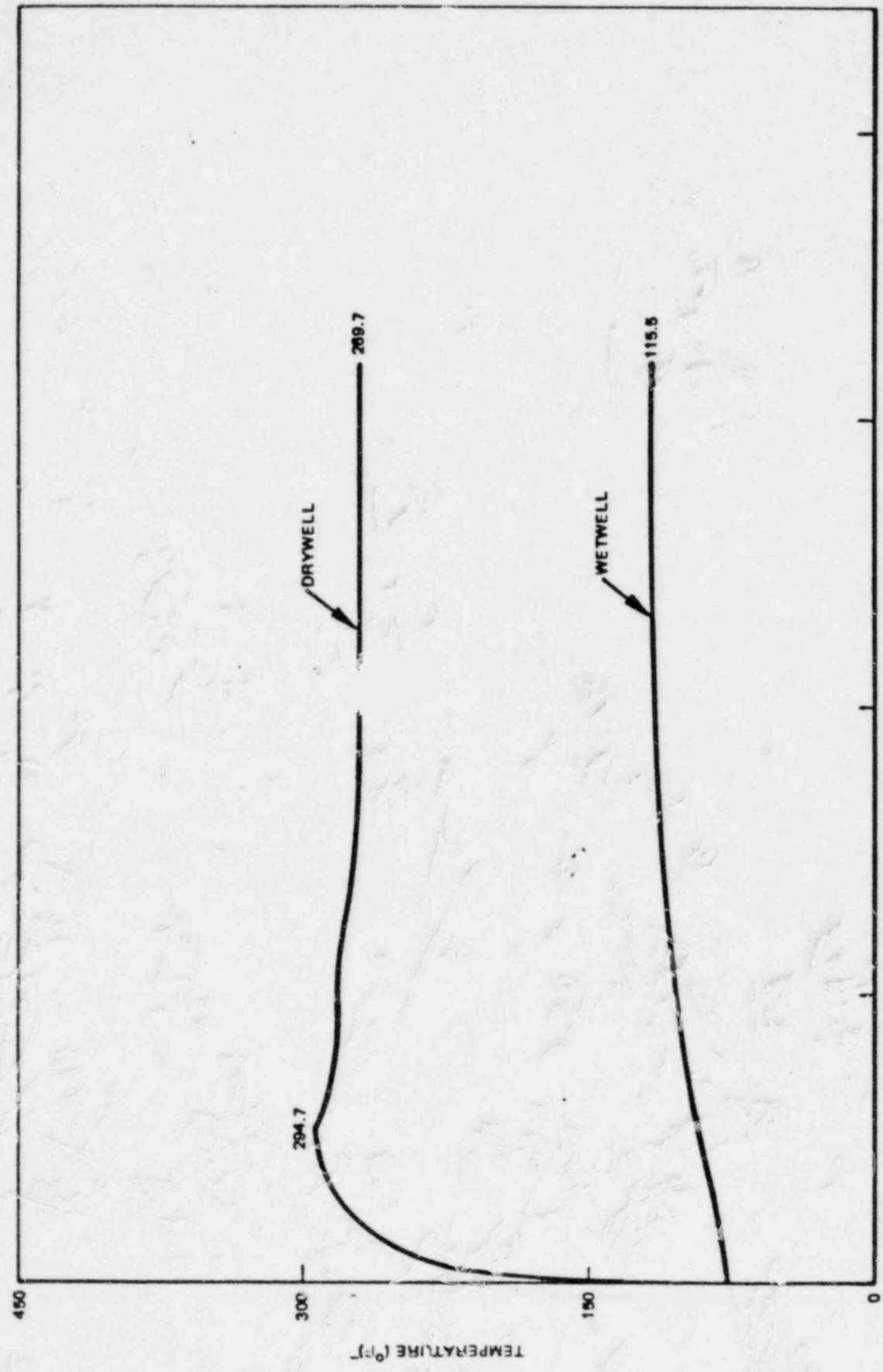

Figure OC 4.1.1-2b. DBA Containment Temperature Response (Zero ΔP), 4.06 ft Submergence

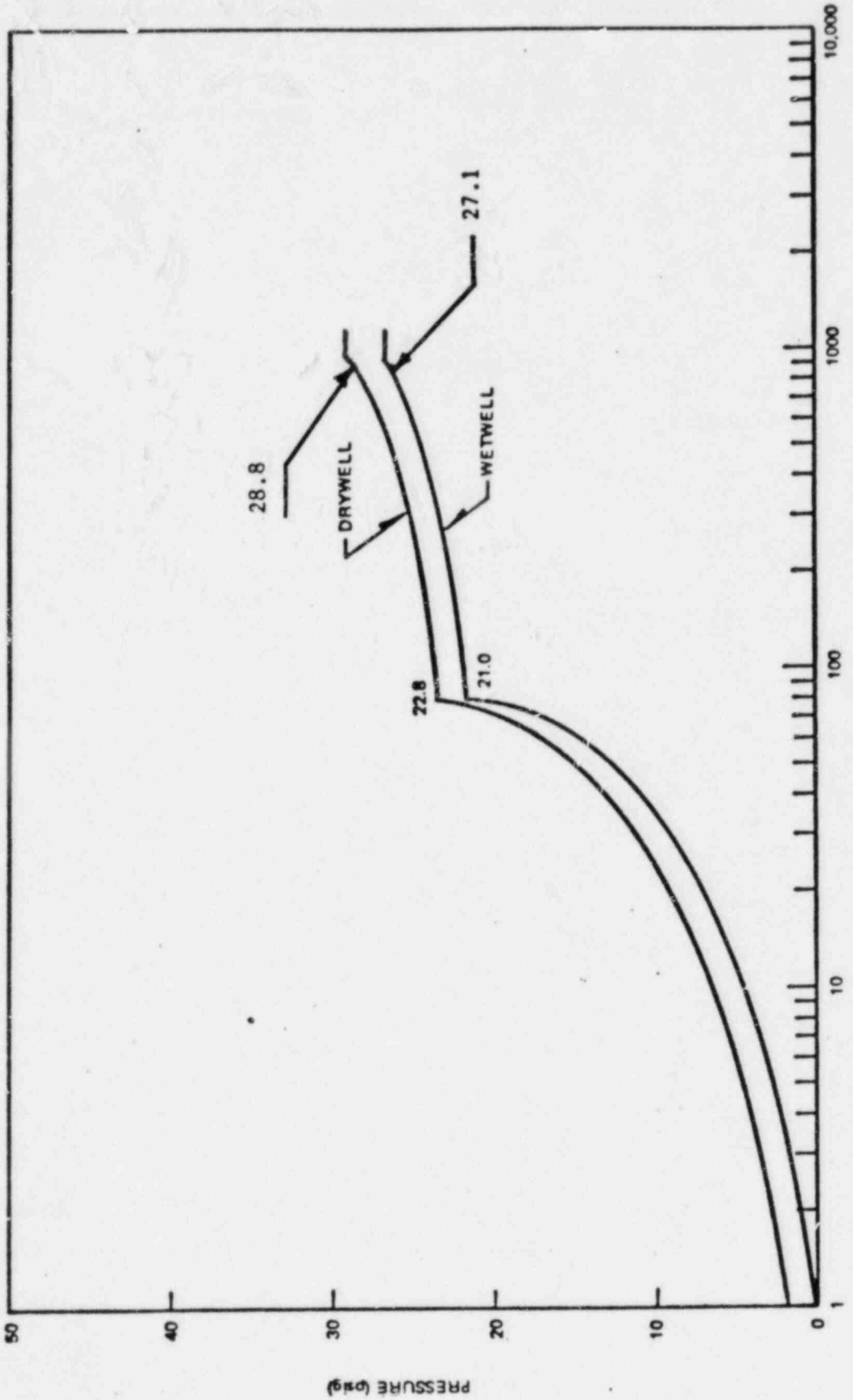

Figure OC 4.1.2-1a. IBA Containment Pressure Response (Zero ΔP), 4.06 ft Submergence

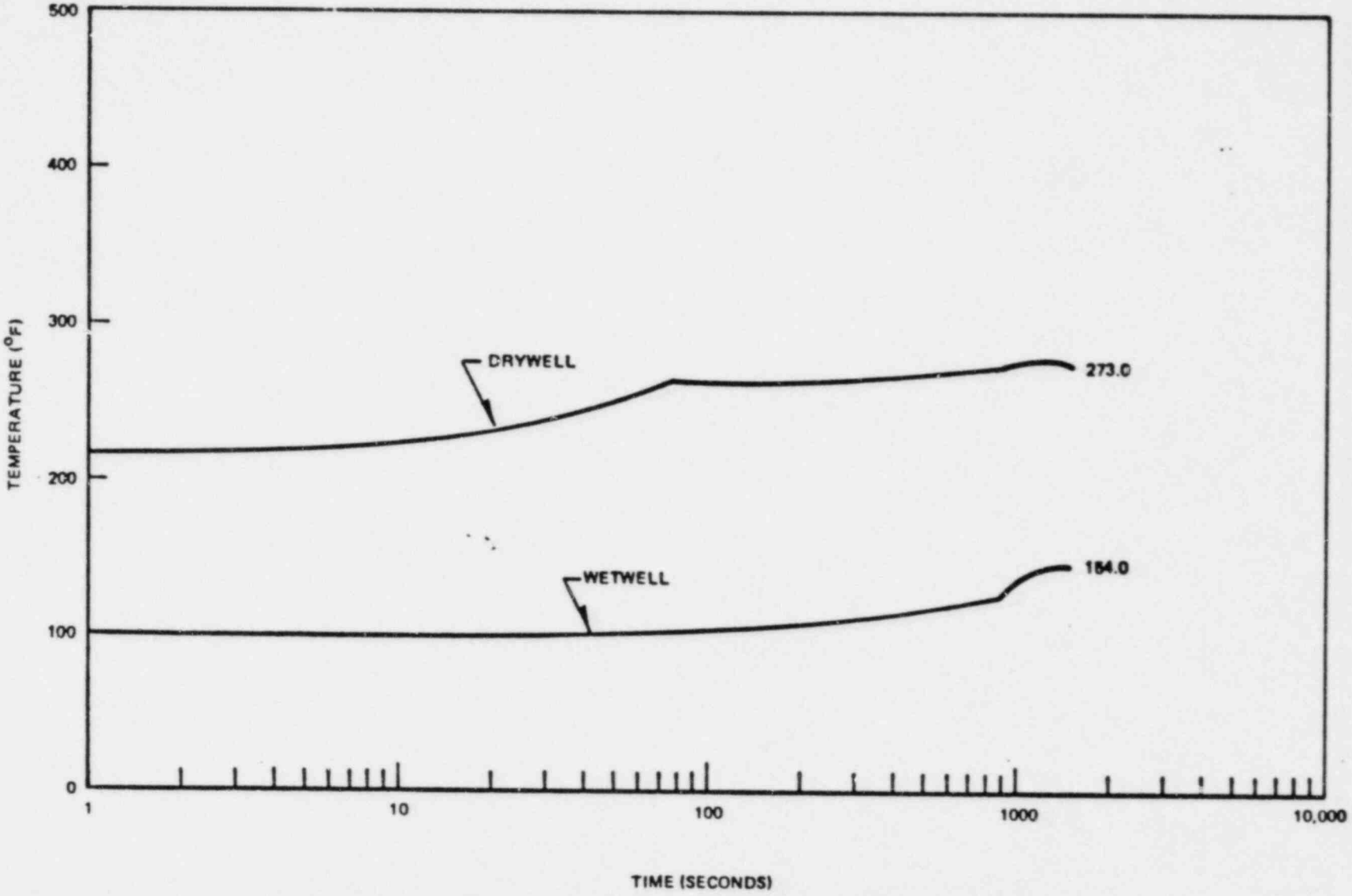

Figure OC 4.1.2-2a. IBA Containment Temperature Response (Zero ΔP), 4.06 ft Submergence

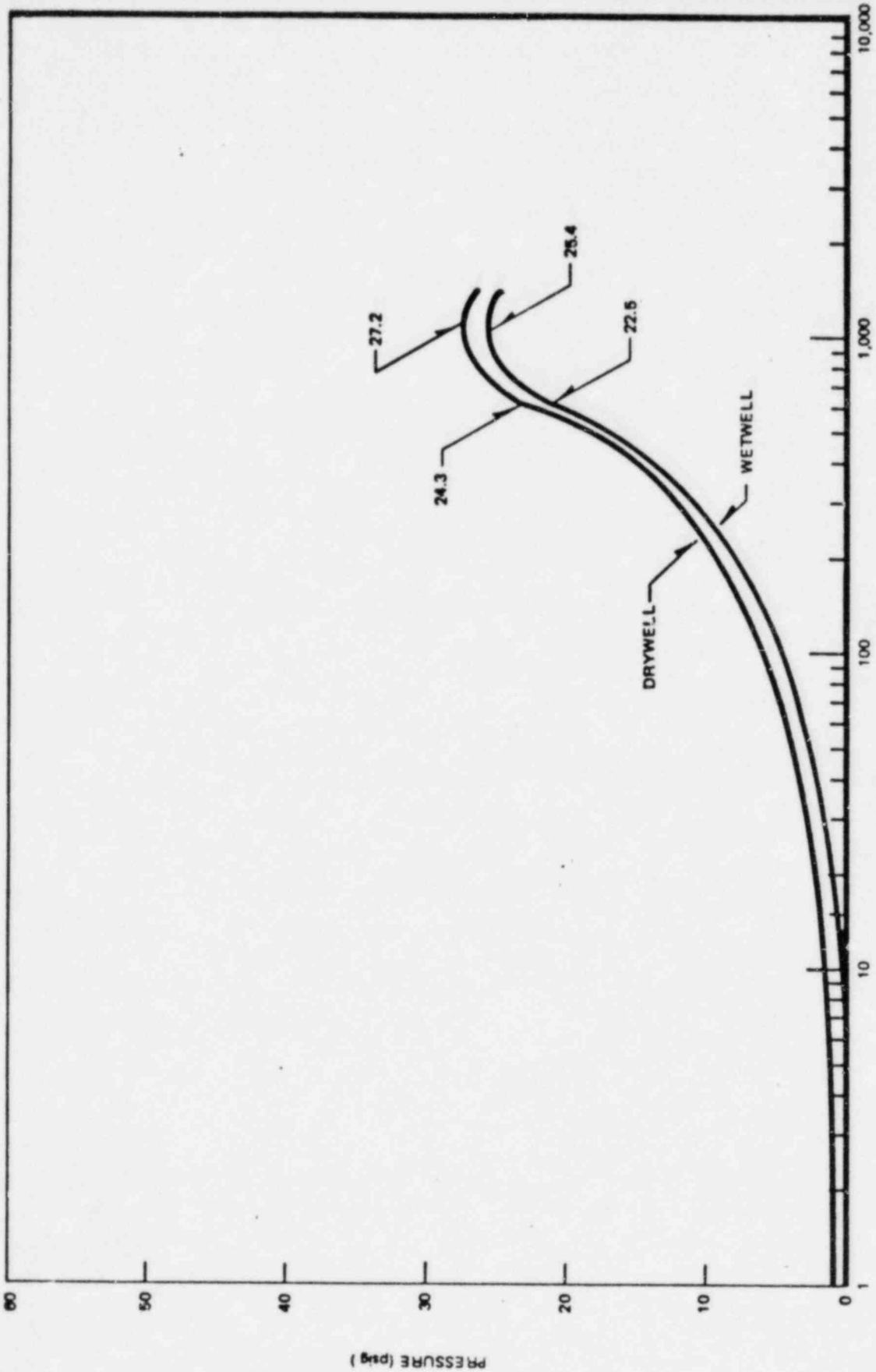

Figure OC 4.1.3-1a. SBA Containment Pressure Response (Zero ΔP), 4.06 ft Submergence

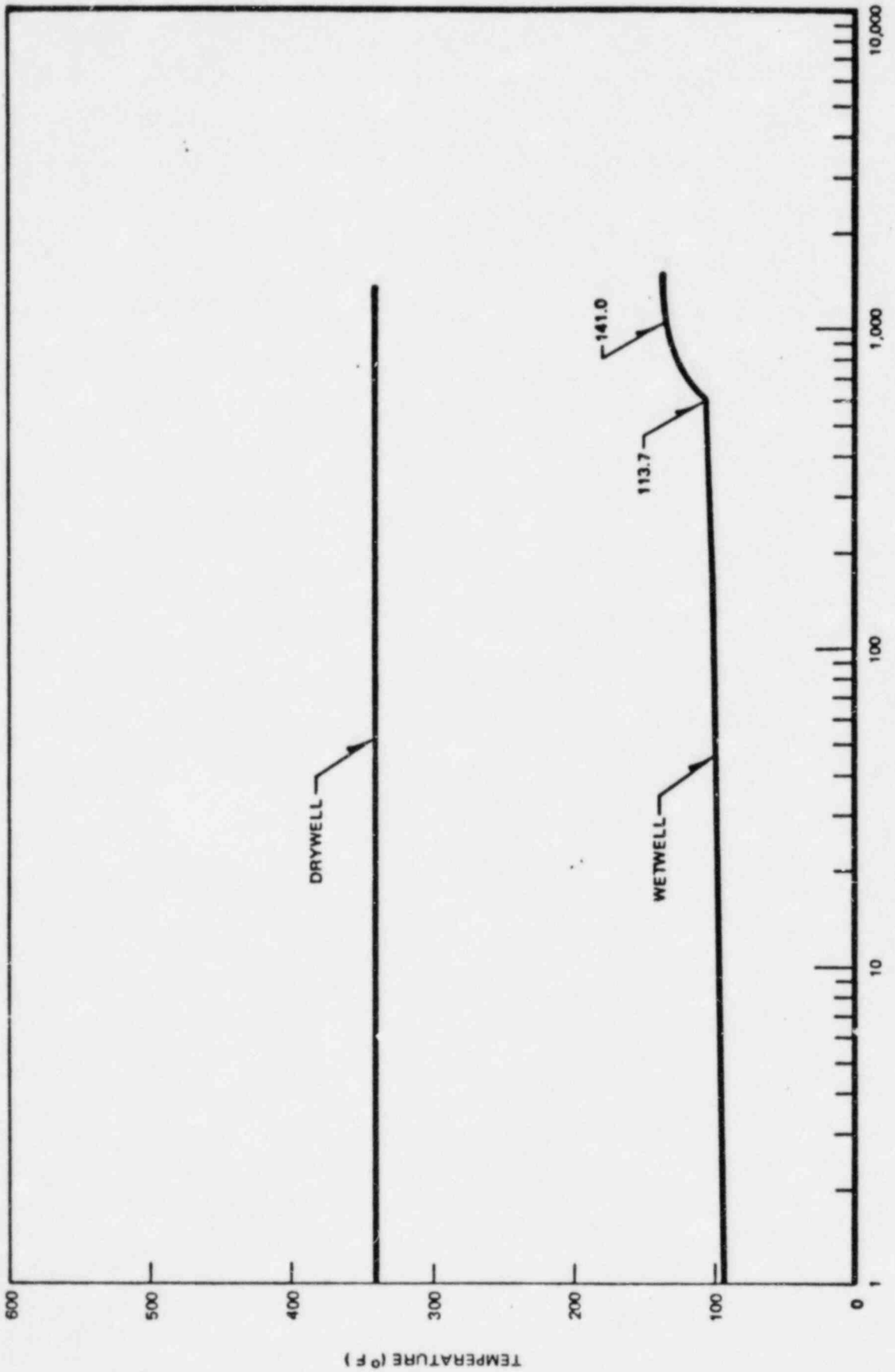

Figure OC 4.1.3-2a. SBA Containment Temperature Response (Zero ΔP), 4.06 ft Submergence

Table OC 4.2-1

NOMENCLATURE FOR DBA VENT SYSTEM THRUST LOAD SECTION

PDW	Drywell pressure
PWW	Wetwell airspace pressure
P1	Main vent pressure
P2	Vent header pressure
P3	Downcomer pressure
F1V1	Vertical force on a single main vent end cap
F1H1	Horizontal force on a single main vent end cap
F1V2	Vertical force on a single main vent mitre bend (applicable to Browns Ferry and Oyster Creek only)
F1H2	Horizontal force on a single main vent mitre bend (applicable to Browns Ferry and Oyster Creek only)
F2V	Vertical force on vent header (per mitre bend)
F2H	Horizontal force on vent header (per mitre bend)
F3V	Vertical force on a single downcomer mitre bend
F3H	Horizontal force on a single downcomer mitre bend
F4V	Vertical force on second mitre bend of a single downcomer (if applicable)
F4H	Horizontal force on second mitre bend of a single downcomer (if applicable)
F1V1T	Total main vent end cap vertical force = F1V1 x number of main vents
F1V2T	Total main vent mitre bend vertical force = F1V2 x number of main vents
F2VT	Total vent header vertical force = F2V x number of vent header mitre bends
F3VT	Total vertical force (first downcomer mitre bend) = F3V x number of downcomers
F4VT	Total vertical force (second downcomer mitre bend) = F4V x number of downcomers
FNETV	FNETV = F1V1T + F1V2T + F2VT + F3VT + F4VT
A_{VH}	Vent header flow area

Table OC 4.2-1 (Continued)

NOMENCLATURE FOR DBA VENT SYSTEM THRUST LOAD SECTION

A_{VP}	Total main vent flow area
A_{DC}	Total downcomer flow area
n_1	Number of main vents
n_2	Number of downcomers
n_3	Number of vent header mitre bends
$\dot{m}_T$	Total mass flow rate
V_1	Fluid velocity in main vent
V_2	Fluid velocity in vent header
V_3	Fluid velocity in downcomer
θ_1	Angle of main vent with horizontal
θ_2	Angle of first downcomer mitre bend with horizontal
θ_3	Angle of second downcomer mitre bend with horizontal
α	Angle of main vent mitre bend with horizontal
β	90° - (vent header mitre bend angle)

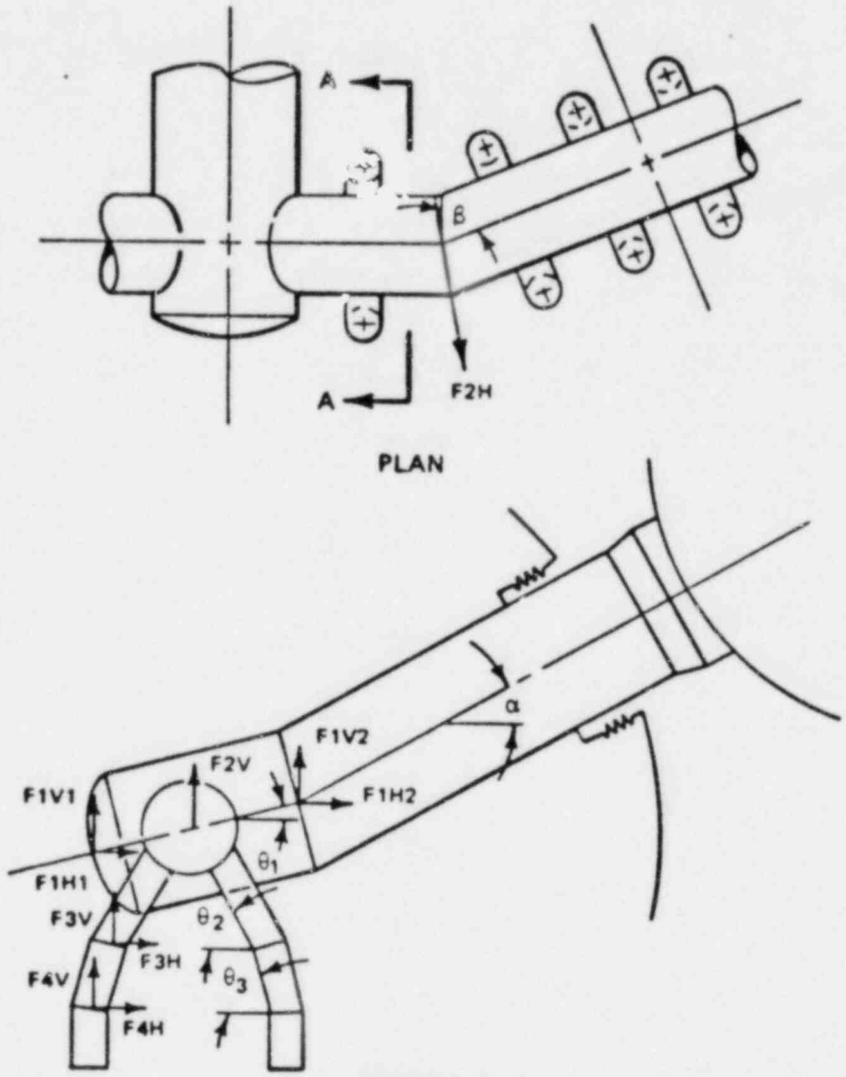

F1V1 = VERTICAL FORCE ON MAIN VENT END CAP
F1H1 = HORIZONTAL FORCE ON MAIN VENT END CAP
F1V2 = VERTICAL FORCE ON MAIN VENT MITRE BEND
F1H2 = HORIZONTAL FORCE ON MAIN VENT MITRE BEND
F2V = VERTICAL FORCE ON VENT HEADER (PER MITRE BEND)
F2H = HORIZONTAL FORCE ON VENT HEADER (PER MITRE BEND)
F3V = VERTICAL FORCE ON DOWNCOMER MITRE BEND
F3H = HORIZONTAL FORCE ON DOWNCOMER MITRE BEND
F4V = VERTICAL FORCE ON SECOND DOWNCOMER MITRE BEND
F4H = HORIZONTAL FORCE ON SECOND DOWNCOMER MITRE BEND

FORCES ARE SHOWN IN THEIR ASSUMED POSITIVE DIRECTION

Figure OC 4.2-1. Definition of Positive Thrust Loads

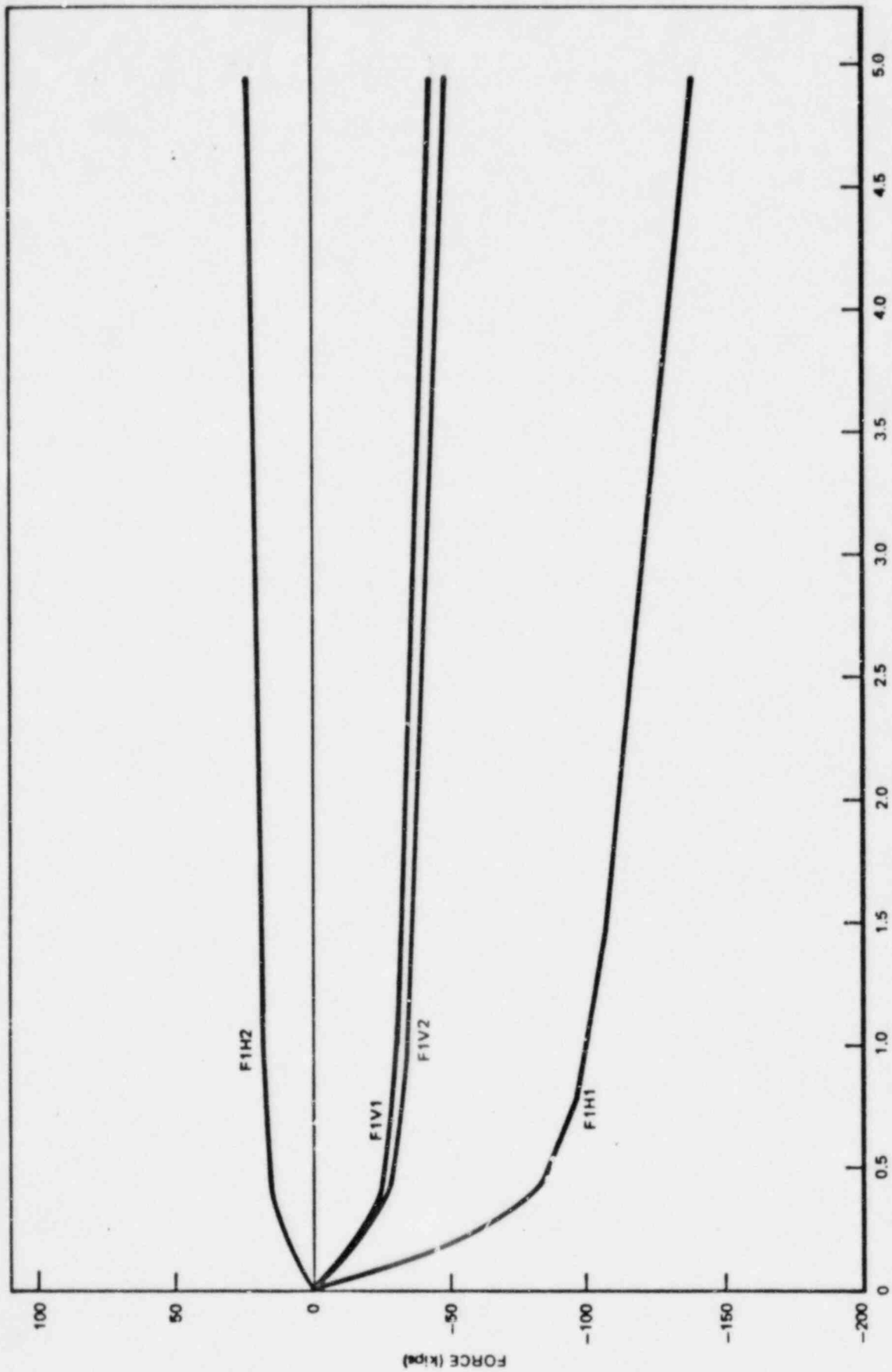

Figure OC 4.2-12. Oyster Creek 3.53 Ft. Submergence (Zero ΔP) Single Main Vent Forces

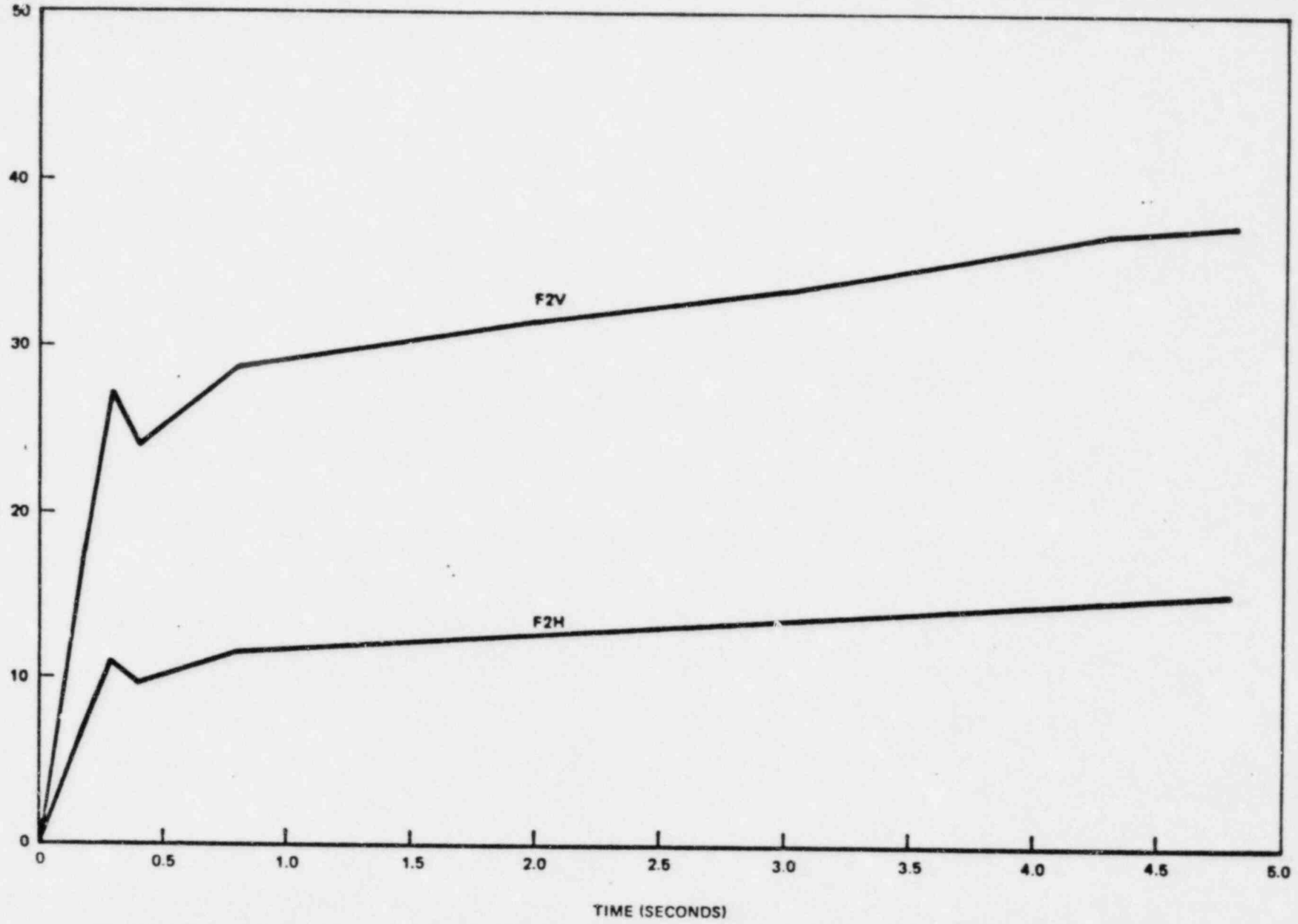

Figure OC 4.2-13. Vent Header Forces Per Mitre Bend (Zero ΔP), 3.53 ft Submergence, 0 to 5 Seconds

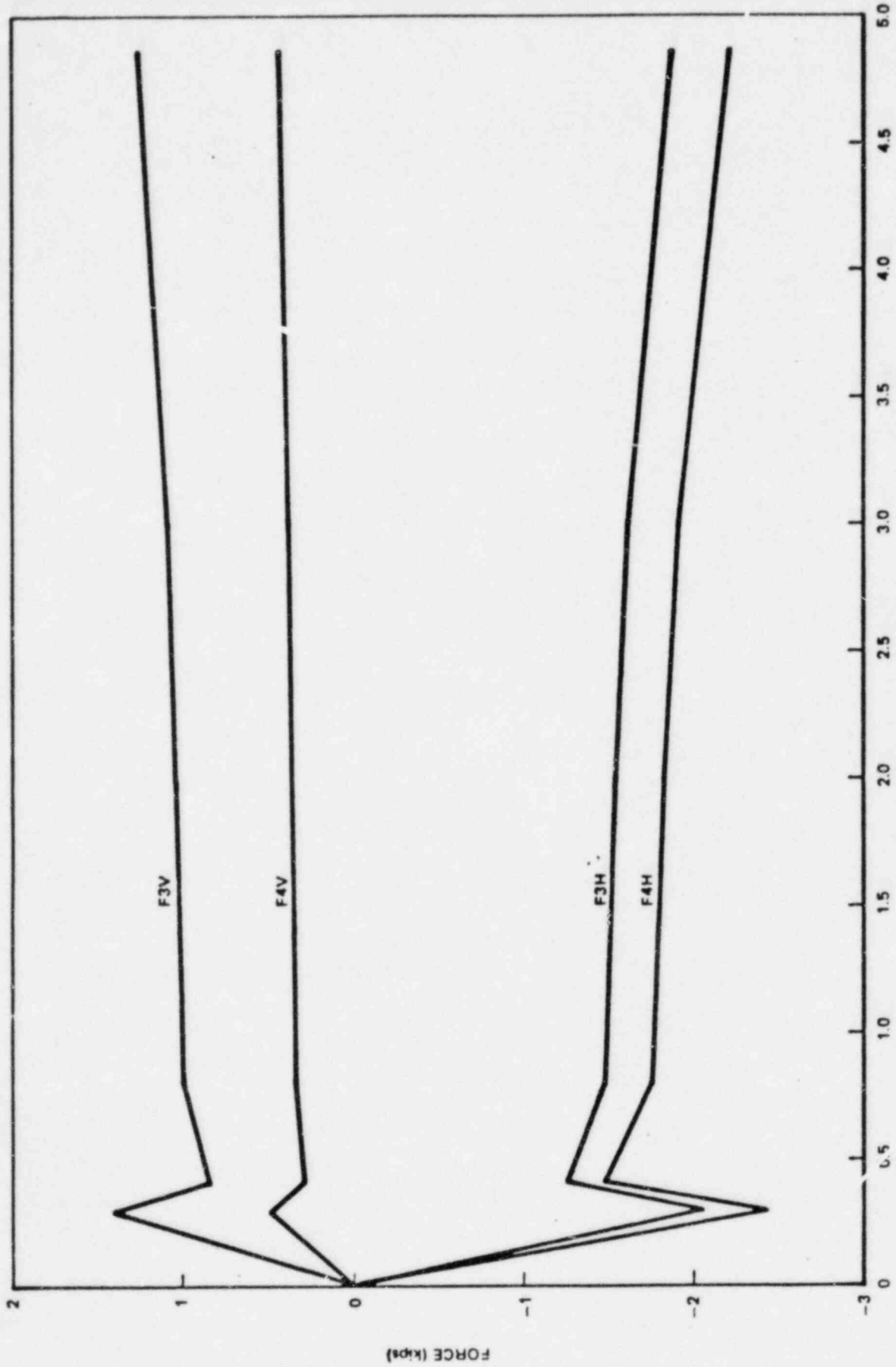

Figure OC 4.2-14. Single Downcomer Forces (Zero ΔP), 3.53 ft Submergence, 0 to 5 Seconds

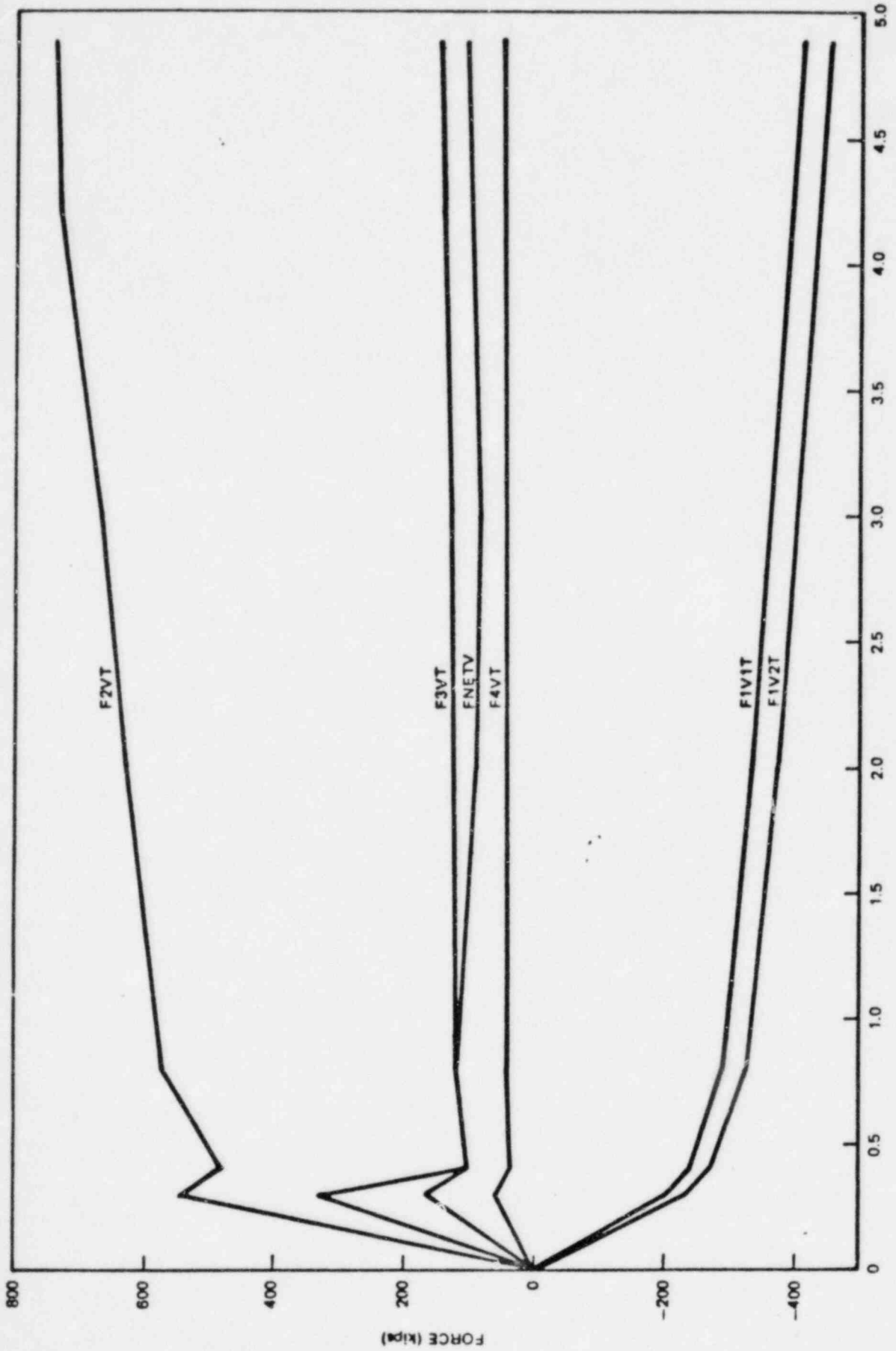

Figure OC 4.2-15. Total and Net Vertical Forces (Zero ΔP), 3.53 ft Submergence, 0 to 5 Seconds

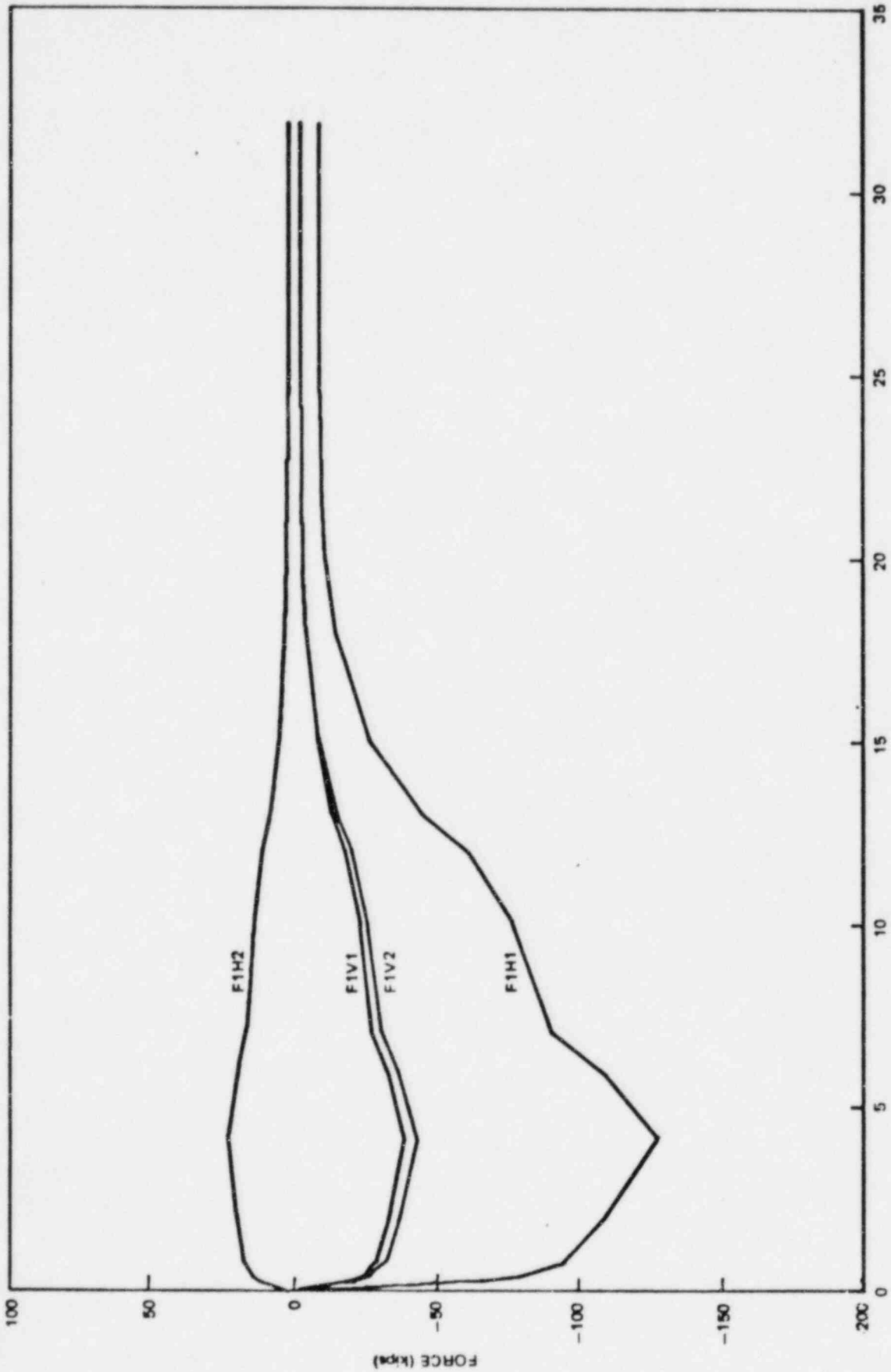

Figure OC 4.2-16. Single Main Vent Forces (Zero ΔP), 3.53 ft Submergence, 0 to 30 Seconds

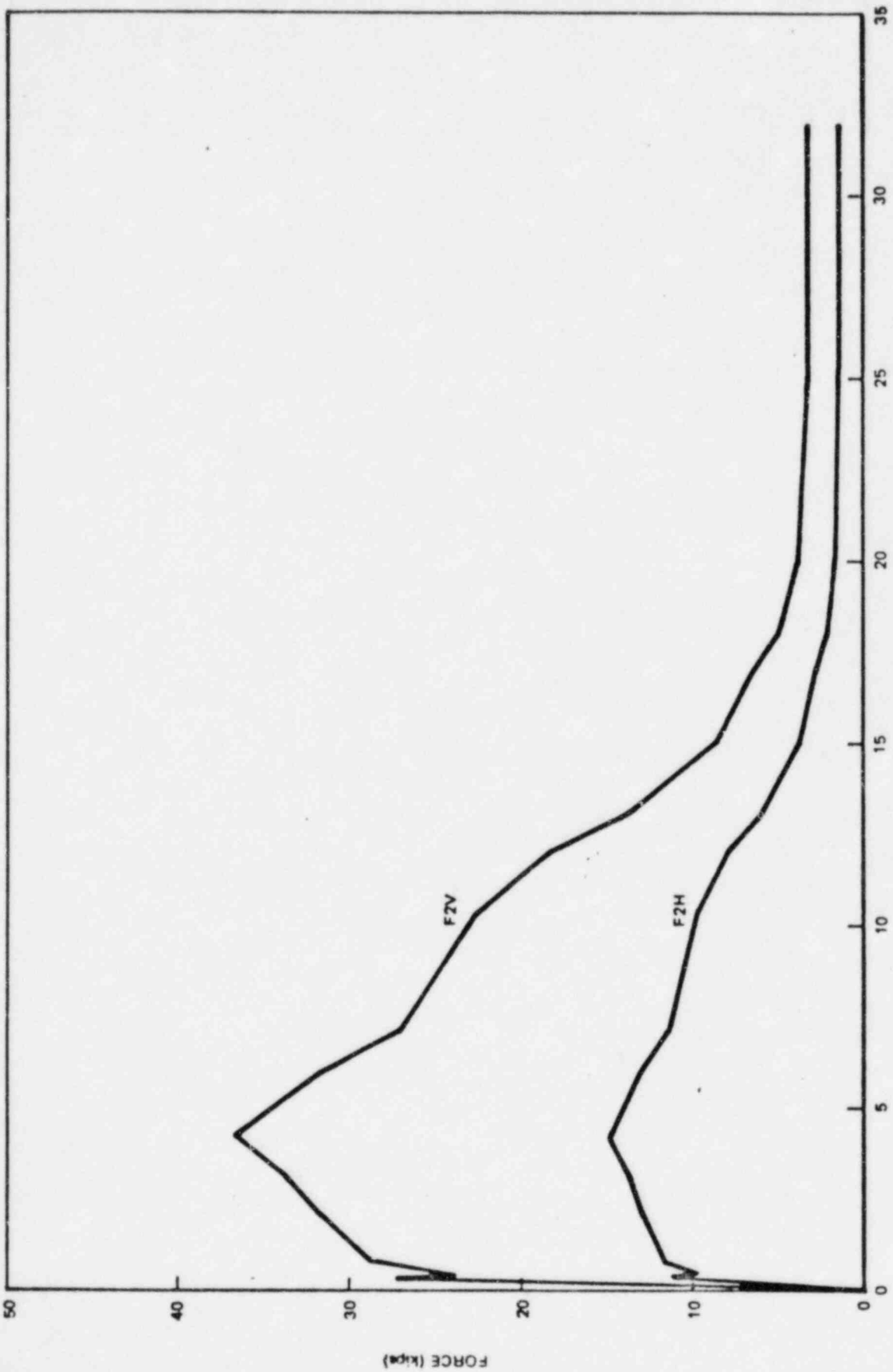

Figure OC 4.2-17. Vent Header Forces Per Mitre Bend (Zero ΔP), 3.53 ft Submergence, 0 to 30 Seconds

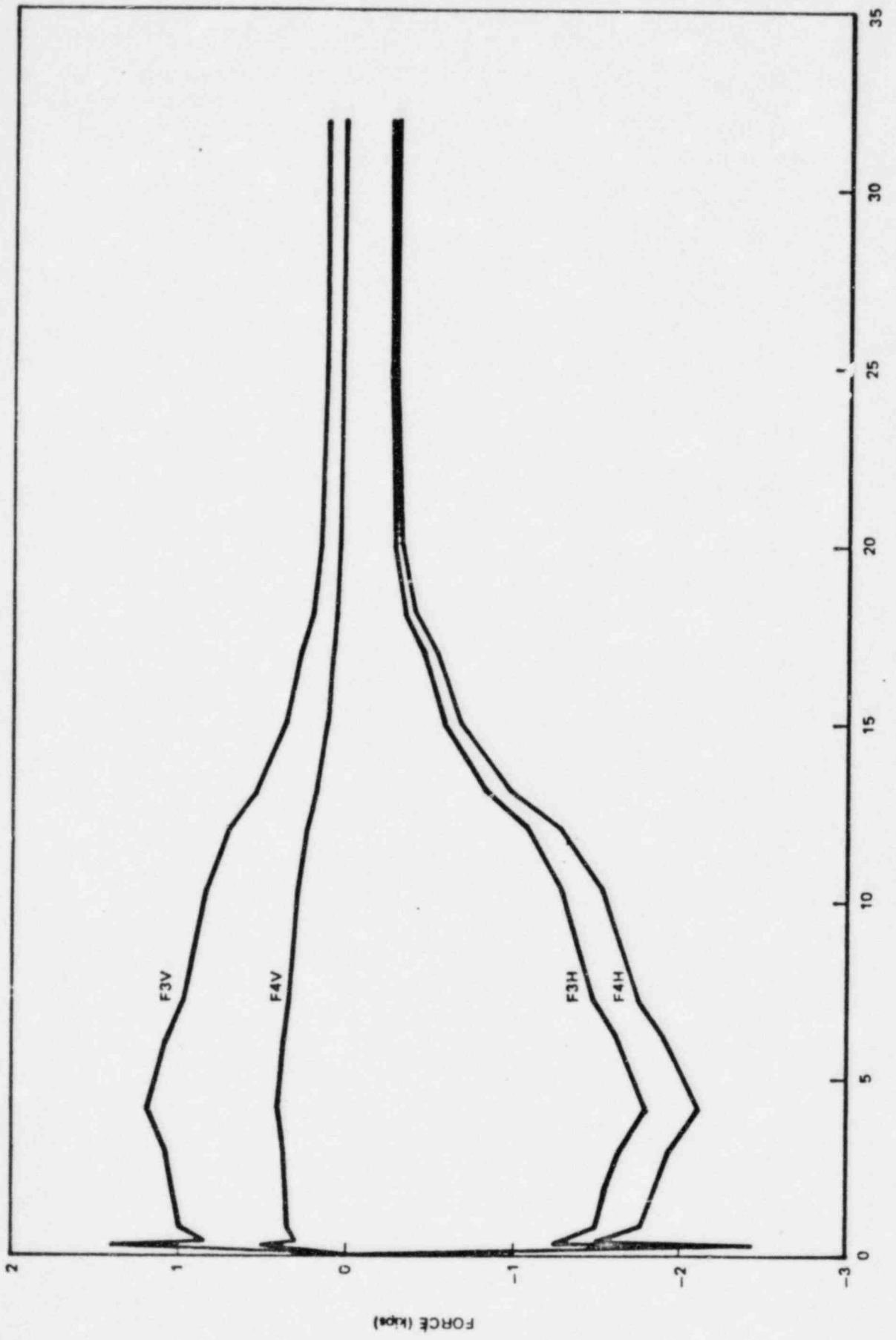

Figure OC 4.2-18. Single Downcomer Forces (Zero ΔP), 3.53 ft Submergence, 0 to 30 Seconds

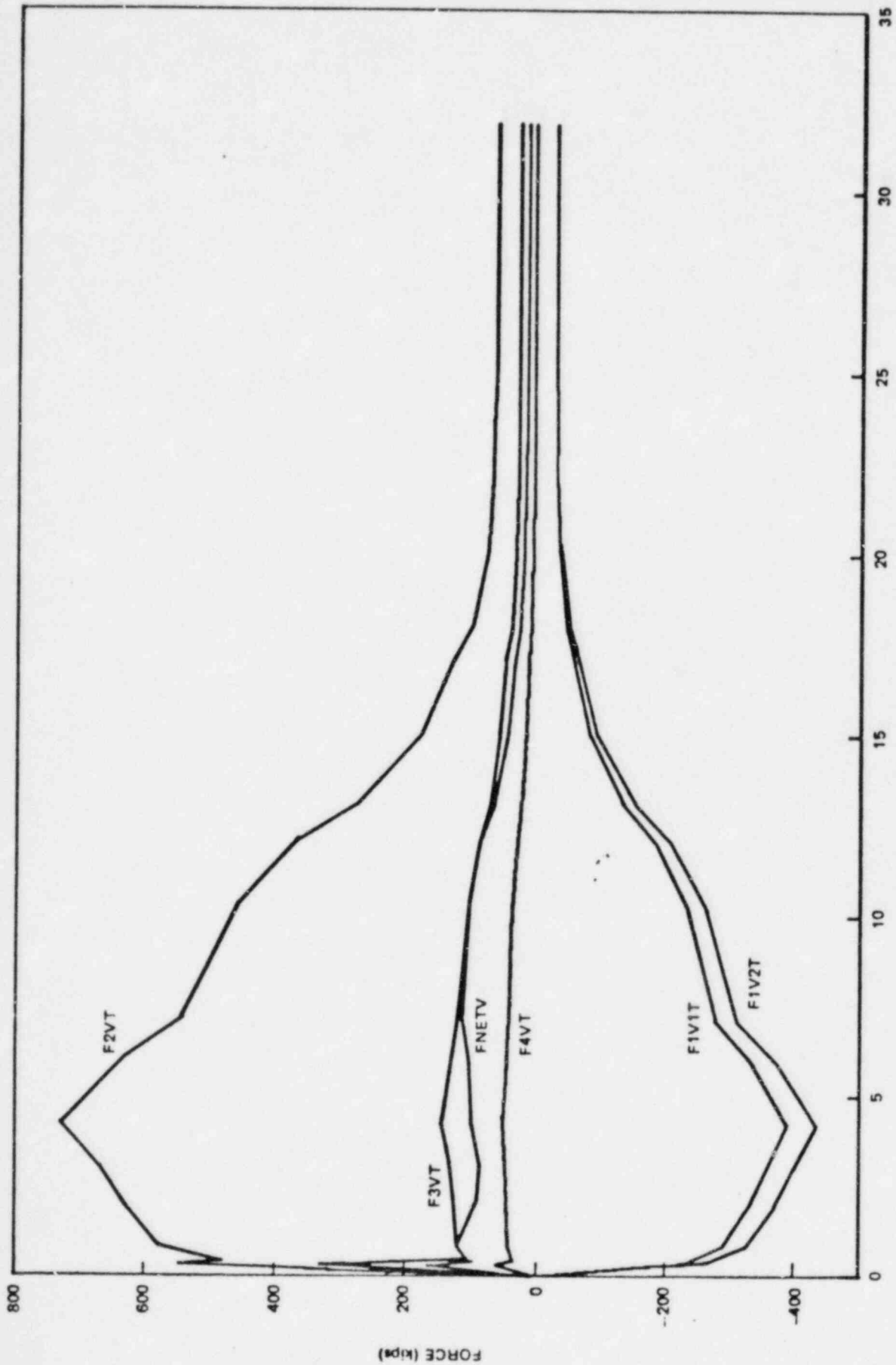

Figure OC 4.2-19. Total and Net Vertical Forces (Zero ΔP), 3.53 ft Submergence, 0 to 30 Seconds

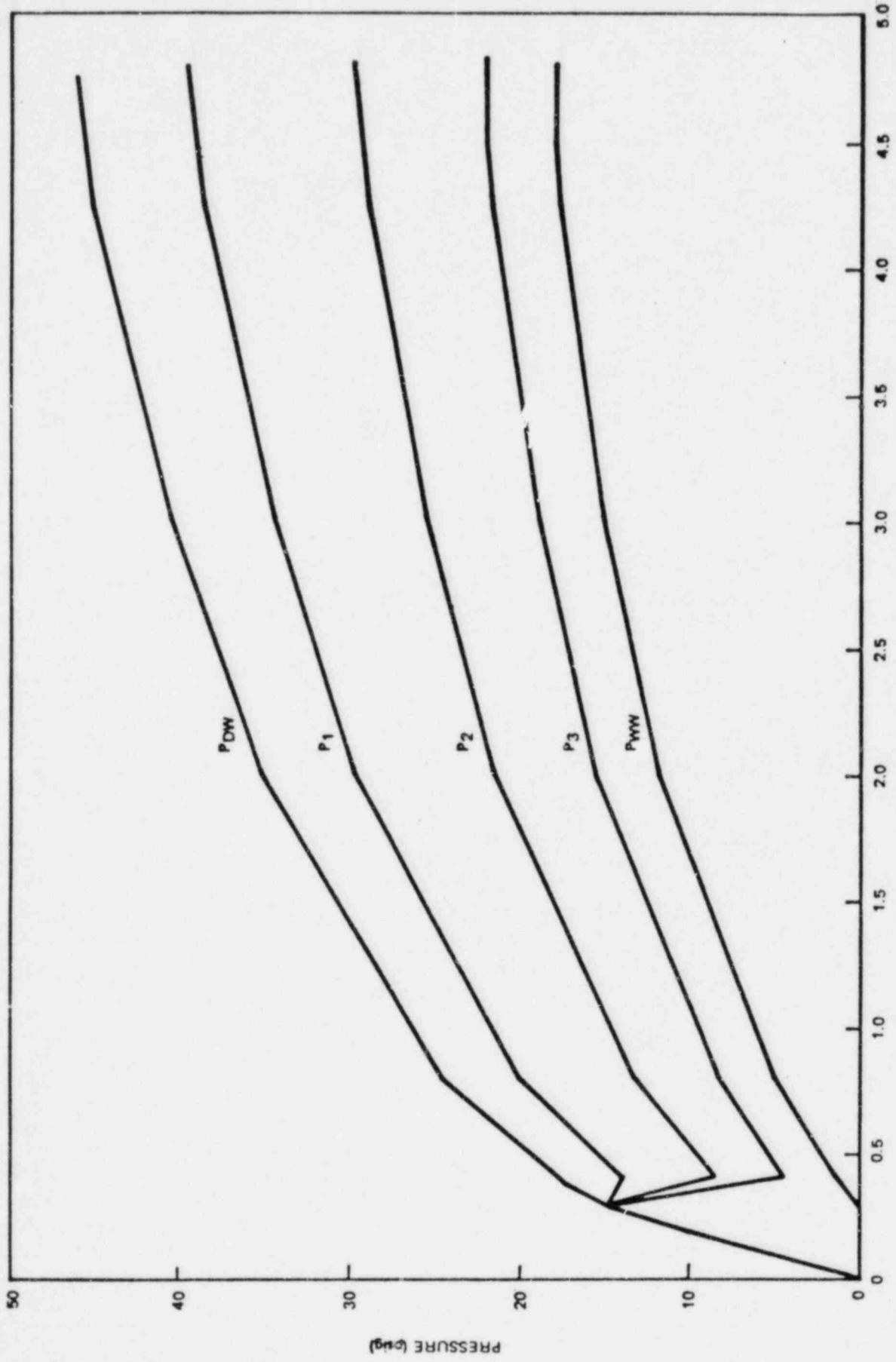

Figure OC 4.2-20. Pressure Time Histories (Zero ΔP), 3.53 ft Submergence, 0 to 5 Seconds

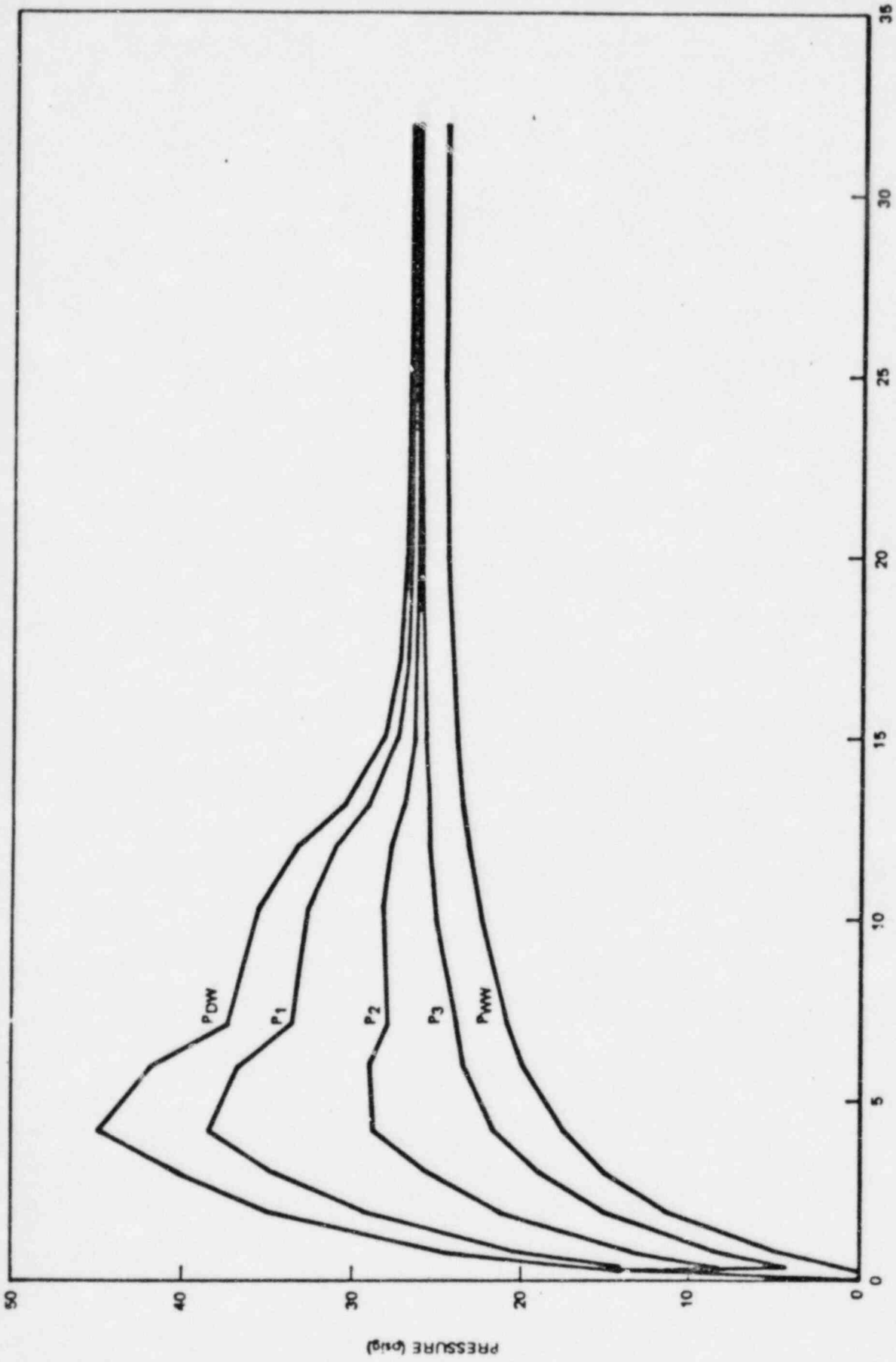

Figure OC 4.2-21. Pressure Time Histories (Zero ΔP), 3.53 ft Submergence, 0 to 30 Seconds

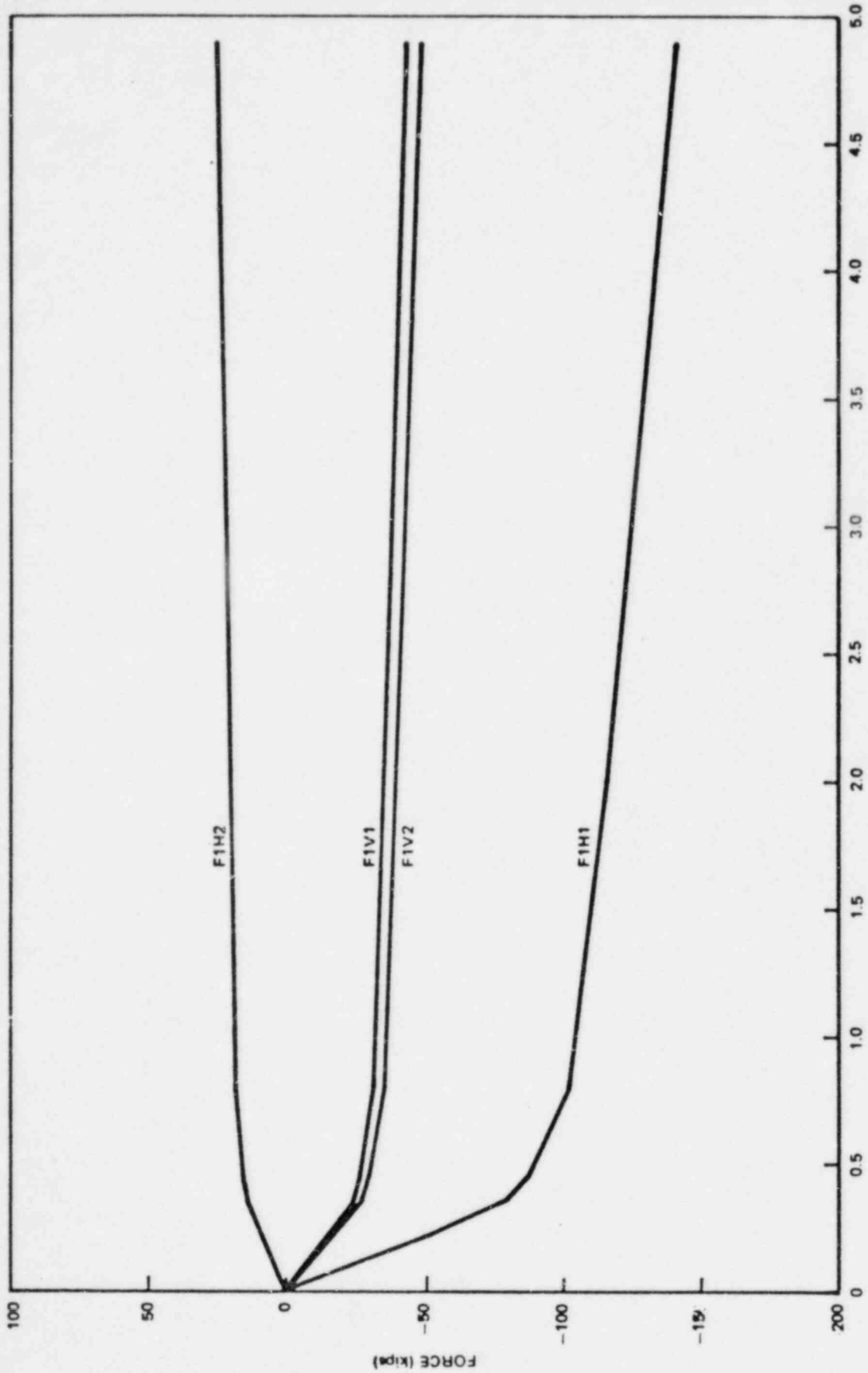

Figure OC 4.2-12a. Single Main Vent Forces (Zero ΔP), 4.06 ft Submergence, 0 to 5 Seconds

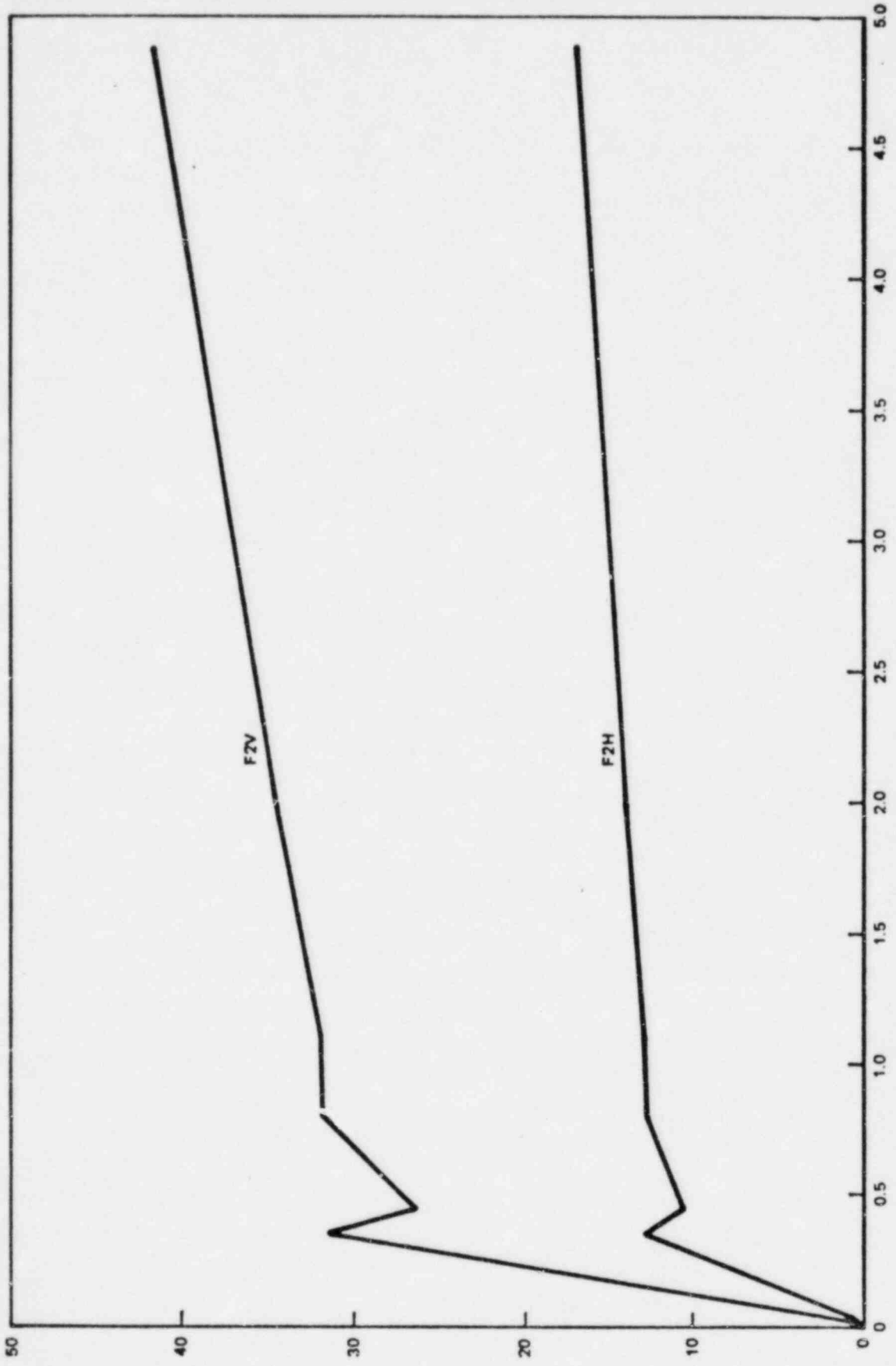

Figure OC 4.2-13a. Vent Header Forces Per Mitre Bend (Zero ΔP), 4.06 ft Submergence, 0 to 5 Seconds

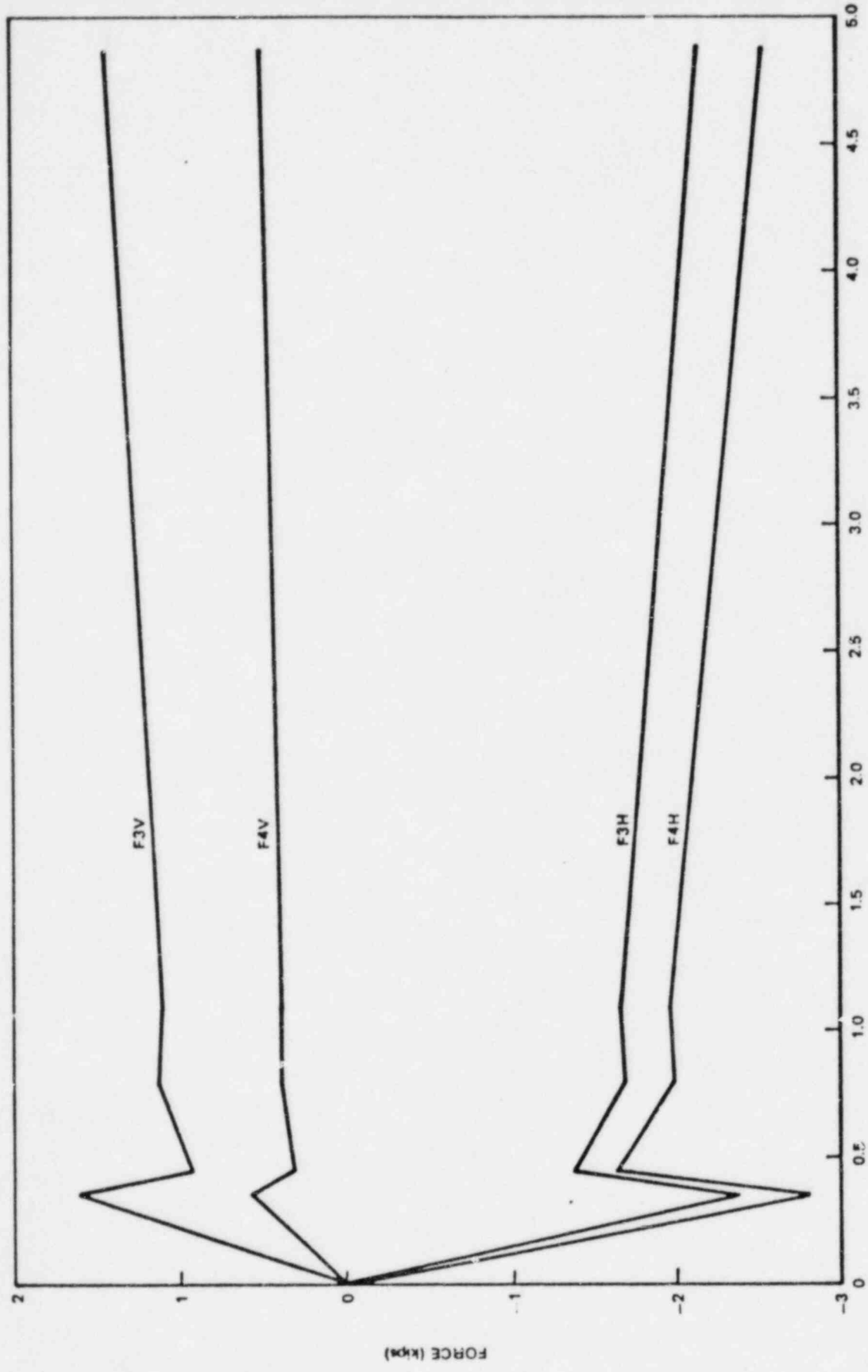

Figure OC 4.2-14a. Single Downcomer Forces (Zero ΔP), 4.06 ft Submergence, 0 to 5 Seconds

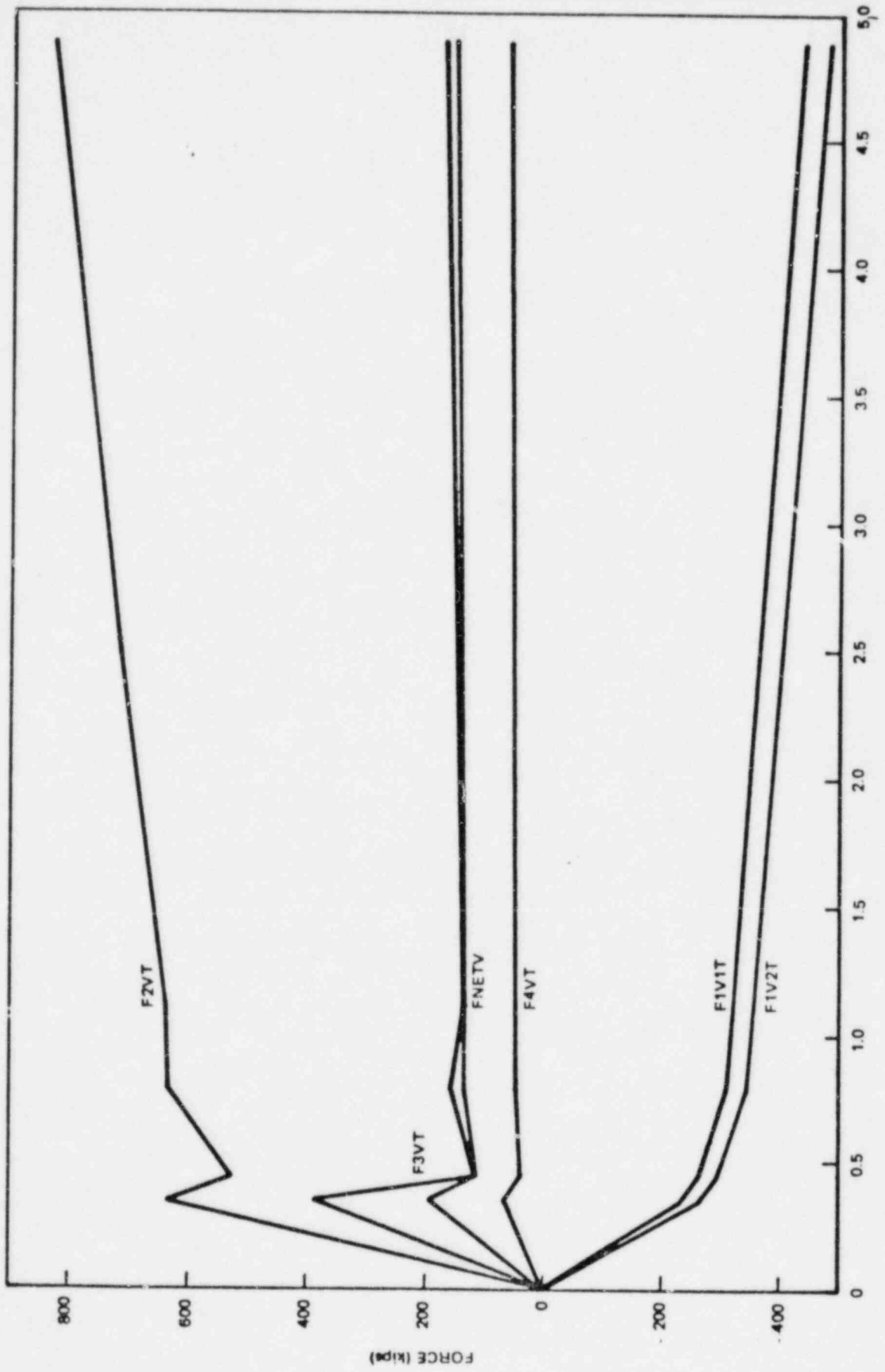

Figure OC 4.2-15a. Total and Net Vertical Forces (Zero ΔP), 4.06 ft Submergence, 0 to 5 Seconds

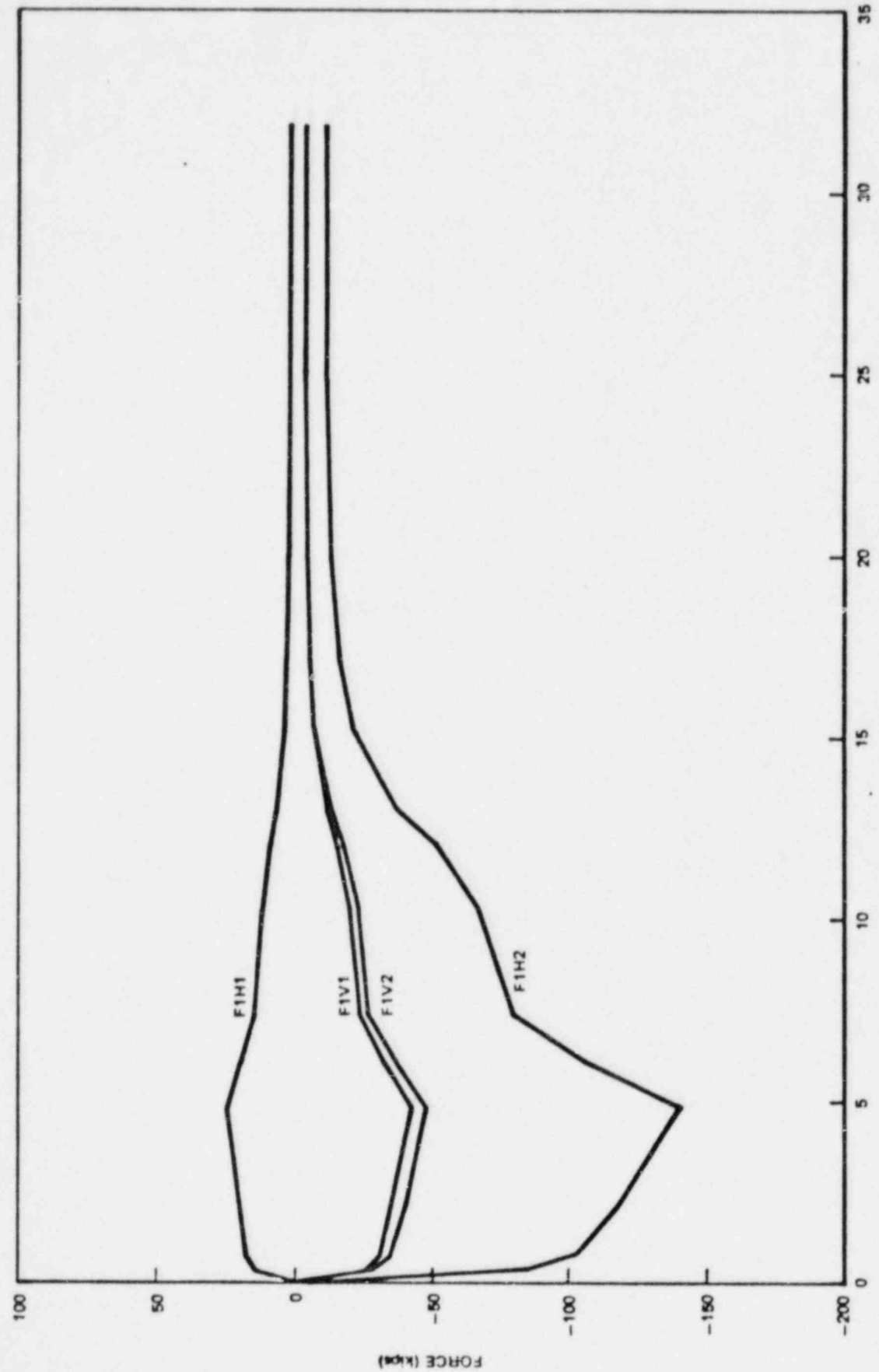

Figure OC 4.2-16a. Single Main Vent Forces (Zero ΔP), 4.06 ft Submergence, 0 to 30 Seconds

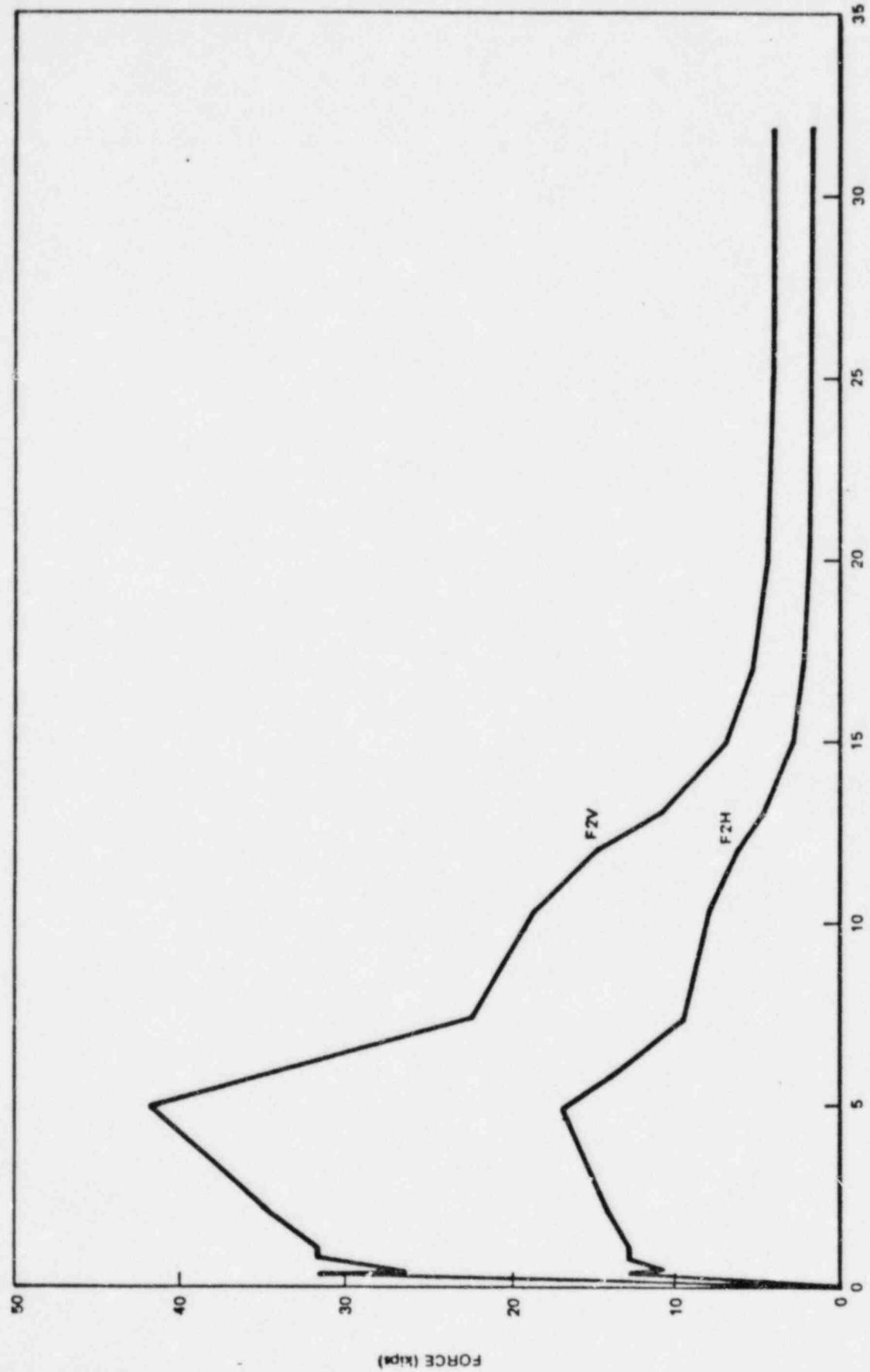

Figure OC 4.2-17a. Vent Header Forces Per Mitre Bend (Zero ΔP), 4.06 ft Submergence, 0 to 30 Seconds

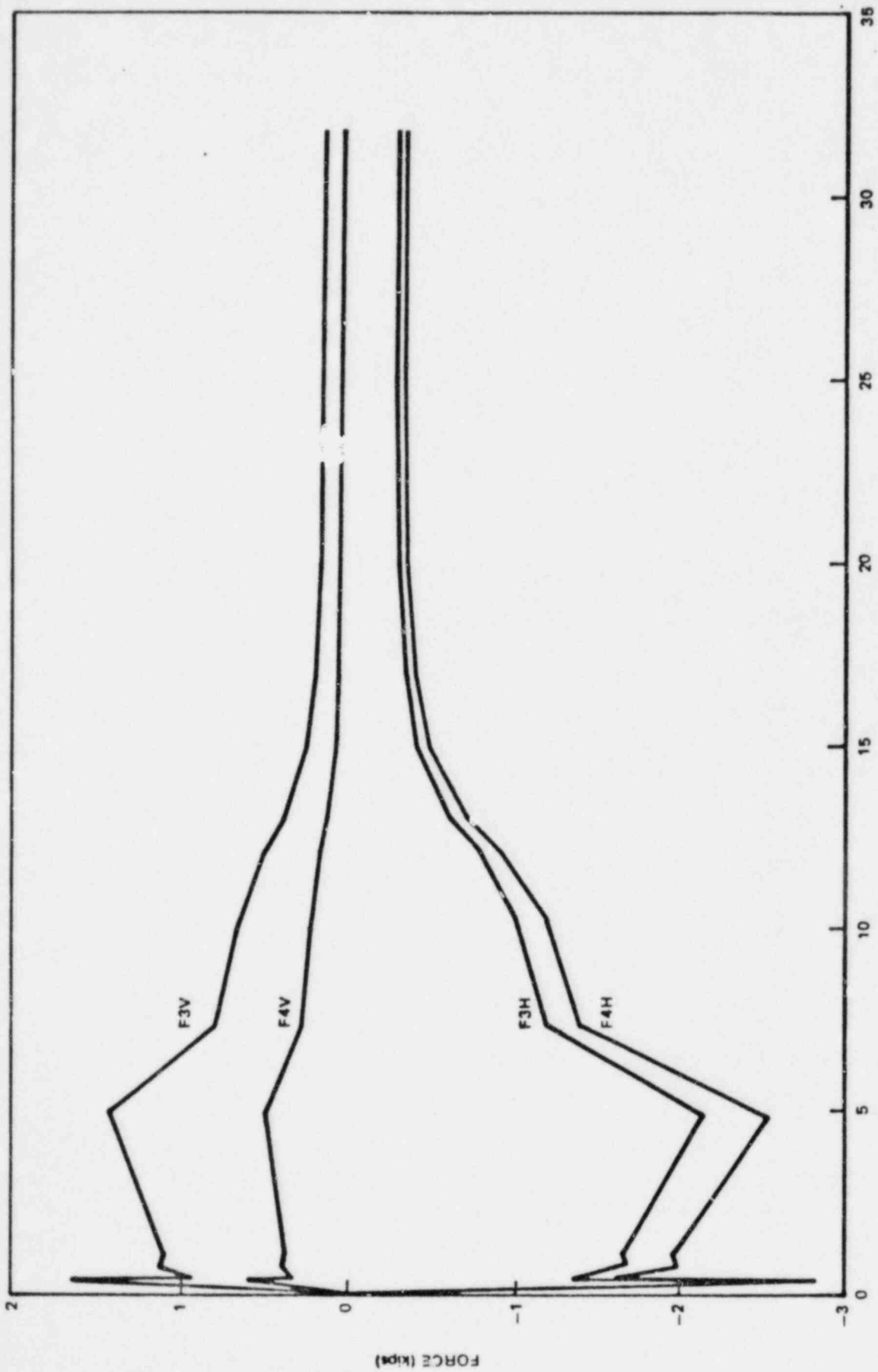

Figure OC 4.2-18a. Single Downcomer Forces (Zero ΔP), 4.06 ft Submergence, 0 to 30 Seconds

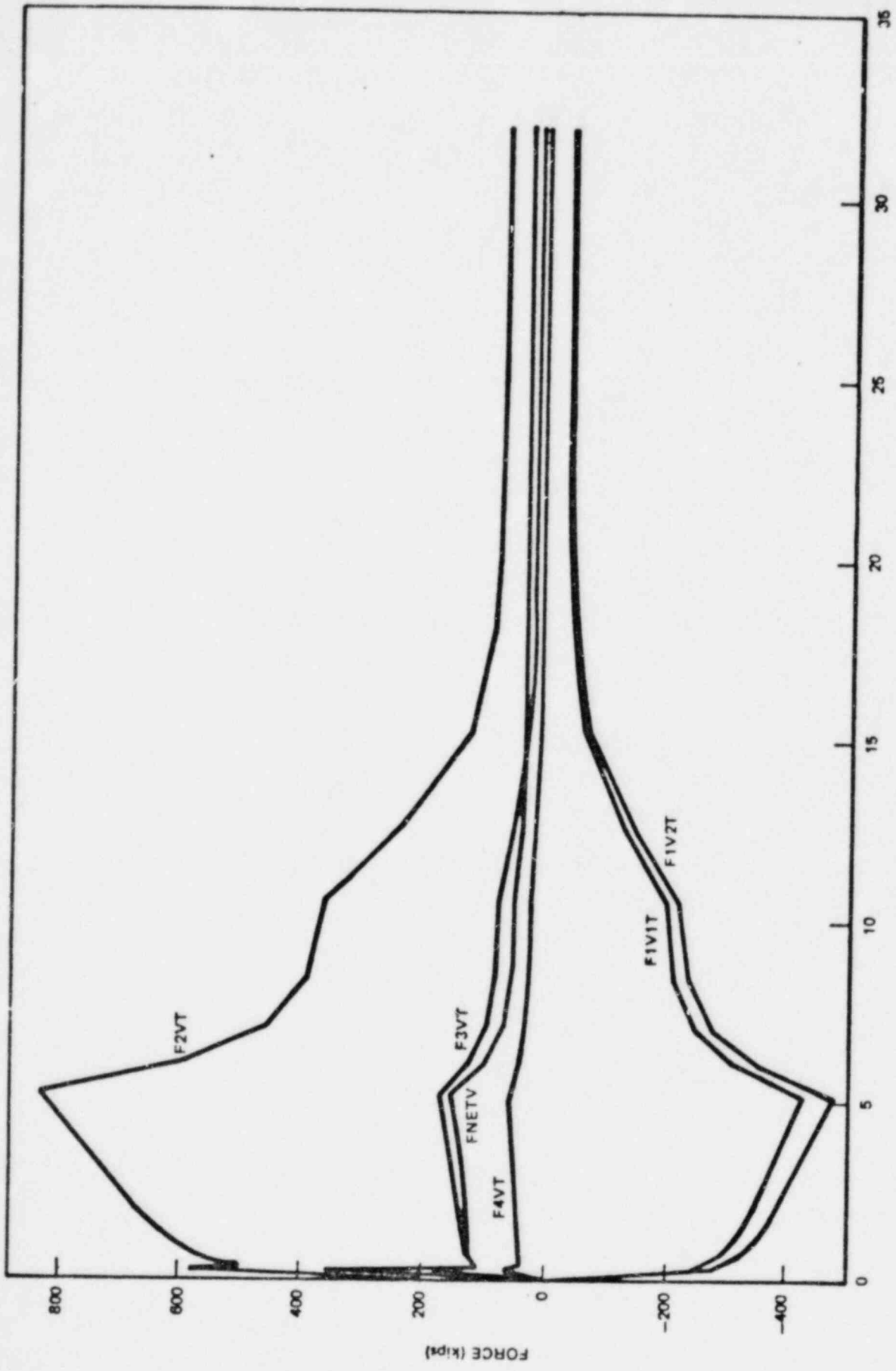

Figure OC 4.2-19a. Total and Net Vertical Forces (Zero ΔP), 4.06 ft Submergence, 0 to 30 Seconds

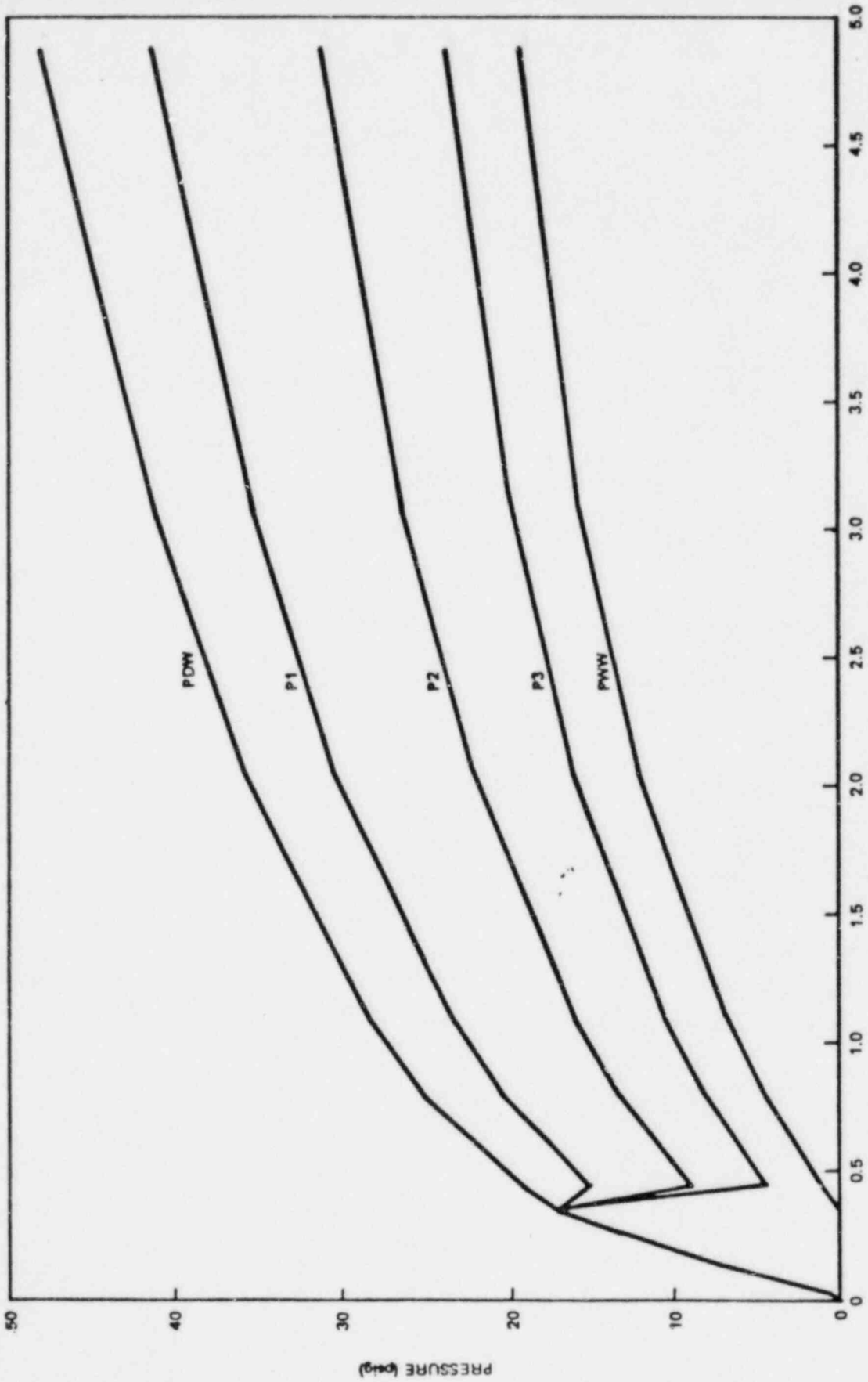

Figure OC 4.2-20a. Pressure Time Histories (Zero ΔP), 4.06 ft Submergence, 0 to 5 Seconds

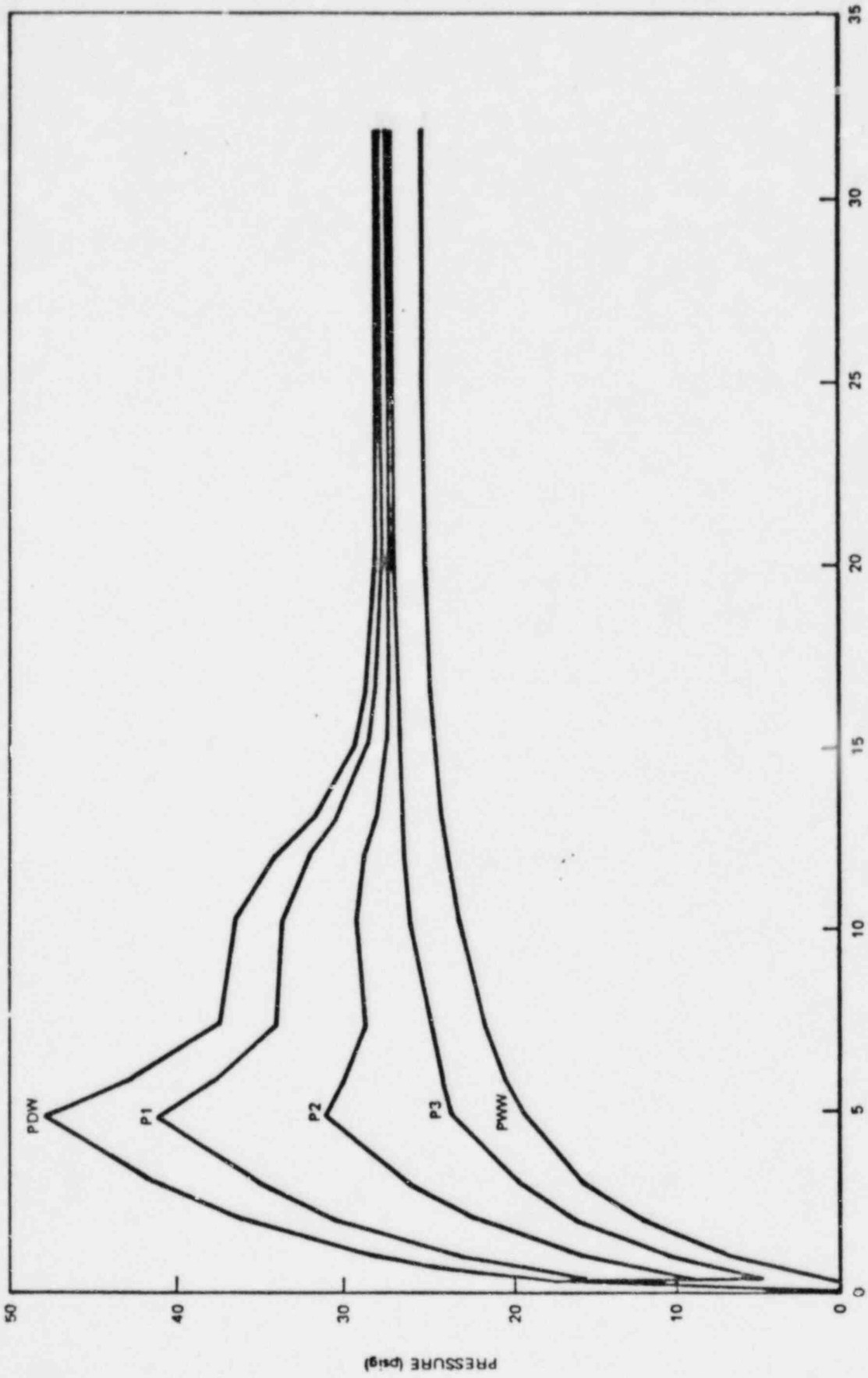

Figure OC 4.2-21a. Pressure Time Histories (Zero ΔP), 4.06 ft Submergence, 0 to 30 Seconds

Table OC 4.3.1-1

NET TORUS VERTICAL LOADS (FILTERED) (ZERO ΔP), AVERAGE SUBMERGED PRESSURE AND TORUS AIR PRESSURE, 4.06 FT SUBMERGENCE

Time (msec)	Net Torus Vertical Load (psid)	Torus Air Pressure (psid)	Average Submerged Pressure (psid)
0.0	0.01	0.0	0.0
2.0	-0.08	0.0	0.08
12.0	0.03	0.0	0.0
22.0	-0.11	0.0	0.11
31.0	-0.11	0.0	0.11
41.0	-0.14	0.10	0.23
51.0	-0.07	0.0	0.02
61.0	-0.18	0.0	0.18
71.0	-0.14	0.0	0.14
81.0	-0.27	0.0	0.27
91.0	-0.07	0.0	0.07
100.0	-0.29	0.0	0.29
110.0	-0.27	0.0	0.27
120.0	-0.29	0.0	0.29
130.0	-0.33	0.0	0.33
140.0	-0.37	0.0	0.37
150.0	-0.23	0.0	0.23
159.0	-0.58	0.0	0.58
169.0	-0.24	0.0	0.24
179.0	-0.59	0.0	0.59
189.0	-0.54	0.10	0.64
199.0	-0.82	0.0	0.82
209.0	-0.80	0.10	0.89
218.0	-1.05	0.10	1.15
228.0	-1.14	0.10	1.24
238.0	-1.63	0.10	1.73
248.0	-2.01	0.10	2.10
258.0	-3.02	0.19	3.21
268.0	-5.93	0.19	6.12
277.0	-11.78	0.19	11.97
279.0	-12.10	0.19	12.29
287.0	-10.22	0.86	11.08
297.0	-10.02	0.38	10.40
307.0	-7.67	0.38	8.06
317.0	-7.43	0.67	8.10
327.0	-6.35	0.76	7.11
336.0	-7.49	0.86	8.34
346.0	-8.53	1.14	9.67
350.0	-8.60	1.14	9.75
356.0	-8.48	1.23	9.69
366.0	-8.01	1.33	9.35
376.0	-7.98	1.62	9.60

Table OC 4.3.1-1

NET TORUS VERTICAL LOADS (FILTERED) (ZERO ΔP), AVERAGE SUBMERGED PRESSURE AND TORUS AIR PRESSURE, 4.06 FT SUBMERGENCE (Continued)

Time (msec)	Net Torus Vertical Load (psid)	Torus Air Pressure (psid)	Average Submerged Pressure (psid)
388.0	-7.16	1.90	9.06
395.0	-6.88	2.38	9.26
405.0	-6.23	2.57	8.80
415.0	-6.03	2.76	8.78
425.0	-5.03	3.23	8.26
435.0	-4.44	3.51	7.96
445.0	-3.80	3.99	7.79
454.0	-3.20	4.47	7.67
464.0	-2.17	5.13	7.30
474.0	-1.53	5.42	6.94
484.0	-0.75	6.17	6.93
494.0	-0.01	6.56	6.57
504.0	0.35	7.32	6.97
514.0	1.06	7.79	6.74
523.0	2.16	8.74	6.58
533.0	2.88	9.31	6.43
543.0	3.57	10.07	6.50
553.0	4.14	10.73	6.60
563.0	4.69	11.50	6.81
573.0	5.04	12.07	7.02
582.0	5.19	12.54	7.35
592.0	5.47	12.92	7.45
600.0	5.60	13.20	7.60
602.0	5.55	13.49	7.95
612.0	5.49	14.06	8.57
622.0	5.39	14.25	8.86
632.0	5.26	14.54	9.27
641.0	5.12	14.82	9.70
651.0	4.75	15.01	10.26
661.0	4.31	15.29	10.98
671.0	4.00	15.39	11.39
681.0	3.55	15.48	11.93
691.0	3.10	15.67	12.58
700.0	2.72	15.87	13.14
710.0	2.44	15.96	13.52
720.0	2.15	16.34	14.19
730.0	1.94	16.63	14.68
740.0	1.87	17.01	15.14
750.0	1.91	17.19	15.29
759.0	1.92	17.48	15.56
769.0	2.07	17.95	15.88
779.0	2.30	18.24	15.94

Table OC 4.3.1-1

NET TORUS VERTICAL LOADS (FILTERED) (ZERO ΔP), AVERAGE SUBMERGED PRESSURE AND TORUS AIR PRESSURE, 4.06 FT SUBMERGENCE (Continued)

Time (msec)	Net Torus Vertical Load (psid)	Torus Air Pressure (psid)	Average Submerged Pressure (psid)
789.0	2.42	18.81	16.39
799.0	2.49	19.00	16.51
809.0	2.51	19.19	16.68
818.0	2.51	19.66	17.15
828.0	2.35	19.85	17.50
838.0	2.44	20.23	17.80
848.0	2.46	20.52	18.06
858.0	2.63	20.90	18.27
868.0	2.52	21.19	18.67
877.0	2.47	21.47	19.00
887.0	2.55	21.66	19.11
897.0	2.60	22.04	19.44
907.0	2.51	22.32	19.82
917.0	2.52	22.70	20.19
927.0	2.54	22.99	20.45
937.0	2.53	23.18	20.65
946.0	2.46	23.37	20.91
956.0	2.39	23.94	21.55
966.0	2.34	23.94	21.60
976.0	2.14	24.31	22.17
986.0	2.23	24.70	22.47
996.0	2.20	24.97	22.77
1005.0	2.24	25.16	22.92
1015.0	2.14	25.47	23.33
1025.0	2.17	25.74	23.57
1035.0	1.87	25.94	24.06
1045.0	1.94	26.32	24.38
1055.0	1.97	26.79	24.81
1064.0	1.85	26.79	24.93
1074.0	1.77	27.17	25.40
1084.0	1.88	27.37	25.49
1094.0	1.83	27.75	25.92
1104.0	1.82	28.03	26.21
1114.0	1.77	28.22	26.45
1123.0	1.86	28.68	26.83
1133.0	1.83	28.80	26.97
1143.0	1.75	28.99	27.25
1153.0	1.79	29.46	27.67
1163.0	1.73	29.54	27.80
1173.0	1.76	29.85	28.09
1182.0	1.63	30.19	28.56
1192.0	1.62	30.31	28.69
1202.0	1.57	30.58	29.01

Table OC 4.3.1-1

NET TORUS VERTICAL LOADS (FILTERED) (ZERO ΔP), AVERAGE SUBMERGED PRESSURE AND TORUS AIR PRESSURE, 4.06 FT SUBMERGENCE (Continued)

Time (msec)	Net Torus Vertical Load (psid)	Torus Air Pressure (psid)	Average Submerged Pressure (psid)
1212.0	1.47	30.77	29.30
1222.0	1.42	30.97	29.54
1232.0	1.44	31.24	29.80
1241.0	1.37	31.55	30.18
1251.0	1.28	31.82	30.54
1261.0	1.30	32.21	30.90
1271.0	1.33	32.40	31.07
1281.0	1.22	32.67	31.45
1291.0	1.23	33.14	31.91
1301.0	1.12	33.25	32.13
1310.0	1.03	33.45	32.42
1320.0	0.99	33.72	32.73
1330.0	0.81	34.03	33.22
1340.0	0.83	34.37	33.54
1350.0	0.72	34.68	33.96
1360.0	0.54	34.68	34.14
1369.0	0.60	35.07	34.47
1379.0	0.56	35.34	34.78
1389.0	0.48	35.42	34.94
1399.0	0.43	35.73	35.30
1409.0	0.42	35.92	35.50
1419.0	0.26	36.19	35.93
1428.0	0.36	36.27	35.91
1438.0	0.36	36.46	36.11
1448.0	0.39	36.58	36.19
1458.0	0.40	36.85	36.45
1468.0	0.38	36.97	36.58
1478.0	0.40	37.05	36.64
1487.0	0.36	37.24	36.88
1497.0	0.32	37.24	36.92
1507.0	0.31	37.32	37.01
1517.0	0.31	37.51	37.20
1527.0	0.46	37.43	36.97
1537.0	0.46	37.51	37.05
1546.0	0.30	37.63	37.33
1556.0	0.23	37.63	37.40
1566.0	0.21	37.51	37.30
1576.0	0.10	37.43	37.33
1586.0	0.03	37.51	37.48
1588.0	-0.02	37.51	37.53

Table OC 4.3.1-2a

NET TORUS VERTICAL LOADS (FILTERED DATA) (ZERO ΔP), AVERAGE SUBMERGED PRESSURE AND TORUS AIR PRESSURE, 3.0 FT SUBMERGENCE

Time (msec)	Net Torus Vertical Load (psid)	Torus Air Pressure (psid)	Average Submerged Pressure (psid)
0.0	-0.08	0.0	0.08
2.0	-0.06	0.0	0.06
12.0	0.01	0.0	0.0
22.0	0.08	0.0	0.0
31.0	-0.01	0.10	0.10
41.0	0.01	0.10	0.09
51.0	-0.18	0.0	0.18
61.0	-0.19	0.0	0.19
71.0	-0.25	0.10	0.35
81.0	-0.19	0.0	0.19
91.0	-0.15	0.0	0.15
100.0	-0.06	0.0	0.06
110.0	-0.28	0.0	0.28
120.0	-0.23	0.0	0.23
130.0	-0.49	0.0	0.49
140.0	-0.35	0.10	0.45
150.0	-0.56	0.0	0.56
159.0	-0.61	0.10	0.71
169.0	-0.68	0.10	0.78
179.0	-0.72	0.10	0.81
189.0	-1.28	0.10	1.37
199.0	-1.15	0.19	1.35
209.0	-2.01	0.19	2.20
218.0	-3.01	0.19	3.20
228.0	-7.70	0.19	7.90
236.0	-9.24	0.19	9.43
238.0	-8.96	0.29	9.25
248.0	-7.49	0.29	7.78
258.0	-7.35	0.39	7.74
262.0	-5.64	0.39	6.03
268.0	-6.44	0.58	7.02
277.0	-7.49	0.48	7.97
283.0	-7.65	0.48	8.13
287.0	-7.50	0.77	8.28
297.0	-6.65	0.87	7.52
307.0	-6.73	1.16	7.89
317.0	-6.74	1.35	8.09
327.0	-5.60	1.54	7.14
336.0	-5.00	1.74	6.74
346.0	-4.90	2.13	7.03
356.0	-4.42	2.32	6.74
366.0	-3.95	2.80	6.75
376.0	-3.24	3.00	6.23

Table OC 4.3.1-2a

NET TORUS VERTICAL LOADS (FILTERED DATA) (ZERO ΔP), AVERAGE SUBMERGED PRESSURE AND TORUS AIR PRESSURE, 3.0 FT SUBMERGENCE (Continued)

Time (msec)	Net Torus Vertical Load (psid)	Torus Air Pressure (psid)	Average Submerged Pressure (psid)
386.0	-2.76	3.48	6.24
395.0	-2.47	3.86	6.33
405.0	-1.47	4.25	5.72
415.0	-0.73	4.64	5.36
425.0	-0.46	5.12	5.58
435.0	0.33	5.70	5.37
445.0	0.55	6.38	5.82
454.0	1.28	6.76	5.48
464.0	1.75	7.25	5.50
474.0	2.39	7.92	5.53
484.0	3.05	8.60	5.55
494.0	3.28	8.98	5.70
502.0	3.34	9.37	6.04
504.0	3.30	9.37	6.08
514.0	3.26	9.75	6.50
523.0	2.96	10.05	7.09
533.0	2.66	10.24	7.57
543.0	2.29	10.43	8.15
553.0	2.17	10.53	8.36
563.0	2.04	10.92	8.88
573.0	1.95	11.21	9.26
582.0	1.91	11.30	9.39
592.0	1.98	11.69	9.71
602.0	1.99	12.17	10.18
612.0	1.94	12.36	10.42
622.0	1.85	12.56	10.71
624.0	1.80	12.94	11.14
632.0	1.96	13.04	11.09
641.0	2.00	13.33	11.34
651.0	2.01	13.62	11.61
661.0	2.05	13.81	11.76
671.0	2.04	14.10	12.07
681.0	1.92	14.39	12.47
691.0	1.92	14.63	12.76
700.0	1.87	14.88	13.01
710.0	1.91	15.17	13.26
720.0	1.97	15.65	13.68
730.0	1.97	15.75	13.78
740.0	2.05	16.13	14.08
750.0	1.96	16.32	14.36
759.0	1.89	16.81	14.92
769.0	1.96	16.81	14.85
779.0	1.97	17.39	15.42

Table OC 4.3.1-2a

NET TORUS VERTICAL LOADS (FILTERED DATA) (ZERO ΔP), AVERAGE SUBMERGED PRESSURE AND TORUS AIR PRESSURE, 3.0 FT SUBMERGENCE (Continued)

Time (msec)	Net Torus Vertical Load (psid)	Torus Air Pressure (psid)	Average Submerged Pressure (psid)
789.0	1.97	17.58	15.61
799.0	1.98	17.87	15.89
809.0	2.05	18.16	16.10
818.0	1.98	18.55	16.56
828.0	1.97	18.64	16.67
838.0	1.99	19.03	17.04
848.0	1.94	19.32	17.38
858.0	1.89	19.61	17.72
868.0	1.95	19.90	17.95
877.0	1.95	20.09	18.14
887.0	1.98	20.38	18.40
897.0	2.03	20.67	18.64
907.0	1.91	21.06	19.15
917.0	1.80	21.25	19.45
927.0	1.83	21.45	19.61
937.0	1.73	21.83	20.10
946.0	1.76	22.03	20.26
956.0	1.78	22.60	20.82
966.0	1.82	22.60	20.78
976.0	2.33	22.99	20.66
986.0	1.93	23.38	21.45
996.0	1.79	23.57	21.78
1005.0	1.72	23.76	22.04
1015.0	1.73	24.24	22.52
1025.0	1.95	24.43	22.48
1035.0	1.77	26.94	25.17
1045.0	1.78	25.01	23.23
1055.0	1.68	25.20	23.52
1064.0	1.62	25.39	23.77
1074.0	1.47	25.90	24.43
1084.0	1.36	26.09	24.73
1094.0	1.33	26.48	25.14
1104.0	1.27	26.67	25.40
1114.0	1.31	26.94	25.63
1123.0	1.25	27.14	25.89
1133.0	1.23	27.45	26.21
1143.0	1.11	27.72	26.60
1153.0	1.00	27.91	26.91
1163.0	0.87	28.30	27.43
1173.0	0.83	28.61	27.78
1182.0	0.83	28.68	27.85
1192.0	0.86	29.07	28.21
1202.0	0.85	29.38	28.53

Table OC 4.3.1-2a

NET TORUS VERTICAL LOADS (FILTERED DATA) (ZERO ΔP), AVERAGE SUBMERGED PRESSURE AND TORUS AIR PRESSURE, 3.0 FT SUBMERGENCE (Continued)

Time (msec)	Net Torus Vertical Load (psid)	Torus Air Pressure (psid)	Average Submerged Pressure (psid)
1212.0	0.75	29.57	28.83
1222.0	0.77	29.85	29.08
1232.0	0.68	30.15	29.47
1241.0	0.50	30.35	29.85
1251.0	0.53	30.74	30.20
1261.0	0.43	30.93	30.50
1271.0	0.42	31.20	30.78
1281.0	0.29	31.47	31.18
1291.0	0.40	31.66	31.26
1301.0	0.40	31.66	31.26
1310.0	0.05	32.17	32.1[illegible]
1312.0	-0.02	32.17	32.1[illegible]

Peak Download = 9.24 psid

Standard Deviation = 0. psid

Peak Upload = 3.34 psid

Standard Deviation = 0. psid

Table OC 4.3.3-2

VENT HEADER LOCAL IMPACT/DRAG PRESSURE TRANSIENTS
(ZERO ΔP), 4.06 FT SUBMERGENCE

Submergence = 4.06 ft, Deflector: 16 in. Pipe with "T" Sections, 30 in. Width

Location T1		Location T2		Location T3		Location T4	
T (msec)	P (psi)	T (msec)	P (psi)	T (msec)	P (psi)	T (msec)	P (psi)
0.0000	0.0000	0.0000	0.0000	0.0000	0.0000	0.0000	0.0000
10.4285	4.7002	26.1691	3.9673	5.9352	1.3590	5.9028	1.2642
12.0024	3.8757	69.4564	1.4504	83.1759	0.0000	31.4817	1.9673
43.6808	5.6001	85.1975	1.7247	46.2387	1.0660	55.0929	2.7042
150.2269	0.0000	194.7637	0.0000	79.6088	0.0000	136.4600	0.0000

Location T5		Location T6		Location T7		Location T8	
T (msec)	P (psi)	T (msec)	P (psi)	T (msec)	P (psi)	T (msec)	P (psi)
0.0000	0.0000	0.0000	0.0000	0.0000	0.0000	0.0000	0.0000
19.6760	0.0539	55.4864	0.4025	6.0996	3.6760	17.5117	0.4265
59.0281	0.5579	90.3130	1.0568	15.9376	5.2506	40.7244	1.6306
98.8002	0.5838	108.0215	0.0000	45.4841	3.9235	68.4726	0.0000
137.7823	0.0000	108.0215	0.0000	117.4789	0.0000	68.4726	0.0000

Location T9		Location T10		Location T11		Location T12	
T (msec)	P (psi)	T (msec)	P (psi)	T (msec)	P (psi)	T (msec)	P (psi)
0.0000	0.0000	0.0000	0.0000	0.0000	0.0000	0.0000	0.0000
1.7708	4.5893	5.7061	17.5754	5.1158	2.9179	0.7870	4.2207
19.8720	4.7603	6.8866	13.6471	22.8242	0.0000	13.7732	1.2721
23.2177	2.6634	13.4700	6.7243	67.0953	0.6057	43.2813	0.6242
219,9828	0.0000	197.7011	0.0000	91.6904	0.0000	82.6394	0.0000

Table OC 4.3.3-1b

VENT HEADER LOCAL IMPACT/DRAG PRESSURE TRANSIENTS (ZERO ΔP), 3.0 FT SUBMERGENCE

Submergence = 3.00 ft, Deflector: 16 in. pipe with "T" sections, 30 in. width

Location T1		Location T2		Location T3		Location T4	
T (msec)	P (psi)	T (msec)	P (psi)	T (msec)	P (psi)	T (msec)	P (psi)
0.0000	0.0000	0.0000	0.0000	0.0000	0.0000	0.0000	0.0000
21.6436	4.6432	21.8404	0.7673	46.2387	0.0390	5.7061	0.0000
31.2849	7.0083	36.2039	2.4731	95.4288	0.0000	47.2225	0.0000
58.4379	4.7452	51.3545	5.2761	95.4286	0.0000	47.2225	0.0000
149.3412	0.0000	130.0587	0.0000	95.4288	0.0000	47.2265	0.0000

Location T5		Location T6		Location T7		Location T8	
T (msec)	P (psi)	T (msec)	P (psi)	T (msec)	P (psi)	T (msec)	P (psi)
0.0000	0.0000	0.0000	0.0000	0.0000	0.0000	0.0000	0.0000
15.7408	0.0000	84.6070	0.0000	32.8590	0.2507	35.8104	0.1299
73.7852	0.0000	108.2182	0.0000	53.5168	0.0000	98.3802	0.0000
73.7852	0.0000	108.2182	0.0000	53.5188	0.0000	98.3802	0.0000
73.7852	0.0000	108.2182	0.0000	53.5188	0.0000	98.3802	0.0000

Location T9		Location T10		Location T11		Location T12	
T (msec)	P (psi)	T (msec)	P (psi)	T (msec)	P (psi)	T (msec)	P (psi)
0.0000	0.0000	0.0000	0.0000	0.0000	0.0000	0.0000	0.0000
12.0024	1.4412	59.0281	0.7393	19.6760	0.0000	19.6760	0.0000
75.9495	0.0000	88.5422	0.0000	60.7990	0.6717	37.7780	2.4417
75.9495	0.0000	88.5422	0.0000	71.8176	0.7253	46.6322	0.0000
75.9495	0.0000	88.5422	0.0000	88.5422	0.0000	46.6322	0.0000

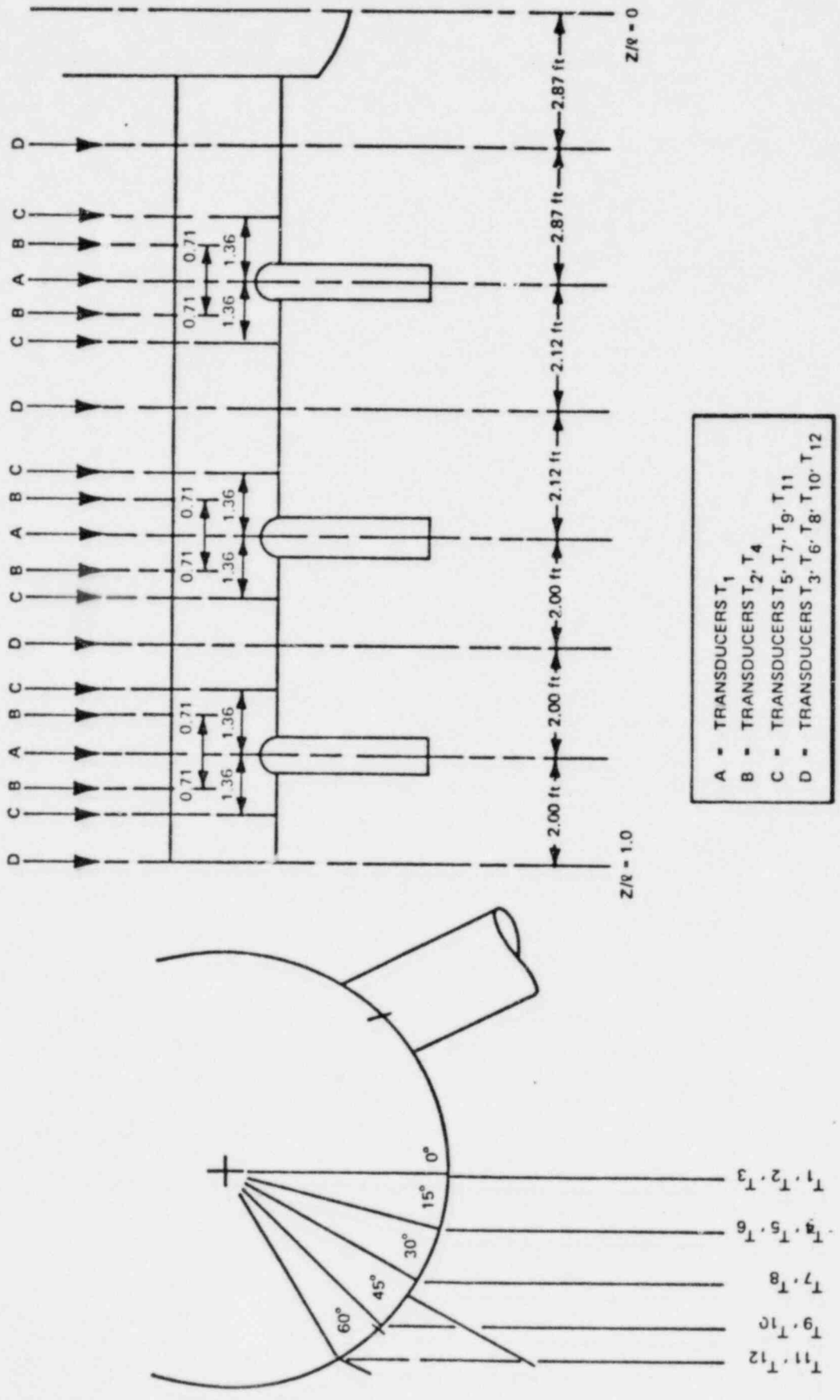

Figure OC 4.3.3-1. Location of Impact/Drag Pressure Transducers on Header

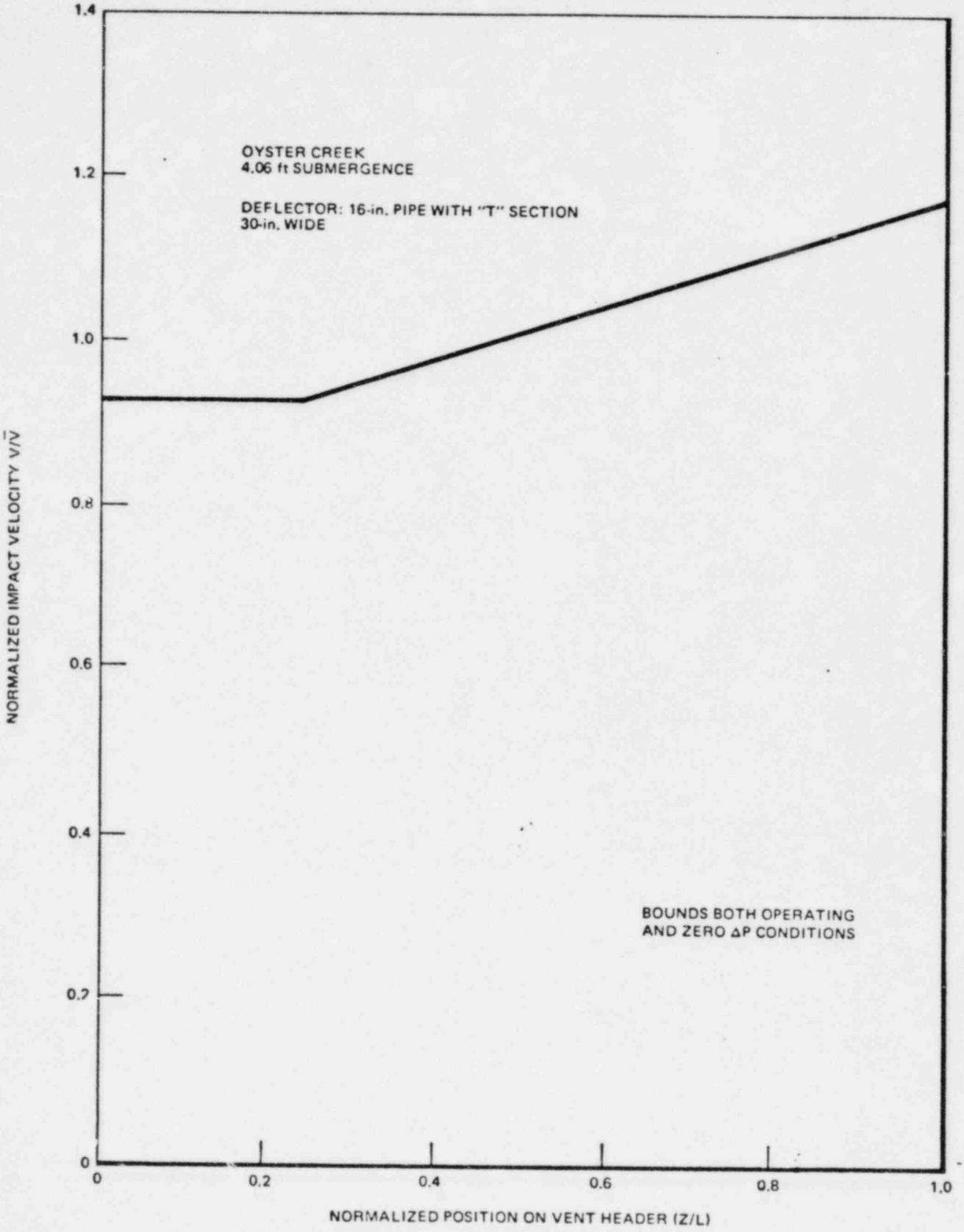

Figure OC 4.3.3-2. Longitudinal Vent Header Impact Velocity Distribution Based on EPRI Main Vent Orifice Tests (Operating and Zero ΔP), 4.06 ft Submergence

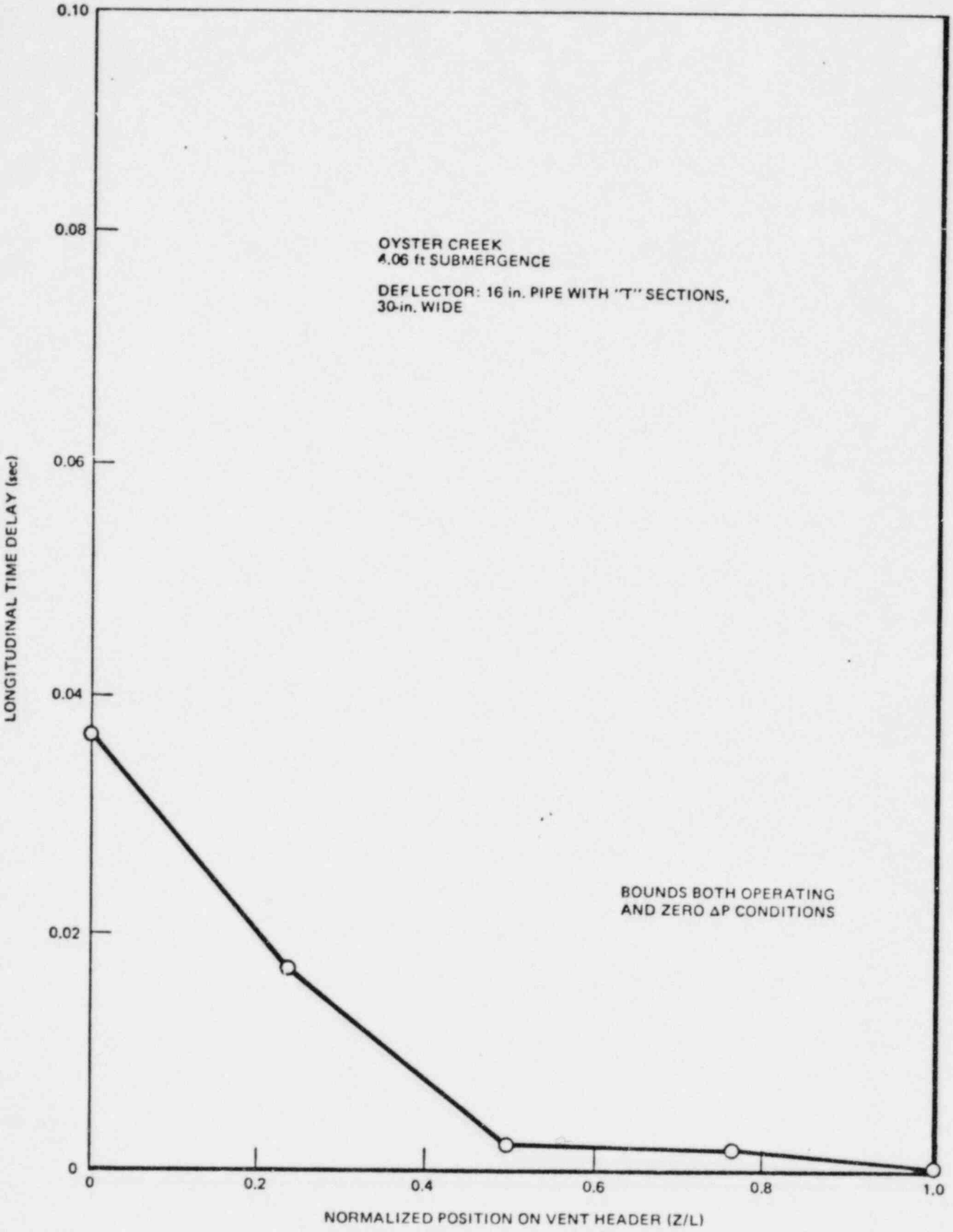

Figure OC 4.3.3-3. Longitudinal Time Delay Distribution Based on EPRI Main Vent Orifice Tests (Operating and Zero ΔP), 4.06 ft Submergence

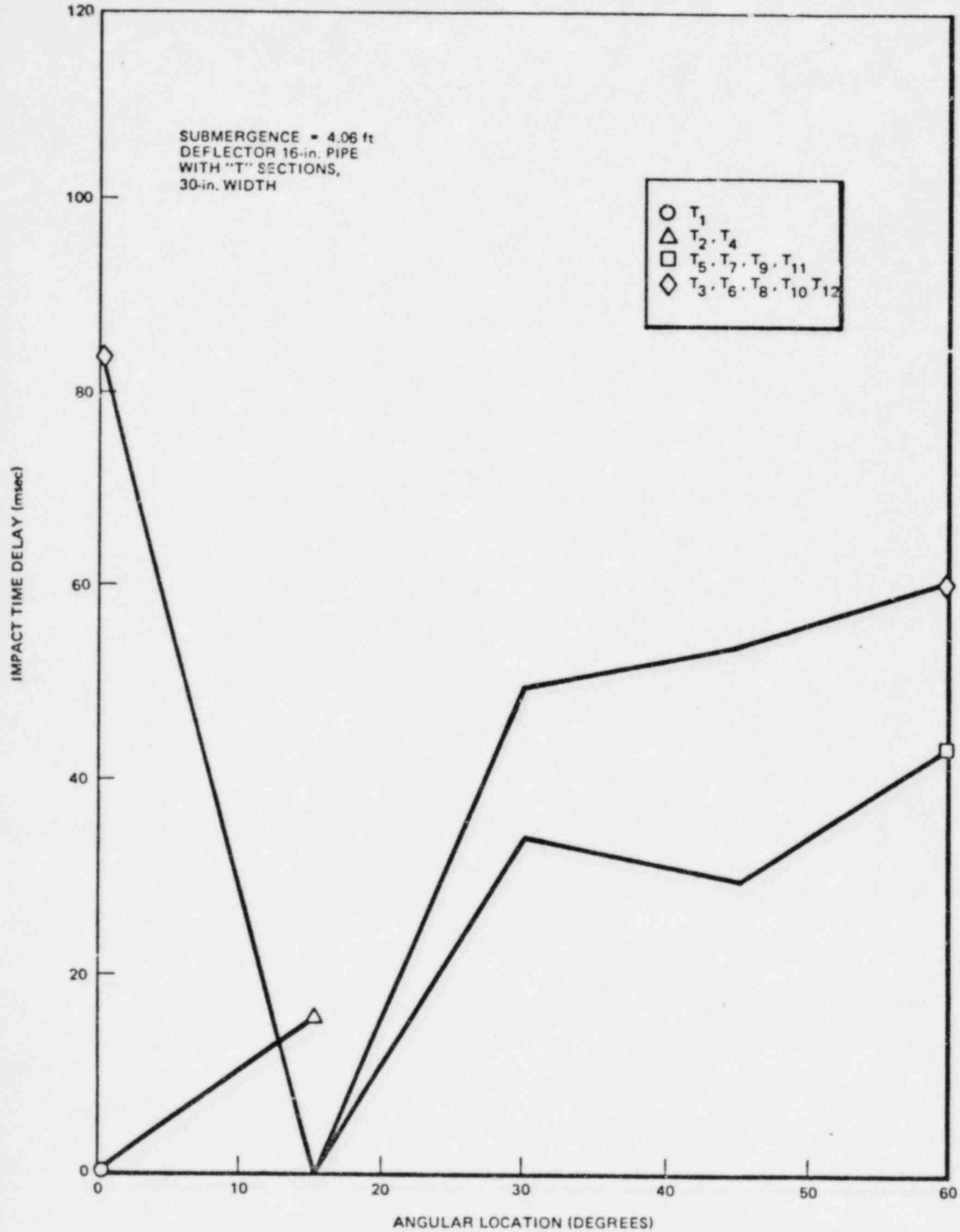

Figure OC 4.3.3-5. Circumferential Time Delay Distribution (Zero ΔP), 4.06 ft Submergence

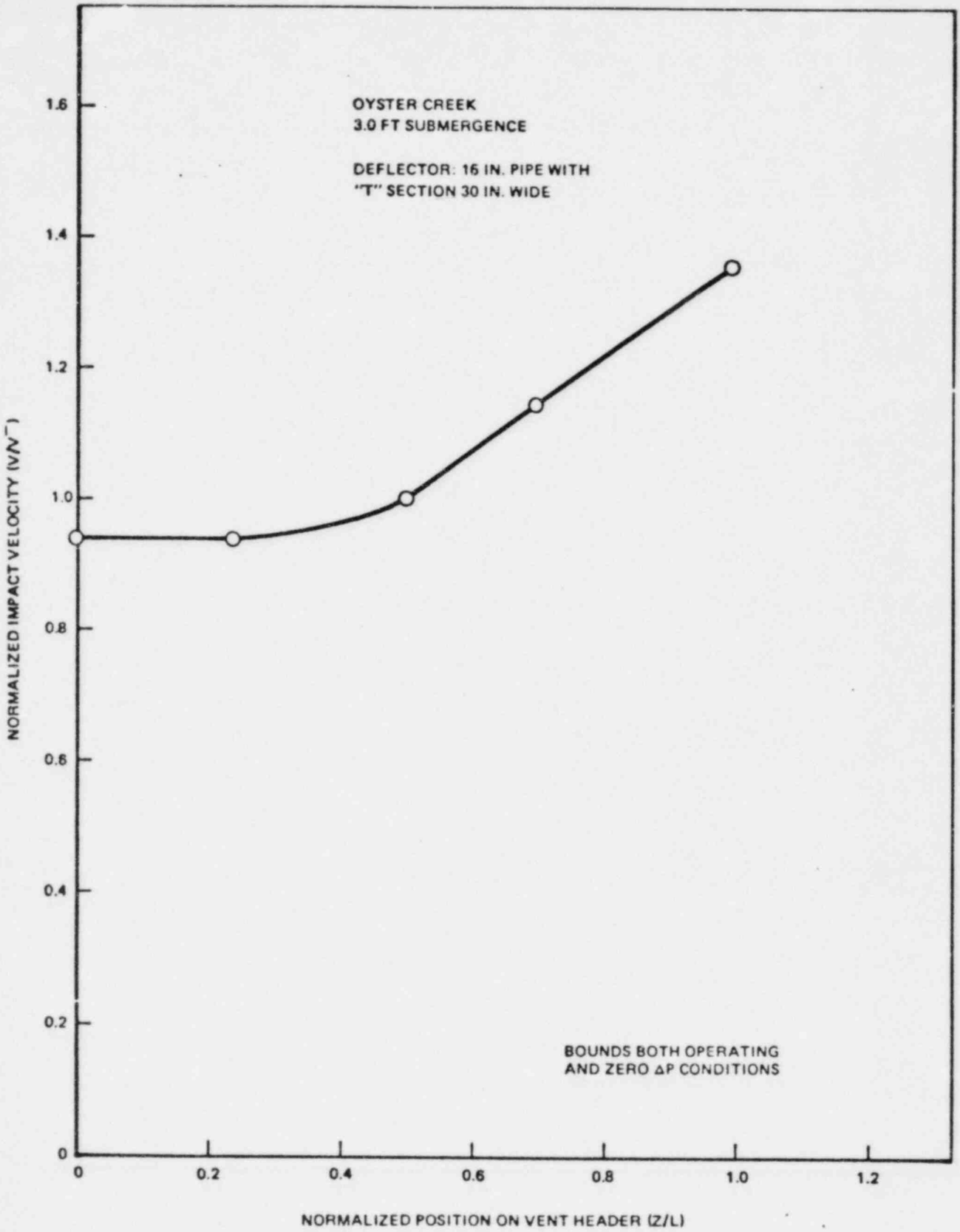

Figure OC 4.3.3-1a. Longitudinal Vent Header Impact Velocity Distribution Based on EPRI Main Vent Orifice Tests (Operating and Zero ΔP), 3.0 ft Submergence

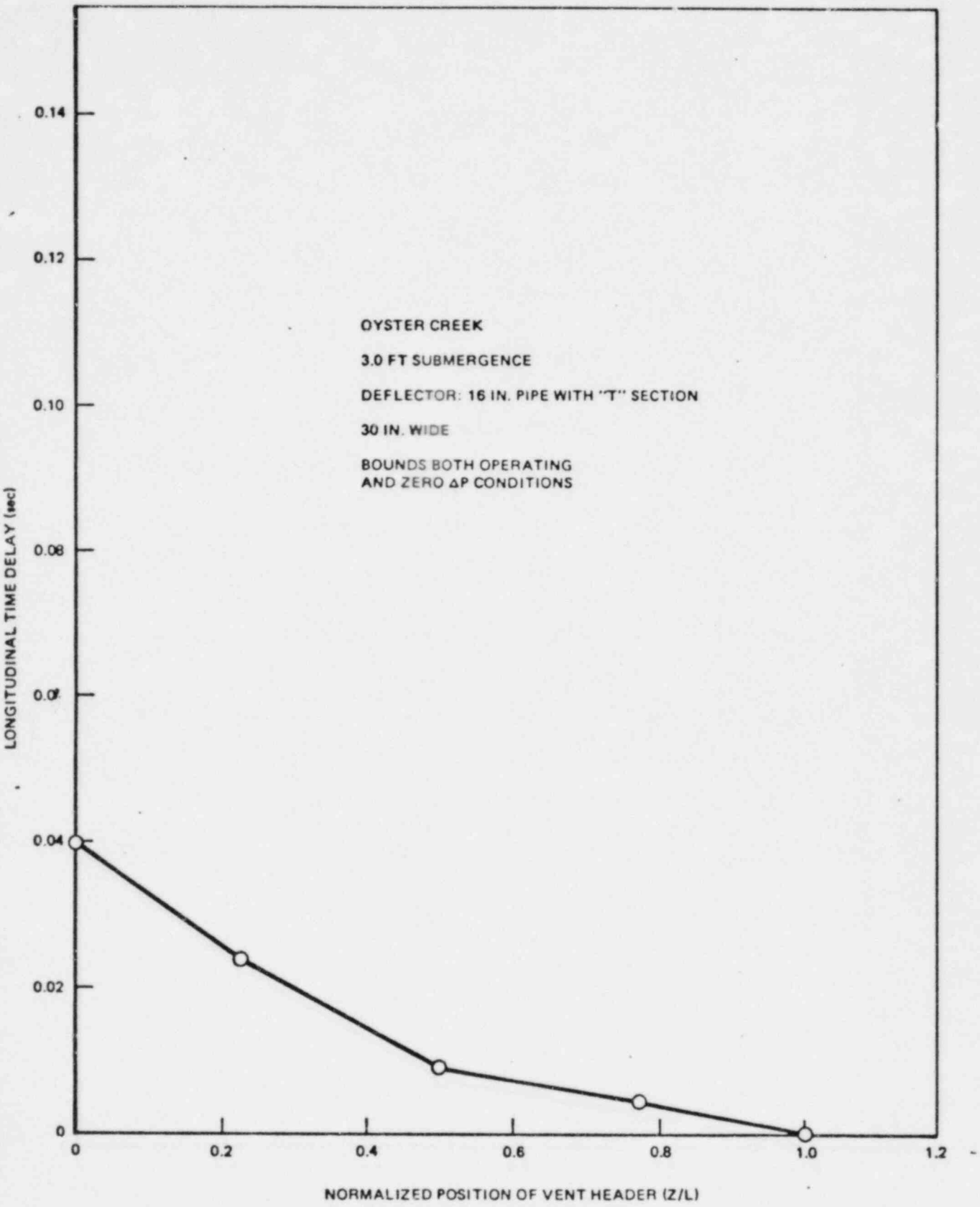

Figure OC 4.3.3-2a. Longitudinal Time Delay Distribution Based on EPRI Main Vent Orifice Tests (Operating and Zero ΔP), 3.0 ft Submergence

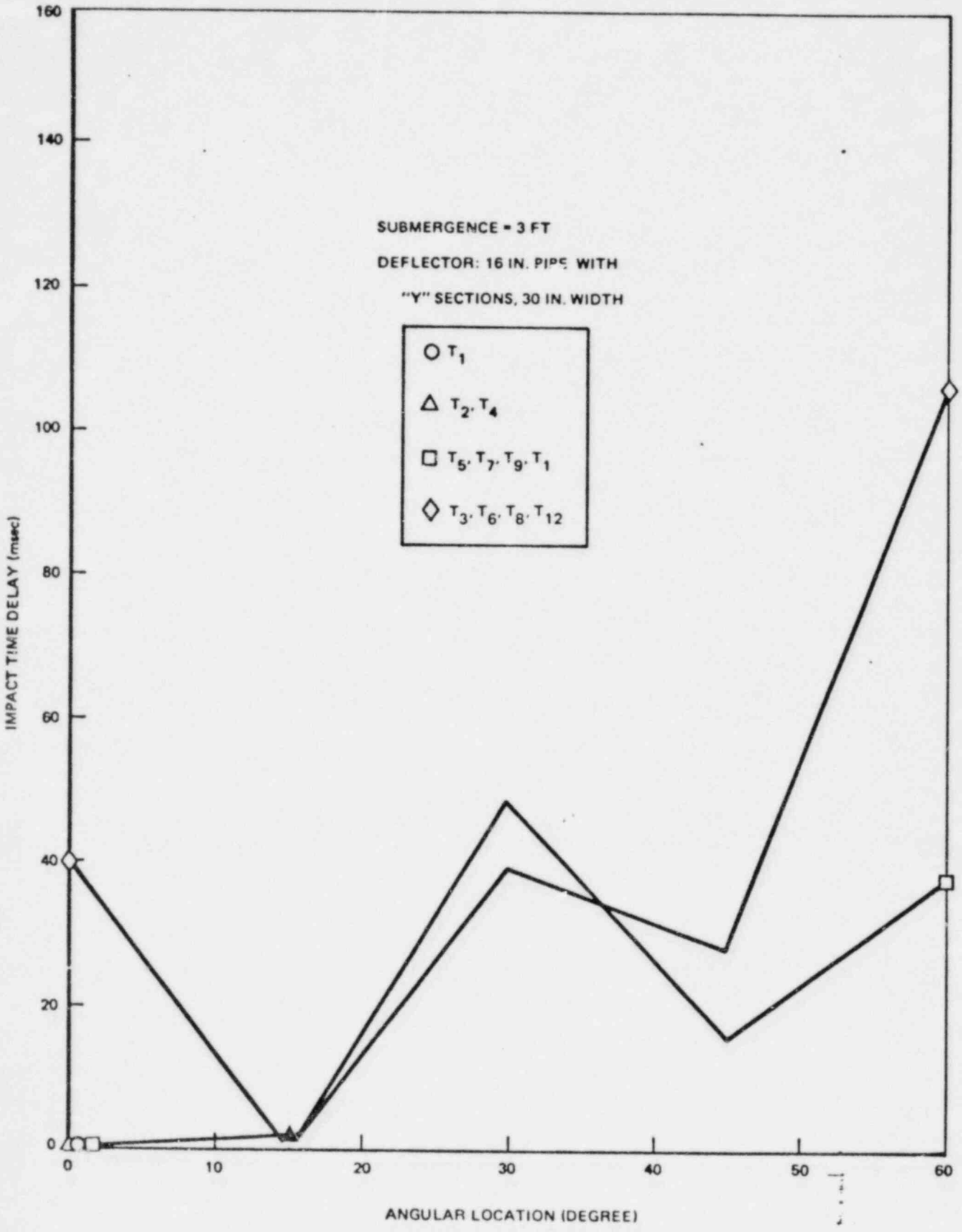

Figure OC 4.3.3-1b. Circumferential Time Delay Distribution (Zero ΔP), 3.0 ft Submergence

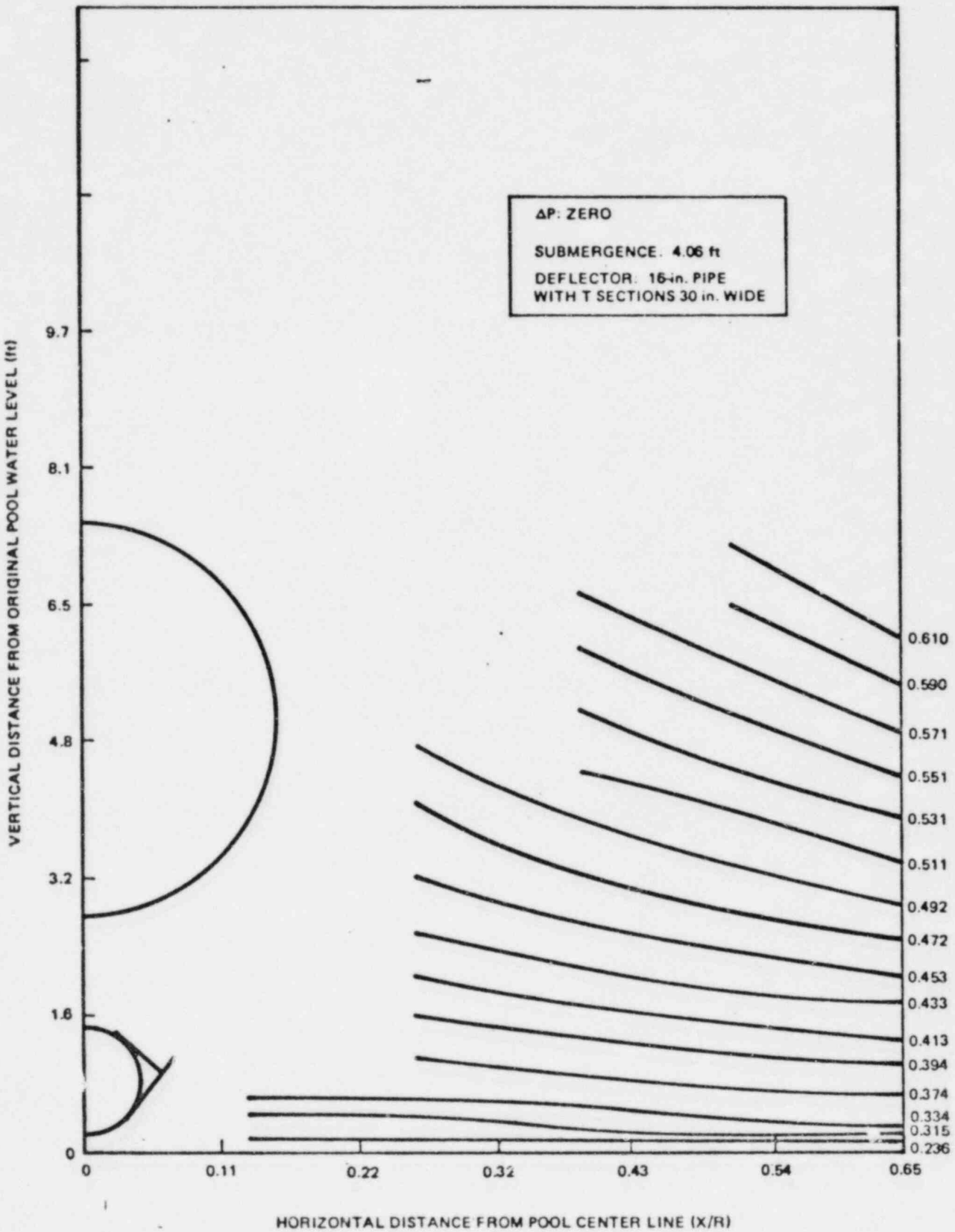

Figure OC 4.3.4-1a. Pool Swell Displacement Distribution (Zero ΔP), 4.06 ft Submergence

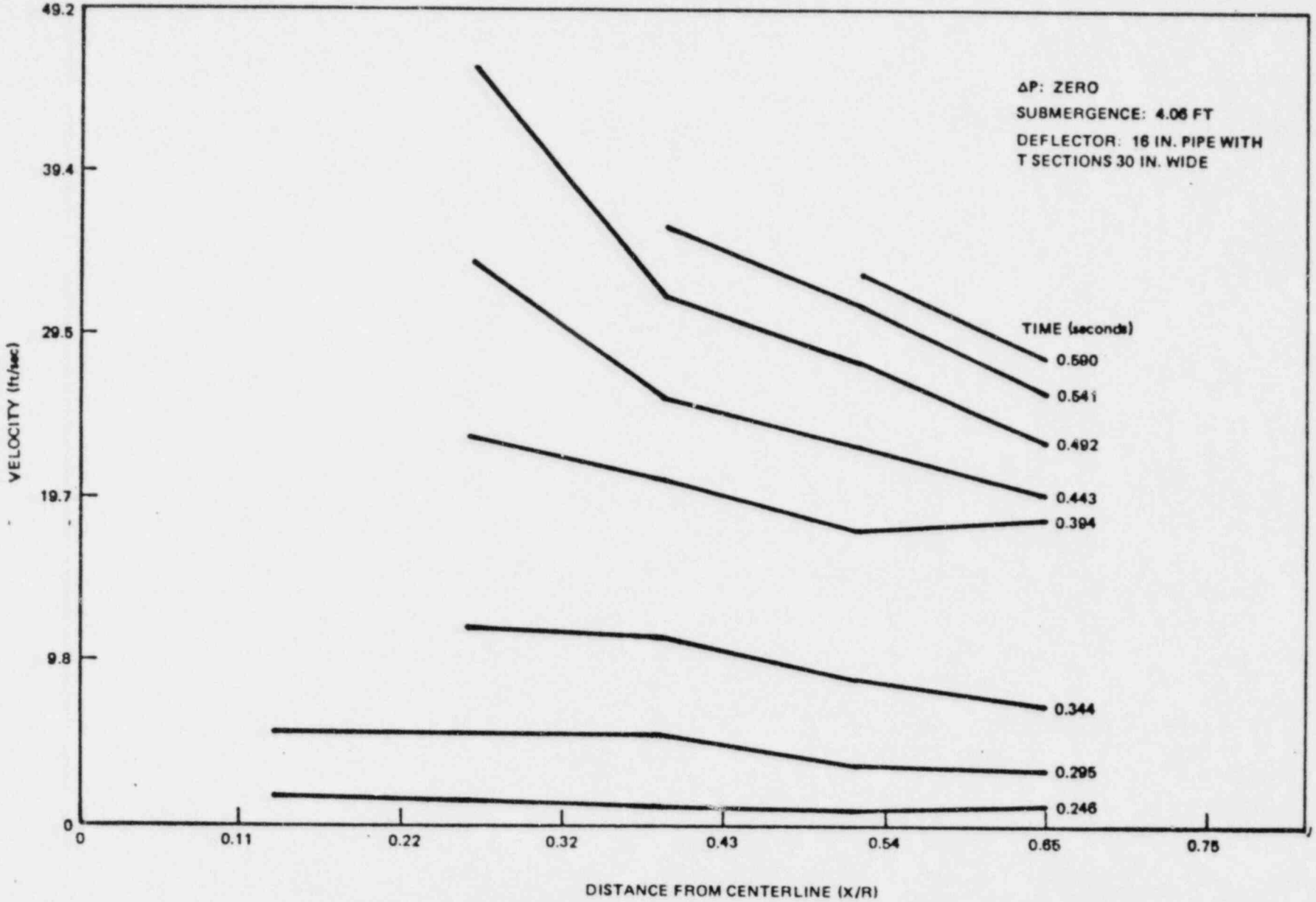

Figure OC 4.3.4-2a. Pool Swell Velocity Distribution (Zero ΔP), 4.06 ft Submergence

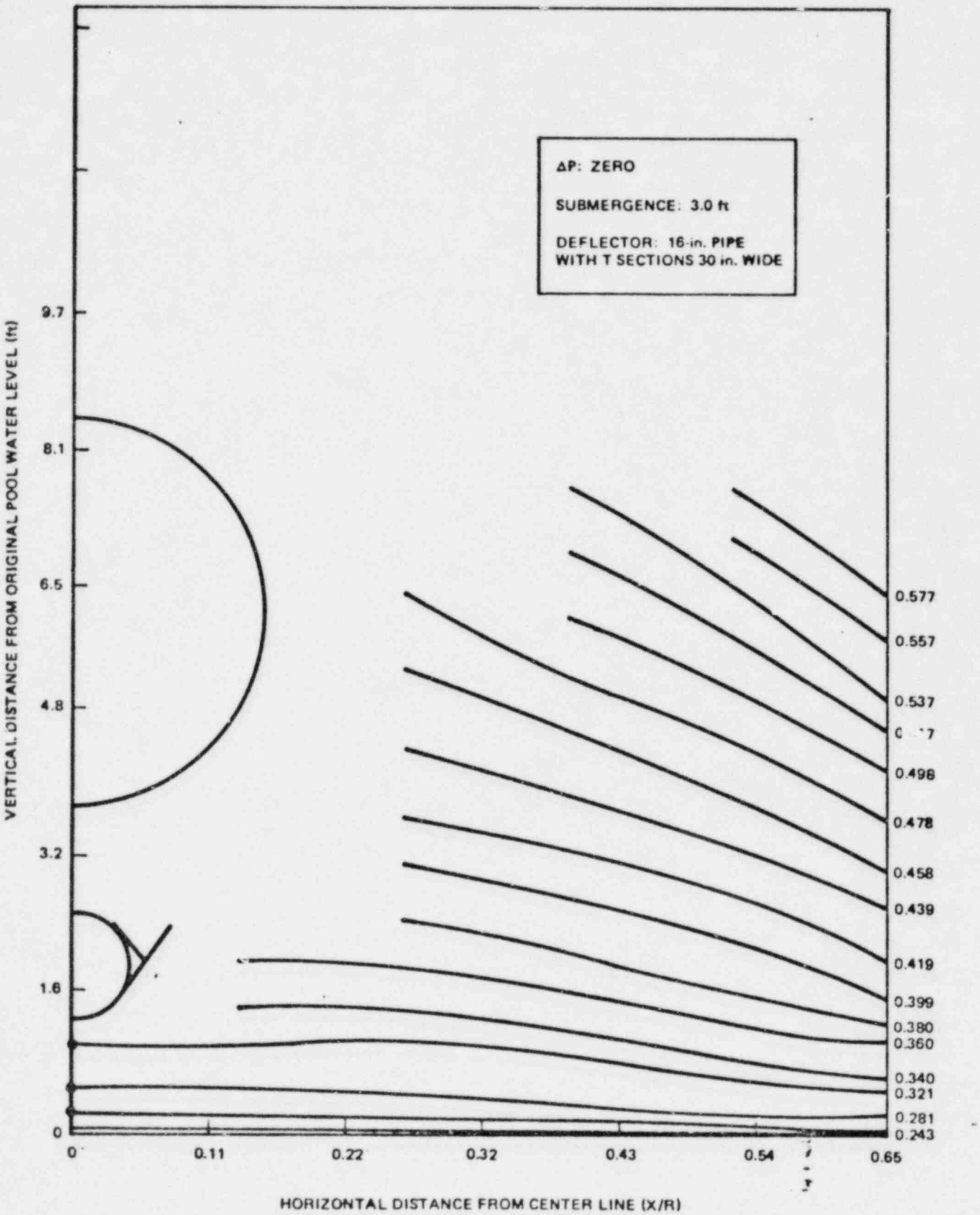

Figure OC 4.3.4-1c. Pool Swell Displacement Distribution (Zero ΔP), 3.0 ft Submergence

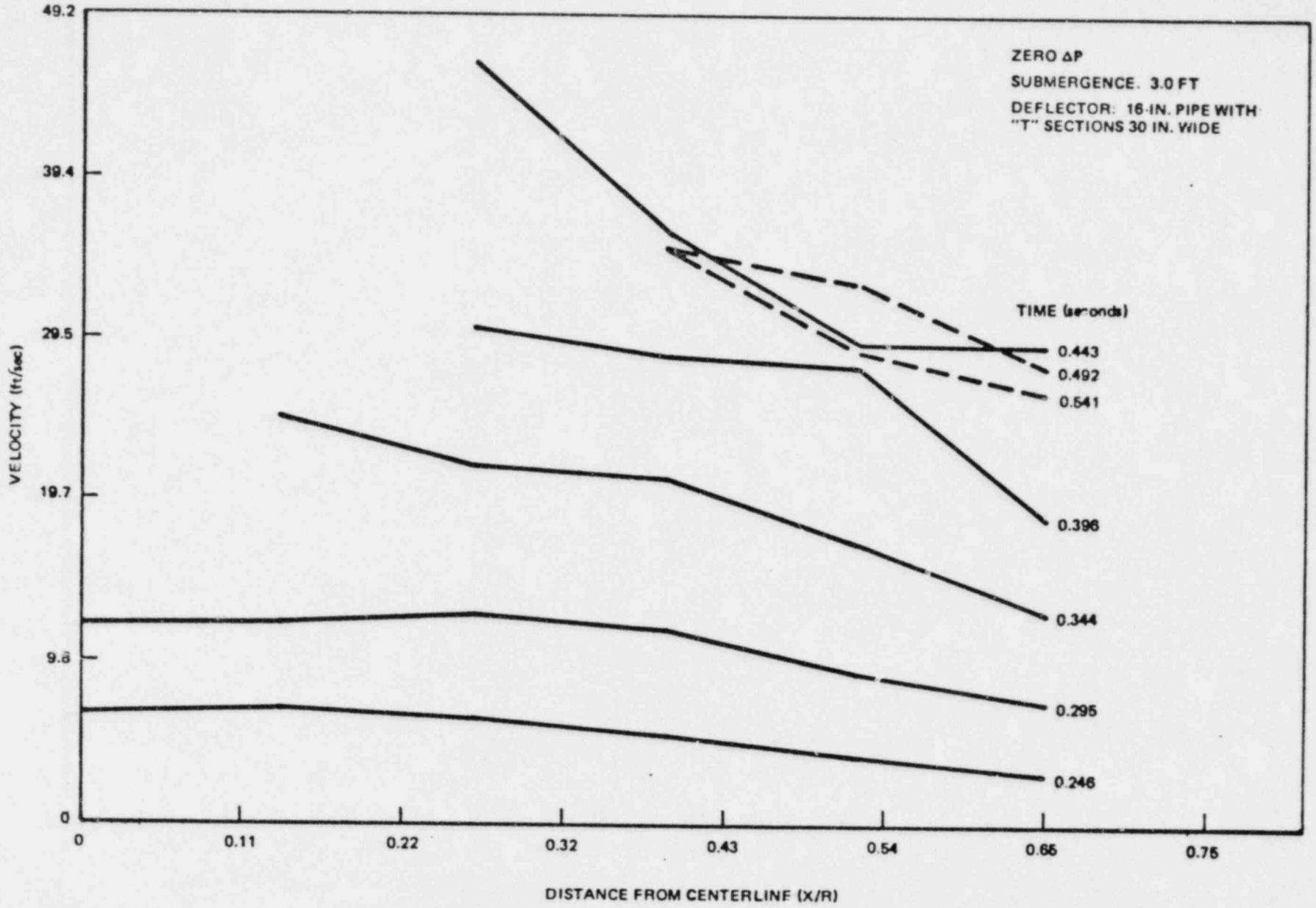

Figure OC 4.3.4-2c. Pool Swell Velocity Distribution (Zero ΔP), 3.0 ft Submergence

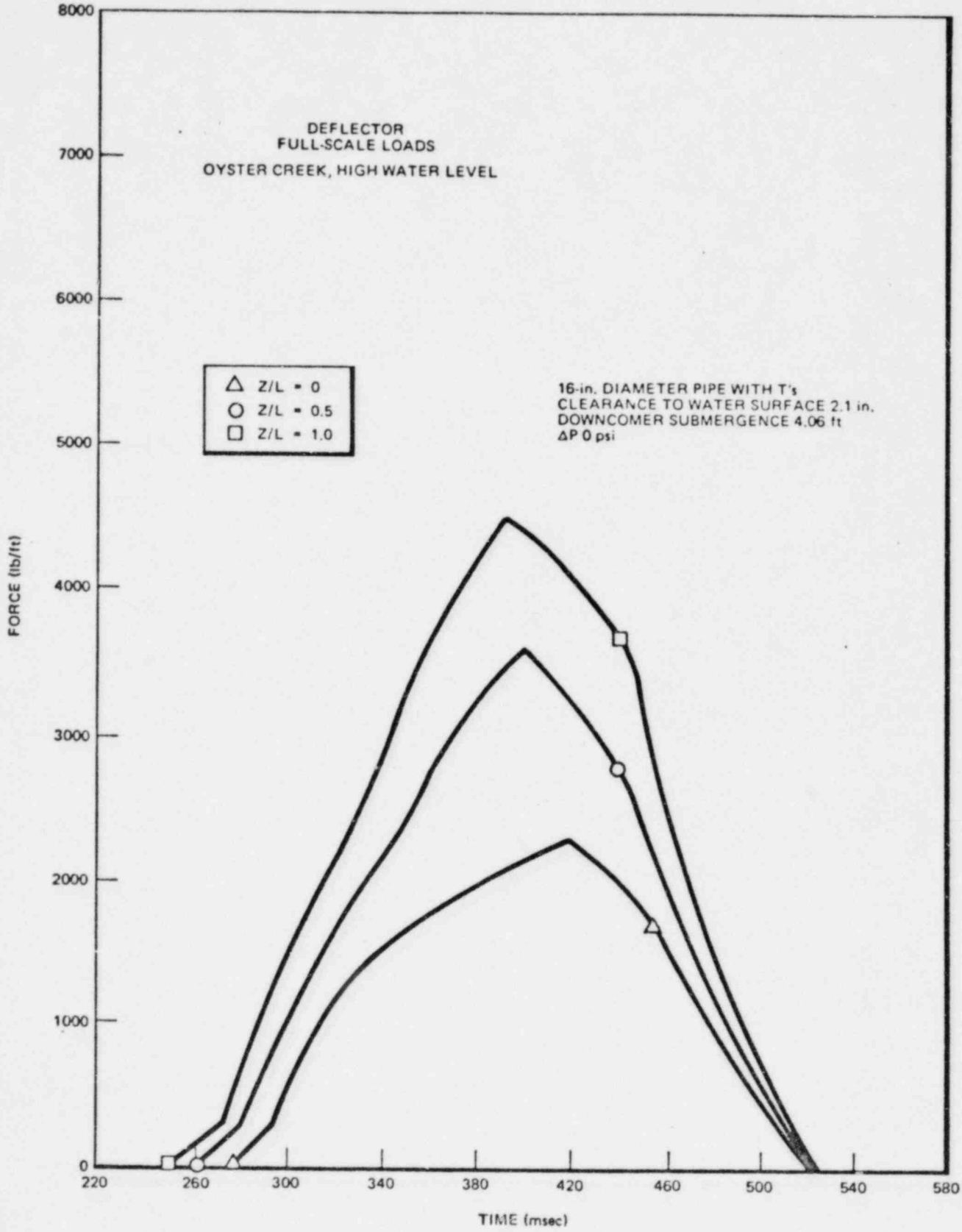

Figure OC 4.3.9-1. Vent Header Deflector Loads (Zero ΔP), 4.06 ft Submergence

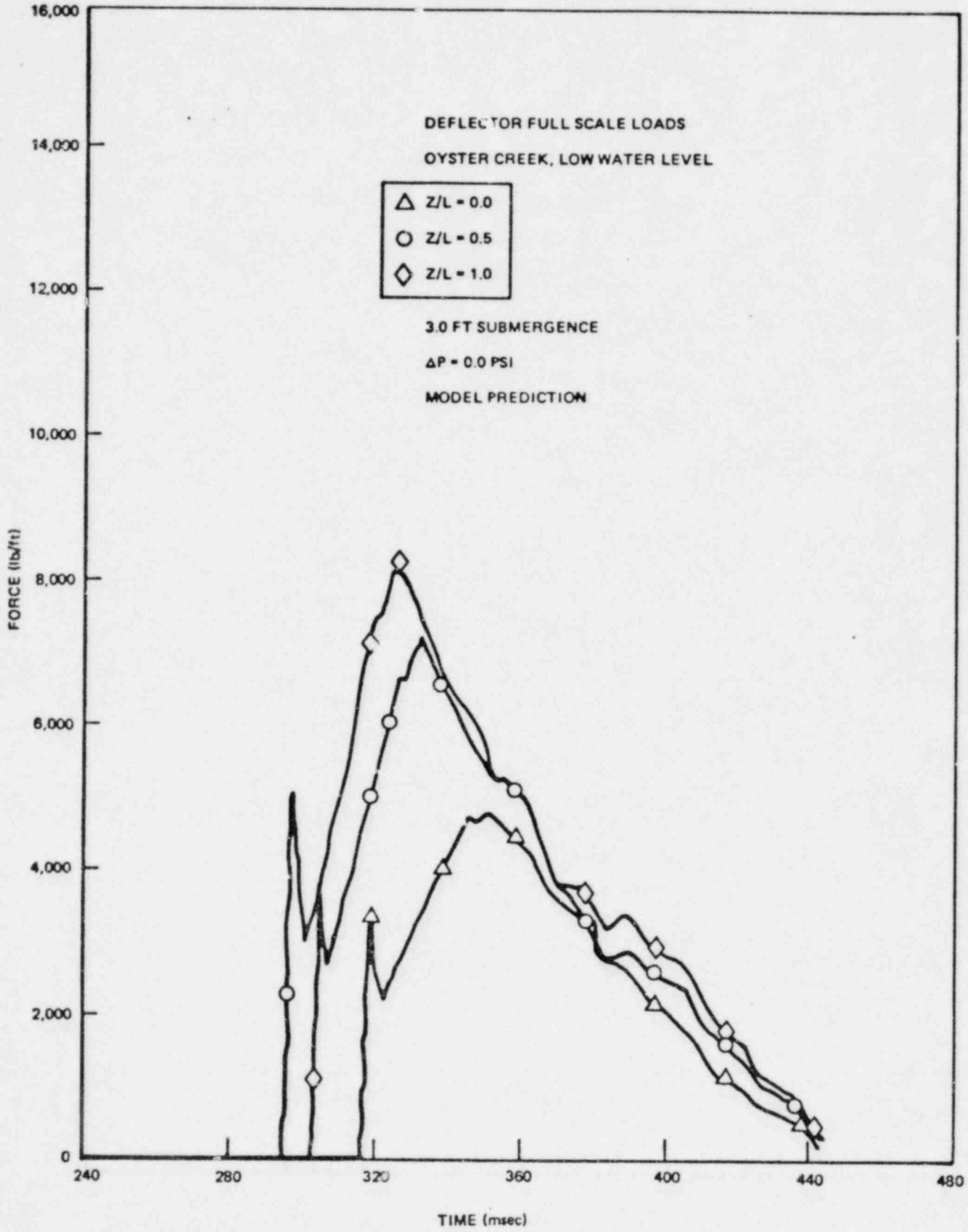

Figure OC 4.3.9-1a. Vent Header Deflector Loads (Zero ΔP), 3.0 ft Submergence